Washington University in St. Louis
Washington University Open Scholarship

All Theses and Dissertations (ETDs)

5-24-2012

Identification of Novel Fluid Biomarkers for Alzheimer's Disease

Rebecca Craig-Schapiro
Washington University in St. Louis

Follow this and additional works at: https://openscholarship.wustl.edu/etd

Recommended Citation
Craig-Schapiro, Rebecca, "Identification of Novel Fluid Biomarkers for Alzheimer's Disease" (2012). *All Theses and Dissertations (ETDs)*. 685.
https://openscholarship.wustl.edu/etd/685

This Dissertation is brought to you for free and open access by Washington University Open Scholarship. It has been accepted for inclusion in All Theses and Dissertations (ETDs) by an authorized administrator of Washington University Open Scholarship. For more information, please contact digital@wumail.wustl.edu.

WASHINGTON UNIVERSITY IN ST. LOUIS

Division of Biology and Biomedical Sciences

Neurosciences

Dissertation Examination Committee:
David M. Holtzman, Chair
Anne Fagan
Alison Goate
Paul Gray
Robert Schmidt
Reid Townsend

Identification of Novel Fluid Biomarkers for Alzheimer's Disease

by

Rebecca June Craig-Schapiro

A dissertation presented to the
Graduate School of Arts and Sciences
of Washington University in
partial fulfillment of the
requirements for the degree
of Doctor of Philosophy

May 2012

Saint Louis, Missouri

Copyright by

Rebecca June Craig-Schapiro

2012

ABSTRACT OF THE DISSERTATION

Identification of Novel Fluid Biomarkers for Alzheimer's Disease

by

Rebecca June Craig-Schapiro

Doctor of Philosophy in Biology and Biomedical Sciences

Neurosciences Program

Washington University in St. Louis, 2012

Dr. David M. Holtzman, Chairperson

Clinicopathological studies suggest that Alzheimer's disease (AD) pathology begins to appear ~10-20 years before the resulting cognitive impairment draws medical attention. Biomarkers that can detect AD pathology in its early stages and predict dementia onset and progression would, therefore, be invaluable for patient care and efficient clinical trial design. To discover such biomarkers, we measured AD-associated changes in the cerebrospinal fluid (CSF) using an unbiased proteomics approach (two-dimensional difference gel electrophoresis with liquid chromatography tandem mass spectrometry). From this, we identified 47 proteins that differed in abundance between cognitively normal (Clinical Dementia Rating [CDR] 0) and mildly demented (CDR 1) subjects. To validate these findings, we measured a subset of the identified candidate biomarkers by enzyme linked immunosorbent assay (ELISA); promising candidates in this discovery cohort (N=47) were further evaluated by ELISA in a larger validation CSF cohort (N=292) that contained an additional very mildly demented (CDR 0.5) group. Levels of four novel biomarkers were significantly altered in AD, and Receiver-operating characteristic (ROC) analyses using a stepwise logistic regression model identified optimal panels containing these markers that distinguished CDR 0 from CDR>0 (tau, YKL-40, NCAM) and CDR 1 from CDR<1 (tau, chromogranin-A, carnosinase-I). Plasma

levels of the most promising marker, YKL-40, were also found to be increased in CDR 0.5 and 1 groups and to correlate with CSF levels. Importantly, the CSF YKL-40/Aβ42 ratio predicted risk of developing cognitive impairment (CDR 0 to CDR>0 conversion) as well as the best CSF biomarkers identified to date, tau/Aβ42 and p-tau181/Aβ42. Additionally, YKL-40 immunoreactivity was observed within astrocytes near a subset of amyloid plaques, implicating YKL-40 in the neuroinflammatory response to Aβ deposition. Utilizing an alternative, targeted proteomics approach to identify novel biomarkers, 333 CSF samples were evaluated for levels of 190 analytes using a multiplexed Luminex platform. The mean concentrations of 37 analytes were found to differ between CDR 0 and CDR>0 participants. ROC and statistical machine learning algorithms identified novel biomarker panels that improved upon the ability of the current best biomarkers to discriminate very mildly demented from cognitively normal participants, and identified a novel biomarker, Calbindin, with significant prognostic potential.

Acknowledgements

I have had the fortunate opportunity to work with several excellent mentors. First and foremost, I want to thank Dr. David Holtzman, who provided invaluable guidance, resources, and advice along the way. I am truly privileged to be able to say I was trained in his lab. I am especially grateful to Dr. Anne Fagan, who was always accessible, even through weekend phone calls and late night emails, to offer me both advice and support. There were at least several times when I was feeling 'stuck' with a project, Anne was there to listen patiently, offer her advice, and get me in touch with people she knew could help me solve the problem. And lastly, my unofficial mentor, Dr. Rick Perrin, who spent countless hours pouring over mass spec data, taking immunohistochemistry images on his microscope, giving feedback on papers and figures, chilling in the 4˚ walk-in, discussing experiments, and offering that all-important sympathetic ear and sounding board which helped make my time in the lab successful and got me through the hard times.

I would also like to thank the members of my thesis committee, Dr. Robert Schmidt, Dr. Reid Townsend, Dr. Paul Gray, and Dr. Alison Goate, for taking time out of their busy schedules to provide advice and feedback on my work.

Over the last year, I have relied on the expertise of many statisticians here at Washington University, including Chengjie Xiong, Cathy Roe, and Martha Storandt, who have patiently taught and assisted me in my statistical analyses. Additionally, Eve Pickering and Max Kuhn at Pfizer contributed considerable statistical help. I would also like to thank Deborah Carter for all her help teaching me immunohistochemistry. Dr. Gray and the members of his lab were very welcoming and kind in teaching me about *in situ* hybridization.

Much of this work would not have been possible without the efforts of the members of the Proteomics Core. In particular, I received a great deal of support and guidance from Reid Townsend, Alan Davis worked with me at the bench teaching me the proteomics techniques, and Jim Malone helped immensely with the 2D-DIGE project.

I have thoroughly enjoyed my time in the Holtzman lab, in large part because the members strive to create an environment that fosters collaboration and camaraderie. Aarti Shah taught me the art of ELISAs, and without her efforts in preparing and managing the CSF sample database, this work would not have been possible. Adam Bero and Joe Castellano kept me laughing along the way. I also made a great friend through the lab, former office-sharer Jae-Eun Kang.

This work was supported by the National Institutes of Health, the Charles and Joanne Knight Alzheimer Research Initiative, the National Center for Research Resources, the Department of Veterans Affairs, the W.M. Keck Foundation, and the National Alzheimer's Coordinating Center.

And finally, words are not enough to express how thankful and lucky I am to have such wonderful and supportive parents. I dedicate this thesis to my parents, who have always been my biggest advocates, encouraged me to have confidence in myself and to work harder and go farther, cheered me up when I was down, tolerated me when I was cranky, and always bragged (embarrassingly) about my accomplishments.

Table of Contents

List of Tables

List of Figures

Chapter 1.

Introduction and Perspective

Portions of this chapter were published in the August 2009 issue of *Neurobiology of Disease.*

Alzheimer's Disease

Alzheimer's disease (AD) is a progressive neurodegenerative disorder estimated to affect 5.3 million Americans (1). Although the course of AD can be heterogeneous among individuals, there are many common symptoms. The initial symptom is often a problem remembering recently learned information, which is frequently mistaken or dismissed as a normal effect of aging. Disease progression is characterized by a gradual decline in memory, orientation, comprehension, and judgment, and in advanced stages, a loss of control over bodily functions. The mean life expectancy following diagnosis is approximately 5 years (2, 3). For most individuals with "late-onset" AD, symptoms first begin after age 65; however, the onset is generally gradual and insidious, leading to a delay between symptom onset and diagnosis of approximately 3 years (4). It has been reported that episodic memory deficits may be detectable by clinical testing up to six years before diagnosis (5). While the majority of AD cases are late-onset, an estimated 200,000 Americans have "early-onset" AD, when symptoms present before age 65 (1). Many of these cases are familial (FAD), caused by autosomal dominant mutations in one of three genes: amyloid precursor protein (*APP*) gene on chromosome 21 (6), presenilin 1 (*PSEN1*) gene on chromosome 14 (7), and presenilin 2 (*PSEN2*) gene on chromosome 1 (8). Studies of the proteins encoded by these genes has furthered our understanding of the molecular mechanisms contributing to AD. A hallmark neuropathological feature of AD is the accumulation of extracellular amyloid plaques consisting primarily of amyloid-beta (Aβ). Aβ is a 38-43 amino acid peptide that is generated by sequential cleavage of APP by β-secretase and γ-secretase; *PSEN1* and *PSEN2* encode components of the γ-secretase enzyme complex (9). *PSEN1* mutations account for the majority of FAD cases, and most *PSEN1*, *PSEN2*, and *APP* mutations

are thought to affect APP processing such that Aβ production, and specifically the more amyloidogenic form, Aβ42, is increased. Additionally, individuals with Down Syndrome (trisomy 21) have three copies of *APP*, resulting in increased Aβ production and early-onset AD neuropathology (10). These findings, as well as evidence that Aβ is the primary component of plaques and that cerebrospinal fluid (CSF) Aβ42 levels are altered in AD, point to a critical role for Aβ in AD pathogenesis. The 'amyloid cascade hypothesis' holds that increased Aβ production and accumulation, whether early in life from genetic causes or later in life in sporadic cases, leads to Aβ oligomerization, aggregation, and deposition in plaques, eventually resulting in synaptic and neuronal injury, glial activation, and ultimately dementia (11). This hypothesis has garnered much support, however, additional work is needed to fill in missing details and perceived weaknesses in the theory, in particular, improved understanding of the relationship between amyloid and neurofibrillary tangle pathology and neurodegeneration (discussed more in depth below), and the identity of the specific Aβ species that drives neurotoxicity.

For late-onset AD, the chromosome 19 gene encoding apolipoprotein E (*APOE*) has been the most extensively investigated, and until recently the only consistently replicated, genetic risk factor for AD (12). ApoE has three isoforms, ε2, ε3, and ε4, that differ by cysteine-arginine interchanges at position 112 and 158 (13). The ApoE ε4 allele has been shown to be a risk factor for late-onset familial and sporadic AD (14), as well as early-onset sporadic cases (15, 16). This risk is dose dependent, with homozygotes at increased risk of disease and demonstrating earlier age of onset than heterozygotes or those not carrying an ε4 allele (12, 14, 17). Conversely, it appears that the ε2 allele may have a protective effect against the development of late-onset AD (18, 19), and confer a reduced risk of cognitive decline among cognitively normal elderly (20-22).

Furthermore, ε2 carriers may have less amyloid and tangle pathology (23-26) than non-carriers. Additionally, ApoE has been found to bind Aβ and to co-localize with cerebral amyloid deposits in AD and cerebral amyloid angiopathy (CAA) (27, 28). Although the ApoE ε4 allele is a well validated risk factor for late-onset AD, there are likely other genetic or environmental factors involved in determining risk, as ε4 is neither necessary nor sufficient for disease. Indeed, recent genome wide association studies utilizing many thousands of individuals have identified apolipoprotein J (CLU) and phosphatidylinositol binding clathrin assembly protein (PICALM) (29-31) as late-onset AD susceptibility loci. The mechanisms underlying these associations remain to be determined.

In addition to amyloid plaques, a second neuropathological hallmark of AD is the accumulation of intracellular neurofibrillary tangles composed primarily of hyperphosphorylated tau (p-tau). Abnormal tau deposition is seen in other conditions as well, including frontotemporal dementia (FTD), progressive supranuclear palsy (PSP), and corticobasal degeneration (CBD), and while no AD-causing mutations have been identified in the tau gene (*MAPT*), tau mutations have been linked with FTD with parkinsonism, suggesting that tau dysfunction can cause neurodegeneration (32, 33). The tau protein is known to bind and stabilize microtubules, and the abnormal phosphorylation of tau that occurs in AD is thought to lead to microtubule disassembly, disruption of intracellular trafficking, and ultimately neuronal dysfunction (34-36). Additionally, abnormal tau aggregates into insoluble paired helical filaments (PHFs) which are hypothesized to further compromise neuronal function by occluding axons and dendrites (35). Whether phosphorylation of tau drives PHF formation (by preventing tau binding to microtubules and thus increasing the availability of unbound tau to aggregate) or whether the converse is true, is unknown. Additionally, understanding of the regulation of tau phosphorylation is largely incomplete. Importantly, the mechanistic relationships between Aβ, tau, and brain degeneration remain unclear. According to the

amyloid cascade hypothesis, Aβ is the primary driver of AD pathogenesis, with tau hyperphosphorylation and neurofibrillary tangle formation downstream events. Unresolved details of the amyloid cascade hypothesis, along with the relatively disappointing results of clinical trials with amyloid-reducing therapeutic agents, have, in part, lent support to a 'tau hypothesis' of AD neurodegeneration; additionally, proponents point to mutations in tau that can cause FTD with parkinsonism, a dementing illness lacking amyloid pathology, as demonstrating that tau dysregulation alone is sufficient to cause neurodegenerative disease. Some in the field have proposed a "dual pathway" model postulating that Aβ and tau pathologies are two distinct processes linked by a common upstream driver, rather than representing a linear cascade (37). What this upstream driver or the signaling pathways between amyloid and tau pathologies may be are unknown. A 'modified' amyloid cascade hypothesis such that Aβ accumulation initiates the disease process, but a secondary event (i.e. tau dysfunction) is necessary for subsequent neurodegeneration is also possible, and is supported by a number of animal studies of AD (38-41).

The pattern and chronology of plaque and tangle formation have been well studied, and their associations with clinical symptoms have been investigated in an attempt to clarify these unresolved relationships. While various findings have strengthened one hypothesized model of AD neurodegeneration or another, no model has yet been conclusively proven. For example, individuals with APP mutations eventually develop plaques and tangles, appearing to suggest that Aβ dysregulation causes or leads to tangle formation. Studies by Braak and Braak have suggested that neurofibrillary tangles, initially appearing in the limbic system and later spreading to the cortex, appear before plaques, which first appear in the frontal cortex and later spread to other regions (42, 43). However, subsequent clinicopathologic studies have strongly suggested that amyloid plaques, followed by neurofibrillary tangles, begin to accumulate

~10-15 years prior to cognitive decline, and that synaptic and neuronal loss best correlate with symptom onset (44, 45). A number of studies have shown that dementia severity better correlates with the number of neurofibrillary tangles than the amount of plaque deposition (46-50), leading some to hypothesize that neurofibrillary tangles are the key factor in the development of dementing symptoms. More recently, however, it has been suggested that neurofibrillary tangles and amyloid plaques are not the neurotoxic agents, but rather the final pathological hallmarks of the disease. Instead, oligomers of Aβ (51-53) or tau forms intermediate between normally phosphorylated protein and hyperphosphorylated fibrils are thought to represent the neurotoxic species (54). It should also be noted that AD pathophysiology does not consist solely of plaque and tangle formation, and that microglia and reactive astrocytes can be found surrounding plaques (55), implicating neuroinflammatory processes in the pathogenesis of AD as well. Whether neuroinflammation is a cause or result of AD is still a matter of debate. The interplay between amyloid, tau, and neurodegeneration is an area that clearly warrants further study, as the mechanisms of neurodegeneration in AD will have important consequences on the time course of biomarker changes that reflect these pathologies, as well as ultimately the choice of therapeutic targets.

The need for biomarkers of AD

Reports that the number of AD deaths increased by 46% from 2000-2006, and that the number of affected is projected to nearly triple by 2050 have made the ability to accurately and reliably diagnose AD in its earliest stages a public health priority (56). Currently, the diagnosis of ‘possible’ or ‘probable’ AD is based on clinical assessment using the criteria of the National Institute of Neurological and Communicative Diseases

and Stroke-Alzheimer's Disease and Related Disorders Association (NINCDS-ADRDA) and *Diagnostic and Statistical Manual of Mental Disorders*, 4th ed (*DSM-IV*-TR) (57), with definitive diagnosis only at autopsy, or rarely, by biopsy. Although the antemortem clinical diagnosis of AD is quite accurate in specialized centers, diagnostic accuracy is much lower in non-specialized settings, and, in particular, sensitivity at milder disease stages can be limited (58-63). Thus, measures to increase diagnostic sensitivity and specificity will be extremely important for improving early detection, and consequently early intervention. Biomarkers may be useful in this regard, facilitating a more accurate and earlier diagnosis, which is particularly difficult given that there are no signs or symptoms unique to AD. The Biomarkers Definitions Working Group of the National Institutes of Health defines a biomarker as "a characteristic that is objectively measured and evaluated as an indicator of normal biological processes, pathogenic processes, or pharmacologic responses to a therapeutic intervention" (64).

Importantly, biomarkers may allow for the identification of individuals with preclinical AD (those with AD neuropathology but do not yet display clinical symptoms) (44, 45, 65-67). Identifying individuals in the preclinical stage is particularly critical, as this group will likely have the greatest chance of benefit from targeted therapeutics. Biomarkers may be instrumental not only in the diagnosis of disease cases, but may aid in following disease progression and response to treatment as well. In these capacities, biomarkers will be crucial for the design and evaluation of clinical trials of disease-modifying therapies by helping to reduce sample size, reduce trial duration, and evaluate treatment efficacy. Finally, biomarkers are key in advancing our understanding of the pathophysiology of AD, which in turn has important implications for patient diagnosis and treatment.

Recognizing the potential utility of biomarkers and the significant scientific advances in the AD field over the last two decades, recent efforts have aimed at revising

the current diagnostic criteria, which, although widely used, have not been modified since their publication in 1984. This effort, led by scientific workgroups convened by the National Institute on Aging and the Alzheimer's Association, seeks to update diagnostic criteria for "Alzheimer's dementia (AD)" and "mild cognitive impairment (MCI)," and proposes a new diagnostic category of "preclinical AD." As such, the proposed guidelines for dementia diagnosis are largely unchanged (cognitive and behavioral symptoms with a progressive decline), with amendments refining "probable" and "possible" AD categories to reflect advances in our understanding of other dementing illnesses, the genetics of AD, and biomarkers. To increase the confidence of AD diagnosis, biomarkers such as CSF Aβ42, tau, p-tau, and imaging measures of brain amyloid, metabolism, and atrophy (discussed more in depth in the relevant sections below) are included in the proposed criteria; however, as there are not yet standardized practices to measure and evaluate these biomarkers, and formal cut-offs have not been identified, biomarkers will not be required for clinical diagnosis, and are mainly intended for use in research settings.

The proposal also includes revised criteria for the diagnosis of MCI, or the symptomatic pre-dementia phase of AD. This stage is analogous to a Clinical Dementia Rating (CDR) of 0.5 in the CDR scale developed at Washington University to rate cognitive and functional performance (68-70). Using informant-based clinical assessment, this scale rates individuals as cognitively normal (CDR 0), very mildly impaired (CDR 0.5), mildly demented (CDR 1), moderately demented (CDR 2), or severely demented (CDR 3) (68). The overall CDR score is based on scores in six functional domains (memory, orientation, judgment and problem solving, community affairs, home and hobbies, and personal care); these six subscores can be combined into a "sum of boxes" score. Under the newly proposed diagnostic criteria (similar to the old criteria),the clinical diagnosis of MCI is based on impairment in one or more cognitive

domains, but an absence of dementia, and a maintenance of independence of function in daily life. The domains in which the cognitive impairment can occur have been widened to include, in addition to memory, executive functioning, language, visuospatial skills, and attentional control. Additionally, as with the proposed AD criteria, biomarker measurements are also included to increase the confidence of diagnosis, although they are intended primarily for research purposes. A major focus of MCI research has been the identification of individuals who will progress to AD from those who will not, as this stage allows for an opportunity for medical intervention to perhaps prevent or postpone disease progression. Annual conversion rates from MCI to AD are approximately 15% in clinic groups, with somewhat lower rates reported for community-recruited groups (71); this difference has been attributed to an increased baseline functional impairment of clinic versus community MCI groups, as measured by the CDR sum of boxes, which most strongly associated with future progression to AD (71). As many here at Washington University use the CDR scale, it is important to note that some individuals receiving a CDR of 0.5 are insufficiently impaired to meet MCI criteria, and can be considered “pre-MCI” (70). A study of these pre-MCI individuals reported a median survival time of ~8 years, approximately twice as long as that of the CDR 0.5 individuals that met MCI criteria (~4 years, comparable to annual rates of progression of MCI to AD of ~15%) (70). These pre-MCI and MCI subjects were followed longitudinally, and 91% and 90%, respectively, of those that came to autopsy had a neuropathological diagnosis of AD. These results, along with others, strongly suggest that MCI usually represents early-stage AD, and that an even earlier stage of AD, pre-MCI, can be identified (69, 70).

Criteria for a new diagnostic category, preclinical AD, are also among the changes recommended by the working group. These preclinical criteria are intended for use only in research settings at this point, to determine the measures that will best define the preclinical stage. This ‘pre-symptomatic stage’ of AD, during which amyloid

plaques and neurofibrillary tangles being to appear, is estimated to be ~10-15 years in duration (44, 66, 72), thus providing a lengthy and crucial period for intervention with disease modifying therapies. Although AD was first described approximately 100 years ago, there are currently no treatments to prevent or delay disease onset or halt disease progression. While over 100 compounds have been tested as potential therapeutics, only five medications are Food and Drug Administration-approved for AD, all of which provide only modest symptomatic benefit of short duration (memantine, donepezil, galantamine, rivastigmine, and tacrine) (73). The largely disappointing clinical trial results are thought to be due, in part, to the focus of many trials on already symptomatic study subjects. It is likely that therapies applied earlier in the disease process (preclinically) will have the greatest opportunity for disease modification, and indeed, animal studies of AD have suggested that therapies may have limited benefit once neurodegeneration has begun. The hope is that the application of these new preclinical criteria, which rely on biomarkers for diagnosis, will facilitate characterization of the sequences of events and the biological players of preclinical AD, and allow for the development of standardized biomarkers panels or biomarker modalities to enhance our ability to identify preclinical individuals and predict clinical course. Ultimately these findings will have important consequences on drug development and the enrollment and end-point monitoring of clinical trials.

The road to biomarker discovery has not been a simple one, however. The identification of reliable biomarkers has been hindered by the fact that patient classification relies on clinical diagnosis which is not always accurate, especially at early stages of the disease. Requiring postmortem confirmation of disease diagnosis has been impractical for biomarker studies. Moreover, control groups are likely to contain individuals with preclinical AD, resulting in the observation of overlapping biomarkers values between clinical groups. Limited patient sample size and lack of adjustment for

covariates such as age, gender, ethnicity, and APOE genotype have restricted the application of results from some studies to the general population. In addition, protocols for sample collection, preparation, and analysis often vary widely between labs, thus contributing additional methodological variability. Adopting standardized protocols for clinical assessment, sample analysis, and statistical evaluation would help overcome many of these shortcomings. Because of these concerns regarding biomarker discovery, it is essential that new candidate biomarkers are validated in independent cohorts by multiple groups, a practice not uniformly applied, and even when carried out, often fails to replicate initial findings. Given the multifactorial nature of the disease, it is unlikely that a single biomarker will meet the needs for clinical diagnosis, while a panel of biomarkers may offer improved sensitivity, specificity, and positive and negative predictive values. These limitations not withstanding, many potential biomarkers have been identified, the most promising of which are discussed below. Furthermore, to appropriately evaluate a newly discovered candidate biomarker, its performance must be considered in the context of existing biomarkers, and, more broadly, the current standing of the AD biomarker field.

The State of the AD Biomarker Field: Fluid Biomarkers

APP

The postmortem pathological diagnosis of an AD brain relies on the presence of amyloid plaques and neurofibrillary tangles. These amyloid plaques are composed of Aβ, a proteolytic fragment of APP. If altered proteolytic processing of APP underlies AD, then measures of APP or its derivatives may serve as diagnostic markers. Indeed, early studies (74-76) observed increased levels of APP and/or its secreted forms in the CSF of AD individuals. However, later studies have reported decreased (77-79) or unchanged

(80) levels. Several studies of AD patients have shown reduced CSF levels of sAPPα, the soluble product released following α-secretase cleavage of APP (79, 81, 82). These inconsistent findings between studies do not currently support a consensus of CSF APP being a useful biomarker for AD.

Aβ

APP is expressed in all tissues and undergoes cleavage by β-secretase to release the ectodomain (sAPP-β) and subsequent cleavage by γ-secretase to release Aβ peptides of 38-43 amino acids (83). Because Aβ42 is the dominant component of the plaques seen in AD (84), many groups have investigated the use of Aβ42, as well as the other Aβ species, as a diagnostic tool. The amount of total Aβ in CSF is not well correlated with the diagnosis of AD (85-87). The majority of studies have demonstrated a decrease in CSF Aβ42 in AD patients (88-112); however, there have been a few reports of increased (113) or unchanged (114, 115) CSF Aβ42. These discrepancies are likely due to differing methods for assaying samples and varying sizes and selection criteria of patient groups, as well as the inclusion of subjects at different points along the disease spectrum.

A number of studies have investigated CSF Aβ42 levels in conjunction with those of CSF tau, the primary protein component of neurofibrillary tangles. In perhaps the most comprehensive analysis of Aβ42 and tau levels to date, Sunderland et al. (2003) assayed 131 AD patients and 72 controls, and performed a meta-analysis of 17 studies of CSF Aβ42 levels and 34 studies of CSF tau levels. In their own patient cohort, they observed significantly lower mean levels of CSF Aβ42 and higher mean levels of CSF tau in AD compared to controls, but with significant overlap between the clinical groups. The results of the meta-analysis mimicked their findings, with an effect size, or difference in levels between AD and controls, of 1.53 for Aβ42 and 1.31 for tau. Several interesting

correlations were observed, with tau correlating with the age of the controls but not of the AD individuals, with gender for the AD group only, and with CDR and Mini Mental State Examination (MMSE) scores, but not duration of illness. While the meta-analysis did not reveal correlations between CSF Aβ42 and any score of dementia severity, age, or duration of illness, there have been studies reporting a negative correlation between Aβ42 and dementia severity (91, 113, 116) and *APOE* ε4 dosage (91).

In addition to distinguishing AD from non-demented subjects, decreased levels of CSF Aβ42 have been shown to be predictive of future dementia in MCI patients (109, 117-124). Additionally, significantly decreased CSF Aβ42 has been observed in patients with very mild dementia (MMSE score of 25-28 or CDR 0.5) (99, 107).

In the evaluation of a candidate biomarker, it is important to consider whether the particular marker makes sense in the context of the disease pathophysiology. Mouse models of AD have shown that CSF Aβ levels are related to the amount of plaque in the brain (125), and human studies have shown that increased neocortical and hippocampal plaque burden and cerebral amyloid angiopathy is highly associated with decreased Aβ42 in postmortem CSF (126). These finding were furthered by Fagan and colleagues (107, 127) who reported an inverse relationship between CSF Aβ42 and in vivo plaque load using the amyloid imaging agent Pittsburgh Compound B (PIB) in living humans, supporting the authors' claim that plaques can function as "sinks" or "traps" of Aβ42, thus decreasing the amount of Aβ42 clearing the brain to the CSF. Other groups have likewise proposed this hypothesis (88, 116). Recent studies have shown that low CSF Aβ42 levels can identify PIB-positive individuals with excellent sensitivity and specificity (128).

One possible limitation of Aβ42 for AD diagnosis is that decreased CSF levels have also been reported in FTD (93, 96, 129), Creutzfeldt-Jakob disease (CJD) (95, 105, 110), Gerstmann-Straussler-Scheinker syndrome (105), amyotrophic lateral sclerosis

(102), multiple system atrophy (130), and dementia with Lewy bodies (DLB) (97, 105, 112). While a number of studies have shown that CSF Aβ40 is unchanged in AD (98, 106, 107, 115, 131), the ratio of Aβ42 to Aβ40, rather than either marker alone, has been shown to better distinguish AD subjects from controls or other dementias and to identify incipient AD in MCI subjects (92, 106, 122, 131). The ratios of other markers such as tau/Aβ (114), tau/Aβ42 (104, 107, 114, 132), and p-tau181/Aβ42 (107, 133) have similarly been used, and the CSF tau/Aβ42 ratio has been shown to predict future dementia in non-demented cohorts (107, 132).

While CSF is thought to more closely reflect what is happening in the brain, CSF is not as routinely obtained as blood. However, there has been little consensus among studies as to the relationship between plasma/serum Aβ and AD. Although increased plasma Aβ40 (98) and decreased plasma Aβ42 (134) have been reported in AD, most groups have reported no difference in plasma/serum Aβ levels between sporadic AD and controls (Aβ40 and Aβ42 (135-137), Aβ42 (98, 112))**.** In contrast, plasma Aβ42 has been found to be increased (137, 138) and Aβ40 decreased (137) in individuals with autosomal dominant, disease-causing mutations (FAD). Based on the findings of an early study showing that plasma Aβ42 is elevated in presymptomatic FAD mutation carriers (138), a recent study investigated the levels of Aβ42 in asymptomatic first-degree relatives of individuals with sporadic AD (139). As compared to controls, plasma Aβ42 was found to be elevated in these subjects, irrespective of *APOE* ε4 or FAD mutations. The difference between the Aβ42 levels of the sporadic AD relatives and the controls was small, however (14.2±0.6 and 12.3±0.7 pM, respectively). It will be interesting to see in longitudinal studies whether these relatives with increased plasma Aβ42 will go on to develop AD dementia.

Interestingly, several longitudinal studies have found that baseline plasma Aβ42 levels were significantly higher in those cognitively normal individuals who later

progressed to AD as compared to those who did not (140, 141). Additionally, Aβ42 levels were observed to decrease over time in these individuals, suggesting that while plasma Aβ42 does not appear to be a suitable diagnostic marker for AD, it may be a marker for progression (141). Similarly, a case-cohort study originating from the prospective Rotterdam study found that increased plasma Aβ40 at baseline was associated with an increased risk of AD as well as vascular dementia (VD) (142).

In a recent study however, any association between plasma Aβ40 or Aβ42 levels and progression from a normal to demented state was lost after adjusting for covariates such as age, cognitive status, cerebrovascular disease, *APOE* genotype, and kidney function (143). A longitudinal study of MCI patients similarly found no correlation between plasma Aβ species and progression to AD (124). This lack of association between plasma Aβ and AD is further supported by studies demonstrating that plasma Aβ40 and Aβ42 levels do not reflect brain Aβ or plaque levels (127, 144) and that there is no correlation between plasma and CSF Aβ42 or Aβ40 (112, 145).

A number of anti-amyloid clinical trials have aimed at slowing or stopping the progression of AD by decreasing the production of Aβ42, increasing its clearance, or reducing its aggregation. Based on animal findings that immunization with Aβ42 resulted in a reduction of brain amyloid plaques (146-148), a phase II clinical trial (AN1792, Elan Pharmaceuticals) was undertaken to study its effects in humans. While this trial was cut short because of an increased incidence of meningoencephalitis (6%), a six-year follow up of a subset of the patients from the earlier phase I trial revealed a positive effect on Aβ load and plaque removal, but no effect on cognitive function, clinical outcomes, or long-term survival (149). These findings would appear to cast doubt on the role of Aβ as a culprit in the cognitive decline characteristic of AD. The lack of correlation between amyloid load and dementia severity in clinicopathologic studies would also support this assertion (46, 48). It may be, however, that the immunizations were given too late in the

disease course, as the subjects already had mild to moderate dementia at the time of treatment. Studies have shown that brain accumulation of Aβ probably begins 10-20 years before clinical manifestations of the disease (150) and can be imaged with a variety of compounds that can be visualized by PET (see below), and that this accumulation may drive the further accumulation of tau aggregates within vulnerable neurons (151). If the phase I demented patients already had substantial tau aggregation, it may be that the reduction of Aβ could not reverse the tau-associated pathology and consequent cognitive impairment once the disease had progressed too far. However, this does not mean that Aβ is not promising as a candidate biomarker of AD. A repertoire of biomarkers that can serve as surrogates of underlying disease pathology would be crucial to our diagnosing of AD and following its progression and response to treatment. While it has been shown that CSF Aβ42 reflects the presence of brain amyloid, the results from the Aβ42 immunization trial suggests that tau is likely a better marker to follow for clinical disease progression and clinical outcomes. However, since Aβ load in the brain does not correlate with dementia severity (46, 48), and some degree of tangle pathology can exist in older individuals in the absence of dementia (152-154), accurate diagnosis and prognosis of AD will most likely require a combination of these pathology-related biomarkers.

Tau and p-tau

The other pathognomic feature of AD brains, neurofibrillary tangles, is composed primarily of tau, a microtubule-associated protein which has similarly been extensively investigated as a biomarker. Many studies have demonstrated that CSF tau is increased in AD patients (88, 91, 92, 96, 97, 100-102, 107, 114, 131, 155-181).

In AD, tau undergoes abnormal hyperphosphorylation at many sites, and enzyme linked immunosorbent assays (ELISAs) have been developed to recognize various

phosphorylated epitopes such as threonine 181 and 231 and serine 199, 235, 396, and 404 (119). As a result of this aberrant phosphorylation, tau is likely unable to bind and stabilize microtubules, possibly leading to axon degeneration (34). Thus, one possibility is that the increase in tau seen in AD CSF is due to the release of tau from degenerating neurons and its subsequent diffusion into the CSF (34). With the disturbance of the tau-microtubule binding equilibrium, there is a resulting increase in the cytosolic unbound levels of tau as well, and consequently an increased likelihood of protein misfolding and subsequent aggregation as neuropil threads in dystrophic neurites and as neurofibrillary tangles (182). While these observations suggest possible reasons for the increases in CSF tau level in AD, it is still unclear what is really happening in the human disease process.

Given that increased levels of CSF tau can be seen in other neurodegenerative disorders, in particular FTD, stroke, corticobasal degeneration, and CJD (179), studies have begun looking specifically at phosphorylated forms of tau as diagnostic markers for AD. Hampel et al., (2004) compared the accuracy of CSF p-tau231, p-tau181, and p-tau199 in discriminating AD from FTD, LBD, VD, and normal controls. They found that all three proteins were significantly increased in AD as compared to the other groups; however, the discriminative power of each differed, with p-tau231 providing for the greatest discrimination between AD and non-AD, AD and controls, and AD and FTD (183). The combined use of the three p-tau markers did not provide further discrimination. Several studies have similarly shown that p-tau231 and p-tau199 can discriminate AD from other neurological disorders with sensitivities and specificities in the 80%-90% range (179, 184, 185).

While Aβ42 and tau are specific markers of AD pathogenesis, a recent study has investigated the utility of a marker of neuronal death in the diagnosis of AD (186). Visinin-like protein 1 (VLP-1), a cytoplasmic calcium sensor protein that is thought to

leak from damaged or dying neurons, was found to be significantly increased in the CSF of AD subjects compared to controls (186). Although VLP-1 is not specific to AD and indeed was originally studied in ischemic stroke subjects (187), the combined use of Aβ42, tau, p-tau, and VLP-1 resulted in increased diagnostic accuracy over any marker individually. Several studies have shown little correlation between amyloid plaque load and dementia severity (46, 48), thus VLP-1, in representing the end-result of the disease process, may provide a better reflection of the degree of dementia. In this preliminary study, only VLP-1 and none of the other markers were found to correlate with MMSE (186). Clearly additional study of this molecule as a potential biomarker of cell death in AD is warranted.

Isoprostanes

Growing evidence suggests that oxidative damage may be important in the pathogenesis of AD. Isoprostanes, the end-products of lipid peroxidation, and in particular F2-isoprostanes, have been found to be increased in the frontal and temporal cortex of AD compared to control and FTD brains, suggesting a specificity for AD (188, 189). Studies have shown F2-isoprostanes to be increased in postmortem ventricular CSF obtained from autopsy-verified AD cases (188, 190, 191), as well as in antemortem CSF from individuals diagnosed with AD dementia (192-196). CSF F2-isoprostanes have been shown to correlate with brain weight, degree of cortical atrophy, and Braak stage (191), as well as with dementia severity (193). Several longitudinal studies have shown that over one and two year periods, CSF F2-isoprostanes increase in MCI and AD patients (197, 198), and that baseline measurements could distinguish individuals that progress to MCI or AD from stable patients with 100% accuracy (199). Moreover, the addition of isoprostane measurements to conventional memory testing or to quantitative MRI measurements resulted in increased diagnostic and prognostic power

(199), although confirmation awaits investigation in a larger number of subjects. Preclinical FAD mutation carriers have been shown to have increased CSF F2-isoprostanes as well, indicating this marker may be suitable for both sporadic and familial AD (200). Using a combined analysis of CSF Aβ42, tau, and F2-isoprostanes, Montine et al., (2001) were able to diagnose AD with a sensitivity of 84% and specificity of 89%, while Grossman et al., (2005) were able to classify 88.5% of patients in accordance with their clinical or autopsy diagnosis using this same panel of markers (194, 196).

Results have been less consistent in regard to peripheral F2-isoprostanes, with reports of increased (193, 195) or unchanged (201-203) plasma levels in AD subjects. Similarly, urinary F2-isoprostanes have been reported to be increased (193, 195, 204) or unchanged (203, 205). The discrepancies concerning peripheral F2-isoprostanes may be due to differences in patient selection criteria between studies, as smoking and other conditions associated with oxidative stress, such as cardiovascular disease and diabetes, can significantly alter isoprostane levels (206).

Inflammatory markers

In addition to the classical pathological features of amyloid plaques and neurofibrillary tangles, AD brains display characteristics of inflammatory processes (207). One well investigated potential inflammatory marker of AD is α_1-antichymotrypsin (ACT), a serine protease inhibitor that is a colocalized with Aβ in senile/neuritic plaques (208-210). Early studies of ACT yielded inconsistent results, however, with reports of increased ACT in AD serum (211-214) or CSF (211, 215), along with reports of unchanged ACT in AD serum (216-218) or CSF (216-218). Four recent studies, however, have attempted to put this controversy to rest by measuring ACT levels in large groups of subjects or by including additional controls. In a study of 196 subjects,

Licastro et al., (2000) observed increased plasma ACT in AD, and found that levels inversely correlated with cognitive performance (219). DeKosky et al., (2003) carried out a large study of 516 individuals, with AD subjects stratified by dementia severity, and similarly found that plasma and CSF ACT were increased, and that levels were negatively correlated with dementia severity. This study excluded those with systemic inflammatory diseases or those taking anti-inflammatory medications in an attempt to achieve as homogeneous a study population as possible. Additionally, plasma ACT was significantly increased in women compared to men, perhaps further explaining why previous studies which did not control for gender yielded inconsistent results (220). In a 700+ subject case-cohort study within the Rotterdam Study, Engelhart et al., (2004) found that increased plasma ACT was associated with increased risk of dementia, AD, and VD (221). A proteomics approach, using gel electrophoresis and mass spectrometry, identified CSF ACT as being increased in AD versus control subjects, and findings were confirmed by ELISA validation in an independent sample set (222). CSF ACT has also been found to be elevated in DLB, suggesting that it may be ineffective in distinguishing between these types of dementia (223).

The results of cytokine studies in AD have been highly inconsistent between groups. For example, in AD patients, CSF interleukin-6 (IL-6) has been found to be increased (224-227), decreased (228), or unchanged (218, 229-233). Plasma/serum IL-6 results have similarly been mixed (218, 219, 233-236). Additionally, whereas one report was able to discriminate VD from AD by CSF IL-6 levels (237), another found no difference in levels between VD and AD (225). These inconsistencies have been mimicked in studies of IL-6 receptor, Gp130, IL-1β, TNF-α, and Hp 2-1 (238). Moreover, most studies have either found no concentration differences or have yielded inconsistent results for additional cytokines such as IL-4, IL-8, IL-10, interferon-gamma, complement C1q, and TGF-β (206). These discrepancies between studies are likely due to several

significant obstacles to the evaluation of cytokines in AD. Cytokine concentration can vary considerably over time, and can be influenced by an individual's genetic background, comorbid systemic inflammatory processes, usage of anti-inflammatory drugs, and exposure to environmental factors (206). Moreover, many studies use subjects with neurological diseases other than AD, such as Parkinson's disease (PD) or amyotrophic lateral sclerosis, as "controls."

Proteomics

A newer field of biomarker studies is moving away from the traditional approach of investigating levels of a single, or several, candidate biomarkers that have been implicated in the pathogenesis of AD, and is instead focusing on nonbiased profiling of human fluids in an attempt to discover novel biomarkers. As a result of improved mass spectrometry (MS) techniques, proteomics has emerged as a powerful tool for biomarker discovery. General methods in proteomic studies typically include protein separation by two-dimensional gel electrophoresis (2-DE), liquid chromatography (LC), or protein-chip arrays, followed by MS or tandem MS and database searches to determine protein identity. Recent efforts to characterize the human CSF proteome have identified 2,594 proteins (239) and 563 peptide forms and 798 proteins (240) using a combination of approaches. By comparing the differences in protein expression levels between AD and control CSF samples, a number of studies have identified potential diagnostic markers (222, 241-246). Additional studies have carried out similar analyses in samples with postmortem neuropathological confirmation of AD (247, 248), with one study analyzing both antemortem and postmortem CSF from the same individuals (249).

An important concern of proteomics-based discovery, however, is that often candidate markers identified by a study are not confirmed in independent studies or by other more quantitative methods, indicating the present need for large validation studies

and corroboration by alternative techniques. While some candidates have been identified in multiple studies, and furthermore have been implicated in AD pathogenesis, they unfortunately have not been consistently reported as increased or decreased in AD CSF. For example, β2-microglobulin, the constant component of the class I major histocompatibility complex, has been identified as increased (241, 243, 245, 250, 251) and decreased (242) in AD CSF. Although the function of this protein is still unclear, it has been shown to accumulate as amyloid fibrils in dialysis patients (252, 253). Similarly, transthyretin has been reported to be increased (241, 245) and decreased (242, 248) in AD CSF. Transthyretin is thought to play a role in AD pathogenesis, as it can form complexes with Aβ40 and Aβ42, thus preventing Aβ aggregation (254-256) and has been shown to negatively correlate with senile plaque abundance (257). Such inconsistencies in proteomics studies, and more broadly in biomarker studies in general, may be due in part to post-translational modifications, such as limited proteolysis *in vivo*, which are often overlooked.

Many studies have formulated panels of proteins for the discrimination of AD from normal cohorts. For example, using 2-DE and tandem MS, Finehout et al., (2006) formulated a panel of 23 protein spots that differentiated AD from non-AD with a sensitivity and specificity of 94% and a predictive error rate of 5.9%; the application of this same panel to a validation cohort yielded only slightly lower values (258). Moreover, panels derived from proteomic studies have been shown to differentiate AD, PD, and DBL with high accuracy (246) and to distinguish MCI individuals who progress to AD from those who do not (250). Interestingly, the fragment signature of four CSF Aβ species (Aβ1-16, Aβ1-33, Aβ1-39, and Aβ1-42) as analyzed by Matrix-Assisted Laser Desorption/Ionization Time-of-Flight MS (MALDI-TOF-MS) has been shown to discriminate AD with a sensitivity of 89%, specificity of 83%, and accuracy of 86% (259). Finally, the few proteomic studies of serum (260, 261) and of plasma (262, 263) have

similarly yielded markers to distinguish AD from controls, as well as to predict progression from MCI to AD (263), although verification in independent cohorts is needed.

Imaging Biomarkers

Neuroimaging techniques have increasingly been used to detect brain changes associated with AD, and thus have potential as markers of disease progression, monitors of therapeutic effects, and predictors of future dementia prior to symptoms. Because the work in this thesis is focused on the search for novel fluid biomarkers of AD, only a cursory overview of imaging biomarkers will be provided. In brief, in MCI and AD subjects, computed tomography (CT) (264, 265) and magnetic resonance imaging (MRI) (266-274) have been used to examine atrophy and rates of atrophy of various brain regions, functional MRI (fMRI) has been used to examine abnormalities in brain activation (275-285), and single photon emission computed tomography (SPECT) (264, 286-298) and arterial spin-labeling perfusion MR imaging (ASL-MRI) (299-301) have been used to study cerebral perfusion defects. Additionally, positron emission tomography (PET) has been employed in a number of AD studies to examine regional cerebral metabolism using ^{18}F-2-deoxy-2-fluoro-D-glucose (CMRglc using FDG-PET) (302-310).

While currently definitive diagnosis of AD relies on the presence of amyloid plaques and neurofibrillary tangles at autopsy, recent studies have aimed at developing compounds for the *in vivo* imaging of AD pathology. These imaging markers would allow for earlier diagnosis, as AD pathology precedes the onset of dementia symptoms by many years, and for the monitoring of disease progression and treatment efficacy. Promising results have been reported using PET and SPECT ligands for microglial

activation ([^{11}C](R)-PK11195 (311, 312) and [^{18}F] FE-DAA1106 (313, 314)). Over the last decade there has been intense interest in PET ligands for brain amyloid, with a proliferation of new tracers in development or clinical trials, such as ^{11}C-SB-13 (315) and ^{11}C-BF-227 (316). The most widely studied amyloid imaging agent, and the one used in our studies, is ^{11}C-labelled Pittsburgh compound B, or PIB, (2-[4'-(methylamino)phenyl]-6-hydrobenzothiazole) (317). In AD, PIB retention is increased in the frontal, parietal, temporal, and occipital cortices and striatum, and studies have consistently shown that nearly all patients diagnosed with Alzheimer's dementia test PIB-positive (318-321). Additionally, the difference in ligand binding in AD versus controls is significantly more robust with PIB than with another commonly used amyloid agent, FDDNP (318, 322-324). PIB binding correlates well with rates of cerebral atrophy in AD (325) and with reductions in CSF Aβ42 (107, 127, 326). PIB retention is also inversely correlated with cerebral glucose metabolism as determined by FDG-PET (318), and is strongly related to the degree of memory impairment in MCI and AD (321, 326, 327). Interestingly, a longitudinal study of early AD patients taking cholinesterase inhibitors and/or the NMDA antagonist memantine, found that PIB retention did not change over a two-year follow-up, although cortical rCMRGlc decreased (327). This suggests that amyloid burden reaches a maximum early in the course of the disease, and indeed, several studies have found that certain MCI individuals have PIB uptake in the AD range (320, 321, 328, 329). Importantly, studies have also shown PIB uptake in a proportion of non-demented elderly controls (127, 320, 321, 329-332), consistent with the known presence of AD pathology in a subset of cognitively normal elders as reported in clinicopathological studies (66, 150). These subjects presumably have preclinical AD, but longitudinal studies are needed to test this hypothesis before we can conclude that brain amyloid has adequate sensitivity and specificity to be considered a viable biomarker of AD. PIB retention is not observed in frontotemporal lobar degeneration (FTLD) (319), or more

specifically in its two syndromes FTD (320) and semantic dementia (333). PIB imaging has also been shown to detect cerebral amyloid angiopathy (334, 335).

Although as of 2008 PIB had been used in over 40 centers and 3000 individuals world-wide (336), the 20 minute half-life of ^{11}C has restricted its use to centers with an on-site or near-by cyclotron. For this reason, recent efforts have focused on the development of tracers labeled with ^{18}F, which has a half-life of 110 minutes, facilitating wider use in research and clinical centers. The first ^{18}F labeled tracer, [^{18}F]FDDNP (324, 337-339), has quickly been followed up by the development at least nine other agents, including ^{18}F-BAY94-9172 (340), ^{18}F-GE-067 (341), ^{18}F-3'-F-PIB (342), and, the particularly promising ^{18}F-AV-45. Currently in FDA phase III clinical trials, ^{18}F-AV-45 has shown favorable brain uptake and amyloid imaging properties (343-345). As detailed above, the great wealth of information on imaging with ^{11}C-PIB suggest that it may be suitable for confirming the diagnosis of AD in symptomatic cases as well as for identifying individuals in the pre-symptomatic (preclinical) stage of the disease. It is likely, however, that in the future, more than one amyloid imaging agent will be commonly used, and the goal of the many ^{18}F studies currently underway is to find a tracer with diagnostic potential similar to that of PIB. No imaging agent selective for tau aggregates has yet been developed, and such a discovery would be a major contribution to the field.

Conclusions

The urgent need for biomarkers is reflected by the growing number of studies aimed at investigating biomarker candidates for AD. Additionally, the biomarker field has experienced a renewed level of enthusiasm due to better reagent availability and novel methods for the assessment of a variety of fluid and imaging measures. Apart from brain

biopsy or brain catheterization, the collection of CSF and blood is the most direct and convenient approach to studying the biochemical changes that occur in the brain. Thus, these fluids, and in particular CSF because of its direct contact with the extracellular space of the brain, have been considered attractive sources for potential AD biomarkers. Indeed, the biomarkers showing the greatest promise to date for use in AD diagnosis and prognosis are CSF Aβ42, tau, and p-tau. CSF Aβ42 and tau have proved particularly promising as potential predictors of cognitive decline in individuals with very mild cognitive impairment, as well as future dementia in non-demented cohorts. Further, low levels of CSF Aβ42 are an excellent marker for the presence of neocortical amyloid deposition, in the presence or absence of dementia. Whether brain amyloid invariably leads to subsequent dementia in AD is currently being studied. Even for these promising biomarkers, however, there is substantial overlap in levels between AD and control groups, and specificity against other dementing conditions is not perfect. Consequently, there remains a need for supplemental biomarkers to improve diagnostic accuracy. More rigorous investigation of fluid markers of inflammation, oxidative damage, and neuronal death is clearly warranted. Plasma and serum analytes have been notoriously difficult to interrogate, with most studies yielding inconsistent results. Improved techniques have lead to the emergence of the field of proteomics as a powerful tool for biomarker discovery; however, an important concern of proteomics-based discovery is that candidate markers are often not confirmed in independent cohorts or by other quantitative methods, indicating the present need for large validation studies and corroboration by alternative techniques. Additionally, most proteomics studies, and the majority of biomarker studies in general, have compared AD subjects to non-demented controls (or controls with other neurological conditions), thus identifying biomarkers with diagnostic potential, but not necessarily prognostic potential. Moreover, of the studies aimed at discovering prognostic biomarkers, most have focused on the search for

markers predictive of progression from MCI to AD. Increased efforts should be placed on identifying markers predictive of the progression from cognitive normalcy or preclinical stages to AD, as emerging therapies will best preserve cognitive function if at-risk individuals are identified in these earlier stages. These studies will require large, well-characterized, longitudinally followed cohorts of study participants, which are not readily available for evaluation at most institutions. The development of imaging agents for the detection of AD pathologies (amyloid, tangles, activated microglia) has propelled the imaging field forward, with PIB-PET imaging emerging as a particularly promising modality. Given the multifactorial nature of the disease, it is unlikely that a single biomarker will meet the needs for clinical diagnosis, while a panel of biomarkers and multiple biomarker modalities, especially combinations of fluid and imaging measures, may offer improved sensitivity, specificity, and positive and negative predictive values. Biomarkers may be useful in the more immediate future in clinical trial design and enrollment, allowing for the enrichment of study populations for characteristics of interest, thereby helping to reduce sample size, trial duration, and ultimately cost. Finally, newly identified candidate biomarkers, regardless of whether they outperform existing biomarkers, may advance our understanding of the pathophysiology of the disease, which in turn may inform new therapeutic targets.

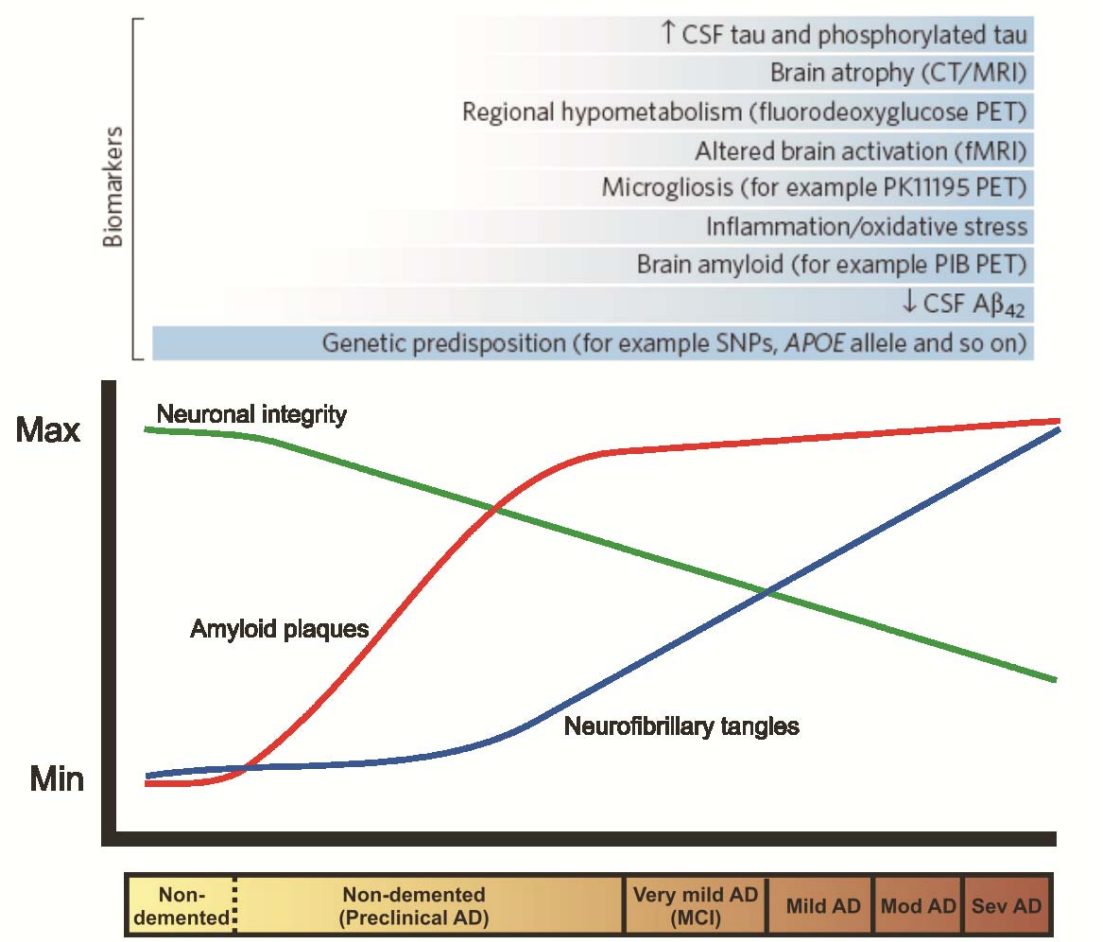

Figure 1.1. Hypothesized relationship between the time course of changes in various biomarkers in relation to the neuropathology and clinical changes of Alzheimer's disease. The stages of AD (bar) are associated with the formation of amyloid plaques (red line), the accumulation of neurofibrillary tangles (blue line), and synaptic and neuronal loss (green line). The most promising biomarker candidates are listed (in chronological order from bottom to top) according to the earliest stage of the pathological process they appear to demonstrate utility. For example, genetic variations (SNPs) may be considered biomarkers that allow the earliest possible estimation of risk, and decreased CSF Aβ42 levels may provide the earliest evidence of AD pathology in the brain.

Abbreviations: CSF, cerebrospinal fluid; CT, computed tomography; MRI, magnetic resonance imaging; PET, positron-emission tomography; fMRI, functional magnetic resonance imaging; PIB, Pittsburgh compound B; SNPs, single nucleotide polymorphisms; AD, Alzheimer's disease; MCI, mild cognitive impairment.

Table 1.1. Select candidate fluid and imaging biomarkers of AD

Fluid	Biomarker	Observations	References
CSF	Aβ42	1. Decreased in AD 2. Decreased in subjects with brain amyloid deposition 3. Predictive of conversion from MCI to AD	1. (88-112, 346) 2. (107, 127) 3. (109, 117, 118, 120-124)
Plasma and/or serum	Aβ42	1. Mostly no difference in AD 2. Mixed results for prediction of conversion from normal or MCI to AD 3. Increased in FAD	1. (98, 107, 112, 134-137) 2. (124, 139-141, 143) 3. (137, 138)
CSF	Aβ40	No difference in AD	(90, 98, 106, 107)
Plasma and/or serum	Aβ40	1. Mostly no difference in AD 2. Mixed results for prediction of conversion from normal or MCI to AD 3. Decreased in FAD	1. (98, 107, 135-137) 2. (124, 142, 143) 3. (137)
CSF	Ratio of Aβ species (Aβ40 and Aβ42)	1. Discriminates AD from normals 2. Predictive of conversion from MCI to AD	1. (92, 106, 107, 131) 2. (122)
CSF	Tau	Increased in AD	(88, 91, 92, 96, 97, 100-102, 107, 110, 114, 131, 155-181, 346)
CSF	p-tau231, p-tau181, and p-tau199	1. Increased in AD 2. p-tau231 predicts conversion from MCI to AD	1. (107, 179, 183, 184, 347) 2. (185)
CSF	Ratio of tau species to Aβ42	1. Increased in AD 2. Predictive of conversion from normal to MCI or AD 3. Predictive of conversion from MCI to AD	1. (104, 107, 114, 133) 2. (107, 132) 3. (348)
CSF	Isoprostanes	1. Increased in postmortem and antemortem AD CSF 2. Predictive of conversion from normal to MCI or AD	1. (188, 190-196) 2. (199) 3. (200)

		3. Increased in preclinical FAD mutation carriers	
Plasma	Isoprostanes	Results mixed, showing increase or no change in AD	(193, 195, 201-203)
Urine	Isoprostanes	Results mixed, showing increase or no change in AD	(193, 195, 203-205)
CSF	α_1-antichymotrypsin	Results mixed, showing increase or no change in AD	(211, 215-217, 218 , 222, 349)
Plasma and/or serum	α_1-antichymotrypsin	1. Results mixed, showing increase or no change in AD 2. Predictive of AD risk	1. (211-214, 216-219, 349) 2. (221)
CSF	Interleukin-6	Results mixed	(218, 224-233)
Plasma	Interleukin-6	Results mixed, showing increase or no change in AD	(218, 219, 233-236)
CSF and plasma	Various markers of inflammation	Results mixed	For reviews see (206, 238)
Imaging Modality		**Observations**	**References**
CT and MRI		1. Regional atrophy in AD 2. Whole brain atrophy in AD 3. Predictive of conversion from MCI to AD 4. Predictive of conversion from normal to MCI	1. (264, 265, 350) 2. (269, 270) 3. (266-268) 4. (351)
fMRI		1. Altered activation in AD 2. Altered activation in MCI	1. (275-278, 283, 352) 2. (276, 277, 279-284)
FDG-PET		1. Regional hypometabolism in AD 2. Predictive of conversion from MCI to AD	1. (302-305) 2. (306-310)
$H_2{}^{15}O$-PET		Altered activation in AD	(353-356)
SPECT		1. Altered regional cerebral perfusion in AD 2. Predictive of conversion from MCI to AD	1. (264, 286-291) 2. (292-297)
ASL-MRI and contrast-based MRI		Regional hypoperfusion in AD	(288, 299-301, 357, 358)
FDDNP-PET		Increased retention in AD and MCI	(324, 337, 339)

	brain	
PIB-PET	1. Increased retention in AD brain 2. Increased retention in a subset of cognitively normal controls 3. Detects cerebral amyloid angiopathy	1.(318-321) 2. (127, 320, 321, 329-332) 3. (334, 335)
Other PET amyloid imaging agents: ^{11}C-SB-13, ^{11}C-BF-227, ^{18}F-BAY94-9172, ^{18}F-GE-067, ^{18}F-3'-F-PIB, ^{18}F-AV-45	Increased retention in AD brain	(315, 316, 340-345)
PET markers of microglial activation: [^{11}C](R)-PK11195 and [^{123}I]iodo-PK11195	Increased retention in AD and MCI brain	(311, 312)

AD, indicates clinical diagnosis of dementia believed to be Alzheimer's disease, not necessarily autopsy confirmed AD cases.
FAD, Familial Alzheimer's disease
MCI, mild cognitive impairment

Chapter 2.

Identification and Validation of Novel Cerebrospinal Fluid Biomarkers for Staging Early Alzheimer's Disease Using Proteomics and ELISA

Summary

Background: Ideally, disease modifying therapies for Alzheimer disease (AD) will be applied during the 'preclinical' stage (amyloid plaques and other pathology present with cognition intact) before severe neuronal damage occurs, or at the first signs of cognitive impairment. Developing and judiciously administering such therapies will require biomarker panels that can identify early AD pathology, classify disease stage, monitor pathological progression, and predict cognitive decline. To discover biomarkers that may be useful in this regard, we measured AD-associated changes in the cerebrospinal fluid (CSF) proteome.

Methods and Findings: Because low CSF Aβ42 has previously been shown to correlate with amyloid deposition, we selected N=24 CSF samples from cognitively normal controls (Clinical Dementia Rating [CDR] 0) with high Aβ42 concentrations and N=24 from mild "probable AD" (CDR 1) individuals with low Aβ42. Samples were subjected to two-dimensional difference-in-gel electrophoresis (2D-DIGE). Gel features (protein spots) with intensity differences between groups were excised, trypsinized, and subjected to liquid chromatography tandem mass spectrometry (LC-MS/MS) for protein identification. Within 119 gel features that differed in intensity between groups, 47 proteins were identified. Eleven candidate biomarker proteins were re-evaluated by enzyme-linked immunosorbent assays (ELISA) in the original sample set. Six of these candidates (NrCAM, YKL-40, chromogranin A, carnosinase I, transthyretin, cystatin C) showed differences in mean concentration between the original AD (CDR 1) and control (CDR 0) groups, and were subsequently evaluated in a larger independent sample set (N=292) that included CDR 0, CDR 0.5 (very mild dementia), and CDR 1 groups. CSF Aβ42, tau and phospho-tau (p-tau181) concentrations were also measured. In this larger

independent sample set, CDR 0 and CDR>0 groups showed significant differences in mean concentrations of YKL-40, carnosinase I, tau, p-tau181 and Aβ42; CDR 1 and CDR <1 groups showed differences in carnosinase I, chromogranin A, NrCAM, tau, p-tau181 and Aβ42. Receiver-operating characteristic curve analyses using a stepwise logistic regression model yielded optimal biomarker panels to distinguish CDR 0 from CDR>0 (tau, YKL-40, NrCAM) and CDR 1 from CDR<1 (tau, chromogranin A, carnosinase I) with areas under the curve of 0.90 (0.85 - 0.94 95% confidence interval [CI]) and 0.88 (0.81 – 0.94 CI), respectively.

Conclusions: This study identifies 47 candidate CSF protein biomarkers for mild AD, and, in an independent cohort, demonstrates that four of these biomarkers (NrCAM, YKL-40, chromogranin A, carnosinase I), can improve upon the ability of CSF Aβ42 and tau to define three clinical categories: cognitive normalcy (CDR 0), very mild dementia (CDR 0.5), and mild dementia (CDR 1). Building upon findings from previous studies of Aβ42 and tau (107, 121, 132), this panel of six CSF biomarkers might aid subject categorization into six early clinicopathological stages (cognitively normal without amyloid, cognitively normal with amyloid ['preclinical AD'], cognitively normal at increased risk for dementia ['at risk'], very mild symptomatic AD, very mild symptomatic AD at increased risk of short-term progression, and mild symptomatic AD). Use of such a biomarker panel to guide subject enrollment might increase the efficiency of clinical trials. Future study of these candidate CSF biomarkers will be required to evaluate their potential for monitoring disease progression and for distinguishing AD from other common causes of dementia.

Introduction

Clinicopathological studies suggest that Alzheimer's disease (AD) pathology (amyloid plaque formation, followed by gliosis and neurofibrillary tangle formation) begins 10-15 years before the onset of very mild dementia (43, 44). This period of 'preclinical AD' could provide an opportunity for disease modifying therapies to prevent or forestall the synaptic and neuronal losses associated with cognitive impairment (65, 67, 359). However, before such interventions can be developed and judiciously administered, accurate tools must be in place to diagnose and monitor the pathophysiological condition of individuals with preclinical AD and very early stage AD dementia. Clinical examination cannot detect preclinical disease or measure cellular and molecular changes within the brain, and has limited accuracy when diagnosing the very earliest symptomatic stages of AD. Therefore, there is an urgent need to identify biomarkers that can do so. Because its composition is rapidly and directly influenced by the brain, the cerebrospinal fluid (CSF) proteome represents an appealing source for such biomarkers.

Indeed, a few CSF proteins have already shown promise as diagnostic biomarkers for clinical AD (Dementia of the Alzheimer Type [DAT]) and even preclinical AD. Lower mean levels of CSF Aβ42 and higher mean levels of tau and phosphorylated tau can distinguish groups with DAT from cognitively normal controls (88, 346). Unfortunately, value ranges for each biomarker show substantial overlap between groups.

Recently, using PET imaging with Pittsburgh Compound B (PIB) to measure brain amyloid in vivo, it has been demonstrated that low CSF Aβ42 can serve as an indicator of amyloid deposition (107, 127), and that CSF tau levels correlate positively with in vivo brain amyloid load (128, 360). Importantly, both of these associations are

independent of clinical diagnosis (107, 128), though CSF tau does correlate with more sensitive measures of cognition (360). These findings suggest that the overlap of biomarker values between clinical groups may, in part, reflect "contamination" of control groups by cognitively normal individuals with amyloid plaques and early neurodegeneration (preclinical AD), low CSF Aβ42 and elevated CSF tau. Supporting this notion, elevated ratios of tau/Aβ42 and p-tau181/Aβ42 (consistent with the presence of amyloid plaques and neurodegeneration) have been associated with increased risk of converting from cognitive normalcy to dementia (107, 132). Together, these findings suggest that CSF biomarkers can describe neuropathological state and trajectory. They also suggest that a pathological staging system based on biomarkers might be a favorable alternative or adjunct to clinical staging for guiding treatment decisions or designing clinical trials.

Beyond amyloid plaque formation, other features of AD pathophysiology might also be exploited as therapeutic targets, sources of diagnostic biomarkers, or measures of disease progression. In addition to Aβ42 and tau, many other candidate AD biomarkers have been identified by either targeted or unbiased proteomics screens (241-243, 245, 246, 250, 263, 361-365). Only a few of these studies have tested large, well-characterized cohorts, however. Even fewer have evaluated biomarkers for their ability to distinguish the very early stages of AD pathophysiology. Thus, there remains a critical need for validated AD biomarkers that can properly categorize individuals by early pathological stage; such markers may have potential for monitoring neuropathological decline and, thereby, for evaluating response to disease-modifying therapies.

The goal of this study, therefore, is to identify such CSF protein biomarkers for AD using the unbiased proteomic technique of two-dimensional difference-in-gel electrophoresis (2D-DIGE) coupled with liquid chromatography and tandem mass

spectrometry (LC-MS/MS), and to evaluate them further in a larger independent cohort using quantitative enzyme-linked immunosorbent assays (ELISA). Our findings suggest that a small ensemble of novel biomarkers may be able to distinguish several stages of cognitive decline in early AD, and improve the ability of current leading biomarkers tau and Aβ42 to discriminate early symptomatic AD from cognitive normalcy.

Methods

Subject selection - Discovery cohort

Subjects (N=48), community-dwelling volunteers from University of Washington (N=18), Oregon Health and Science University (N=11), University of Pennsylvania (N=11), and University of California San Diego (N=8), were 51-87 years of age and in good general health, having no other neurological, psychiatric, or major medical diagnoses that could contribute to dementia, nor use of exclusionary medications (e.g. anticoagulants) within 1-3 months of lumbar puncture (LP). Cognitive status was evaluated based on criteria from the National Institute of Neurological and Communicative Diseases and Stroke-Alzheimer's Disease and Related Disorders Association (57). In the morning after overnight fasting, CSF was collected in polypropylene tubes by LP and immediately frozen at -80°C. Subjects who were cognitively normal (CDR 0, N=24) or had mild "probable AD" (CDR 1, N=24), were selected from a larger group of 120 samples on the basis of CSF Aβ42 (relatively high and low values, respectively), and, when possible, CSF tau (relatively low and high values, respectively) to increase the likelihood of CDR 1 subjects having and CDR 0 subjects not having AD pathology. CSF Aβ42 and tau levels for the discovery cohort were all measured in a single laboratory using well-established ELISA assays (366).

Although quantitative thresholds were not defined prior to sample selection, the lowest CDR 0 value and the highest CDR 1 value for CSF Aβ42 in this discovery cohort were 609 and 361 pg/mL, respectively; ranges for CSF tau were 141-461 pg/mL for CDR 0 and 215-1965 pg/mL for CDR 1.

Subject selection - Validation cohort

Subjects (N=292), community-dwelling volunteers enrolled at the Knight Alzheimer Disease Research Center at Washington University (WU-ADRC), were ≥60 years of age and met the same exclusion criteria as the discovery cohort. Cognitive status was determined as with the discovery cohort. Subjects who were cognitively normal (CDR 0, N=198), very mildly demented (CDR 0.5, N=65) or mildly demented (CDR 1, N=29) at the time of LP were selected without regard to previously measured biomarkers. Some CDR 0.5 subjects met criteria for mild cognitive impairment (MCI) and some were more mildly impaired, or "pre-MCI" (70). All CDR 1 individuals had received a diagnosis of DAT (demographic characteristics in Table 2.1). Apolipoprotein E (*APOE*) genotypes were determined by the WU-ADRC Genetics Core. Fasted CSF was collected, gently mixed, centrifuged, and frozen at -80°C in polypropylene tubes (107).

Multi-affinity immunodepletion of CSF

A pooled CSF sample, containing an equivalent volume from every 'discovery' cohort sample, was prepared as an internal standard for 2D-DIGE to facilitate the matching of gel features, and to allow for normalization of the intensity of each gel feature among different gels. To enrich for proteins of low-abundance prior to 2D-DIGE, each CSF sample was depleted of six highly-abundant proteins (albumin, IgG, IgA, haptoglobin, transferrin, and α-1-antitrypsin) by immunoaffinity chromatography (Agilent Technologies, Palo Alto, CA) according to the manufacturer's instructions and as

described previously (251). Depleted samples were then concentrated using 10 kDa exclusion filters to retain larger molecules. As a 'benchmark' of immunodepletion column performance, an aliquot of reference CSF was depleted after every group of seven experimental chromatographic depletions. Non-depleted reference CSF, depleted CSF and the proteins that were retained by the column were analyzed by 2D-DIGE as previously described (222, 251); gel images obtained from all reference CSF depletion analyses were similar (data not shown).

2D-DIGE

2D-DIGE was performed as described previously (222, 251). Briefly, CDR 0 and CDR 1 samples were randomly paired. Fifty-micrograms of protein from each paired sample and from an aliquot of the pooled CSF sample were labeled with one of three N-hydroxysuccinimide cyanine dyes (Cy2, Cy3, or Cy5). The labeled proteins and 100 micrograms of unlabeled protein from each sample were mixed and equilibrated with an immobilized pH gradient strip for isoelectric focusing (first dimension), after which the strip was treated with reducing and alkylating solutions prior to SDS-PAGE (second dimension). Cy2, Cy3 and Cy5-labeled images were acquired on a Typhoon 9400 scanner (GE Healthcare) at excitation/emission wavelengths of 488/520, 532/580, and 633/670 nm, respectively.

Gel image and statistical analysis

The comparative two-dimensional gel analysis was performed using an established experimental design (367) in which the high variation between gels is minimized by including a common, labeled pooled sample in all gels. Intra-gel feature detection and quantification, and inter-gel matching and quantification were performed using the Differential In-Gel Analysis (DIA) and Biological Variation Analysis (BVA)

modules of DeCyder software v 6.5 (GE Healthcare), respectively, as described previously (251). This process (DIA analysis) resulted in approximately 5,000 gel features per gel image. In five gels, one sample contained significant amounts of hemoglobin indicating possible blood contamination. Therefore, all images from gels with these hemoglobin-containing samples were removed from further analysis. Remaining gel images were separated into three sets: standard (pool of all samples), CDR 0 and CDR 1. The pooled sample image with the largest number of well-resolved gel features was chosen as a master image. Gel features in each remaining pooled sample image were hand matched to gel features in the master image. For each gel feature that was matched across >50% of the gels (N=764), a Student's t-test (α=0.05) was performed to determine the statistical significance of CDR 0/CDR 1 ratios, using the DeCyder EDA (Extended Data Analysis) module. To maximize discovery rate and minimize type II error, no multiple test correction was applied. The image intensity data for the statistically significant gel features (N=119) were then subjected to unsupervised hierarchical clustering (DeCyder EDA module).

Protein/peptide identification by LC-MS/MS

Gel features with significant intensity differences were targeted by a robotic gel sampling system (ProPic; Genomics Solutions, Ann Arbor, MI) and transferred into 96 well plates for in-gel digestion with trypsin using a modification of a method (368) described previously (222). Aliquots of these digests were processed for and analyzed by LC-MS/MS using a capillary LC (Eksigent, Livermore CA) interfaced to a nano-LC-linear quadrupole ion trap Fourier transform ion cyclotron resonance mass spectrometer (nano-LC-FTMS) (369), QStar (370), or LTQ (369). The tandem spectra were searched against the National Center for Biotechnology Information non-redundant protein database NR (downloaded on 02-18-2007) using MASCOT, version 2.2.04 (Matrix

Sciences, London). The database searches were constrained by allowing for trypsin cleavage (with up to two missed cleavage sites), fixed modifications (carbamidomethylation of Cys residues) and variable modifications (oxidation of Met residues and N-terminal pyroglutamate formation). Protein identifications were considered genuine if at least two peptides were matched with individual MASCOT ion scores ≥ 40.

Using nano-LC-MS/MS, multiple proteins were identified in the majority of individual gel features. The frequent observation of multiple proteins in single gel features was attributed to the sensitivity and greater peptide coverage that can be achieved with nano-LC-MS methods as compared to, for example, MALDI-MS analysis of peptides from gel features. Assignment of the major protein(s) from each gel feature was achieved using quantitative proteomics from spectra counting (371). The detection of multiple proteins within single gel features could also be attributed to artifacts and technical issues associated with 2D gel electrophoresis: 1) incomplete resolution of proteins by gel electrophoresis (due to similar charge and size characteristics, excessive abundance of neighboring proteins, or artifactual streaking); 2) changes in molecular weight associated with cyanine dye labeling, particularly for lower molecular weight proteins; and 3) sample 'carryover' during robotic gel sampling or during nano-LC-MS/MS.

Enzyme Linked Immunosorbent Assays (ELISAs) and statistical analyses

CSF samples were analyzed by ELISA in duplicate for Aβ42, total tau, and phospho-tau181 (Innotest, Innogenetics) after one freeze-thaw cycle, and in triplicate for all other ELISAs after two freeze-thaw cycles. Samples were evaluated using commercially available ELISAs for NrCAM (R&D Systems), YKL-40 (Quidel), apolipoprotein E (Medical and Biological Laboratories), clusterin/apolipoprotein J

(ALPCO Diagnostics), pigment epithelium-derived factor (PEDF)/serpin-F1 (Chemicon International), β-2 microglobulin (ALPCO Diagnostics), ceruloplasmin (Assaypro), chromogranin A (ALPCO Diagnostics, low binding capacity manufacturing protocol), transthyretin (Assaypro), and cystatin C (US Biological), according to manufacturer's instructions, with adjustments for the analysis of CSF. A sandwich ELISA was developed for carnosinase I using goat anti-human carnosinase I antibody (2 µg/mL, R&D Systems) for capture, rabbit anti-human carnosinase I antibody (1 µg/mL, Sigma) for detection, goat anti-rabbit:horseradish peroxidase (1:5000, Upstate) for reporting, and TMB Super Slow (Sigma) for color development; recombinant carnosinase I (R&D Systems) was used as standard.

Statistical analyses were performed using commercially available software: SAS 9.2 (SAS Institute Inc, Cary, NC) for ROC/AUC calculations and logistic regression analyses, and SPSS 18 (SPSS Inc, Chicago, IL) for all other analyses.

Comparisons between CDR 0 and CDR 1 groups of the discovery cohort (one sample was unavailable for re-evaluation, N=47) were performed using unpaired t-test. For the validation cohort (N=292), correlations with age and gender were evaluated using the Spearman rho correlation coefficient (α=0.05). Chi-square analyses were performed to evaluate need for adjustment for observed correlations. Comparisons between the three CDR groups were performed using one-way analysis of variance (ANOVA), with Bonferroni and LSD post-hoc tests for pair-wise group comparisons, with the following exceptions: one-way ANOVA with Welch's correction was applied for markers (transthyretin) demonstrating unequal variances (Levene <.05); markers correlating with age (tau, p-tau181, Aβ42, YKL-40) were evaluated by analysis of covariance (ANCOVA) adjusting for age, followed by Bonferroni and LSD post-hoc tests. Multiple post-hoc tests were applied in recognition of their different levels of stringency (Bonferroni > LSD), and their non-uniform popularity among statisticians. For CDR 0 vs

>0 comparisons and CDR 1 vs <1 comparisons, unpaired t-test was used; Welchs' correction for unequal variances was applied for YKL-40, p-tau, tau, and Aβ42. For each biomarker measured in the larger 'validation' cohort, the receiver operating characteristic (ROC) curve and the area under the ROC curve (AUC) were calculated for predicting CDR 0 versus CDR>0. A stepwise logistic regression analysis was used to identify an optimal combination of these biomarkers for this data set. These analyses were repeated for CDR 1 vs CDR<1.

Results

Sample processing and 2D-DIGE analysis

To identify new candidate biomarkers for AD, we utilized an unbiased proteomics approach, 2D-DIGE LC-MS/MS (222, 251), to compare the relative concentrations of CSF proteins in individuals with mild "probable AD" (CDR 1, N=24) to those in individuals without dementia (CDR 0, N=24). The two clinical groups were selected on the basis of relative biomarker values for CSF Aβ42 and tau (see Methods), and differed somewhat with respect to age at LP and gender (CDR 0: 64.8 ± 8.8 yrs, 38% female; CDR 1: 72.8 yrs ± 7.9 yrs, 54% female). Five samples showed evidence of blood contamination by 2D-DIGE; the five gels containing these samples were excluded from subsequent image analysis. The remaining individual sample images (N=38, from 19 gels) were aligned using the BVA modules (see Methods).

Among the 764 gel features that were present in >50% of the gels, 119 were found to have significant intensity differences between CDR 0 and CDR 1 groups (Student's t-test [α=0.05]) (Figure 2.1A). The image intensity data for these 119 gel features were subjected to unsupervised hierarchical clustering (EDA module, DeCyder software) and the gel features themselves were analyzed for protein composition.

Protein identification by LC-MS/MS

LC-MS/MS identified single dominant proteins in 77 of the 119 gel features (Table 2.2). In 30 gel features, our analyses identified two or more co-dominant proteins. The 12 remaining gel features were not annotated from the nano-LC-MS/MS data. Among the characterized gel features, there was considerable redundancy in protein identifications, with some proteins appearing in multiple gel features. Such 'redundant' gel features, likely representing a modified form or variant of the same 'parent' protein, generally migrated with some proximity on 2D-gel electrophoresis (Figure 2.1). Forty-seven unique proteins were identified (Table 2.2). Thirteen of these unique proteins had been identified in our previous studies (222, 251) (including chromogranin B, cystatin C, prostaglandin H2 D-isomerase/beta trace, neuronal pentraxin receptor, gelsolin, β-2 microglobulin, carnosinase I, angiotensinogen, apolipoprotein H, secretogranin III, α-1-antichymotrypsin, chitinase 3-like 1 / YKL-40, and kininogen I) and others have been reported by other groups (243, 245, 246, 361, 363, 364). These previous reports provide supporting evidence that this list of proteins may contain viable candidate biomarkers for AD that are worthy of pursuit in validation experiments.

Unsupervised clustering analysis

The intensity data from the 119 gel features of interest were subjected to an unsupervised clustering analysis to evaluate their ability to segregate the CDR 0 and CDR 1 subjects, and to assess their collective potential as a diagnostic biomarker panel (Figure 2.2). The 'heatmap' generated from this analysis appeared to segregate CDR 0 and CDR 1 individuals (indicated by green and red squares, respectively) almost completely, with only four subjects 'misclassified.' However, closer examination revealed an additional layer of segregation on the basis of *APOE* genotype (indicated by

'ApoE 4+ Cluster' and 'ApoE 4 – Cluster') which showed perfect subject segregation. Given that the *APOE-ε4* allele is a dominant genetic risk factor for AD, some clustering of individuals by *APOE* genotype might be expected simply from successful segregation of CDR 0 and CDR 1 subjects. However, we hypothesize that the apoE protein exerts a dominant clustering influence through the markedly different electrophoretic profiles of its different isoforms derived from *APOE-ε2*, *APOE-ε3* and *APOE-ε4* alleles (illustrated in Figure 2.3). ApoE was present in 24 of the 119 gel features found to differ in intensity between the CDR groups, and was found to be the primary protein in 12 of these gel features. This heterogeneous electrophoretic mobility of apoE results from the inherent charge differences of the three major apoE isoforms (-E2, -E3, -E4) and the appearance of each isoform as an array of multiple distinct gel features caused by post-translational modifications. These isoform-specific differences are reflected in the prominent red and green clusters, located within the lower third of Figure 2.2 (corresponding to gel features 83-90 and 107-116), that correlate very closely with subject *APOE* genotypes. Recognizing this correlation, we hypothesized that *APOE* genotypes were in large part driving the clustering of subjects in Figure 2.2. To test this hypothesis, we performed a second unsupervised clustering analysis, including only those gel features from the initial analysis that did not contain apoE protein (Figure 2.4). Although this 'apoE-free' analysis segregated CDR 1 and CDR 0 groups less completely, it appropriately re-clustered (by CDR status) several subjects (#12, 36, 37) who were aberrantly segregated in Figure 2.2, potentially due to their *APOE* genotypes. Moreover, clustering of subjects into *APOE* genotype subgroups in Figure 2.4 appears negligible. The underlying benefit of this 'apoE-free' analysis is that it reveals the subject-clustering potential of other gel features, which was previously obscured by the inclusion of apoE-containing gel features. As can now be better visualized in Figure 2.4, gel features appearing within the upper three-fourths of the heatmap appear to show greater intensity

in CDR 1 subjects; the converse is true of gel features within the lower fourth. It is important to note that measurements of Aβ42 and tau (two proteins measured by ELISA and not detected by 2D-DIGE) were not included in these clustering analyses; because these subjects were selected on the basis of CSF Aβ42 and tau levels, such inclusion would presumably yield perfect or near-perfect segregation by CDR status in this 'discovery' cohort. Therefore, this analysis reflects the potential of these candidate biomarkers to segregate CDR 0 and CDR 1 subjects *independent* of any contribution from current leading CSF biomarkers Aβ42 and tau. It does not address whether these biomarker candidates might improve upon the utility of Aβ42 and tau, however.

Validation of candidate biomarkers by ELISA

Before evaluating a subset of these candidate biomarkers in a larger independent sample set, we first assessed the capacity of protein-specific quantitative ELISAs to detect significant differences between the CDR 0 and CDR 1 subject groups of the original discovery cohort. When possible, to facilitate future reproduction of our findings by other groups and potential translation to clinical use, we applied commercially available ELISA kits.

Of the eleven ELISAs applied to the discovery cohort (N=47, one sample was unavailable for validation), six (NrCAM, YKL-40, chromogranin A, carnosinase I, transthyretin, cystatin C) showed statistically significant or near-significant differences between CDR 0 and CDR 1 groups (Figure 2.5); five others (PEDF, β-2 microglobulin, clusterin/apoJ, ceruloplasmin, apoE) did not.

The six ELISAs that measured differences between the CDR 0 and CDR 1 CSF samples of the discovery cohort were subsequently applied to a larger, independent set of CSF samples (N=292) collected from volunteer participants studied by the WU-ADRC. This 'validation' cohort included a CDR 0.5 group in addition to CDR 0 and CDR 1

groups, allowing for biomarker assessment in the very early clinical stage of AD. Demographic, clinical, and genetic characteristics of these subjects at time of sample collection are presented in Table 2.1. Unlike the discovery cohort, this validation cohort was not preselected on the basis of prior biomarker values (CSF Aβ42 and tau), although assays for CSF Aβ42, tau, and p-tau181 were performed.

Because the age and gender compositions differed among the clinical groups of the validation cohort, we evaluated each of the 9 biomarkers (six novel candidates, Aβ42, tau, and p-tau181) for age and gender correlations in order to apply covariate analyses appropriately. Correlating with age were: tau (r=0.318, p<0.0001), p-tau181 (r=0.2216, p<0.001), Aβ42 (r=-0.2334, p<0.0001) and YKL-40 (r=0.4001, p<0.001); no biomarkers correlated with gender (p>0.05).

As shown in Figure 2.6, statistically significant differences between clinically defined groups were measured for Aβ42, tau, p-tau181, NrCAM, YKL-40, chromogranin A, and carnosinase I; for transthyretin and cystatin C, non-significant trends were measured. These differences appeared in three patterns: Aβ42 showed a pronounced decrease from CDR 0 to CDR 0.5 and a lesser reduction from CDR 0.5 to CDR 1; tau, p-tau 181, and YKL-40 showed increases that were equivalent in CDR 0.5 and CDR 1 relative to CDR 0; NrCAM, chromogranin A, and carnosinase I showed decreases relative to CDR 0 only in CDR 1, and not in CDR 0.5.

Diagnostic utility of validated candidate biomarkers

To evaluate and compare the potential of the validated candidate biomarkers and Aβ42, tau, and p-tau181 for identifying either very mild to mild dementia (combined CDR 0.5 and CDR 1) or mild dementia (CDR 1), ROC curves and AUCs were calculated for each biomarker using data from the validation cohort (Figure 2.7A, B, Table 2.3A, B). Stepwise logistic regression analyses indicated that, among the nine biomarkers under

consideration, YKL-40, NrCAM, and tau yielded an AUC of 0.896 in discriminating cognitive normalcy (CDR 0) from very mild to mild dementia (CDR>0) (Figure 2.7C,Table 2.3A); for discriminating mild dementia (CDR 1) from CDR<1, carnosinase I, chromogranin A and tau yielded an AUC of 0.876 (Figure 2.7D, Table 2.3B).

Discussion

The results from the 2D-DIGE LC-MS/MS portion of this study suggest that many of the recognized neuropathological changes of AD are represented by changes in the CSF proteome. Most of the 47 candidate biomarker proteins identified in this study can be placed into structural and/or functional categories (e.g. synaptic adhesion, synaptic function, dense core synaptic vesicle proteins, inflammation/complement, protease activity/inhibition, apolipoproteins, etc.) associated with accepted neuropathophysiological changes in AD (Table 2.4). Unsupervised clustering analyses of this 2D-DIGE data, performed without the influence of CSF Aβ42, tau, p-tau and *APOE* genotype, additionally suggest that these biomarker candidates collectively show utility for discriminating groups with and without mild DAT (Figure 2.4).

In the second phase of this study, designed to measure a subset of candidate biomarker proteins in two independent sample sets by ELISA, four of the eleven candidate biomarkers tested showed capacity to distinguish clinical groups. However, seven candidate biomarkers did not show statistically significant differences between clinical groups in either the smaller discovery cohort or the larger validation cohort. Superficially, this 'failure rate' might cast doubt on the list of candidate biomarkers identified through 2D-DIGE. However, it is important to note that 2D-DIGE is sensitive to changes in concentrations of minor protein isoforms and post-translational modifications that may not significantly alter the global concentrations of a 'parent' protein, which

would be measured by ELISA. Therefore, it is not surprising that some of the candidate biomarker ELISAs did not replicate the findings from 2D-DIGE. Transthyretin provides a prime example: all of the significant gel-features ascribed to transthyretin (gel features # 20, 52, 57, 58, 60, 77, 78, 79, 84, 87, 110, 115; Table 2.2) showed unusual electrophoretic patterns and were dwarfed by the canonical transthyretin gel features that did not individually show statistical differences (Figure 2.1B). In fact, whereas most of the significant transthyretin 2D-DIGE gel features were decreased in AD, the global transthyretin levels measured by ELISA in the discovery and validation cohorts were actually mildly increased in groups with cognitive impairment (CDR>0) relative to those without (CDR 0) (Figures 2.5 and 2.6). To measure the sub-species of transthyretin that were identified by 2D-DIGE as decreasing in AD will require assays that specifically target relevant post-translational modifications and exclude other forms of transthyretin. Similarly, other 2D-DIGE biomarker candidates may also require specifically tailored assays for accurate, high-throughput measurement.

Nevertheless, four candidate biomarkers were successfully validated in both cohorts, and two others showed non-significant trends by ELISA in the larger validation cohort (Figure 2.6). This larger cohort represented three different cognitive stages: normalcy, very mild dementia, and mild dementia (CDR0, CDR 0.5, CDR 1, respectively), and revealed different patterns of CSF biomarker levels, vis-a-vis cognitive status. The CSF concentration of YKL-40, an astrocytic marker of plaque-associated neuroinflammation (372-383), is increased by the very earliest stage of clinical disease (CDR 0.5). Transthyretin (241, 248, 384-390) and cystatin C (362, 390-394), two proteins with neuroprotective qualities that are implicated in preventing amyloidogenesis of Aβ peptide, show a similar pattern. In contrast, the concentrations of NrCAM, a synaptic adhesion molecule (361, 395-398), chromogranin A, a dense core synaptic vesicle protein (361, 362, 399-402), and carnosinase I, a neuronal dipeptidase

responsible for degradation of the anti-oxidant and metal-chelating dipeptide carnosine (403-405), do not decline until mild dementia ensues (CDR 1).

Like the current leading CSF biomarkers for AD (Aβ42, tau and p-tau181), all of these biomarker candidates show ranges with substantial overlap between clinically defined subject groups. This issue of overlapping values, common among candidate AD CSF biomarkers reported to date, suggests that any one biomarker will be insufficient to accurately identify early AD, and that an ensemble of complementary biomarkers will be required to provide adequate sensitivity and specificity. Therefore, to identify an optimal combination of these biomarkers that can distinguish the early clinical stages of AD from cognitive normalcy, we applied stepwise logistic regression analyses to the ELISA data from our 'validation' cohort (Figure 2.7, Table 2.3). These analyses suggest that four candidate AD biomarkers (YKL-40, NrCAM, chromogranin A, carnosinase I) can improve the ability of tau to classify individuals into CDR0, CDR 0.5 and CDR 1 groups with appreciable accuracy.

It may appear counter-intuitive that Aβ42 and p-tau, which individually discriminate very mild AD and mild AD from cognitively normal groups quite well, were not incorporated into either 'optimal' biomarker panel by the stepwise linear regression analyses. Likewise, NrCAM was included in the optimal CDR 0 vs CDR>0 biomarker panel (AUC 0.896) even though its mean levels did not independently show a statistical difference between CDR 0 and CDR>0 groups. In considering this outcome, it may be worth noting that if NrCAM, transthyretin, chromogranin and cystatin C are removed from consideration, the stepwise linear regression model for the CDR 0 vs CDR>0 comparison yields an 'optimal' biomarker panel that includes only tau, Aβ42 and carnosinase I, with an AUC of 0.849. In this restricted analysis, the paired contribution of Aβ42 and carnosinase I to tau is apparently greater than that of YKL-40. These analyses illustrate how 'unpredictable' and context-dependent optimal biomarker

combinations can be, and suggest that biomarker complementarity may be more important to consider than each biomarkers' independent performance, when choosing a biomarker panel. Of course, it will be important to replicate these findings in additional independent cohorts. It will also be important to evaluate a greater number of candidate biomarkers in similar fashion, in order to construct a biomarker panel with even greater accuracy.

Nevertheless, by providing proof of concept, this study outlines a scheme to categorize the early stages of AD using CSF protein biomarkers that reflect established features of the pathophysiological evolution of the disease (Figure 2.8). Building upon previous findings that low CSF Aβ42 can identify cognitively normal individuals with plaques (preclinical AD) (127), and that tau/Aβ42 and YKL-40/Aβ42 ratios can predict risk of developing cognitive impairment (107, 132, 372), this minimal panel of six CSF biomarkers (YKL-40, NrCAM, chromogranin A, carnosinase I, tau and Aβ42) begins to segregate subjects into six clinicopathological categories: normal cognition without amyloid plaques, normal cognition with amyloid plaques (preclinical AD), normal cognition at increased risk to develop dementia (converters), very mild dementia (CDR 0.5), very mild dementia at increased risk for progression, and mild dementia (CDR 1) (Figure 2.8).

We acknowledge that this minimal panel of biomarkers currently has insufficient sensitivity and specificity for clinical application, particularly because it has not been fully evaluated for its ability to discriminate AD from non-AD causes of dementia (Aβ42, p-tau181, tau, and specific fragments of chromogranin A and cystatin C have shown some ability to distinguish AD from FTLD (362, 406, 407). The incorporation of additional biomarkers that are likely to discriminate early AD from cognitive normalcy, such as those identified in the first phase of this study, or other biomarkers that have already shown promise for distinguishing AD from other leading causes of dementia (e.g. agouti

related peptide, eotaxin-3, and hepatocyte growth factor (361), complement C3a des-arg and integral membrane protein 2B CT (362) for FTLDs; and alpha-synuclein (408), ApoH and vitamin D binding protein (246) for Lewy body disorders), would likely improve the panel's diagnostic utility. However, even in its current form, this initial panel might show value if applied in the context of clinical trial design, wherein simple enrichment of study populations for characteristics of interest would increase efficiency and power and reduce duration and cost. A biomarker panel like this one might also allow clinical trials to evaluate stage-specific responses to treatment, which may differ. Finally, because most of these biomarkers reflect underlying pathological changes in real time, it is appealing to speculate that these biomarkers may have additional utility for evaluating clinically imperceptible treatment responses (as in (409)) and for monitoring neuropathological – rather than cognitive – decline.

Table 2.1. Demographic, clinical, genotype characteristics of validation cohort

Characteristic	CDR 0	CDR 0.5	CDR 1
Number of Participants	198	65	29
Gender (% Female)	63%	54%	52%
APOE genotype, % ε4+	35%	51%	59%
Mean MMSE score (SD)	28.9 (1.3)	26.3 (2.8)	22.3 (3.9)
Mean age at LP (SD), yrs	71.0 (7.3)	73.8 (6.8)	76.5 (6.2)
Mean CSF Aβ42 (SD), pg/mL	605 (240)	446 (230)	351 (118)
Mean CSF tau (SD), pg/mL	304 (161)	539 (276)	552 (263)
Mean CSF ptau181 (SD), pg/mL	55 (25)	85 (44)	77 (38)

Abbreviations: CDR, Clinical Dementia Rating; APOE, apolipoprotein E;MMSE, Mini-Mental State Examination; LP, lumbar puncture; SD, standard deviation; CSF, cerebrospinal fluid; Aβ42; ptau181, tau phosphorylated at threonine 181.

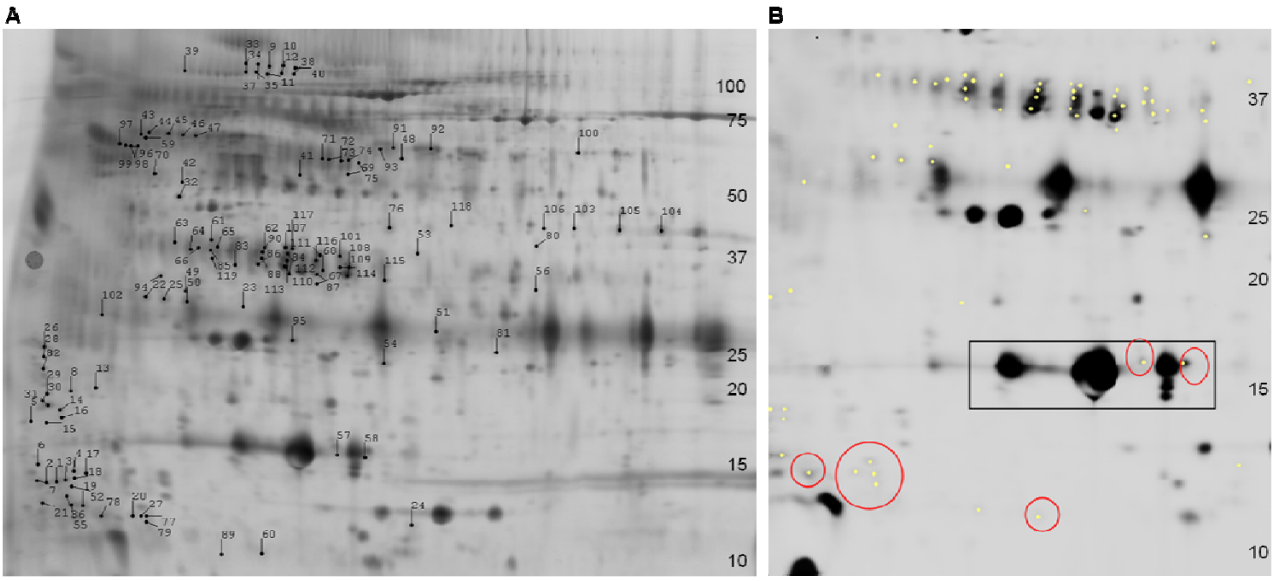

Figure 2.1. Two-dimensional difference in gel electrophoresis (2D-DIGE) of cerebrospinal fluid immunodepleted of six high abundance proteins.

A) Representative 2D-DIGE (grayscale) image with labeled locations of 119 gel features that differed in intensity between CDR 0 and CDR 1 groups. Gel features are numbered 1 through 119, and relevant information about each is listed in Table 2.2. Approximate molecular weight (in kDa) is indicated along the right border; pI ranges from 3 (left) to 11 (right) and is non-linear. **B)** Two-dimensional gel electrophoresis pattern of transthyretin. The large, intense, protein spots commonly attributed to transthyretin are boxed; those appearing in our study as differentially abundant between cognitively normal (CDR 0) and mildly demented participants (CDR 1) are circled in red, and are partially obscured by yellow dots (yellow dots indicate sites targeted by robotic sampling for mass spectrometric identification of proteins).

Table 2.2. Proteins that were identified by 2D-DIGE and LC-MS/MS to have differences in mild DAT versus non-demented control CSF

Spot	BVA	GI number(s)	Protein	Change	p value	Protein #
1	4709	31543193	hypothetical protein LOC146556	-1.36	7.02E-04	1
2	5659	4502807	chromogranin B	-1.31	1.18E-03	2
3	4683	4502101	annexin I	-1.31	9.54E-04	3
4	4608	62089004	chromogranin B	-1.24	6.49E-03	
		181387	cystatin C			4
		134464	Secretogranin-2			5
5	4297	4502807	chromogranin B	-1.26	0.0157	
6	4545			-1.34	3.86E-03	
7	4695	4502807	chromogranin B	-1.27	0.0115	
8	4044	4502807	chromogranin B	-1.32	2.15E-03	
9	1314	1621283	neuronal cell adhesion molecule (NrCAM)	-1.22	0.0119	6
10	1320	1621283	neuronal cell adhesion molecule (NrCAM)	-1.33	6.31E-04	
11	1382	6651381	neuronal cell adhesion molecule (NrCAM)	-1.28	9.53E-04	
12	1383	6651381	neuronal cell adhesion molecule (NrCAM)	-1.25	6.64E-03	
13	4033	4502807	chromogranin B	-1.21	0.0419	
14	4191	4502807	chromogranin B	-1.23	0.0107	
15	4293	4502807	chromogranin B	-1.33	4.64E-03	
		825635	calmodulin			7
16	4266	62089004	chromogranin B	-1.22	0.0315	
17	4615			-1.22	0.0188	
18	4677			-1.3	9.63E-03	
19	4906	5454032	S100 calcium binding protein A1	-1.3	1.36E-04	8
		62898141	prosaposin			9

		627391	brain-associated small cell lung cancer antigen / NCAM-140 / CD56			10
		17136078	VGF nerve growth factor inducible precursor			11
20	5014	443295	transthyretin	-1.3	2.10E-03	12
21	4884	224917	apolipoprotein CIII	-1.34	9.78E-04	13
		337760	prosaposin / cerebroside sulfate activator protein			
22	3423	39654998	Chain A, Hr1b Domain From Prk1	-1.27	0.0133	14
		32171249	prostaglandin H2 D-isomerase / beta trace			15
23	3470	17402888	neuronal pentraxin receptor	-1.25	7.23E-03	16
24	4954	34616	beta-2 microglobulin	-1.3	4.15E-03	17
25	3436	32171249	prostaglandin H2 D-isomerase	-1.22	0.0266	
		178775	proapolipoprotein			18
		39654998	Chain A, Hr1b Domain From Prk1			
26	3714			-1.27	0.03	
27	4922	39654998	Chain A, Hr1b Domain From Prk1	-1.27	0.0194	
28	3786	2072129	chromogranin A	-1.38	8.96E-03	19
29	4076	7341255	brain acetylcholinesterase putative membrane anchor	-1.25	0.0375	20
30	4111	62089004	chromogranin B	-1.28	0.0206	
31	4167	4502807	chromogranin B	-1.29	0.0207	
32	2652	28373309	gelsolin	-1.23	0.0346	21
33	1313	6651381	neuronal cell adhesion molecule (NrCAM)	-1.19	8.08E-03	
34	1372	1620909	ceruloplasmin	-1.19	9.00E-03	22
		1483187	inter-alpha-trypsin inhibitor family heavy chain-related protein (IHRP)			23
		31874098	hypothetical protein (NrCAM)			
		6651381	neuronal cell adhesion molecule (NrCAM)			
35	1387	68534652	neuronal cell adhesion molecule (NrCAM)	-1.29	8.16E-05	
		1620909	ceruloplasmin			

36	4808	337760	prosaposin / cerebroside sulfate activator protein	-1.22	0.0114	
37	1319	68534652	neuronal cell adhesion molecule (NrCAM)	-1.19	0.0198	
		1942284	ceruloplasmin			
38	1386	6651381	neuronal cell adhesion molecule (NrCAM)	-1.29	1.24E-03	
39	1353	21706696	calsyntenin 1	-1.22	0.0417	24
40	1329	1621283	neuronal cell adhesion molecule (NrCAM)	-1.22	4.61E-03	
41	2456	5802984	UDP-GlcNAc:betaGal beta-1,3-N-acetylglucosaminyltransferase 1	-1.13	0.0449	25
42	2550	20178323	pigment epithelium-derived factor precursor (PEDF) / Serpin-F1 / EPC-1	-1.15	0.022	26
43	2125	21071039	carnosinase 1	-1.21	0.0245	27
44	2131	21071039	carnosinase 1	-1.19	0.049	
45	2152	21071039	carnosinase 1	-1.15	0.0366	
46	5614	21071039	carnosinase 1	-1.18	0.0109	
47	2166	21071039	carnosinase 1	-1.21	0.0122	
48	2328	416180	Man9-mannosidase / a1,2-mannosidase IA	-1.16	0.0464	28
49	3360			-1.15	0.045	
50	3447	32171249	prostaglandin H2 D-isomerase / beta trace	-1.19	0.0334	
51	3546	1621283	neuronal cell adhesion molecule (NrCAM)	-1.17	0.0368	
		32171249	prostaglandin H2 D-isomerase / beta trace			
52	4745	443295	transthyretin	-1.26	0.0181	
53	3032	11056046	Nectin-like molecule-1 / SynCAM3 / TSLL1	-1.13	0.0472	29
		4506147	protease, serine, 2 preproprotein			30
54	3718	39654998	Chain A, Hr1b Domain From Prk1	-1.14	0.0455	
		32171249	prostaglandin H2 D-isomerase / beta trace			
55	4902	14277770	apolipoprotein C-Ii	-1.19	0.0495	31
		337760	prosaposin / cerebroside sulfate activator protein			
		2072129	chromogranin A			

56	3290	409725	carbonic anhydrase IV	-1.14	0.0141	32
57	4379	17942890	transthyretin	-1.15	0.0219	
		39654998	Chain A, Hr1b Domain From Prk1			
		34999	cadherin 2 precursor			33
58	4388	32171249	prostaglandin H2 D-isomerase / beta trace	-1.14	0.0218	
		39654998	Chain A, Hr1b Domain From Prk1			
		443295	transthyretin			
59	2192	21071039	carnosinase 1	-1.34	6.56E-03	
		532198	angiotensinogen			34
		5531817	secretogranin III			35
		9665262	EGF-containing fibulin-like extracellular matrix protein 1 / Fibulin-3			36
		177933	alpha-1-antichymotrypsin			37
		4504893	kininogen 1			38
		36573	vitronectin			39
60	5336	443295	transthyretin	-1.17	0.0301	
61	3009	178855	apolipoprotein J / clusterin	-1.26	0.0288	40
		4557325	apolipoprotein E			41
		4506147	protease, serine, 2 preproprotein			
62	3042	4557325 / 178853	apolipoprotein E	-1.21	0.047	
		338305	apolipoprotein J / clusterin			
63	3016	338305	apolipoprotein J / clusterin	-1.32	6.69E-05	
64	3050	4557325 / 178853	apolipoprotein E	-1.24	5.19E-04	
		178855	apolipoprotein J / clusterin			
65	3075	4557325 / 178853	apolipoprotein E	-1.42	5.59E-06	
		178855	apolipoprotein J / clusterin			
66	3038	4557325 / 178853	apolipoprotein E	-1.41	2.84E-05	

		178855	apolipoprotein J / clusterin			
67	3301	178849	apolipoprotein E	-1.4	1.29E-05	
68	3182	4557325 / 178853	apolipoprotein E	-1.41	3.43E-04	
		178855	apolipoprotein J / clusterin			
69	2443	532198	angiotensinogen	-1.2	6.85E-03	
70	2493	4503009	carboxypeptidase E precursor	-1.23	6.09E-03	42
71	5621	532198	angiotensinogen	-1.17	0.0434	
72	5624	532198	angiotensinogen	-1.22	0.0147	
73	5622	553181	angiotensinogen	-1.17	0.04	
74	5625	532198	angiotensinogen	-1.16	0.0423	
75	5627			-1.22	0.0113	
76	2849	4557325	apolipoprotein E	-1.28	6.26E-03	
77	5009	443295	transthyretin	-1.24	0.0268	
78	5033	443295	transthyretin	-1.27	4.59E-03	
79	5078	443295	transthyretin	-1.2	0.0144	
80	2958	4504067	aspartate aminotransferase 1	-1.22	8.60E-03	43
81	3657	32171249	prostaglandin H2 D-isomerase / beta trace	-1.22	3.07E-03	
82	3867			-1.28	0.0437	
83	3176	4557325	apolipoprotein E	-1.63	3.03E-04	
84	3228	4557325	apolipoprotein E	-1.4	1.39E-03	
		443295	transthyretin			
85	3074	4557325 / 178853	apolipoprotein E	-2.36	4.41E-09	
86	5647	4557325	apolipoprotein E	-2.35	2.92E-07	
87	3224	4557325 / 178853	apolipoprotein E	-2.13	6.36E-07	
		443295	transthyretin			
88	3126	4557325 / 178853	apolipoprotein E	-1.93	7.55E-06	

89	5297			-1.44	0.0473	
90	3083	4557325	apolipoprotein E	-1.7	2.82E-05	
91	2218	112911	alpha-2-macroglobulin	1.22	0.0282	44
92	2226	6573461	apolipoprotein H	1.27	0.0305	45
93	2252	112911	alpha-2-macroglobulin	1.26	0.0267	
		4557327	apolipoprotein H			
94	3255			1.24	0.0315	
95	3630	178775	proapolipoprotein	1.24	0.0287	
		32171249	prostaglandin H2 D-isomerase / beta trace			
		39654998	Chain A, Hr1b Domain From Prk1			
96	2229	177933	alpha-1-antichymotrypsin	1.42	3.09E-03	
97	2235	177933	alpha-1-antichymotrypsin	1.35	0.0388	
98	2261	177933	alpha-1-antichymotrypsin	1.3	6.04E-03	
99	2262	177933	alpha-1-antichymotrypsin	1.25	0.0294	
100	2220			1.29	0.0158	
101	3084			1.16	0.0211	
102	3508	32171249	prostaglandin H2 D-isomerase / beta trace	1.22	9.21E-03	
103	2825	23512215	chitinase 3-like 1 / YKL-40 / HC-gp39	1.41	0.0167	46
104	2863	4557018	chitinase 3-like 1 / YKL-40 / HC-gp39	1.5	0.0144	
105	2846	29726259	chitinase 3-like 1 / YKL-40 / HC-gp39	1.46	7.88E-03	
106	2843	23512215	chitinase 3-like 1 / YKL-40 / HC-gp39	1.32	0.0241	
107	3030	4557325	apolipoprotein E	2.46	3.70E-05	
108	3152	4557325 / 178853	apolipoprotein E	2.39	8.73E-07	
109	3203	178853	apolipoprotein E	3.23	3.13E-07	
110	3185	4557325 / 178853	apolipoprotein E	1.9	9.72E-04	
		443295	transthyretin			

111	3069	338305	apolipoprotein J / clusterin	1.5	6.40E-04	
112	3079			1.64	4.47E-04	
113	3133	178853	apolipoprotein E	1.49	8.66E-04	
		338057	apolipoprotein J / clusterin			
114	3151	178853	apolipoprotein E	1.28	9.25E-03	
		338057	apolipoprotein J / clusterin			
115	3249	4557325	apolipoprotein E	1.37	2.46E-03	
		178855	apolipoprotein J / clusterin			
		443295	transthyretin			
116	3118	4557325 / 178853	apolipoprotein E	1.64	9.96E-04	
117	5698	178855	apolipoprotein J / clusterin	1.73	5.82E-04	
118	2819	40737343	C4B3	2	0.038	47
119	3137	4557325	apolipoprotein E	-2.5	8.52E-07	

Table 2.2. Proteins that were identified by 2D-DIGE and LC-MS/MS to have differences in mild DAT versus non-demented control CSF. Column 1, coded protein spot ID (as in Figure 2.1). **Column 2**, biological variation analysis (BVA) number for that spot generated by the DeCyder software. **Column 3**, GI accession number(s) assigned to the proteins identified by MASCOT. **Column 4**, name of the protein identified by MASCOT. **Column 5**, fold change in protein abundance comparing CDR 1 with CDR 0 samples (negative values indicate decreases in abundance in CDR 1 samples compared to controls (CDR 0)). **Column 6**, p value of the CDR 0 versus CDR 1 comparison (Student's t test). **Column 7**, consecutive numbering identifying proteins as unique.

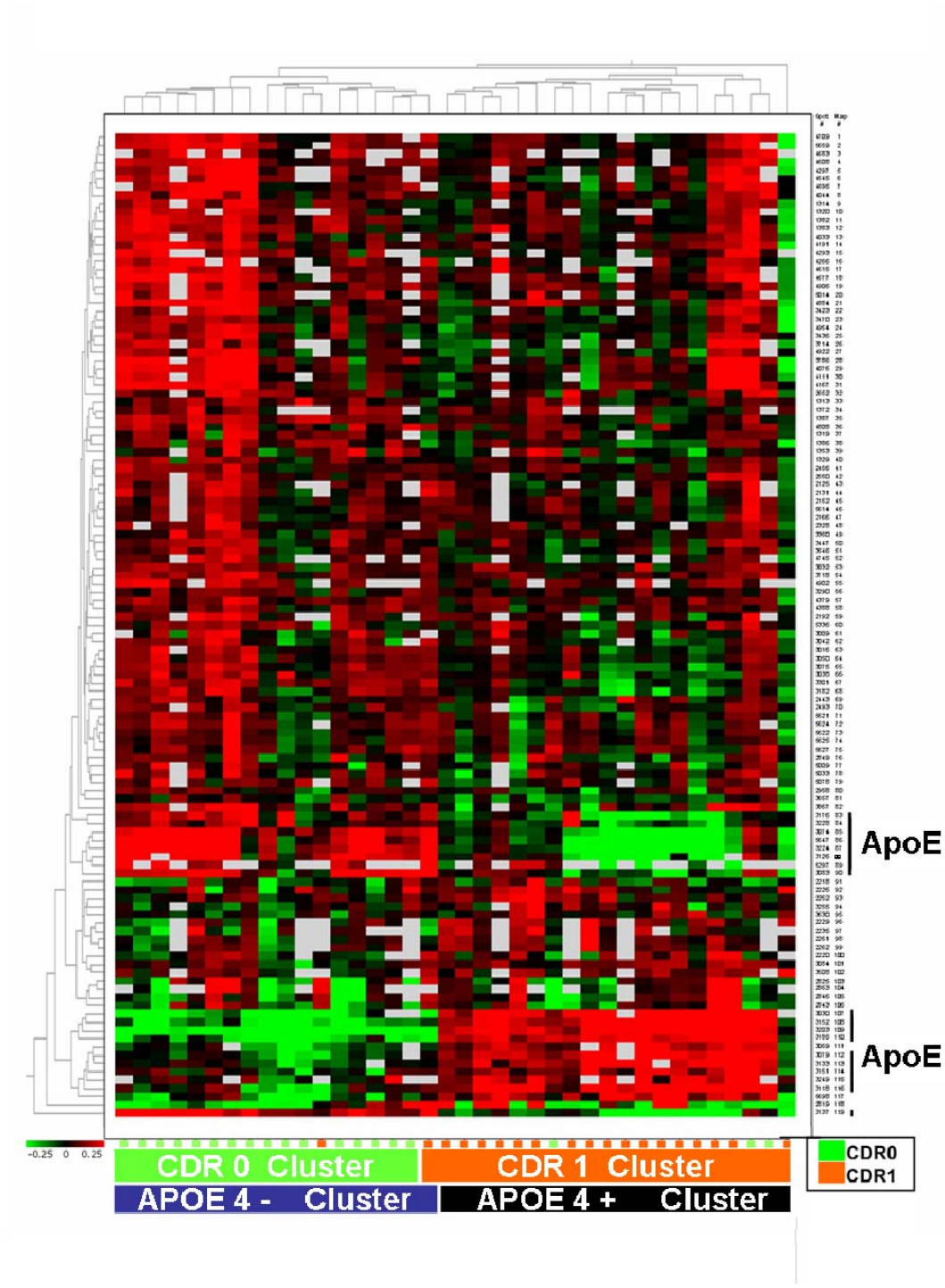

Figure 2.2. Unsupervised Clustering of CSF Samples by 2D-DIGE data from the 119 statistically significant gel features (Student's t-test, α=0.05, present in >50% of images). Five gels containing hemoglobin (N=10 samples) were excluded. Columns represent samples; rows, numbered 1 through 119 from top to bottom, represent gel features

depicted in Figure 2.1A. Gel feature intensity is encoded colorimetrically from red (high in AD) to green (low in AD). CDR status of individual subjects at time of CSF collection is encoded below by small green and orange squares; CDR 0 and CDR 1 clusters are indicated below by green and orange bars, respectively. *APOE-ε4* allele status of individuals and groups, alike, is indicated by black (possessing one or two *APOE-ε4* alleles) or blue (possessing no *APOE-ε4* alleles). Rows representing gel features containing ApoE protein are indicated along the lower right border.

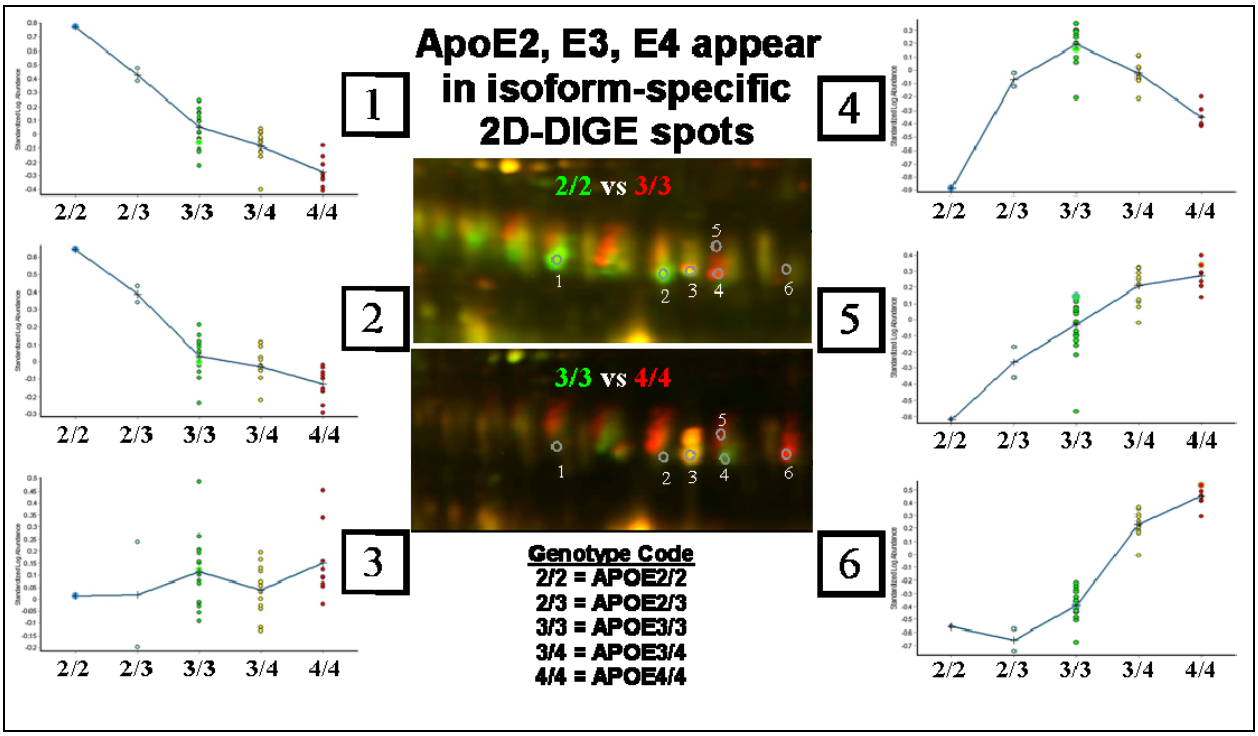

Figure 2.3. ApoE protein isoforms appear in different gel features on 2D-DIGE. Overlays of fluorescent 2D-DIGE images from gels representing CSF from two individuals with homozygosity for *APOE-ε2* (green) or *APOE-ε3* (red) (center, upper image) and for *APOE-ε3* (green) or *APOE-ε4* (red) (center, lower image) illustrate the heterogeneity of signal distribution by isoelectric point and molecular weight among ApoE protein isoforms derived from different alleles. Signal intensities of individual CSF samples, grouped by genotype (2/2, 3/3 and 4/4 represent homozygotes; 2/3, 3/4 represent heterozygotes) is indicated for six ApoE gel features, illustrating that gel features 1 and 2 represent ApoE2; gel feature 3 represents multiple forms; gel feature 4 represents ApoE3; and gel features 5 and 6, ApoE4.

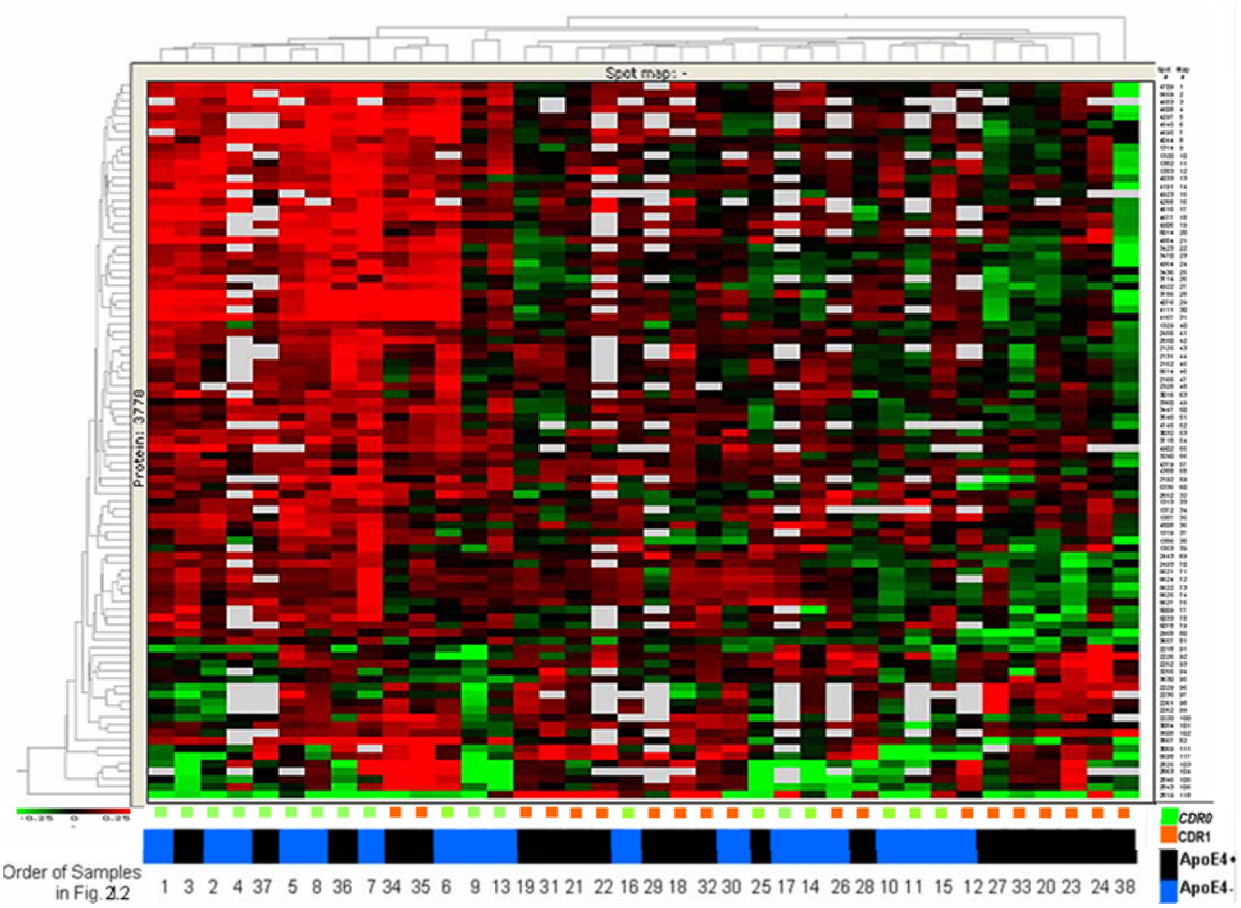

Figure 2.4. Unsupervised Clustering of CSF Samples by 2D-DIGE data, excluding gel features containing ApoE protein; all other statistically significant gel features (Student's T-test α=0.05, present in >50% of images) are retained. As in Figure 2.2, five gels containing hemoglobin (N=10 samples) were excluded. Columns represent samples, numbered by position in Figure 2.2; rows represent gel features, numbered by position in Figure 2.2, with ApoE-containing features removed. Gel feature intensity is encoded colorimetrically from red (high in AD) to green (low in AD); white indicates absent data. CDR status of subjects at time of CSF collection is encoded below, by small green and orange squares. *APOE-ε4* status is indicated in blue or black. Clustering pattern of samples relative to Figure 2.2 is indicated below.

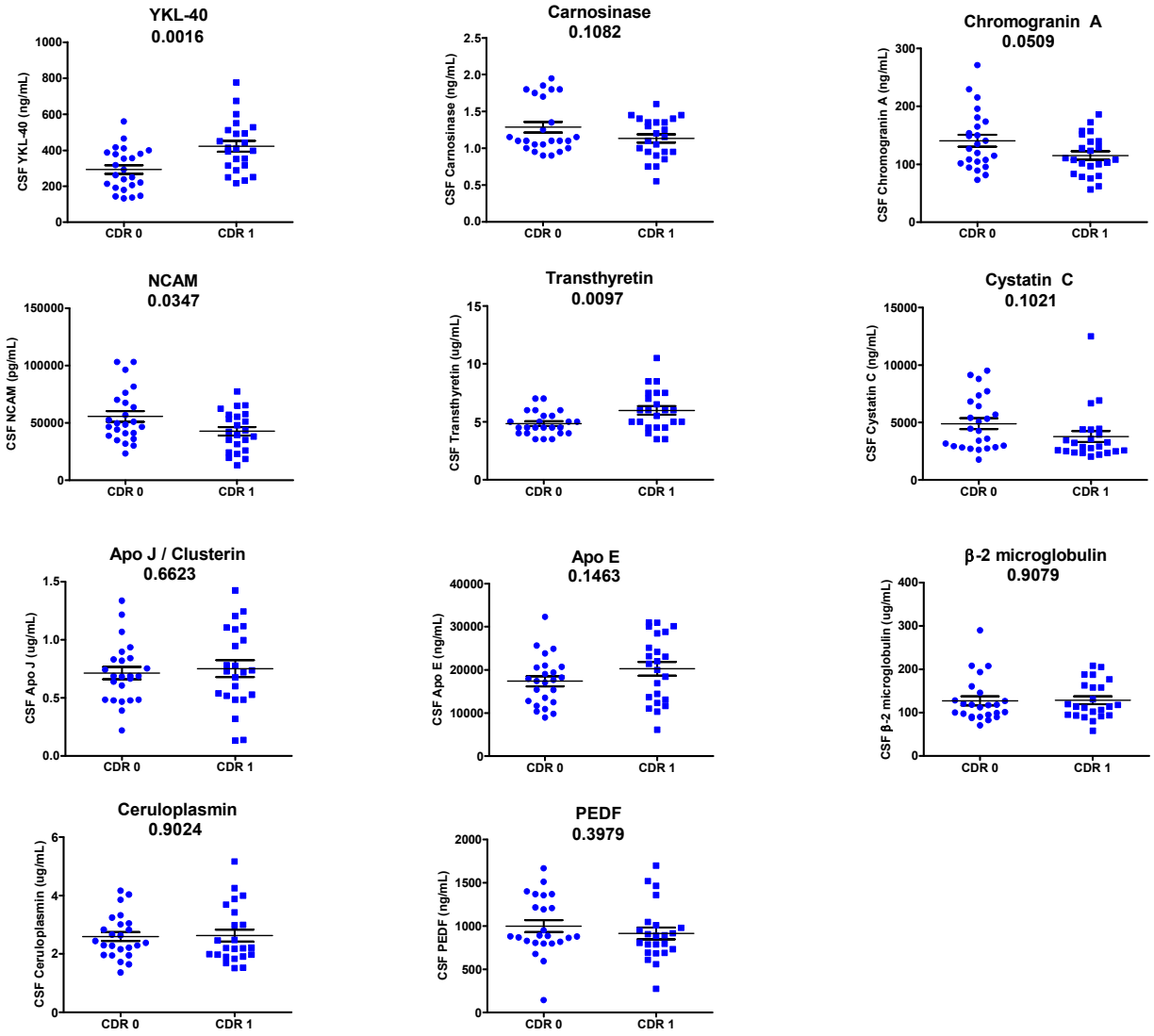

Figure 2.5. Quantitative ELISAs for 11 biomarker candidates were applied to the discovery cohort of CSF samples (one sample was unavailable for analysis, N=47). Each assay was performed in triplicate, with one mean value reported for each sample. The six assays represented in the upper row (NrCAM, YKL-40, chromogranin A, carnosinase I, transthyretin, and cystatin C) measured promising differences between these relatively small CDR 0 and CDR 1 groups (Student's T-test).

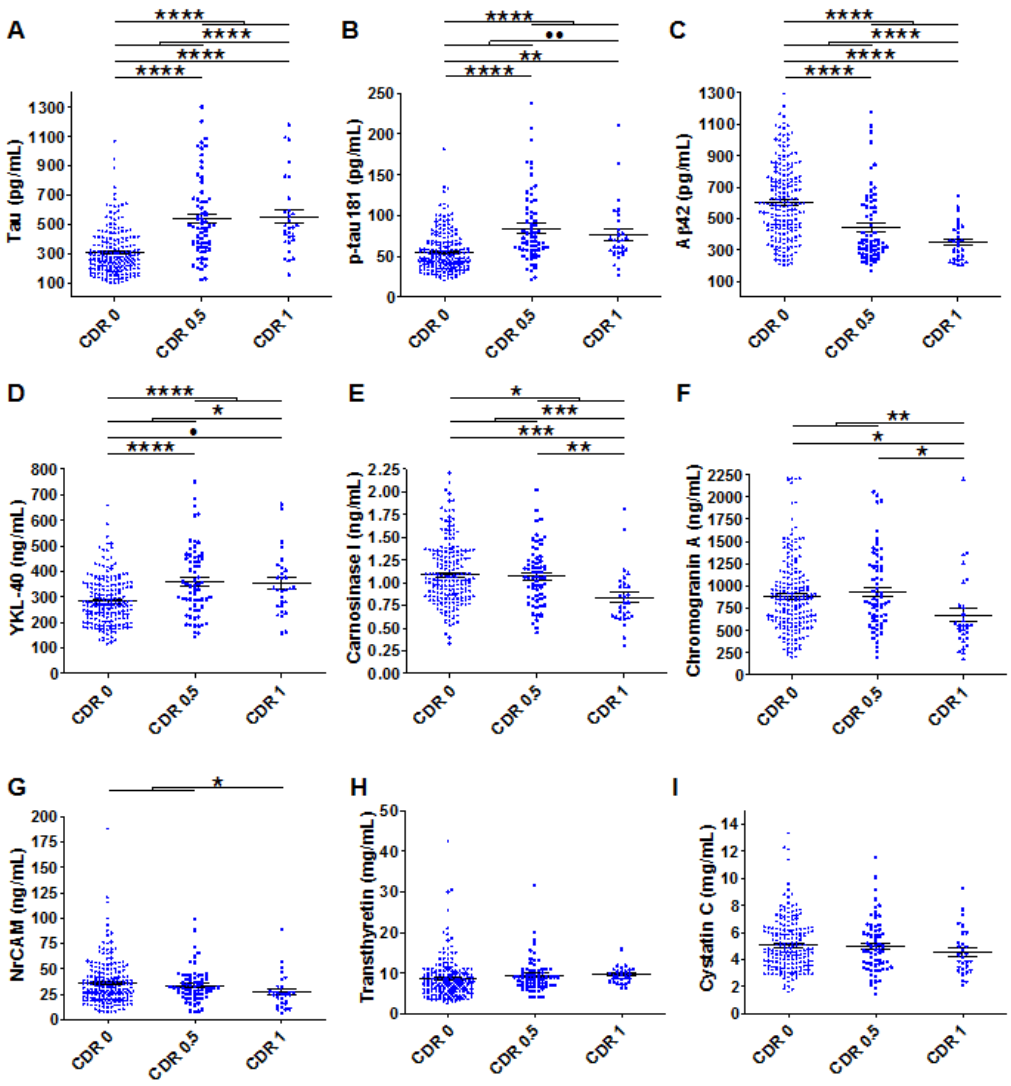

Figure 2.6. ELISAs for six biomarker candidates and established biomarkers tau, p-tau181 and Aβ42 applied to validation cohort CSF samples (N=292). Each candidate biomarker assay was performed in triplicate, with one mean value reported for each sample; assays for tau, p-tau181 and Aβ42 were performed in duplicate. In addition to **A**. tau, **B**. p-tau181 and **C**. Aβ42 (top row), four assays (**D**. YKL-40, **E**. carnosinase I, **F**. chromogranin A, **G**. NrCAM) measured statistical differences between clinically defined groups, as indicated; **H**. transthyretin and **I**. cystatin C did not reach criterion (α=0.05) for any comparisons. * p<0.05; * * p<0.01; * * * p< 0.001;

* * * * p<0.0001; solid circle p<0.05 by LSD only; double solid circle p<0.05 by unpaired T-test and Mann-Whitney, not by unpaired T-test with Welchs correction.

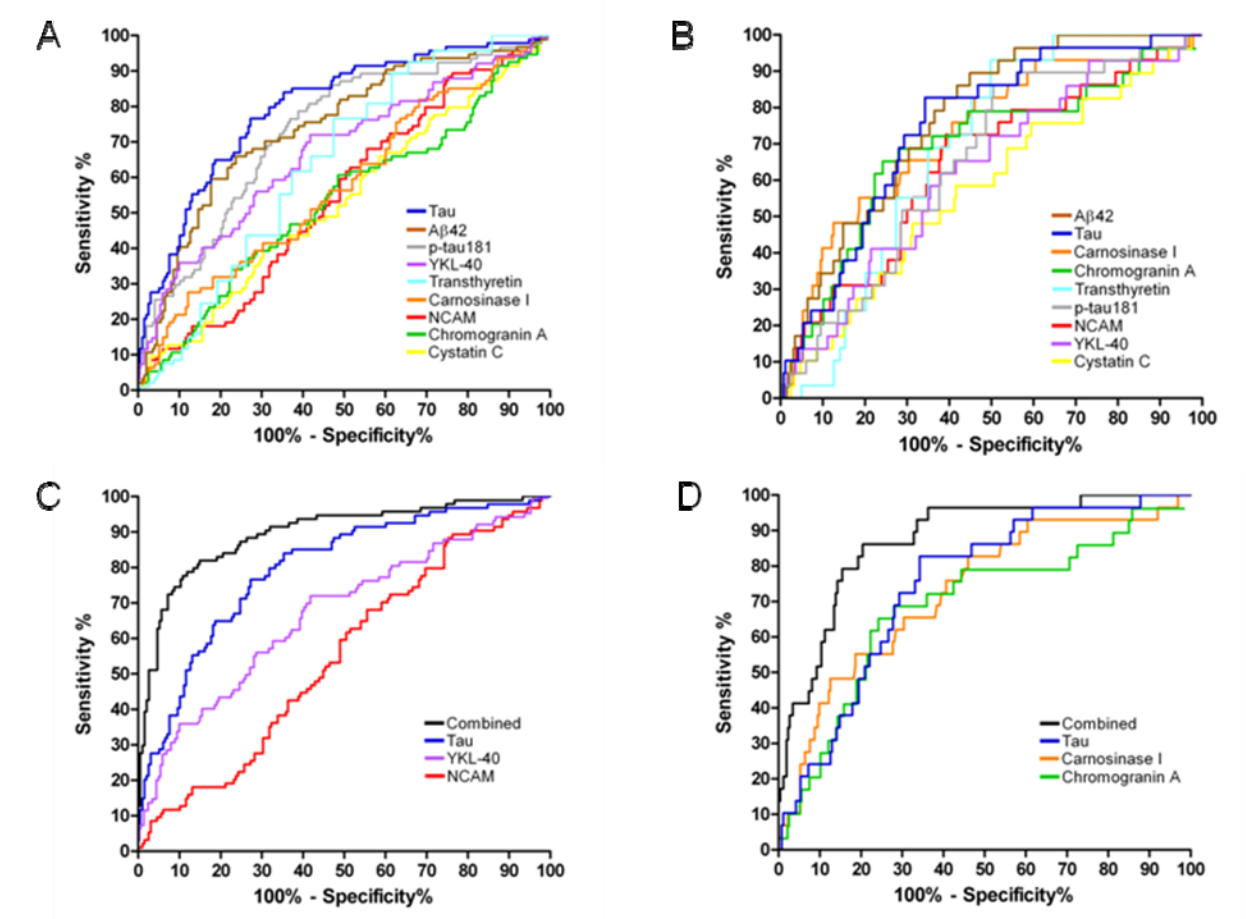

Figure 2.7. Receiver Operating Characteristic (ROC) curves of ELISA data from validation cohort. Simple ROC analyses were performed for each biomarker to distinguish **a)** CDR>0 from CDR 0 ("earlier diagnosis") and **b)** CDR 1 from CDR<1 ("early diagnosis"). Stepwise logistic regression models were used to identify combinations of these biomarkers that would distinguish **c)** CDR>0 from CDR 0 ("earlier diagnosis"), AUC = 0.90 and **d)** CDR 1 from CDR<1 ("early diagnosis"), AUC = 0.88.

Table 2.3A. Receiver Operating Characteristic Curve Areas for CDR 0 vs >0 Comparison

Biomarker	Area Under Curve	Standard Error	95% Confidence Interval
Tau	0.8004	0.0279	0.7457 - 0.8551
Aβ42	0.7429	0.0315	0.6812 – 0.8046
p-tau181	0.7339	0.0315	0.6721 – 0.7956
YKL-40	0.6717	0.0349	0.6033 – 0.7401
Transthyretin	0.6190	0.0331	0.5541 – 0.6838
Carnosinase I	0.5735	0.0365	0.5020 – 0.6450
NrCAM	0.5422	0.0355	0.4726 – 0.6118
Chromogranin A	0.5303	0.0373	0.4572 – 0.6034
Cystatin C	0.5297	0.0366	0.4579 – 0.6014
Logistic Regr.	0.8955	0.0212	0.8539 – 0.9372

Table 2.3B. Receiver Operating Characteristic Curve Areas for CDR 1 vs <1 Comparison

Biomarker	Area Under Curve	Standard Error	95% Confidence Interval
Aβ42	0.7690	0.0376	0.6953 - 0.8427
Tau	0.7502	0.0420	0.6679 – 0.8325
Carnosinase I	0.7277	0.0512	0.6273 – 0.8281
Chromogranin A	0.6879	0.0566	0.5771 – 0.7988
Transthyretin	0.6605	0.0380	0.5860 – 0.7350
p-tau181	0.6512	0.0483	0.5566 – 0.7458
NrCAM	0.6411	0.0553	0.5326 – 0.7495
YKL-40	0.6271	0.0532	0.5228 – 0.7313
Cystatin C	0.5752	0.0565	0.4645 – 0.6858
Logistic Regr.	0.8762	0.0314	0.8147 – 0.9377

Table 2.3. Statistical analyses associated with Receiver Operating Characteristic (ROC) curves of ELISA data from validation cohort. ROC analyses were performed for each biomarker to distinguish **A.** CDR>0 from CDR 0 ("earlier diagnosis") and **B.** CDR 1 from CDR<1 ("early diagnosis"). Stepwise logistic regression models were applied to identify a complementary combination of these biomarkers for each analysis

that would optimize accuracy (maximize area under the curve [AUC]) without including additional non-contributory biomarkers. In **A**, the stepwise logistic regression model accepted tau, YKL-40 and NrCAM and yielded an AUC of 0.8955 (Logistic Regr.). In **B**, the model accepted tau, carnosinase I and chromogranin A, yielding an AUC of 0.8762 (Logistic Regr.).

Table 2.4. CSF biomarkers grouped by functional/structural category

Functional / Structural Category	**Protein**
Adhesion molecules	N-Cadherin
	NrCAM
	Calsyntenin
	Neuronal Pentraxin Receptor
	Brain Associated Small Cell Lung Cancer Antigen (NCAM-140/CD56)
	Nectin-like molecule-1 / TSLL1 / SynCam3
Dense core vesicles	Chromogranin A
	Chromogranin B
	Secretogranin II
	Secretogranin III
	VGF NGF Inducible precursor
	Carboxypeptidase E
Synaptic/Neuronal metabolism	Aspartate aminotransferase I
Synaptic Function	S100A1 (binds synapsins)
	Neuronal Pentraxin Receptor (presynaptic)
	Brain Acetylcholinesterase Putative Membrane Anchor (CutA1)
	Calsyntenin (postsynaptic)
Neuroprotection	PEDF (Serpin-F1)
	Annexin I
	Prosaposin
	Secretogranin II
	Carnosinase I
Apoptosis / actin remodeling	Gelsolin
	Prk-1 (PKN)

Synaptic plasticity / learning and memory	VGF NGF inducible precursor
	NrCAM
	B3GnT1
	Carnosinase I
	Carbonic Anhydrase IV
	S100A1
	Carboxypeptidase E
	Calmodulin
Inflammation / Complement	YKL-40 / Chitinase 3-Like 1
	PEDF (Serpin-F1)
	Annexin I
	IHRP / ITIH4
	Vitronectin
	Complement C4B3
	Kininogen I
	Chromogranin A
	Secretogranin III
	Apolipoprotein J
	Beta 2-microglobulin
Prostaglandin metabolism	Prostaglandin H2 D Isomerase / Beta-trace
Amyloid beta peptide binding / amyloidogenesis	Apolipoprotein A1 (proapolipoprotein)
	Apolipoprotein E
	Apolipoprotein J
	Transthyretin
	Gelsolin
	Vitronectin
	Cystatin C

	Prostaglandin H2 D Isomerase / Beta-trace
	a-2-macroglobulin
	a-1-antichymotrypsin
Protease activity	a-1-antichymotrypsin
	a-2-macroglobulin
	Cystatin C
	Carboxypeptidase E
Matrix proteins	Fibulin 3 (EFEMP1)
	Vitronectin
Phospholipase activity	Annexin I (Lipocortin)
	Prosaposin
Apolipoproteins	Apolipoprotein A1 (proapolipoprotein)
	Apolipoprotein CII
	Apolipoprotein CIII
	Apolipoprotein E
	Apolipoprotein J
	Apolipoprotein H
Calcium binding / homeostasis	Calmodulin
	S100A1
	Annexin I (Lipocortin)
	Calsyntenin (post-synaptic cytoplasmic domain)
	Gelsolin
Metal (Copper and Iron) Binding	Carnosinase I
	Ceruloplasmin
	Brain Acetylcholinesterase Putative Membrane Anchor (CutA1)
Chaperone complex / activity	S100A1
	Transthyretin (prealbumin)

Endoplasmic Reticulum - Associated Degradation (ERAD)	Man9-mannosidase
Extracellular and Intraneuronal pH	Carbonic Anhydrase IV
	Carnosinase I
Glycobiology (lactosamine synthesis)	B3GnT1 (lactosamine synthesis)
CNS renin-angiotensinogen system	Angiotensinogen
Thyroid hormone transport	Transthyretin (prealbumin)
Unknown	Hypothetical protein

Table 2.4. Candidate CSF biomarkers reflect AD-related pathophysiological changes. Candidate CSF biomarkers are grouped according to reported function(s) and, when appropriate, cellular locations.

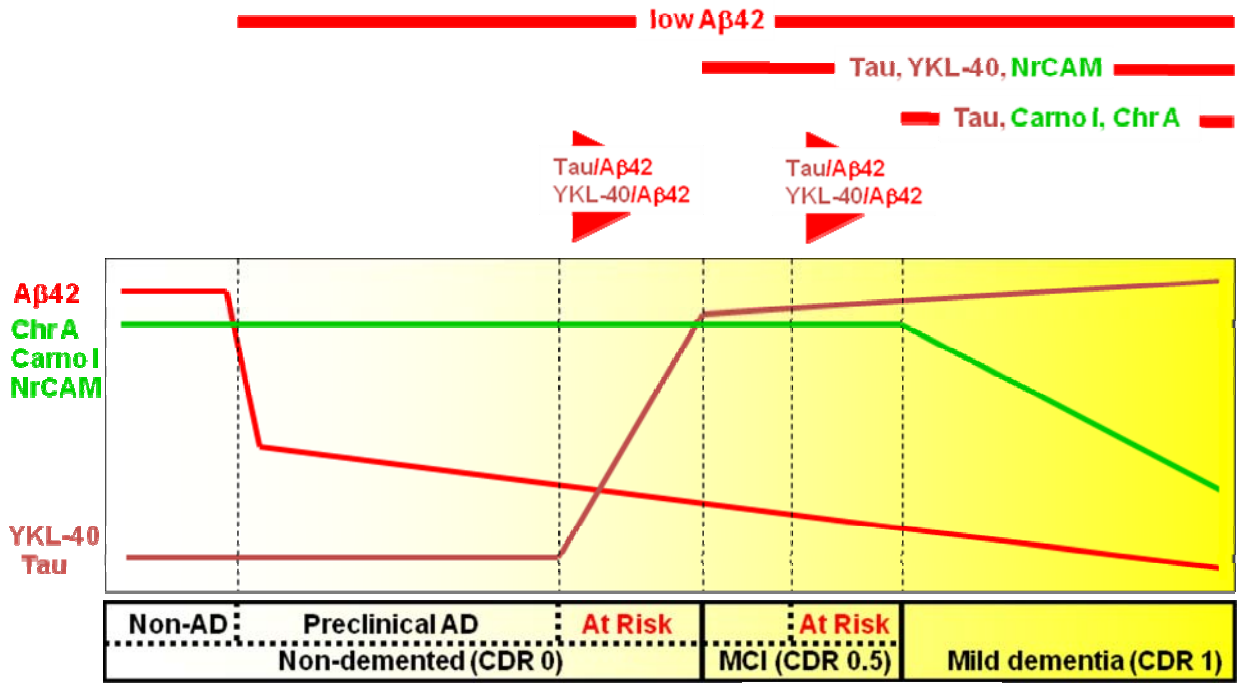

Figure 2.8. Hypothetical model to define early stages of AD by temporal pattern of CSF protein biomarker levels. The horizontal bar (below) describes the early clinicopathological progression from non-AD to mild dementia (CDR 1) in six stages. As depicted by the curves above, '**Non-AD**' CSF has high Aβ42 (red line), high chromogranin A (Chr A), carnosinase I (Carno I) and NrCAM (green line), and low YKL-40 and tau (blue line). Reduced CSF Aβ42 correlates with amyloid plaque deposits, the first sign of neuropathologically identifiable AD ("**preclinical AD**") (127). CSF Aβ42 appears to decline further as cognition declines from CDR 0 to 0.5 to 1. When considered as ratios with Aβ42, CSF markers of neuroinflammation (e.g. YKL-40) and neurofibrillary tangle pathology (e.g. tau) appear to increase before and predict the onset of very mild cognitive impairment (CDR 0.5), defining a **CDR 0 group 'At Risk'** for cognitive decline (107, 121, 132, 372); YKL-40 and tau also appear to be higher among those who progress rapidly from very mild to mild dementia, defining a **CDR 0.5 group 'At Risk'** for cognitive decline. Reductions in synapse-associated (NrCAM,

chromogranin A) and neuronal (carnosinase I) proteins, and increases in tau mirror the progression and anatomical spread of synaptic and neuronal losses and tau pathology associated with cognitive decline, and can be used to define **CDR 0.5** and **CDR 1**.

Chapter 3.

YKL-40: A Novel Diagnostic and Prognostic Fluid Biomarker for Preclinical and Early Alzheimer's Disease

Portions of this chapter will appear in the November 2010 issue of *Biological Psychiatry.*

Summary

Background: Disease-modifying therapies for Alzheimer's disease (AD) would be most beneficial if applied during the 'preclinical' stage (pathology present with cognition intact) before significant neuronal loss occurs. Therefore, biomarkers that can detect AD pathology in its early stages and predict dementia onset and progression will be invaluable for patient care and efficient clinical trial design.

Methods: Previously, 2D-difference gel electrophoresis and liquid chromatography tandem mass spectrometry were used to measure AD-associated changes in cerebrospinal fluid (CSF). Concentrations of one of the most promising candidates identified by this method, CSF YKL-40, were further evaluated by enzyme-linked immunosorbent assay in the discovery cohort (N=47), an independent sample set (N=292) with paired plasma samples (N=237), frontotemporal lobar degeneration (N=9), and progressive supranuclear palsy (PSP, N=6). Human AD brain was studied immunohistochemically to identify potential source(s) of YKL-40.

Results: In the discovery and validation cohorts, mean CSF YKL-40 was higher in very mild and mild AD-type dementia (Clinical Dementia Rating [CDR] 0.5 and 1) vs. controls (CDR 0) and PSP. Importantly, CSF YKL-40/Aβ42 ratio predicted risk of developing cognitive impairment (CDR 0 to CDR>0 conversion) as well as the best CSF biomarkers identified to date, tau/Aβ42 and p-tau181/Aβ42. Mean plasma YKL-40 was higher in CDR 0.5 and 1 vs. CDR 0 groups, and correlated with CSF levels. YKL-40 immunoreactivity was observed within astrocytes near a subset of amyloid plaques, implicating YKL-40 in the neuroinflammatory response to Aβ deposition.

Conclusions: These data demonstrate that YKL-40, a putative indicator of neuroinflammation, is elevated in AD, and that, together with Aβ42, has potential prognostic utility as a biomarker for preclinical AD.

Introduction

Clinicopathological studies suggest that the pathological hallmarks of AD, amyloid plaques and neurofibrillary tangles, begin to appear ~10-20 years before the synaptic and neuronal loss that accompany dementia onset (44, 66, 72). Identifying and treating individuals during this preclinical stage will maximize benefit from disease-modifying therapies. By definition, this preclinical phase of AD will elude detection by conventional clinical examination, and will therefore require the use of biomarkers for diagnosis. Beyond diagnosis, biomarkers may also provide prognostic information and facilitate the monitoring of disease progression and response to treatment. In addition, novel biomarkers may advance our understanding of AD pathophysiology, and thereby inform future treatment strategies.

Because many proteins expressed in the brain are present in the cerebrospinal fluid (CSF), the CSF proteome is a logical source for potential AD biomarkers. Indeed, CSF amyloid-β42 (Aβ42), tau, and phosphorylated forms of tau (p-tau) have already shown great promise for use in AD diagnosis and prognosis (410-413). Nevertheless, there remains a need for supplemental biomarkers that represent different aspects of AD pathophysiology and can improve diagnosis and prognosis at early disease stages.

To discover additional CSF biomarkers for early AD, we used two-dimensional difference gel electrophoresis in conjunction with tandem mass spectrometry (2-D DIGE LC-MS/MS) to identify proteins that increase or decrease in the setting of early AD relative to age-matched cognitively normal controls (see Chapter 2 for details). One protein found in that study to be significantly more abundant in AD CSF, YKL-40 (chitinase-3 like-1 [CHI3L1], human cartilage glycoprotein-39 [HC-gp39], and chondrex), is a secreted 40-kDa glycoprotein with sequence homology to bacterial and fungal chitinases and chitin binding ability, but no chitinase activity (379). Reports suggest a

role in inflammation and tissue remodeling, and an upregulation in AD brain (373), but its physiological function remains unclear (414, 415). Nevertheless, plasma/serum and/or CSF levels of YKL-40 have been proposed as a candidate biomarker for arthritis, asthma, multiple sclerosis, and myriad cancers (414-416).

In this study, we evaluate the potential of CSF and plasma YKL-40 to serve as diagnostic and prognostic biomarkers for AD; additionally, using immunohistochemistry, we investigate the source(s) of YKL-40 in the brain in the setting of AD. Our data suggest that CSF YKL-40 is produced by astrocytes, is significantly elevated in very mild and mild AD, and predicts conversion from cognitive normalcy to very mild cognitive impairment.

Methods

Subjects

Discovery cohort: Subjects (N=48), community-dwelling volunteers from University of Washington (N=18), Oregon Health and Science University (N=11), University of Pennsylvania (N=11), and University of California San Diego (N=8), were 51-87 years of age and in good general health, having no other neurological, psychiatric, or major medical diagnoses that could contribute importantly to dementia, nor use of exclusionary medications within 1-3 months of lumbar puncture (LP) (e.g. neuroleptics, anticonvulsants, anticoagulants). Study protocols at each institution were approved by their respective Institutional Review Boards and written informed consent was obtained from each participant. Cognitive status was evaluated based on criteria from the National Institute of Neurological and Communicative Diseases and Stroke-Alzheimer's Disease and Related Disorders Association (57). CSF was collected in the morning by LP after overnight fasting and immediately frozen at -80°C. Subjects with a clinical dementia rating (CDR) of 0 (N=24), indicating no dementia, and CDR 1 (N=24), indicating mild

dementia, were selected from a larger group of 120 samples on the basis of CSF Aβ42 (relatively high and low values, respectively), and, when possible, CSF tau (relatively low and high values, respectively) to increase the likelihood of CDR 1 subjects having and CDR 0 subjects not having AD pathology. CSF Aβ42 and tau levels were measured in a single laboratory using well-established ELISAs ((366) and Innotest, Innogenetics, respectively). Quantitative thresholds were not defined prior to sample selection; the lowest CDR 0 and highest CDR 1 CSF Aβ42 value were 572 and 399 pg/mL, respectively; CSF tau ranges were CDR 0: 141-448 pg/mL, CDR 1: 216-1965 pg/mL.

Validation cohort: Subjects (N=292), community-dwelling volunteers enrolled in longitudinal studies of healthy aging and dementia at the Washington University Alzheimer Disease Research Center (WU-ADRC), were ≥60 years of age and met the same exclusion criteria as the discovery cohort. The study protocol was approved by the Human Studies Committee at WU, and we obtained written and verbal informed consent from participants at enrollment. CDR status was determined as with the discovery cohort, with an additional category of CDR 0.5, indicating very mild dementia; some of these met criteria for MCI and some were more mildly impaired, or "pre-MCI" (70). A subset of subjects (N=159) underwent positron emission tomography (PET) imaging with Pittsburgh Compound-B (PIB) for assessment of in vivo amyloid burden (127, 318, 330). Apolipoprotein E (*APOE*) genotypes were determined by the WU-ADRC Genetics Core. Fasted CSF was collected, mixed, centrifuged, and frozen at -80°C in polypropylene tubes; blood was collected at the time of LP, and plasma prepared by centrifugation and stored at -80°C (107).

FTLD/PSP Cohort: Volunteer subjects were diagnosed with frontotemporal lobar degeneration (FTLD) (N=9) or progressive supranuclear palsy (PSP) (N=6) at the

University of California San Francisco (UCSF) Memory and Aging Center using published criteria (417, 418). Subjects in the FTLD group met criteria for one of the three clinical syndromes that comprise FTLD: frontotemporal dementia (FTD) (N=6), semantic dementia (SD) (N=1), and progressive non-fluent aphasia (PNFA) (N=2) (417). The study protocol was approved by the UCSF Committee on Human Research, and informed consent was obtained from all participants. CSF was collected by LP and immediately frozen at -80°C.

2-D DIGE LC-MS/MS Proteomic Analysis

Details for sample processing and analysis can be found in Chapter 2. In brief, discovery cohort CSF samples and a pooled reference sample were immunodepleted of six highly abundant proteins (albumin, IgG, α1-antitrypsin, IgA, haptoglobin, transferrin). Samples were randomly paired (CDR 0 and CDR 1), labeled with one of three cyanine dyes, and loaded with the labeled reference sample onto the same 2-D gel. Protein spot quantification and between-gel spot matching were performed on digitized images. To focus efforts on candidate biomarkers more likely to be measurable in the CSF of a majority of individuals, only gel features with significant intensity differences between CDR 0 and CDR 1 groups (Student's t-test, $\alpha=0.05$) that were present in >50% of gels were excised, trypsinized, and subjected to LC-MS/MS. Proteins were identified from peptide fragmentation spectra using MASCOT (v2.8, Matrix Sciences) and the NCBI non-redundant protein database (downloaded 11/11/2008).

Enzyme Linked Immunosorbent Assays (ELISAs)

CSF and plasma samples were analyzed by ELISA for Aβ42, total tau, and phospho-tau181 (Innotest, Innogenetics) after one freeze-thaw, and for YKL-40 (Quidel) after two freeze-thaw cycles. Intra- and inter-assay coefficient of variation for CSF YKL-40 were 5.27% and 6.03%, respectively; for plasma, 5.73% and 11.26%.

Statistical Analyses

Correlations were evaluated using the Pearson rho correlation coefficient (α=0.05). Survival analyses assessed the ability of baseline biomarkers and biomarker ratios to predict time to conversion from cognitive normalcy (CDR 0) to very mild or mild dementia (CDR 0.5, 1) and time to progression from very mild dementia (CDR 0.5) to more severe dementia (CDR>0.5). Data from subjects who did not convert/progress were statistically censored at the date of last assessment. Biomarker measurements were converted to standard Z-scores to allow comparison of hazard ratios between different biomarkers. Cox proportional hazard models adjusted for age and gender were conducted treating the CSF biomarkers as continuous and categorical variables. Categorical analyses compared subjects within the highest tertile of baseline values to those within the lowest two tertiles; this tertile-based assessment was applied because Kaplan-Meier curves illustrating the unadjusted time to CDR>0 for each tertile of each biomarker suggested similar outcomes for the lower two tertiles. The difference between the survival curves reflecting the upper tertile versus the lower tertiles of each biomarker was tested using the log-rank test. Survival analyses were conducted using baseline CDR scores determined at clinical assessment prior to LP; analyses using scores determined at clinical assessment closest to LP yielded almost identical results. Similar survival analyses were carried out for plasma YKL-40.

Immunohistochemistry

Six-µm-thick sections of formalin-fixed, paraffin-embedded human postmortem brain tissue (middle frontal gyrus, post mortem interval <6 hrs) from the WU-ADRC Neuropathology Core were double-labeled using rabbit anti-human YKL-40 antibody (Quidel) in series with either goat anti-human GFAP (Santa Cruz), mouse anti-human HLA Class II antigen, LN-3 (Novocastra), RCA-1 (Vector), or mouse anti-human PHF-1 (gift of Dr. Peter Davies), followed by staining with the ImmPress kit (Vector). In control experiments, the primary antibody was omitted and replaced with 1% bovine serum albumin-PBS. Thioflavin S stain (1% aqueous) was applied for 20 minutes and destained with 50% ethanol.

Results

Proteomic Analysis Identifies YKL-40 as Increased in AD CSF

To identify new candidate biomarkers for AD, we utilized an unbiased proteomics approach, 2-D DIGE LC-MS/MS (222, 251), to compare the concentrations of CSF proteins in individuals with mild dementia (CDR 1, N=24) of the Alzheimer's type to those in individuals without dementia (CDR 0, N=24) (see Chapter 2 for details of this portion). The two groups differed with respect to age at LP and gender (CDR 0: 64.8 yrs, 38% female; CDR 1: 72.8 yrs, 54% female). From this proteomic analysis, we identified 47 proteins that differed in abundance between the CDR 0 and CDR 1 groups (Chapter 2); one of the most promising, in terms of fold-change and novelty, was YKL-40. Interestingly, in a smaller, previous study, we identified YKL-40 as being significantly more abundant in CSF from CDR 0.5 relative to CDR 0 subjects (251). YKL-40 appeared in four gel features that were more abundant in the CDR 1 group (Figure

3.1A). Tryptic peptides from these spots collectively provide amino acid sequence coverage of 52% and span virtually the full length of the protein (Figure 3.1B), suggesting that these spots represent full-length secreted YKL-40. We hypothesize that this pattern of four spots may be due to allelic differences, post-translational modifications, or both.

ELISA Confirms Increased CSF YKL-40 in AD in Original and Independent Cohorts

To validate our 2-D DIGE findings, we applied a YKL-40 ELISA to the original 'discovery' cohort samples (one sample was unavailable for re-evaluation, N=47). Mean CSF YKL-40 was increased 43% in the CDR 1 vs CDR 0 group (p=.0016) (Figure 3.2A), consistent with the fold-changes measured by 2-D DIGE. We next assayed a larger, independent set of CDR 0, 0.5, and 1 CSF samples collected at the WU-ADRC (N=292) that was not preselected on the basis of CSF Aβ42 and tau values (characteristics at baseline assessment in Table 3.1). In this validation cohort, mean CSF YKL-40 was significantly (27%) higher in the CDR 0.5 and CDR 1 groups vs. CDR 0 ($p<.0001$ and $p=.004$, respectively) (Figure 3.2B). An analysis of covariance (ANCOVA) revealed that this increase remained significant after adjusting for age, $F(2, 288) = 9.075$, $p<.0001$.

CSF YKL-40 is Increased in FTLD and Decreased in PSP

In an effort to determine whether CSF YKL-40 might have potential to distinguish AD from other dementing illnesses, we evaluated levels in two other neurodegenerative diseases: frontotemporal lobar degeneration (FTLD, N=9) and progressive supranuclear palsy (PSP, N=6). Mean CSF YKL-40 was increased in FTLD relative to AD, although a wide range of values was observed, possibly reflecting the pathological heterogeneity of FTLD; in contrast, PSP cases showed relatively low levels and range of CSF YKL-40 (Figure 3.3A). Although this study does not evaluate the complete differential diagnosis

for mild cognitive impairment or mild dementia, these data suggest that CSF YKL-40 may be useful to distinguish AD from some other forms of neurodegenerative disease.

Correlation of CSF YKL-40 With Demographic Features and Other Biomarker Values

Because the CDR 0, 0.5, and 1 groups show somewhat different distributions with regard to age at LP, gender, and *APOE* genotype, levels of CSF YKL-40 were evaluated for potential correlation with these variables. CSF YKL-40 levels did not vary based on gender (p=.8355) or *APOE* genotype (not shown) but did correlate with increasing age (r=.3943, p<.0001) (Figure 3.4). Next, seeking insight into the role of YKL-40 in AD pathology, we evaluated its associations with CSF Aβ42, CSF tau, and cortical amyloid burden measured by PIB-PET imaging. In this validation cohort, CSF YKL-40 did not correlate with CSF Aβ42 (r=-.02463, p=.6745), but did correlate with CSF tau (r=.6331, p<.0001), and p-tau181 (r=.5947, p<.0001), and modestly with cortical amyloid burden (r=.2093, p=.0081) (Figure 3.4). Interestingly, a similar correlation of CSF YKL-40 with tau was observed in FTLD (r=.9109, p=.0006), but not in PSP (r=.2434, p=.6422) (Figure 3.3B,C), suggesting that these two biomarkers are not inextricably linked, and that they may reflect separate but interrelated pathophysiological processes.

Ability of CSF YKL-40 To Predict Onset and Progression of Dementia

Recognizing the need for preclinical diagnosis and prognosis, we applied survival analyses to evaluate whether CSF YKL-40 can predict risk of developing cognitive impairment (conversion from CDR 0 to CDR>0) and of dementia progression (CDR 0.5 to CDR>0.5). Of the 174 CDR 0 subjects with at least one follow-up clinical assessment, 26 received a CDR>0 at follow-up, and thus were classified as "converters." Since CSF

tau/Aβ42 and p-tau181/Aβ42 ratios have been shown to predict cognitive decline in cognitively normal (107, 132) and MCI (348, 419) cohorts, survival analyses were also conducted for these biomarkers. Treated as categorical variables, subjects with high ratios (upper tertile) of CSF YKL-40/Aβ42, tau/Aβ42, and p-tau181/Aβ42 were faster to convert to CDR>0 than were subjects with lower ratios (lower tertiles) (Figure 3.5A), even after adjusting for age and gender (Figure 3.6). Likewise, when treated as continuous variables, CSF YKL-40/Aβ42, tau/Aβ42, and p-tau181/Aβ42 ratios again predicted conversion from CDR 0 to CDR>0 ($p=0.0003$, $p=0.0001$, $p<.0001$, respectively) after adjustment for age and gender (Figure 3.6). Importantly, when evaluated individually, CSF YKL-40, Aβ42, tau, and p-tau181 did not perform as well as the YKL-40/Aβ42, tau/Aβ42, and p-tau181/Aβ42 ratios at predicting conversion from CDR 0 to CDR>0 (Figure 3.7). Thus, the CSF YKL-40/Aβ42 ratio, as a prognostic biomarker of future cognitive impairment in normal individuals, is comparable to the best CSF biomarkers of this type to date, tau/Aβ42 and p-tau181/Aβ42.

Of the 59 CDR 0.5 subjects with at least one follow-up clinical assessment, 24 received a CDR>0.5 at follow-up, and thus were classified as "progressors." Kaplan-Meier estimates of the rate of progression suggest that those with high CSF YKL-40/Aβ42 ratios (upper tertile) were faster to progress to CDR>0.5 than those with lower CSF YKL-40/Aβ42 ratios (lower two tertiles) ($p=.0648$) (Figure 3.5B). The tau/Aβ42 and p-tau181/Aβ42 ratios showed similar patterns (Figure 3.5B). After adjustment for age and gender, similar results were found for all three categorical biomarker variables (Figure 3.6). Treated as a continuous variable and adjusted for age and gender, p-tau181/Aβ42 and YKL-40/Aβ42 ratios showed trends associated with time to progression that did not reach statistical significance (Figure 3.6).

Plasma YKL-40 Demonstrates Limited Utility as AD Biomarker

To evaluate plasma YKL-40 as a potential AD biomarker, we applied the ELISA to 237 plasma samples from the validation cohort. Mean plasma YKL-40 was significantly higher in the CDR 0.5 and CDR 1 vs CDR 0 group (p=.046, p=.031, respectively, One-way ANOVA, Tukey post-hoc), with percent increases similar to those observed in CSF (Figure 3.8A). Plasma and CSF YKL-40 levels correlated modestly (*r*=.2376, p=.0002) (Figure 3.8B), with levels roughly 5-fold higher in CSF. Plasma YKL-40 also correlated with increasing age (*r*=.2284, p=.0004), but not with gender (p=.6558), CSF Aβ42 (*r*= -.07902, p=.2255), CSF tau (*r*=.03769, p=.5637), CSF p-tau181 (*r*=-.02738, p=.6749), or cortical amyloid load (*r*=.01789, p=.8576) (Figure 3.9). Plasma YKL-40 did not demonstrate utility for predicting cognitive decline (not shown).

In AD Brain, YKL-40 is Expressed in Astrocytes in Vicinity of Plaques and in Rare White Matter Neurons

To investigate potential source(s) of YKL-40 in AD, we performed single and double-label immunohistochemistry on human frontal cortex. YKL-40 immunoreactivity was observed in the vicinity of a subset of thioflavin S-positive amyloid plaques (Figure 3.10A,B,C) within GFAP-positive astrocytes (Figure 3.10D), and not within microglia stained with LN-3 (Figure 3.10E,F) or lectin RCA-1 (not shown). YKL-40 immunoreactivity was also present in plaque-associated cell processes (Figure 3.10G) that lacked reactivity for dystrophic neurite marker PHF-1 (Figure 3.10H) and microglial marker LN-3 (Figure 3.10J,K,L representing adjacent focal planes), and that may represent astrocytic processes (suggested in Figure 3.10I by the plaque-associated YKL-40-positive astrocyte in lower left quadrant). YKL-40 immunoreactivity was also observed within the superficial cortical white matter in rare neurons (Figure 3.10M,N,O) with occasional PHF-1-positive neurofibrillary tangles (Figure 3.10N,O). These neurons

may represent cells of multiform layer VI and/or 'interstitial neurons' of the white matter (420).

Discussion

This study suggests that CSF YKL-40, a novel inflammatory biomarker for AD, is increased in AD, and, together with Aβ42, will assist in prognosis of patients and clinical trial participants who are under examination for the preclinical and early clinical stages of AD.

Having identified CSF YKL-40 as a potential AD biomarker through non-biased proteomics, we verified this finding using a commercially available ELISA, and more importantly, validated the results in a much larger, independent cohort. By including very mildly impaired (CDR 0.5) individuals who may be classified at some other institutions as having MCI, or even "pre-MCI," as some were insufficiently impaired to meet MCI criteria, this validation cohort revealed the promise of CSF YKL-40 as a biomarker for very early stage AD. By including individuals with FTLD and PSP, albeit in small numbers, we also demonstrated that CSF YKL-40 shows promise for distinguishing AD from PSP.

By including individuals who were cognitively normal at the time of CSF collection, but subsequently developed cognitive impairment, this validation cohort also revealed the potential utility of YKL-40, coupled with Aβ42, to predict cognitive decline. It has previously been shown that ratios of CSF tau/Aβ42 and p-tau181/Aβ42 can predict conversion from cognitively normal to cognitively impaired over a 2-4 year period (107, 132). Here we confirm those findings in a cohort of twice the size, and show that CSF YKL-40/Aβ42 has predictive value comparable to that of these best current CSF measures. This finding is particularly notable because, whereas CSF tau is derived

principally from neurons, YKL-40 appears to be secreted predominantly from astrocytes. To our knowledge, YKL-40 is the first astrocyte-derived marker shown to be useful in such a way. CSF YKL-40/Aβ42 also showed promise in predicting progression of dementia from CDR 0.5 to CDR>0.5. However, tau/Aβ42 and p-tau181/Aβ42 appear to show greater utility for predicting progression.

We also evaluated plasma YKL-40 as a potential AD biomarker. While plasma YKL-40 levels displayed a pattern of elevation in the CDR 0.5 and 1 groups similar to that observed for CSF, and plasma and CSF levels were modestly correlated, plasma YKL-40 did not show similar prognostic utility. Whether this increase in plasma YKL-40 reflects passive or active export of central nervous system (CNS)-derived YKL-40 or coincident peripheral production in response to a systemic inflammatory signal is unclear. Similar coincident elevations of CSF and serum YKL-40 levels have been reported with aneurysmal subarachnoid hemorrhage (421) and multiple sclerosis (416). However, in the setting of CNS infection, CSF levels of YKL-40 appear to rise without a concomitant increase in serum levels (375, 376), suggesting that YKL-40 produced in the brain does not influence serum/plasma levels. Data to address the converse- whether YKL-40 produced in the periphery can influence CSF levels- have not yet been reported. This issue is important to assess in future studies because peripheral inflammatory and neoplastic conditions are not uncommon within populations most likely to be screened for AD.

To examine its role in AD and to identify potential sources of CSF YKL-40, we immunohistochemically double-labeled human AD brain tissue for YKL-40 and other cell-specific markers, and observed YKL-40 in a subset of plaque-associated astrocytes and in rare white matter neurons. These results should help to clarify the origins of CSF YKL-40, which have been controversial among the small number of relevant studies (375, 383, 422). Additionally, the pattern of expression within a subset of plaque-associated

astrocytes may account for the positive correlation we observe between CSF YKL-40 and cortical amyloid load (Figure 3.4); as amyloid plaque burden increases, so does the amount of plaque associated-astrocyte activation, and likely, the amount of CSF YKL-40. It may also account for the lack of correlation we observe between CSF YKL-40 and CSF Aβ42, and for the relatively equal levels of CSF YKL-40 between CDR 0.5 and CDR 1 groups; once plaque formation commences, which is estimated to occur ~15 years prior to cognitive decline (410, 411, 413), CSF Aβ42 remains at a low steady state (94, 127, 128, 423), so no correlation with YKL-40 would be expected. Likewise, amyloid burden appears close to its maximal extent once cognitive decline begins (107, 127, 128), so plaque burden and CSF YKL-40 levels might be expected to be similar in CDR 0.5 and CDR 1 groups. More importantly, these results implicate YKL-40 in the astrocytic neuroinflammatory response to fibrillar Aβ deposition that appears to play a role in AD pathogenesis (207, 424, 425).

What induces YKL-40 expression in the presence of AD pathology, and how increased YKL-40 expression may influence the disease process are unknown. In models of peripheral inflammation such as asthma and arthritis, tumor necrosis factor-α (TNF-α) and interleukin-1β (IL-1β) appear to stimulate YKL-40 synthesis in macrophages and chondrocytes (382, 426). Since TNF-α and IL-1β are implicated in AD neuroinflammation, it is reasonable to hypothesize that astrocytic expression of YKL-40 may be similarly induced. Given that TNF-α and IL-1β can cross the blood brain barrier, it is also reasonable to hypothesize that YKL-40 levels in plasma and CSF might be modulated by systemic or central inflammation. Defining the factors required to induce YKL-40 expression in astrocytes will be an important first step in understanding the role of YKL-40 in AD and, more generally, in the CNS.

Defining the targets of YKL-40 in the brain is also critically important for understanding its role in AD. In the periphery, YKL-40 can reportedly stimulate

connective tissue cell growth (427, 428); modulate the effects of inflammatory cytokines in fibroblasts (381); bind collagen and influence its fibrillogenesis (429); stimulate endothelial cell migration (430); modulate vascular smooth muscle cell adhesion and migration (431); support antigen-induced Th2 inflammatory responses (432); and stimulate alveolar macrophages to release metalloproteinases and pro-inflammatory and fibrogenic chemokines (382). In the brain, YKL-40 is reported to release extracellular matrix-bound bFGF (375). Clearly, further study of YKL-40 in AD and, more generally, within the CNS and periphery, is warranted to define its pathophysiological role(s).

This study identifies YKL-40 as a novel astrocyte-derived CSF biomarker that can distinguish groups of AD and control subjects and predict risk of developing dementia among cognitively normal subjects. Nevertheless, like all AD biomarker candidates to date, YKL-40 is likely to have less value when applied in isolation, and, alone, will be insufficient to provide definitive information for an individual patient. While significant differences in mean CSF and plasma YKL-40 levels exist between CDR 0 and CDR 0.5, and CDR 0 and CDR 1 groups, the ranges of YKL-40 values among the groups show considerable overlap. This overlap may stem from several sources. The greatest contribution is likely due to the inclusion of individuals with asymptomatic (preclinical) AD pathology in the CDR 0 group; AD neuropathology is present in ~25% of non-demented individuals age ≥75 years (150, 433). It is also possible that different alleles of the *CHI3L1* gene may influence baseline or reactive levels of YKL-40 protein expression, or that members of this cohort may be afflicted by other diseases that affect CSF YKL-40 levels. For example, elevated CSF YKL-40 has been reported in the setting of other CNS pathologies (375, 376, 416, 421); however, most of these conditions would be easily distinguishable from early AD on the basis of clinical assessment. It is important to note that the overlap observed for CSF YKL-40 is comparable to that seen for the best biomarkers identified to date, CSF Aβ42 and CSF tau (Figure 3.2 D&E)

(346). The best use of YKL-40 may be in a panel of biomarkers that provide complementary information to guide diagnosis, prognosis, clinical trial design, and treatment decisions. Indeed, in other work stemming from this 2-D DIGE study, stepwise logistic regression analyses indicate that YKL-40, as part of a panel with other CSF biomarkers, contributes additional sensitivity and specificity for discriminating mildly demented individuals from cognitively normal individuals (see Chapter 2). Additionally, YKL-40 may confer specificity to a panel by distinguishing PSP or other illnesses from AD, as our early results suggest. It will be of interest in future studies to confirm these results and to evaluate CSF YKL-40 levels in the setting of additional dementing conditions. Perhaps more importantly, YKL-40, for its own part, might contribute diagnostic sensitivity for early cognitive impairment, prognostic information for risk of cognitive decline in normal and very mildly impaired individuals, and, more fundamentally, a direct estimate of neuroinflammation, which tau and Aβ42 do not provide.

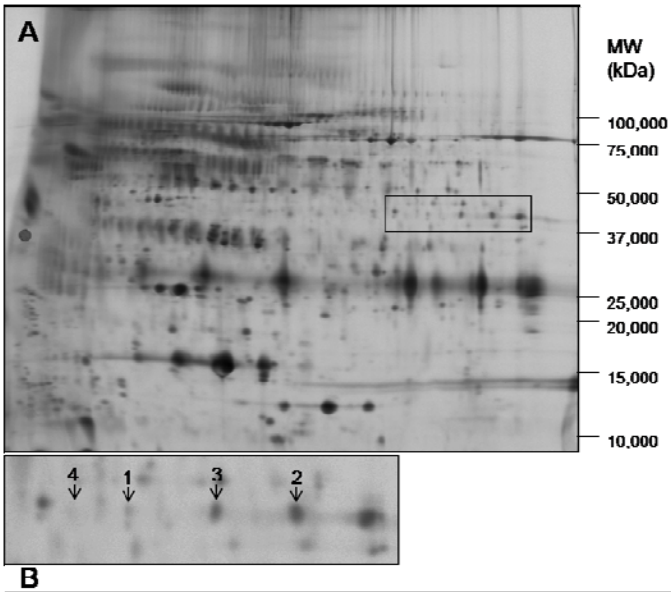

Figure 3.1. **(A)** A representative 2-D DIGE image of CSF from the discovery cohort. Samples were depleted of six highly abundant proteins, fluorescently labeled, and subjected to isoelectric focusing followed by SDS-PAGE. YKL-40 is more abundant in four spots in the CDR 1 group (labeled 1-4 in the inset, with mean fold changes of 1.41, 1.50, 1.46, 1.32, respectively). The near invisibility of spot 4 in this printed representation illustrates the great sensitivity of 2-D DIGE to detect proteins of low abundance. **(B)** Sequence coverage of human YKL-40 by mass spectrometry. Indicated in red is the compilation of peptides identified in the four spots. The signal sequence is shown in green, and polymorphisms are indicated by boxes.

Table 3.1. Demographic, Clinical, and Genotypic Characteristics of Validation Cohort			
Characteristic	**CDR 0**	**CDR 0.5**	**CDR 1**
n	198	65	29
Gender (% Female)	63%	54%	52%
***APOE* genotype, % ε4+**	35%	51%	59%
Mean MMSE score (SD)	28.9 (1.3)	26.3 (2.8)	22.3 (3.9)
Mean age at LP (SD), yrs	71.0 (7.3)	73.8 (6.8)	76.5 (6.2)
Mean CSF Aβ42 (SD), pg/mL	605 (240)	446 (230)	351 (118)
Mean CSF tau (SD), pg/mL	304 (161)	539 (276)	552 (263)
Mean CSF ptau181 (SD), pg/mL	55 (25)	85 (44)	77 (38)

Table 3.1. Demographic, Clinical, and Genotypic Characteristics of Validation Cohort.

Abbreviations: CDR, Clinical Dementia Rating; *APOE*, apolipoprotein E; MMSE, Mini-Mental State Examination; LP, lumbar puncture; SD, standard deviation; CSF, cerebrospinal fluid; Aβ-42, amyloid-beta peptide 1-42; ptau181, tau phosphorylated at threonine 181.

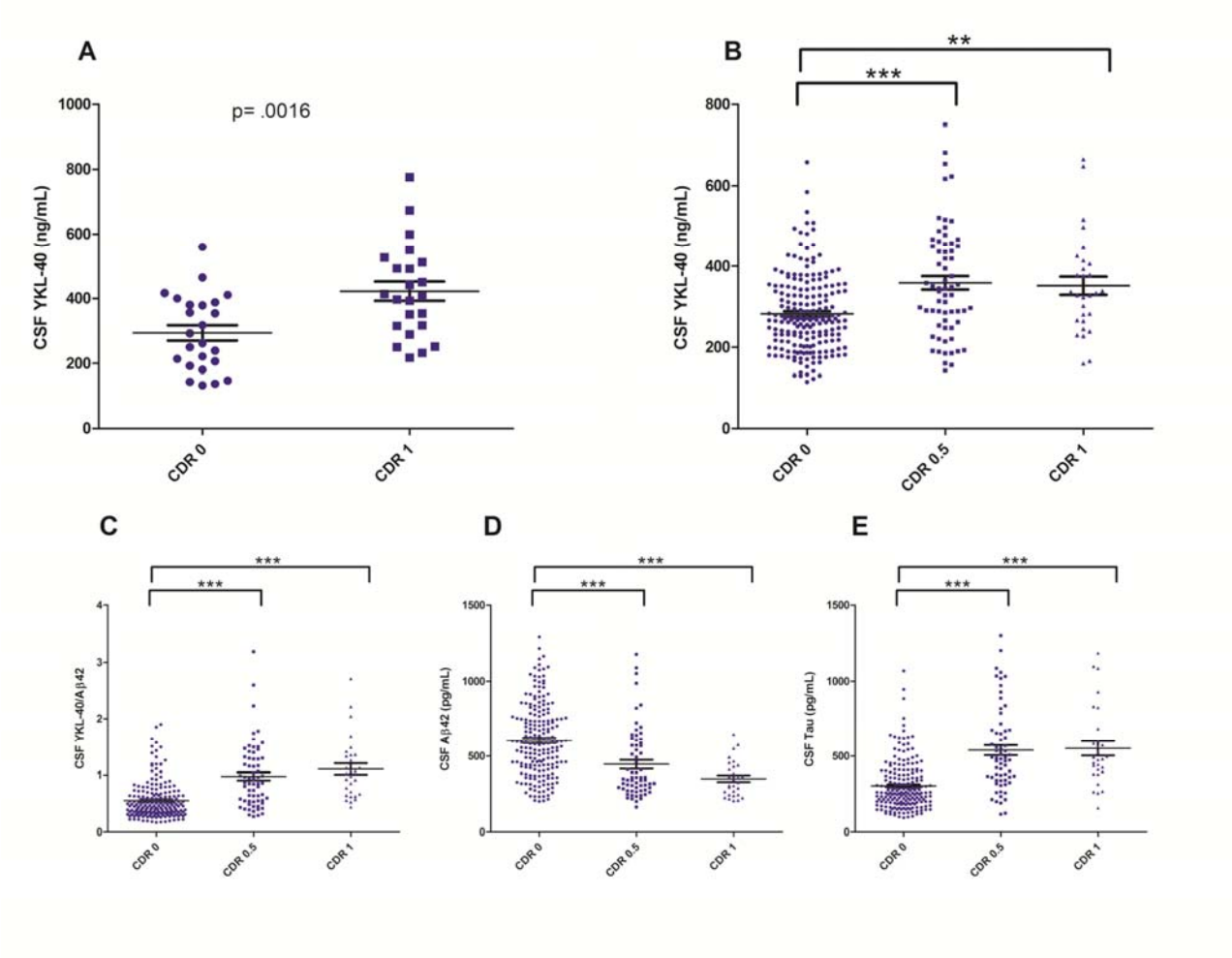

Figure 3.2. Mean YKL-40 is increased in the CSF of CDR 0.5 and CDR 1 subjects. **(A)** CSF from the discovery cohort (CDR 0, N= 24; CDR 1, N=23) was analyzed for YKL-40 by ELISA (CDR 0= 293.6 +/- 23.9; CDR 1= 422.2 +/- 30.0, ng/mL, mean +/- SEM). CSF YKL-40 was significantly higher in the CDR 1 group as compared to the CDR 0 group (p=.0016, unpaired student's t-test). **(B)** CSF from a larger, independent sample set (N=292) was analyzed for YKL-40 by ELISA. Mean CSF YKL-40 was significantly higher in the CDR 0.5 and CDR 1 groups as compared to the CDR 0 group (** p=.004, *** p<.0001; One-way ANOVA with Welch's correction for unequal variances, Tukey post-hoc Test) (CDR 0= 282.1 +/- 6.7; CDR 0.5= 358.9 +/- 16.9; CDR 1= 351.7 +/- 22.6, ng/mL, mean +/- SEM). **(C)** Mean CSF YKL-40/Aβ42 was significantly higher in the CDR

0.5 and CDR 1 groups as compared to the CDR 0 group (*** p<.0001; One-way ANOVA with Welch's correction for unequal variances, Tukey post-hoc Test). **(D & E)** Mean CSF Aβ42 was significantly higher while mean CSF tau was significantly lower in the CDR 0.5 and CDR 1 groups as compared to the CDR 0 group (*** p<.0001; One-way ANOVA with Welch's correction for unequal variances, Tukey post-hoc Test). The degree of overlap between clinical groups is comparable for all biomarkers evaluated.

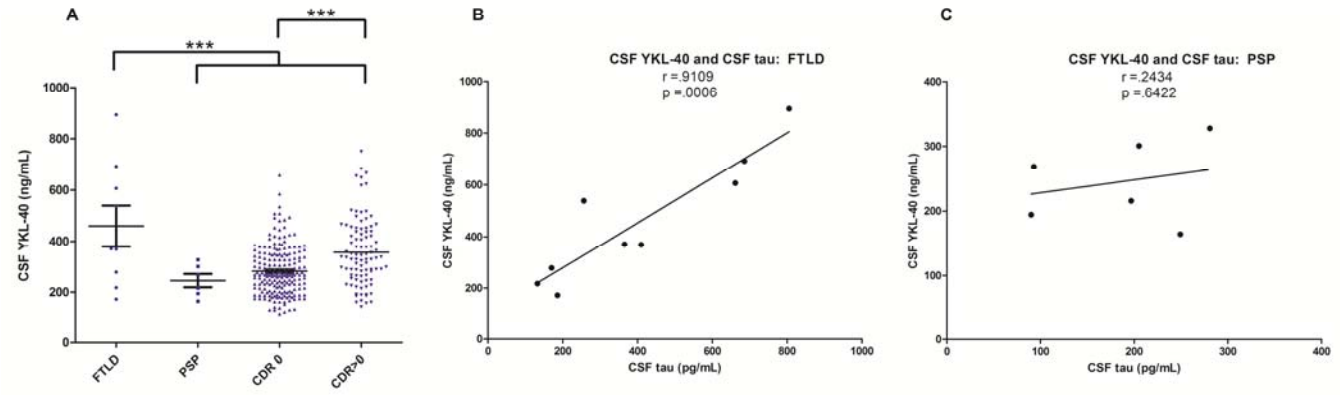

Figure 3.3. (A) CSF samples from subjects with FTLD (N=9) and PSP (N=6) were analyzed for YKL-40 by ELISA, and levels were compared to those of the validation cohort (CDR 0 and CDR>0 [CDR 0.5&1 combined], N=292). Because the groups differed with respect to mean age at LP (FTLD: 59 yrs, PSP: 66 yrs, CDR 0: 71 yrs, CDR 0.5&1: 75 yrs), analyses were adjusted for age. CSF YKL-40 was significantly higher in the FTLD group as compared to the PSP, CDR 0, and CDR>0 groups (*** p<.0001; ANCOVA, LSD post-hoc Test). While not reaching statistical significance (defined here as α=0.05), CSF YKL-40 levels trended lower in the PSP group as compared to the CDR>0 group. **(B-C)** CSF YKL-40 and CSF tau values correlated strongly in the FTLD group, but did not correlate in the PSP group.

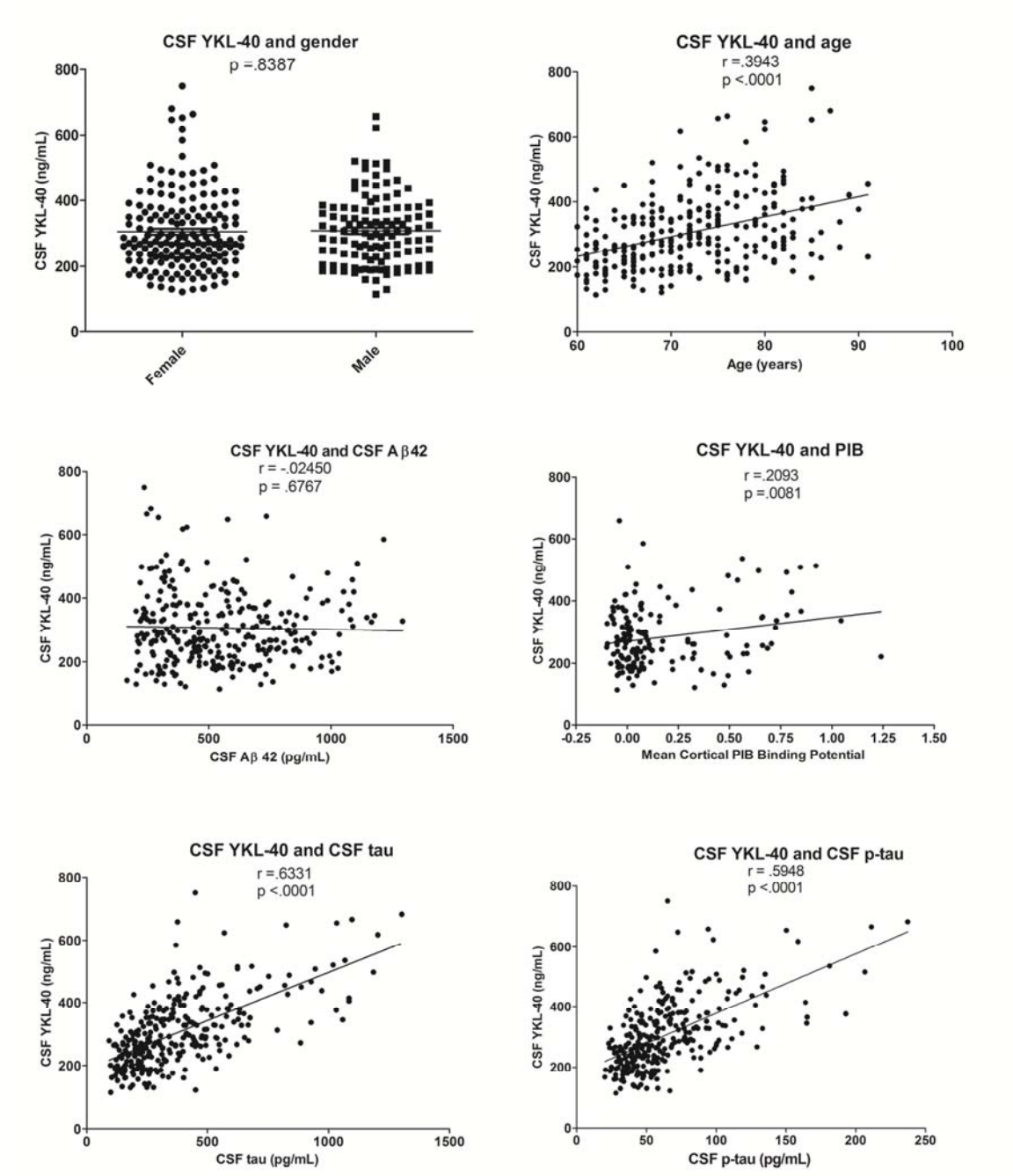

Figure 3.4. In the validation cohort, CSF YKL-40 levels do not vary based on gender and are not correlated with CSF Aβ42. However, CSF YKL-40 levels are correlated with age, CSF tau, CSF p-tau181, and mean cortical PIB binding potential.

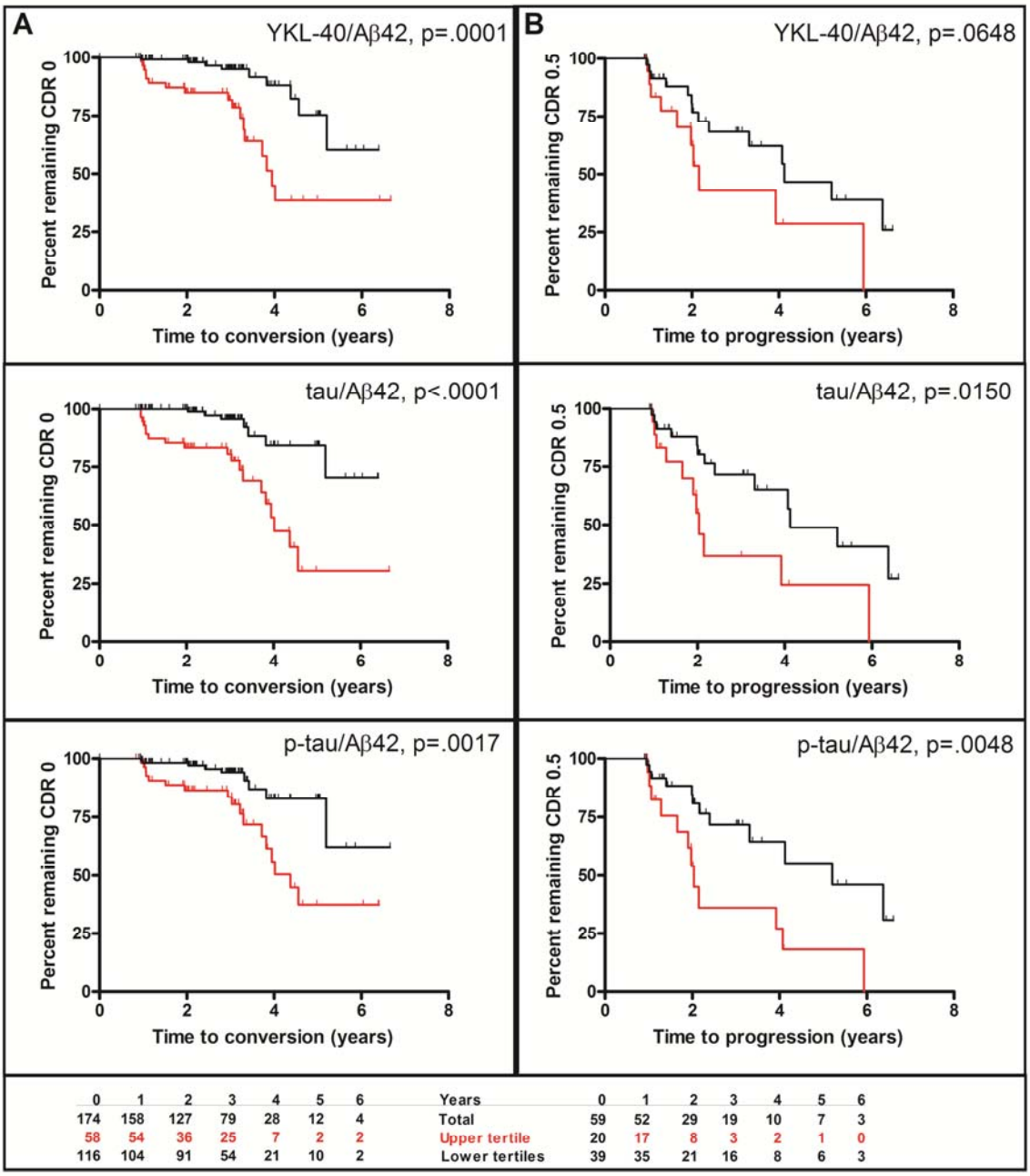

Figure 3.5. CSF YKL-40/Aβ42, tau/Aβ42, and p-tau/Aβ42 as predictors of **(A)** conversion from CDR 0 to CDR>0 and **(B)** progression from CDR 0.5 to CDR>0.5. Kaplan-Meier estimates of rates of conversion and progression are shown with red curves representing the upper tertile and black curves representing the lower two

tertiles. The bottom panel shows for the CSF YKL-40/Aβ42 analyses the number of subjects in the upper and lower tertiles at baseline and at each year of follow-up.

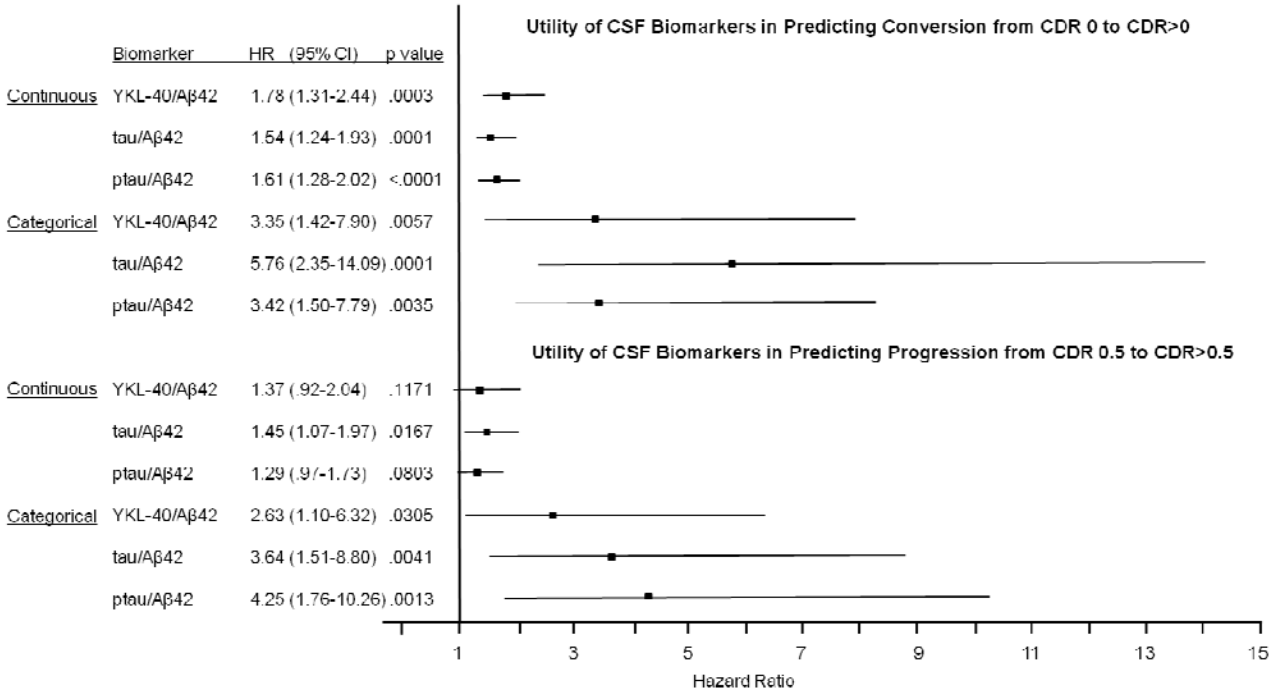

Figure 3.6. Cox proportional hazards models were used to assess the ability of CSF YKL-40/Aβ42, tau/Aβ42, and ptau/Aβ42 to predict **(top)** conversion from cognitive normalcy (CDR 0) to cognitive impairment (CDR>0) and **(bottom)** progression from very mild dementia (CDR 0.5) to mild or moderate dementia (CDR>0.5). Biomarker measures were analyzed as both continuous and categorical variables, and were converted to standard Z-scores to allow comparison of hazard ratios between different biomarkers. In evaluating risk, analyses were adjusted for age and gender. Abbreviations: HR, hazard ratio; CI, confidence interval.

3.7 (A)

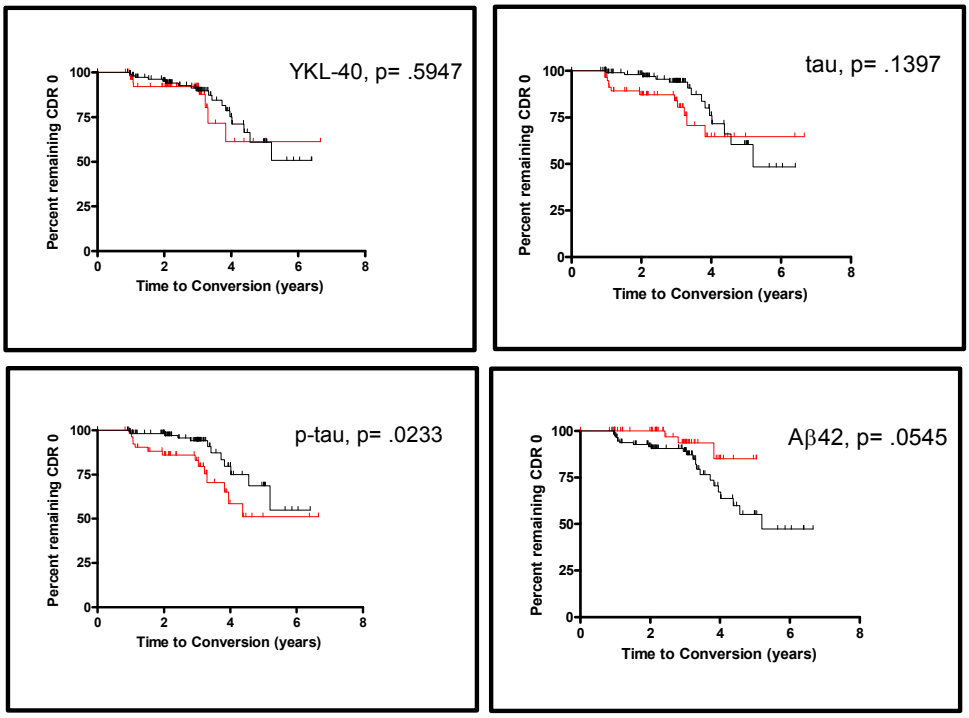

3.7 (B) Utility of CSF Biomarkers In Predicting Conversion from CDR 0 to CDR>0

	YKL-40			tau			ptau			Aβ42		
	HR	95% CI	p value	HR	95% CI	p value	HR	95% CI	p value	HR	95% CI	p value
Biomarker-continuous	0.95	0.61-1.47	.8081	1.45	1.11-1.90	.0072	1.47	1.14-1.91	.0036	0.41	0.23-0.73	.0021
Age, yr	1.06	1.01-1.12	.0211	1.07	1.01-1.12	.0170	1.07	1.01-1.12	.0146	1.05	1.00-1.10	.0672
Women	0.50	0.22-1.12	.0919	0.50	0.22-1.12	.0914	0.51	0.23-1.13	.0981	0.50	0.23-1.12	.0923
	YKL-40			tau			ptau			Aβ42		
	HR	95% CI	p value	HR	95% CI	p value	HR	95% CI	p value	HR	95% CI	p value
Biomarker-categorical	1.00	0.42-2.33	.9901	1.88	0.86-4.09	.1114	2.69	1.22-5.93	.0139	0.34	0.10-1.16	.0841
Age, yr	1.06	1.01-1.11	.0225	1.08	1.01-1.12	.0211	1.07	1.01-1.13	.0105	1.05	1.00-1.11	.0429
Women	0.51	0.23-1.13	.0968	0.52	0.24-1.16	.1097	0.55	0.25-1.23	.1449	0.49	0.22-1.08	.0754

Figure 3.7. (A) CSF YKL-40, tau, p-tau181, and Aβ42 as predictors of conversion from CDR 0 to CDR>0. Kaplan-Meier estimates of rates of conversion are shown with red curves representing the upper tertile and black curves representing the lower two tertiles. **(B)** Cox proportional hazards models were used to assess the ability of CSF YKL-40, tau, p-tau181, and Aβ42 to predict conversion from cognitive normalcy (CDR 0) to cognitive impairment (CDR>0). Biomarker measures were analyzed as both continuous and categorical variables. In evaluating risk, "Biomarker" analyses (YKL-40, tau, p-tau181, Aβ42) were adjusted for age and gender. Likewise, analyses for "Age" were adjusted for biomarker and gender, and analyses for "Women" were adjusted for biomarker and age. Abbreviations: HR, hazard ratio; CI, confidence interval.

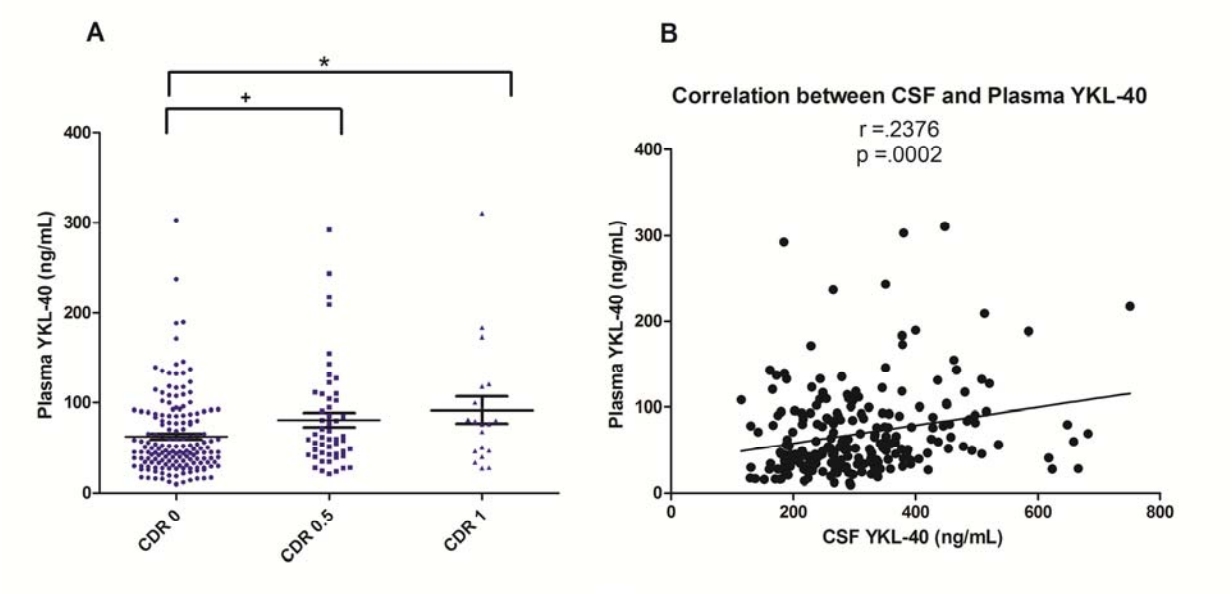

Figure 3.8. Plasma samples of the validation cohort (N=237) were evaluated for YKL-40 by ELISA. **(A)** Mean plasma YKL-40 was significantly higher in the CDR 0.5 and CDR 1 groups as compared to the CDR 0 group (+ p=.046, * p=.031; One-way ANOVA, Tukey post-hoc Test) (CDR 0= 62.5 +/- 3.4; CDR 0.5= 81.1 +/- 8.0; CDR 1= 91.9 +/- 15.0, ng/mL, mean +/- SEM). **(B)** CSF and plasma YKL-40 levels are significantly correlated (*r* =.2376, p=.0002).

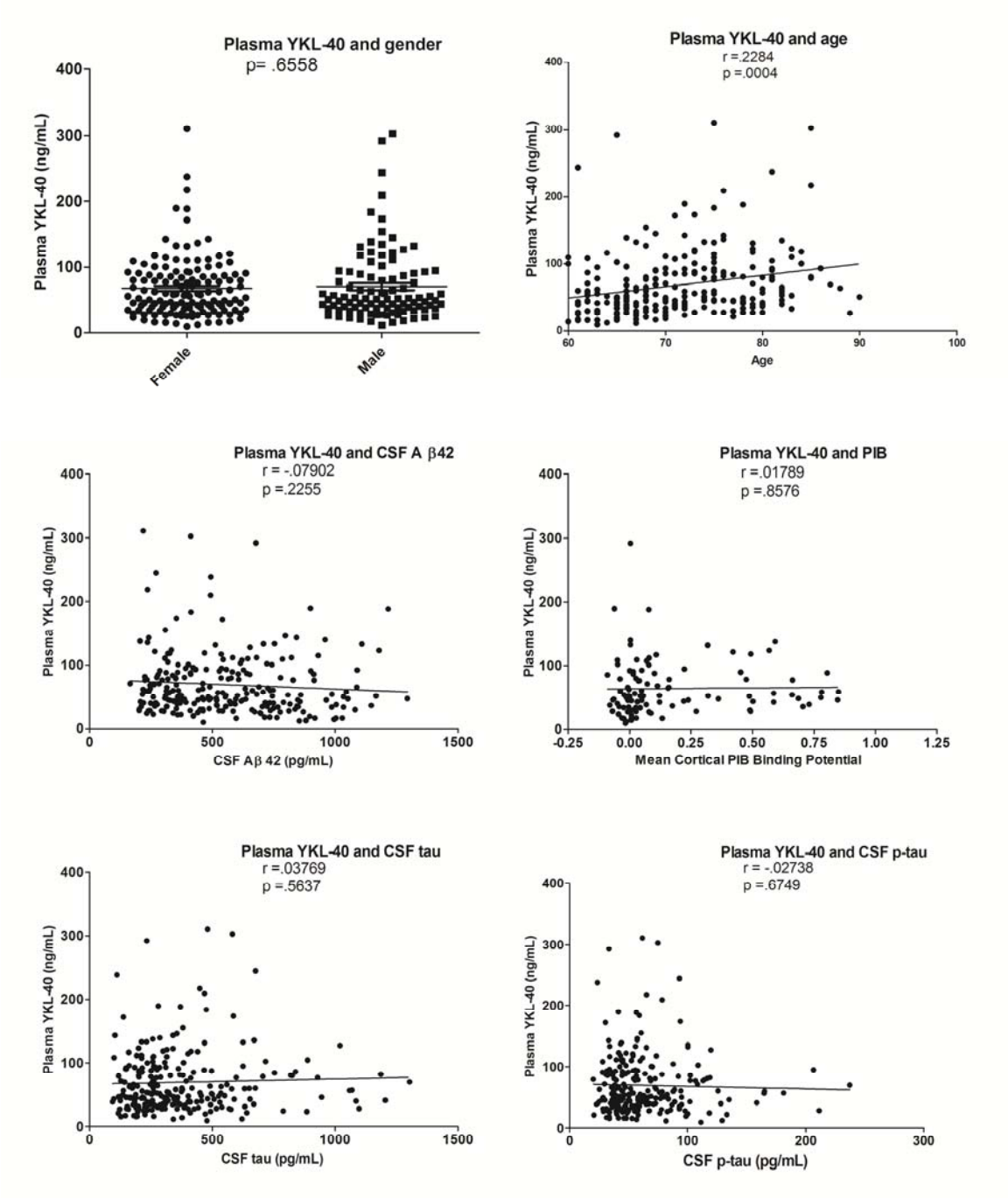

Figure 3.9. Plasma YKL-40 levels do not vary based on gender, but are correlated with age. Plasma YKL-40 levels are not correlated with other CSF biomarkers such as Aβ42, tau, p-tau181, or with mean cortical PIB binding potential.

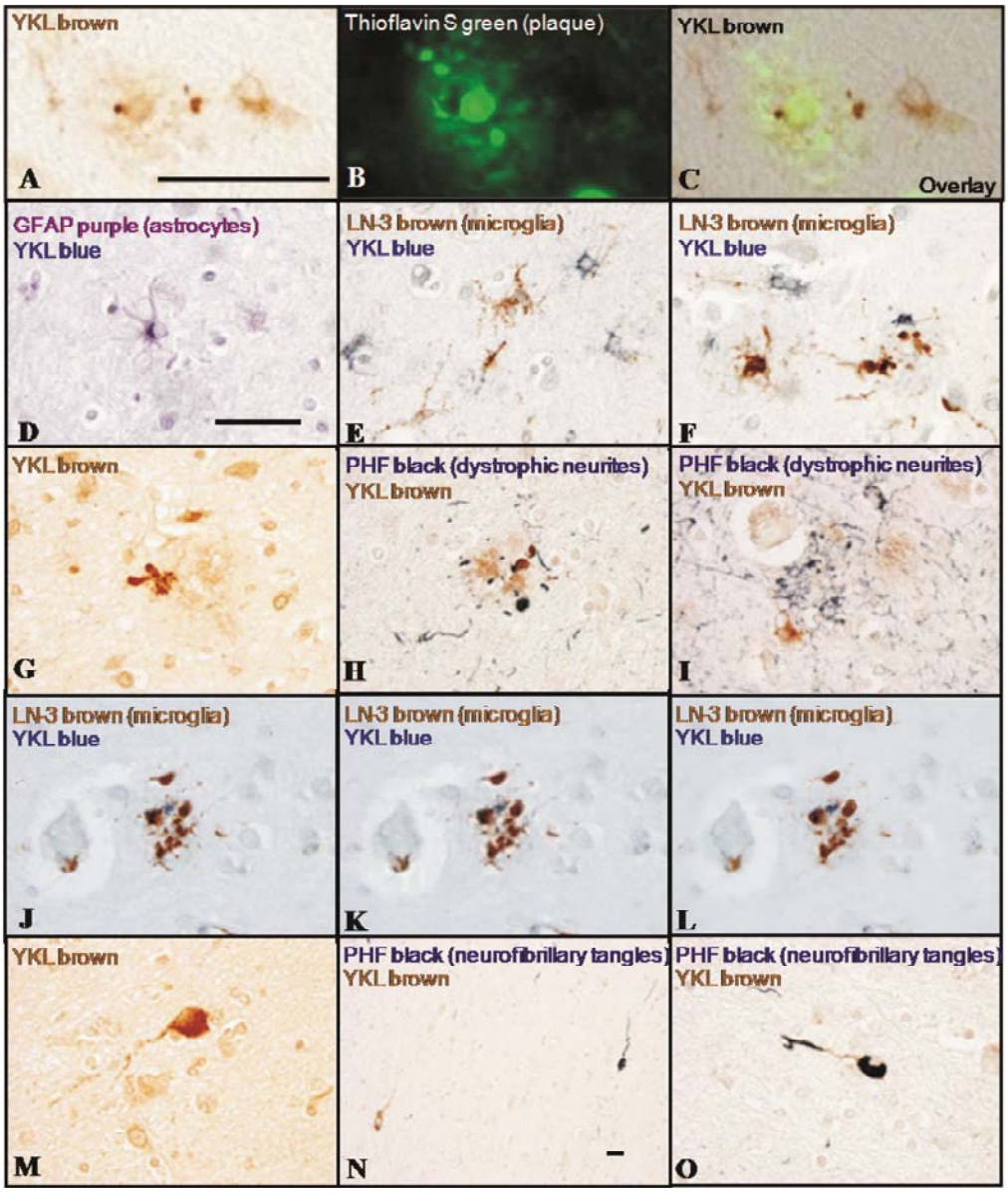

Figure 3.10. In AD neocortex, YKL-40 immunoreactivity is observed in the vicinity of thioflavin S-positive fibrillar amyloid plaques (A,B,C). YKL-40 immunoreactivity is present within a subset of GFAP-positive astrocytes (D) and not in LN-3-positive microglia (E,F). YKL-40 is also observed in cell processes associated with plaques (G); these processes lack reactivity for dystrophic neurite marker PHF-1 (H,I) and microglial marker LN-3 (J,K,L representing adjacent focal planes), and may represent astrocytic processes.

YKL-40 immunoreactivity is also observed in occasional neurons in the superficial white matter (M,N,O), some of which contain neurofibrillary tangles (evidenced by PHF-1 staining, N,O). These neurons may represent cells of multiform layer VI or 'interstitial neurons' of the white matter. Scale bars = 50 μm; scale bar in A applies to A-C; scale bar in D applies to D-O, with the exception of N.

Chapter 4.

Follow-up study: Quantitation by ELISA of four candidate biomarkers identified by 2D-DIGE LC-MS/MS

Prior to the experiments described in Chapters 2 and 3, a similar series of proteomics experiments utilizing 2-D DIGE, but on a smaller scale, were performed by the Holtzman lab in conjunction with the Proteomics Core. As in Chapter 2, a number of candidate biomarkers were identified in these preliminary studies, and were subsequently evaluated by ELISA in an independent cohort. To follow up on these studies, I sought to evaluate several of these biomarkers on a larger scale; these experiments are described below.

Introduction

The efficacy of emerging Alzheimer's disease (AD) modifying treatments will likely rely on the ability to accurately and reliably diagnose individuals early in the disease process. Currently, diagnosis of AD is based upon clinical assessment, with definitive diagnosis requiring pathological evaluation at autopsy. The identification of biomarkers for AD may allow for a less invasive and more accurate diagnosis in the antemortem period. Additionally, biomarkers may facilitate early diagnosis, which is particularly difficult given that there are no signs or symptoms unique to AD. Indeed, a few cerebrospinal fluid (CSF) proteins (most notably Aβ42, tau, and phosphorylated tau) have already shown great promise as diagnostic biomarkers for AD (346).

To identify new candidate biomarkers for AD, our lab used an unbiased proteomic approach of two-dimensional difference in gel electrophoresis (2D-DIGE) coupled with liquid chromatography and tandem mass spectrometry (LC-MS/MS) to compare the relative concentrations of CSF proteins of individuals with mild dementia (Clinical Dementia Rating [CDR] 1, N=6) to those of cognitively normal individuals (CDR 0, N=6) (222) [a larger validation/expansion 2D-DIGE study can be found in Chapter 2].

From this analysis, 11 candidate biomarkers were identified, 6 of which were subsequently evaluated by enzyme-linked immunosorbent assay (ELISA) in the same discovery cohort (N=12) and in a larger, independent cohort (N=81). In the independent cohort, which also included very mildly demented (CDR 0.5) individuals, CSF levels of α1-antichymotrypsin (ACT), antithrombin III (ATIII), and zinc-α2-glycoprotein (ZAG) were significantly higher in the very mild/mild AD (CDR 0.5 and 1) group, confirming the 2D-DIGE findings. Levels of carnosinase 1 (CNDP1) were lower in the very mild/mild AD group, but did not reach statistical significance (p=0.076). In contrast to the 2D-DIGE findings, levels of gelsolin (GSN) and angiotensinogen (AGT) were not found by ELISA to be significantly different between the clinical groups. Importantly, the combination of these promising novel biomarkers (ACT, ATIII, ZAG, CNDP1) with more 'established' biomarkers CSF Aβ42 and tau, resulted in a higher AUC and sensitivity than for any biomarker individually. This increase in AUC did not reach statistical significance, but it is worth noting that this study may have been underpowered to detect the biological differences between groups. It will be of interest whether the changes observed in this panel of markers will reach statistical significance in a larger, independent data set or if alternative combinations of biomarkers (including fluid or imaging markers) will result in improved performance. The current study was undertaken to address these issues. However, evaluation of the levels of ACT, ATIII, ZAG, and AGT by ELISA in 138 CSF samples from cognitively normal, very mildly, and mildly demented individuals did not demonstrate any significant differences between the clinical groups.

Methods

Study Participants

Participants (N=138) were community-dwelling volunteers at the Knight Alzheimer's Disease Research Center at Washington University (ADRC-WU). Informed consent was obtained from all study participants, and protocols were approved by the WU institutional review board for human studies. At sample collection, subjects were 37 to 90 years of age and in good general health, having no other neurological, psychiatric, or major medical diagnoses that could contribute importantly to dementia. Cognitive status was evaluated and rated by the ADRC Clinical Core based on criteria from the National Institute of Neurological and Communicative Diseases and Stroke-Alzheimer's Disease and Related Disorders Association (57). A clinical dementia rating (CDR) of 0 (N=81) indicated no dementia, CDR 0.5 (N=41) indicated very mild dementia, CDR 1 (N=14) indicated mild dementia, and CDR 2 (N=2) indicated moderate dementia. Some of the CDR 0.5 participants met the criteria for mild cognitive impairment (MCI) and some were more mildly impaired and could be considered "pre-MCI" (70). Twenty-five to 30 mL of CSF was collected by lumbar puncture (LP) at 8 AM following overnight fasting. Samples were inverted to avoid gradient effects, centrifuged (2,000g, 5 minutes, 4°C) to remove any cellular elements, and aliquoted into polypropylene tubes for freezing and storage at -80°C.

Enzyme Linked Immunosorbent Assays (ELISAs)

CSF samples were analyzed for Aβ42, total tau, and phospho-tau181 in duplicate by quantitative ELISA after a single freeze-thaw cycle according to the manufacturer's instructions (Innotest, Innogenetics, Ghent, Belgium). CSF samples were analyzed for ACT, ATIII, ZAG, and AGT in triplicate after two freeze-thaw cycles using ELISAs

developed 'in-house.' A sandwich ELISA was developed for α1-antichymotrypsin (ACT) using rabbit anti-human ACT antibody (1:1000; DAKO, Carpinteria, CA) for capture, sheep anti-human ACT antibody (1:1000; The Binding Site, San Diego, CA) for detection, biotinylated rabbit anti-sheep antibody (1:5000; Vector, Burlingame, CA) for reporting, poly-HRP streptavidin (Vector, Burlingame, CA), and Elite ABC (Vector, Burlingame, CA) for color development; ACT purified from human plasma was used as standard (Sigma, St. Louis, MO). A sandwich ELISA was developed for antithrombin III (ATIII) using rabbit anti-human ATIII antibody (1:1000; DAKO, Carpinteria, CA) for capture, mouse anti-human ATIII antibody (1:2000; Antibody Shop, Denmark) for detection, biotinylated rabbit anti-mouse antibody (1:5000; Jackson, West Grove, PA) for reporting, poly-HRP20 streptavidin (1:2000; Fitzgerald, Concord, MA), and Super Slow TMB (Sigma, St. Louis, MO) for color development; ATIII purified from human plasma was used as standard (Sigma, St. Louis, MO). A sandwich ELISA was developed for zinc-α2-glycoprotein (ZAG) using rabbit anti-human ZAG antibody (1:1000; gift from Dr. Iwao Ohkubo, Shiga University of Medical Science, Japan) for capture, mouse anti-human ZAG antibody (clone 1D4, 1:100; Santa Cruz Biotechnology, Santa Cruz, CA) for detection, biotinylated rabbit anti-mouse antibody (1:5000; Jackson, West Grove, PA) for reporting, poly-HRP20 streptavidin (1:2000; Fitzgerald, Concord, MA),and Super Sensitive TMB (Sigma, St. Louis, MO) for color development; ZAG purified from human seminal plasma was used as standard (gift from Dr. Iwao Ohkubo). A sandwich ELISA was developed for angiotensinogen (AGT) using mouse anti-AGT antibody (clone F8A2, 1:288; gift from Dr. Claus Oxvig, University of Aarhus, Denmark) for capture, chicken anti-AGT antibody (1:1200; gift from Dr. Claus Oxvig) for detection, rabbit anti-chicken: horseradish peroxidase antibody (1:15,000; Sigma, St. Louis, MO) for reporting, and Super Sensitive TMB (Sigma, St. Louis, MO) for color development; AGT purified from human plasma was used as standard (Calbiochem, San Diego, CA).

Statistical Analyses

Statistical analyses were performed in PASW 18 (SPSS Inc, Chicago, IL). The distributions of analytes were tested for normalcy by Shapiro-Wilk test, and, when appropriate, log10 transformed to approximate a normal distribution. Analysis of covariance (ANCOVA) using the General Linear Model (GLM) procedure in PASW was used to determine analytes that differed in concentration between AD (CDR>0) and control (CDR 0) groups while adjusting for the effects of age and gender. Because nearly identical results were obtained for analyses using log transformed data as for analyses using data in the original scale (non-transformed), results are reported using the original scale data.

Results

To follow-up on the candidate biomarkers identified in the initial discovery study (222), we used ELISAs to measure the levels of ACT, ATIII, ZAG, and AGT in CSF from 63 cognitively normal (CDR 0), 36 very mildly demented (CDR 0.5), and 11 mild-moderately demented (CDR 1&2) individuals. In the initial discovery study, for the very mild/mild AD group, ACT, ATIII, and ZAG levels were significantly higher, CNDP1 levels trended lower, and GSN and AGT levels were unchanged. Because GSN did not demonstrate promise in the initial study and because of CNDP1 reagent limitations, these two markers were not chosen for further analysis in the current study.

Although the CDR 0 and CDR>0 groups were well matched with regard to age (CDR 0= 71.9 +/- 7.1, CDR>0= 72.4 +/- 9.7, mean +/- SD), they differed with respect to gender (CDR 0= 63% female, CDR>0= 43% female). Additionally, because our initial study found some of the analytes to correlate with these variables, we evaluated the

levels of each analyte for potential correlation with age and gender. CSF ACT and AGT levels correlated modestly with increasing age (r=0.265, p=0.005, and r=0.242, p=0.024, respectively), while levels of ACT, ATIII, and ZAG were significantly higher in males than in females (p=.047, p=.019, p<.001, respectively, Student's t-test). Additionally, participants with very mild to moderate dementia exhibited the typical AD CSF biomarker profile characterized by significantly lower mean levels of CSF Aβ42 (CDR>0= 406.8 +/- 200.9, CDR 0=573.8 +/- 269.7 pg/mL, mean +/- SD) and higher mean levels of CSF tau (CDR>0= 538.5 +/- 280.9, CDR 0=313.3 +/- 188.5 pg/mL, mean +/- SD) and CSF p-tau181 (CDR>0= 76.8 +/- 38.0, CDR 0=52.8 +/- 24.7 pg/mL, mean +/- SD).

No difference in ACT, ATIII, ZAG, or AGT levels was found between the AD (CDR>0) and control (CDR 0) group by analysis of covariance adjusting for the effects of age and gender (p=0.535, p=0.332, p=0.403, p=0.651, respectively). These observations were not qualitatively different from those using the log-transformed or unadjusted data.

The ELISA protocols used here varied slightly from those of the initial study due to changes in personnel, reagent availability, and optimizations for assay performance. To assess whether these changes may have contributed to the inability to validate our initial findings, 28 samples (CDR 0, N=18; CDR>0, N=10) of the initial study were re-assayed ('overlap' samples). Although concentrations measured for these overlap samples correlated strongly between the two experiments (ACT r=0.849, ATIII r=0.837, ZAG r=0.798, AGT r=0.823), absolute values were approximately 50% higher for the new ATIII, ZAG, and AGT measurements. For these 28 overlap samples, levels of ZAG were significantly higher in the CDR>0 group compared to the CDR 0 group (p=0.014), while levels of ACT, ATIII, and AGT were not different between the clinical groups (p=0.184, p=0.131, p=0.480, respectively). Combining the 110 new CSF samples of this study with the 28 overlap samples still did not reveal any differences in ACT, ATIII, ZAG,

or AGT levels between the clinical groups (p=0.939, p=0.772, p=0.982, p=0.417, respectively) (Figure 4.1).

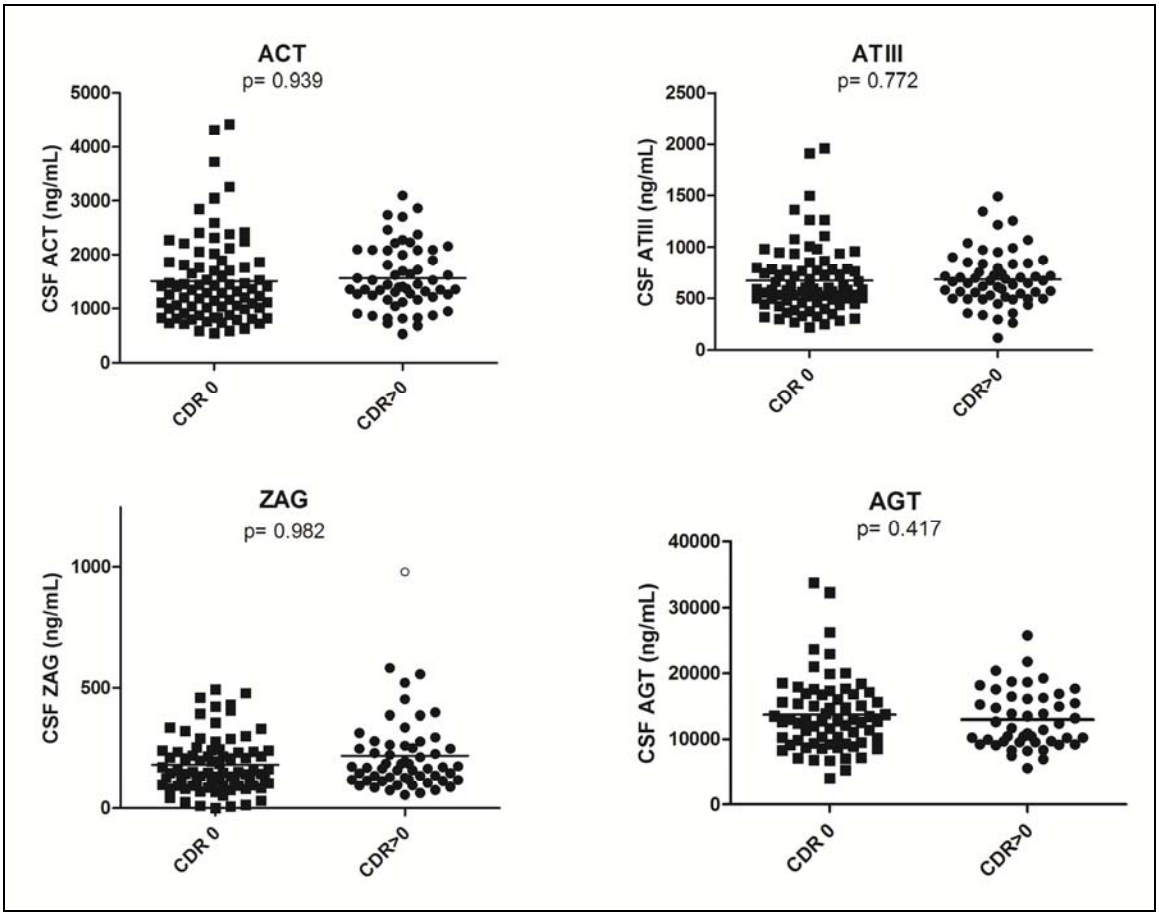

Figure 4.1. Mean levels of CSF ACT, ATIII, ZAG, and AGT are not significantly different between AD (CDR>0) and control (CDR 0) groups (analysis of covariance, adjusting for age and gender). CSF from a total of 81 CDR 0 and 57 CDR>0 participants (110 samples from this study + 28 samples overlapping from initial discovery study) was analyzed by ELISA (original-scale data shown; outlier indicated by the unfilled circle for ZAG was removed from analyses).

Discussion

In a 138-subject cohort we were unable to validate the findings of an initial report of increased ACT, ATIII, and ZAG levels in AD (CDR>0) CSF. However, interestingly, an increase in ZAG levels in the AD group was observed for the 28 samples that overlapped between the initial report and this study, suggesting that the results of the initial study may have been cohort-dependent. The inconsistency in ACT results between our two studies may not be particularly surprising, given that a number of other studies have found either increased (211, 215, 220) or unchanged ACT levels in AD CSF (216-218). The other markers (i.e. ATIII, ZAG, and AGT) have not been well studied in AD, and to our knowledge, changes in their levels in AD CSF have not been evaluated by other groups. These findings would appear not to support a role for ACT, ATIII, ZAG, or AGT as biomarkers for AD. However, it is important to note that these four proteins were first identified as differing significantly in abundance between the AD and control group by 2D-DIGE, a technique sensitive to concentration changes of minor protein isoforms and post-translational modifications which may not substantially alter global concentrations of a 'parent' protein. For ELISAs that measure the parent protein, or total protein level, it is perhaps to be expected that some candidate biomarkers identified by 2D-DIGE would not be validated by ELISAs not tailored to detect only specific isoforms or protein 'sub-species.' Indeed, ATIII, ZAG, and AGT are known to have different isoforms (434-437), and ACT, ATIII, and AGT were identified in multiple protein spots on the 2-D gels of the discovery study, suggesting different protein isoforms. Therefore, a thorough evaluation of the potential of these analytes as biomarkers for AD would appear to require either high-throughput 2D-DIGE of every sample to be analyzed or the design of ELISAs targeting specific post-translational modifications or specific 'sub-species' of interest.

Chapter 5.

Development of a Solid Phase Extraction Protocol For Peptides From Cerebrospinal Fluid In Conjunction with Tandem Mass Spectrometry to Identify Novel Biomarkers for Alzheimer's Disease

Chapters 2-4 of this work have focused on relatively intact, large molecular weight proteins, just as the bulk of published biomarker research. A relatively unexplored avenue for research is the CSF peptidome. The following chapter describes the development of methods for such an analysis, as well as some preliminary results from their application to a small number of CSF samples.

Introduction

Improved proteomics technologies, in particular advances in mass spectrometry (MS) techniques, have solidified proteomics as a valuable tool for biomarker discovery. Indeed, during the last two years, over one thousand articles have been published on the subject, including recent efforts to characterize the human cerebrospinal fluid (CSF) proteome (239, 240). General methods in proteomic studies typically include protein separation by two-dimensional gel electrophoresis (2-DE), liquid chromatography (LC), or protein-chip arrays, followed by MS or tandem MS and database searches to determine protein identity. Powerful proteomic approaches, allowing for the simultaneous screening of large numbers of proteins in a given sample, expand the possibilities for biomarker discovery beyond standard targeted techniques, such as enzyme linked immunosorbent assay, that assess single or small numbers of proteins. Applied to Alzheimer's disease (AD), proteomic studies comparing the differences in protein expression levels between AD and control CSF samples have identified a number of potential diagnostic markers (222, 241-246). Few studies, however, have investigated the low molecular weight (MW) components of CSF for potential AD biomarkers. This is primarily due to a lack of techniques for isolating and detecting low

MW, low abundance species for mass spectrometry. In our prior proteomic studies (Chapter 2 and 4), for example, CSF samples were initially processed with 10 kDa MW exclusion filters to remove salts and to retain and analyze the larger molecules (222, 251). Additionally, many proteomics studies utilize 2-DE, a technique which is usually unable to resolve peptides and proteins smaller than 15 kDa (438). Because the low MW components of CSF remain a relatively untapped source for potential novel biomarkers, we have developed a protocol for the extraction and identification of peptides from CSF. With this protocol, the ≤10 kDa fraction can be probed for peptides that differ in abundance between AD and control groups. More generally, this protocol can be applied to the search for novel biomarkers or altered proteolytic pathways of a number of central nervous system (CNS) diseases.

Methods

CSF sampling:

CSF samples were obtained by lumbar puncture (LP) from volunteer participants enrolled in longitudinal studies of healthy aging and dementia at the Knight Alzheimer's Disease Research Center at Washington University (ADRC-WU). Study protocols were approved by the WU Institutional Review Board, and written informed consent was obtained from each participant. Cognitive status was evaluated and rated based on criteria from the National Institute of Neurological and Communicative Diseases and Stroke-Alzheimer's Disease and Related Disorders Association (57). A clinical dementia rating (CDR) of 0 indicated no dementia, whereas CDR 1 indicated mild dementia. For a 'mixed clinical sample,' de-identified, discarded CSF from diagnostic LPs was pooled

from 20+ patients with a variety of medical conditions to provide a large source of CSF for protocol development and testing.

Sample preparation, solid phase extraction, and mass spectrometry:

To isolate low MW species, CSF samples were passed through a 10-kDa MW cut-off centrifugal filter unit (Amicon Ultra-4 centrifugal filter units). Sample filtrates were then acidified with trifluoroacetic acid (TFA) and spiked with a mixture of tryptic peptides from bovine serum albumin (BSA) as an internal standard (1% TFA final, 2 pmol BSA/200 uL CSF). For desalting and concentrating low MW proteins and peptides, solid phase extraction procedures were developed using Hypercarb (porous graphitic carbon) material in both a column (Hypersep, Thermo Scientific) and tip (NuTip, Glygen) format. For the tips, the Hypercarb chromatography material was first washed with 60% acetonitrile (ACN)/ 1% formic acid (FA) and then equilibrated with 1% ACN/1% FA. A more stringent initial wash sequence was used for the columns, involving washes with 95% ACN/1% TFA, 60% ACN/1% TFA, and 90% ACN/1% TFA, to remove polymer contamination likely leaching from the column. Samples were loaded onto washed columns or tips; peptides that did not bind the first column or tip were sequentially extracted from the same sample with additional columns or NuTips. Columns and tips were rinsed with 1% ACN/1% FA, and peptides were eluted with sequential applications of 60% ACN/1% FA and 90% ACN/1% FA. MALDI-TOF/TOF (Proteomics 4700, Applied Biosystems) was used to evaluate the recovery of the internal standard BSA peptides and to assess intra- and inter-sample preparation reproducibility. Samples were then evaporated to dryness in a Speed-Vac centrifuge, and dissolved in 1% ACN/1% FA for LC-MS/MS (nano-LC-linear quadrupole Fourier transform ion cyclotron) for peptide

identification and quantification. Tandem spectra were searched against the National Center for Biotechnology Information non-redundant database NR using MASCOT, version 1.9 (Matrix Science, London) and neurloProSight (University of Illinois). Relative peptide quantification was determined using X-calibur (Thermo Fisher Scientific) and Rosetta Elucidator (Rosetta Biosoftware).

Results and Discussion

In developing a solid phase extraction protocol for CSF peptides, we evaluated the performance of Hypercarb chromatography material in both column and tip formats (Figure 5.1). In the tip format, the chromatography material is embedded in the inner surface of a pipette tip. Hypercarb material is composed of flat sheets of hexagonally arranged carbon atoms, and is capable of separating very closely related compounds, including geometric isomers and diastereoisomers. Analyte binding is multimodal, with interactions through both hydrophobic and electrostatic mechanisms. The efficiency of CSF processing with the two formats differed; initially, all NuTips were processed manually one-at-a-time, while the columns could be connected to a vacuum manifold, allowing for the processing of 16 samples simultaneously (Figure 5.1). Subsequently, we integrated a robot with the NuTip protocol, allowing up to 96 samples to be processed simultaneously with excellent tip-to-tip reproducibility.

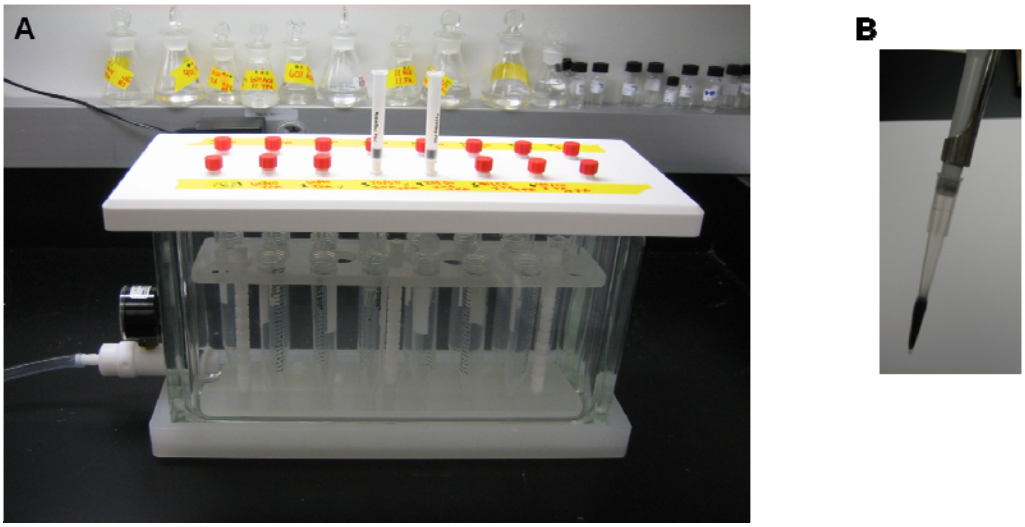

Figure 5.1. Solid phase extraction procedures were developed using Hypercarb (porous graphitic carbon) material in both **A)** column (Hypersep, Thermo Scientific) and **B)** tip (NuTip, Glygen) format. The columns can be connected to a vacuum manifold **(A)**, while the tips can be processed using a pipettor **(B)** or can be interfaced with a robot (not pictured).

The general steps of a typical solid phase extraction involve 0) (may not be necessary) washing the cartridge (i.e. column or tip), 1) equilibrating or conditioning of cartridge with a non-polar or slightly polar solvent that prepares/'wets' the surface, 2) loading the sample, 3) rinsing the cartridge to remove residual unbound species, and 4) eluting with solvents of varying strengths. For our analyses, initial sample preparation involved filtering the samples (10-kDa MWCO) to obtain peptides and low molecular weight proteins, acidifying the filtrate, and spiking it with a mixture of tryptic peptides from BSA as an internal standard. This BSA standard allowed us to compare the reproducibility between columns/tips and between runs, and to assess recovery performance.

Using the columns, many of our initial spectra contained a series of peaks with a major mass difference between them of 44 Da, suggesting polyethylene glycol contamination that was likely a by-product of column manufacturing. Therefore, we tested a series of different column washes to remove the polymer contamination, and found that sequential 95% ACN/1% TFA, 60% ACN/1% TFA, and 90% ACN/1% TFA washes were successful. We did not observe polymer contamination with the tips. Indeed, one advantage reported by the NuTip manufacturer is the lack of polymers or glue, thus avoiding potential contamination or permeability problems (Glygen).

Initial recovery of BSA peptides was low; however, the flow-through lacked BSA peptides, indicating that the issue was not with binding to the column, but with elution from the column. Thus, to increase percent recovery, we tested various elution solvents and electronic modifiers, including 60% ACN, 90% ACN, 60% ACN/1% TFA, 90% ACN/1% TFA, 60% ACN/1% FA, 90% ACN/1% FA, 20% IPA/50% ACN, 40% IPA/50% ACN, 20% IPA/50% ACN/1% TFA, and 40% IPA/50% ACN/1% TFA (TFA= trifluoroacetic acid; ACN= acetonitrile; FA= formic acid; IPA= isopropanol). We found that 60% ACN/1% FA gave the greatest peptide recovery, and that following it with 90% ACN/1% FA eluted additional (albeit fewer) peptides of a different general profile.

In developing a protocol for the extraction and identification of peptides from CSF, we discovered that Hypercarb material yielded better results in the NuTip format (higher signal intensity, more recovered peptides) than in the column format. Although we tested a number of elution solvents of varying strengths, used 25 mg and 50 mg capacity columns and loaded varying CSF volumes, incorporated additional wash steps after sample loading to remove residual salt that can cause signal attenuation, and employed other 'troubleshooting' techniques, the performance of the columns appeared

inferior to that of the tips. To test whether multiple tips would be needed for each sample to ensure maximal peptide recovery, unbound peptides were sequentially extracted from the same sample using three NuTips. The majority of the BSA peptides were extracted with the first tip, with the number of peptides and the signal intensity decreasing dramatically for the second and third tips (Figure 5.2).

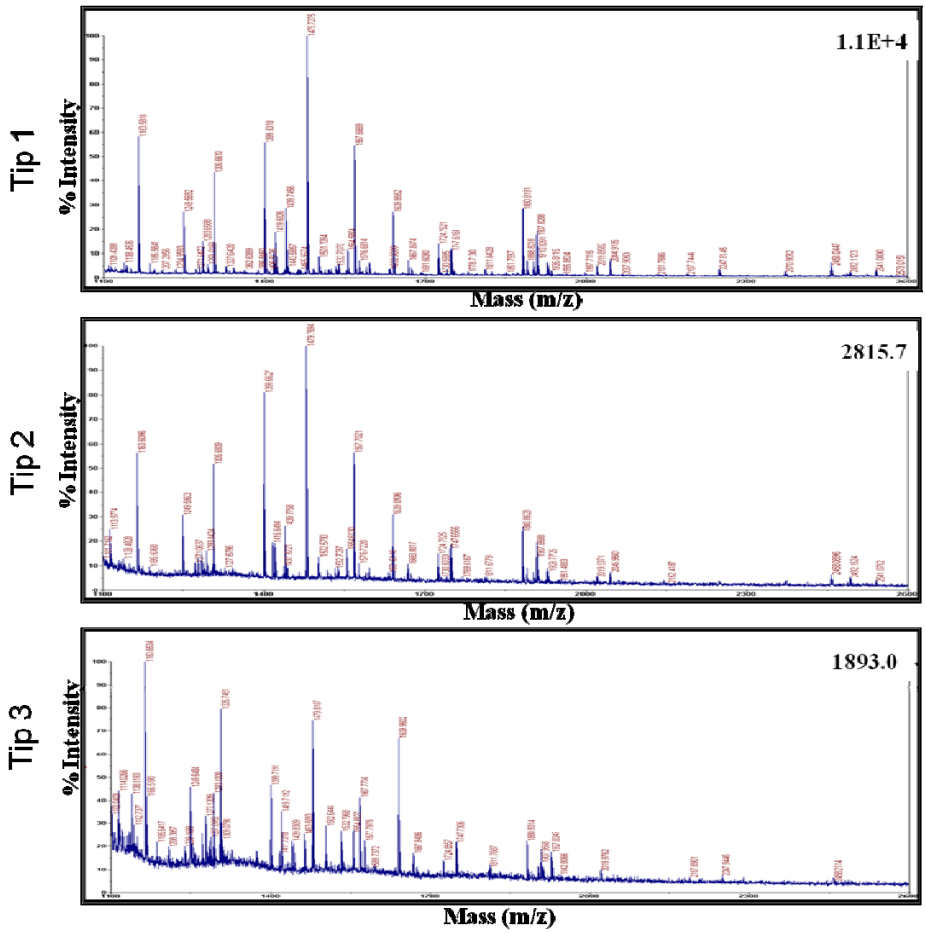

Figure 5.2. Sequential extraction of spiked internal standard BSA peptides from CSF, evaluated by MALDI-TOF/TOF. The flow-through from Tip 1 (containing any unbound peptides) was applied to Tip 2; the flow-through from Tip 2 was applied to Tip 3. As demonstrated, most peptides were extracted with the first tip. The signal intensity (upper right corner of each spectrum) decreased significantly after the first tip.

We then applied our NuTip protocol to CSF from a cognitively normal individual (CDR 0), an individual with mild dementia of the Alzheimer's type (CDR 1), and a mixed clinical sample (20+ subjects with a variety of medical conditions). In this preliminary

study, MALDI-TOF/TOF and LC-MS/MS analysis of internal standard BSA peptide recovery demonstrated good method reproducibility, thus providing confidence of the validity of endogenous peptides detected and identified. Specifically, MASCOT search of the LC-MS/MS data identified 100+ BSA peptides, ten of which were randomly selected for quantitation using X-calibur (Table 5.1). No differences were detected for BSA across the three samples (p=.1204, general linear model procedure in SAS).

BSA Peptides	Peptide Sequence	m/z	Peptide Score	Area- Pooled	Area- CDR 1	Area- CDR 0
1	QTALVELLK	997.600	54	595119	973332	258666
2	LVVSTQTALA	501.798	61	5478748	2772177	3542690
3	EACFAVEGPK	554.264	65	722101	525554	759671
4	KQTALVELLK	571.862	82	5874598	4220647	2259844
5	FKDLGEEHFK	625.317	66	344566	276029	373076
6	HLVDEPQNLIK	653.362	80	33534198	25793920	52492392
7	TVMENFVAFVDK	708.350	101	8518997	2571714	1152917
8	FYAPELLYYANK	746.382	64	635892	163799	26189
9	DAFLGSFLYEYSR	784.377	78	325794	14264	2874
10	HPYFYAPELLYYANK	630.316	74	328289	10188	13008

Table 5.1. Ten random BSA peptides, shown here, were selected for quantitation. No differences were detected for BSA across the three samples (Area- pooled, CDR 1, CDR 0) (p=.1204).

Fifty-six unique peptides (with MASCOT scores ≥30), representing nineteen unique proteins, were identified by tandem MS in the CDR 0, CDR 1, and mixed clinical CSF (Table 5.2). Five proteins were selected for further study based on their well shown association with AD (amyloid-beta precursor protein, tau, apolipoprotein E) or because our previous studies have identified them as being differentially expressed in AD versus control CSF (chromogranin B, VGF nerve growth factor (222)). For these five selected proteins, quantification of peptides from the ion currents that comprised the selected ion

chromatogram (illustrated in Figure 5.3, 5.4) revealed differences in abundance in these peptides between CDR 0, CDR 1, and mixed clinical CSF samples (Table 5.3).

Using the protocol presented here, we have extracted and identified endogenous peptides from CSF. Quantification of a subset of these peptides revealed differences in abundance among pooled, CDR 1, and CDR 0 CSF samples, albeit with a limited sample number. Additionally, recovery of internal standard BSA peptides (~2 pmol from 200 uL) was not statistically significantly different between sample runs, demonstrating the reproducibility of the extraction and LC-MS method. Sample preparation and obtaining high quality MS data are perhaps the largest challenges of proteomic analysis, and during our protocol development, many different experimental variations were tested, not all of which are represented here. Subsequent efforts to purify and concentrate the fractions eluted from the NuTips increased the number of peptides detected and the number of unique proteins (now, 36) represented. It will be of interest in future studies to find whether further protocol optimization, in particular sample digestion, can improve the detection and identification of peptides in CSF. For complex biological samples it is often necessary to digest prior to mass spectrometry; sample digestion generates peptides with molecular masses in the optimal range of the mass spectrometer that can also be fragmented more efficiently. Indeed, initial experiments have shown that our ability to identify peptides was increased upon trypsin digestion. The future application of this protocol to larger numbers of AD and control CSF samples may identify many novel candidate biomarkers for AD; additionally, this protocol for the low molecular weight species in CSF may be used for discovery studies of other neurological disorders as well.

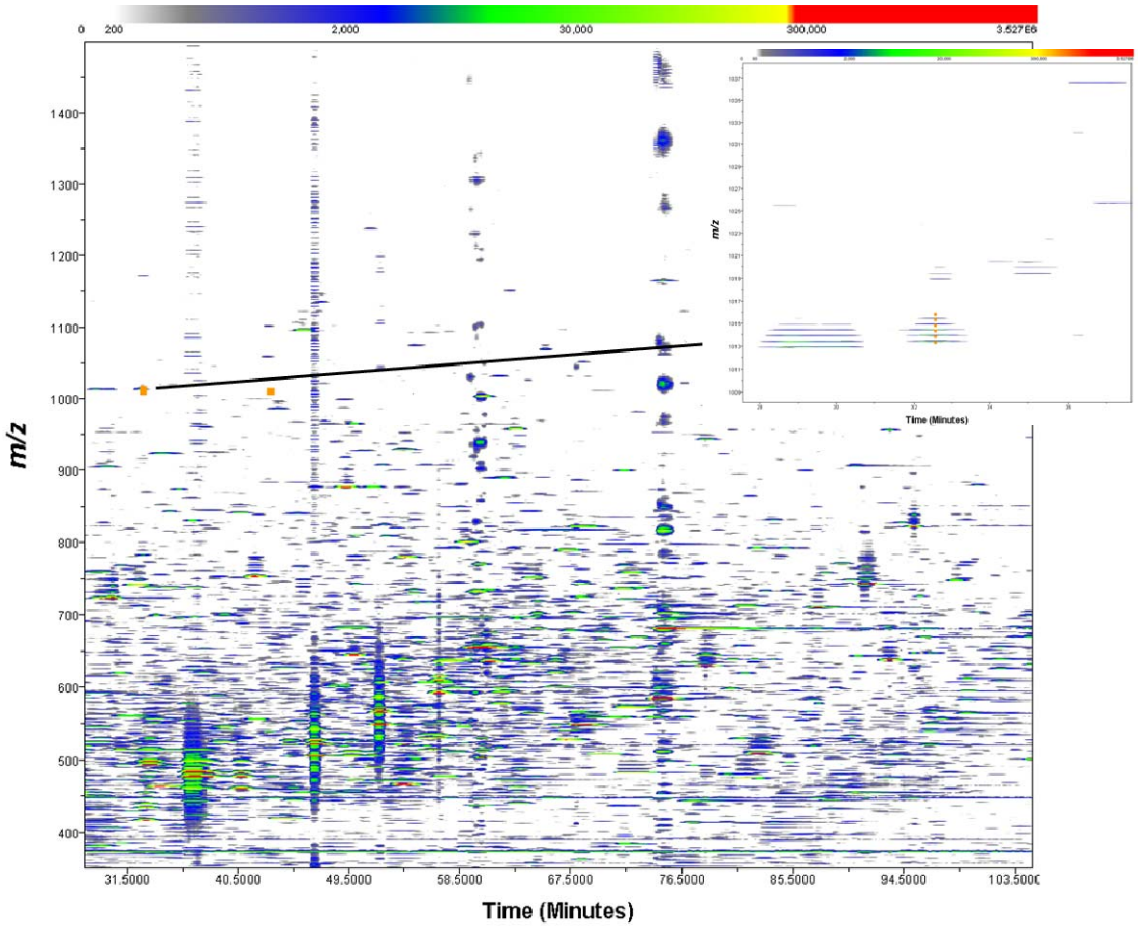

Figure 5.3. High-resolution two-dimensional LC-MS peptide map.

Shown is a representative example of a two-dimensional LC-MS peptide map from one of the samples. Visualization of the LC-MS data in this way allows for assessment of the overall sample complexity and of the quality of the LC separation. Along the x-axis is shown retention time in minutes, while along the y-axis is shown the mass (m) to charge (z) ratio. Signal intensity is represented colormetrically, with yellow-red indicating features of greater intensity. The inset (a feature shown at greater magnification) shows the isotopic cluster for the doubly-charged chromogranin B peptide with m/z of 1013.41.

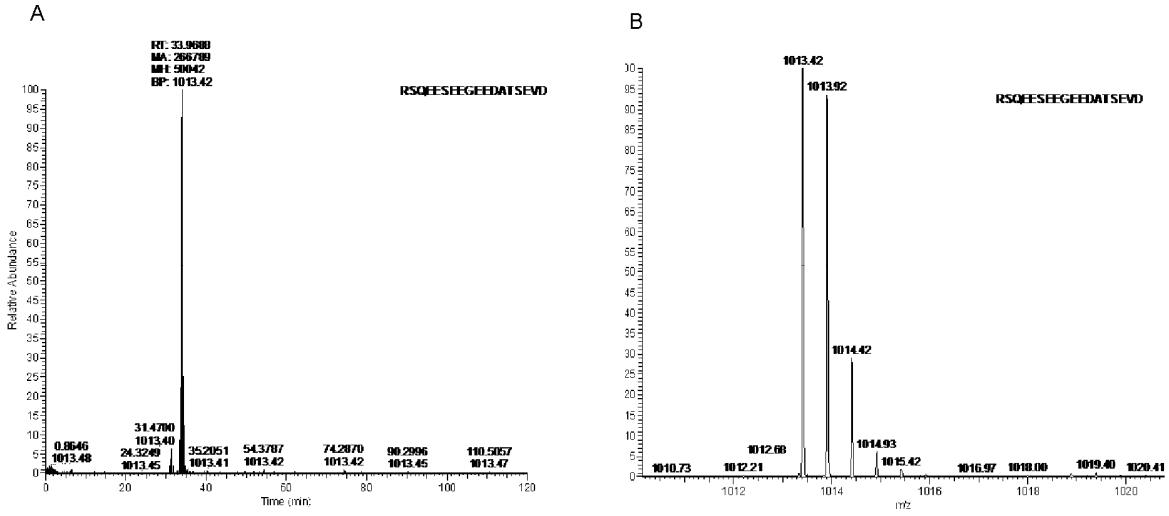

Figure 5.4. A) Representative LC-MS/MS data from low MW CSF eluate.

(A) Selected ion chromatogram showing a single peak at the accurate mass of 1013.41, representing a chromogranin B peptide; **(B)** corresponding mass spectrum demonstrating the isotopic distribution of peak represented in (A).

Table 5.2. Peptides detected and identified by tandem MS in pooled, CDR 0, and CDR 1 CSF

	Protein	Peptide Sequence	m/z	Score
1	chromogranin B precursor	RPQSEESWDEED	753.8056	55
		RSQEESEEGEEDATSEVD	1013.4159	97
		SKGQPRSQEESEEGEEDATSEVD	842.0328	90
		SSQGGSLPSEEKGHPQEESEESNVS	873.0621	60
		SSQGGSLPSEEKGHPQEESEESNVSMASLGE	1069.1471	67
		SSQGGSLPSEEKGHPQEESEESNVSMASLGE	1069.4847	57
2	VGF nerve growth factor inducible precursor	LGGSEAGERL	494.7592	73
		LFAEEEDGEAGAED	741.3054	106
		QQETAAAETETRTHT	828.8937	55
		GLQEAAEERESAREEEEAEQE	807.361	55
		GLQEAAEERESAREEEEAEQE	807.365	63
		GGEERVGEEDEEAAEAEAEAEEAERA	922.0626	91
3	testican	AVTEDDEDEDDDK	748.2952	51
		AVTEDDEDEDDDKE	812.8209	110
		AVTEDDEDEDDDKEDE	935.859	90
		AVTEDDEDEDDDKEDEVG	1013.3917	65
		AVTEDDEDEDDDKEDEVGY	1095.424	110
4	neuron-specific protein	VLSEEKLSEQETEAAEKSA	693.684	87
5	extracellular matrix protein FRAS1 precursor	QMMKHGNLEQ	625.3168	73
		LSEVSNFTMEDIN	757.4318	40
6	amyloid beta A4 precursor protein	DHSKLVDVPFQVEFPAPKNELVQKF	729.6345	62
		DHSKLVDVPFQVEFPAPKNELVQKF	729.6364	52
		DHSKLVDVPFQVEFPAPKNELVQKF	729.8872	75
7	fibrinopeptide A	DSGEGDFLAEGGGV	655.2823	92
		ADSGEGDFLAEGGGVR	768.8611	116
8	fibrinogen alphaA	DSGEGDFLAEGGGV	655.2823	92
		ADSGEGDFLAEGGGVR	768.8611	116
		SMGSWNSGSSGTGSTGNQNP	643.2718	38
9	TPA: microtubule-associated protein tau	TGSSGAKEMKLKGAD	741.3054	69
10	hemicentin 1	FNAIGSF	756.3593	35
		EQVTNVSVLLNQL	732.3136	40
		QCTVSNAAGKQAKD	741.3054	79
		SGISTPARIDLLEL	495.2418	33
11	SLC43A2 protein	VSCLLIAYGASK	642.3611	67
		DANQCVGRAGAPAPSPQP	897.863	33
12	poly(A) binding protein, cytoplasmic 3	HQAKEATQKAVNSA	741.8063	72
		QKAVDEMNGKELNGKQIYVG	747.7208	56
13	glycine-, glutamate-, thienylcyclohexylpiperidine-binding protein	RATDAEMRARRKAATEEAEKQ	807.365	72
14	leptin receptor isoform 2	SLYPIFMEGVGK	671.3491	44
		EQDRNCSLCADNIEGK	637.5971	37
		EQDRNCSLCADNIEGK	955.898	69
		EQDRNCSLCADNIEGK	956.4018	53

		EQDRNCSLCADNIEGK	956.8949	64
		EQDRNCSLCADNIEGK	957.3944	52
15	apolipoprotein E	KVKQAVETEPEPEL	799.9102	71
		KVKQAVETEPEPEL	800.41	71
		KVEQAVETEPEPEL	799.9102	84
		KVEQAVETEPEPEL	800.9118	58
16	unnamed protein product (GI # 34534986)	HQAKETAQKAVNSA	741.8063	88
17	unnamed protein product (GI # 6551993)	EQVTNVSVLLNQL	732.3136	40
		QCTVSNAAGKQAKD	741.3054	79
18	hypothetical protein (GI # 47027976)	TCAEKEEENQEN	741.3054	70
19	unnamed protein product (GI # 70905151)	MQNIGEQGHMA	417.2122	54
		MQNIGEQGHMA	417.2133	65
		MQNIGEQGHMA	625.818	69
		MQNIGEQGHMA	625.8196	63

Table 5.2. Nineteen unique proteins (56 unique peptides with MASCOT scores ≥30) were identified by tandem MS in the CDR 0, CDR 1, and mixed clinical CSF. Abbreviations: m/z = mass to charge ratio. "Score" is the MASCOT ion score, which is a measure of the reliability of each identification; scores above 30 are generally considered significant.

Table 5.3. Quantification of selected peptides

	Peptide Sequence	m/z	Peptide Score	Area-Pooled	Area-CDR 1	Area-CDR 0
chromogranin B precursor	RPQSEESWDEED	753.806	55	107119	3256	3962
	RSQEESEEGEEDATSEVD	1013.416	97	266789	50777	148372
	SKGQPRSQEESEEGEEDATSEVD	842.033	90	245278	2048	4162
	SSQGGSLPSEEKGHPQEESEESNVS	873.062	60	2218	37165	88850
	SSQGGSLPSEEKGHPQEESEESNVSMASLGE	1069.147	67	0	46270	133
	SSQGGSLPSEEKGHPQEESEESNVSMASLGE	1069.485	57	0	27048	0
VGF nerve growth factor inducible precursor	LGGSEAGERL	494.759	73	98051	6903	992
	LFAEEEDGEAGAED	741.305	106	307906	0	592
	QQETAAAETETRTHT	828.894	55	5473	47895	3E+06
	GLQEAAEERESAREEEEAEQE	807.361	55	14947	72131	405950
	GLQEAAEERESAREEEEAEQE	807.365	63	14947	72131	405950
	GGEERVGEEDEEAAEAEAEAEEAERA	922.063	91	73079	0	9045
amyloid beta A4 precursor protein	DHSKLVDVPFQVEFPAPKNELVQKF	729.635	62	431472	145650	87484
	DHSKLVDVPFQVEFPAPKNELVQKF	729.636	52	431472	145650	87484
	DHSKLVDVPFQVEFPAPKNELVQKF	729.887	75	345224	114203	79671
TPA: microtubule-associated protein tau	TGSSGAKEMKLKGAD	741.305	69	307906	0	592
apolipoprotein E	KVKQAVETEPEPEL	799.910	71	4359929	4357	7075

	KVKQAVETEPEPEL	800.410	71	1943888	1157	2180
	KVEQAVETEPEPEL	799.910	84	4359929	4357	7075
	KVEQAVETEPEPEL	800.912	58	565296	0	0

Table 5.3. Quantification of peptides from the ion currents that comprised the selected ion chromatogram for each peptide are listed. Differences in peptide abundance can be seen between the samples; for example, the first chromogranin B peptide listed appears much higher in the pooled, or mixed clinical, sample as compared to the CDR 0 and CDR 1 samples.

Chapter 6.

Use of a Multiplexed Immunoassay Panel for the Identification of Novel CSF Biomarkers for Alzheimer's Disease Diagnosis and Prognosis

Chapters 2-5 of this work reflect efforts to identify novel biomarkers for AD through unbiased approaches. Alternatively, targeted approaches focusing on molecules or processes already implicated in disease can also be used for biomarker discovery. A convenient compromise between these two approaches is offered by established targeted multiplexed immunoassay platforms, which allow for the simultaneous quantitation of large numbers of molecules. We utilized one such resource, Rules Based Medicine, which has assembled a platform for the analysis of 190 markers of varied functional classes, many of which have not been investigated in AD, in an attempt to identify novel biomarkers of AD.

Introduction

With the growing prevalence of Alzheimer's disease (AD), the ability to accurately and reliably diagnose AD in its earliest stages has become a public health priority. The concept of 'earliest stages,' however, warrants revision as it is increasingly clear there exists a 'preclinical' or 'presymptomatic' stage during which the pathological changes associated with AD, amyloid plaques and neurofibrillary tangles, begin to appear without concomitant clinical features. This period has been estimated to be ~10-15 years in duration. Means to identify this preclinical phase of AD may facilitate medical intervention to prevent or slow neurodegeneration and the resulting cognitive impairment. Because clinical examination cannot detect preclinical disease and has limited accuracy with very mild stages of AD, there is a pressing need for biomarkers for AD. Furthermore, biomarkers may have significant utility in clinical trial design, providing greater diagnostic certainty for enrollment than is possible by clinical diagnosis alone, and allowing for the selective enrollment of individuals at greater risk of developing

future cognitive impairment, ultimately resulting in trials of shorter duration, smaller size, and reduced cost.

The cerebrospinal fluid (CSF) is a logical source of potential AD biomarkers, as it reflects biochemical changes in the brain. Indeed, the fluid biomarkers thus far showing the greatest promise for use in AD diagnosis and prognosis are CSF amyloid-β42 (Aβ42), tau, and phosphorylated forms of tau (p-tau) (119, 410-413). Concentrations of CSF Aβ42 decrease in association with the deposition of Aβ42 into plaques within the brain (107, 127, 128, 360). This process occurs years prior to the clinical onset of AD and may mark the earliest phase of AD pathology. CSF Aβ42 levels remain low throughout the disease course (94, 127, 423). In contrast, CSF tau and p-tau levels progressively increase with the advancing stages of AD, and in some individuals, begin to rise several years prior to diagnosis (107, 439, 440). The ratios of tau or p-tau to Aβ42 have also proven useful for predicting clinical progression in individuals who have very mild dementia or mild cognitive impairment (MCI), and for predicting future AD dementia among those who are cognitively normal (107, 132, 348). Nevertheless, even for these analytes, there is substantial overlap between control and AD groups (346). Consequently, there remains a need for supplemental biomarkers to improve diagnosis and prognosis at different disease stages. Given the multifactorial nature of AD pathophysiology, it is likely that there will be other CSF biomarkers that will be useful in this regard. While proteomic screens have identified a number of other candidate AD biomarkers (222, 241-243, 245, 246, 250, 361, 362, 364), few studies have utilized large, well-characterized cohorts or have looked for biomarkers of preclinical or very early stage disease.

In this study, a large number of CSF samples (N=333) selected from well-characterized MCI/very early stage-AD and cognitively normal control cohorts were chosen for protein profiling using a commercially available panel that measures a variety of cytokines, chemokines, metabolic markers, growth factors, and other markers. Multiplex immunoassay platforms such as the one used here, Rules Based Medicine Discovery MAP 1.0 panel, allow for the simultaneous quantitation of many analytes, and by adhering to clinical laboratory improvement amendments (CLIA) standards, are amenable for clinical trial work. Using multiple statistical approaches, our findings suggest novel biomarkers that may improve the ability of traditional AD biomarkers, Aβ42 and tau, to distinguish MCI/early-stage AD from cognitive normalcy and to predict the development of future cognitive impairment (i.e. detection of preclinical AD).

Methods

Participant Selection

Participants (N=333) were community-dwelling volunteers enrolled in longitudinal studies of healthy aging and dementia at the Knight Alzheimer's Disease Research Center at Washington University (WU-ADRC). The study protocol was approved by the Human Studies Committee at Washington University, and written and verbal informed consent was obtained from participants at enrollment. At sample collection, participants were ≥60 years of age and in good general health, having no other neurological, psychiatric, or major medical diagnoses that could contribute importantly to dementia. Cognitive status was evaluated based on criteria from the National Institute of Neurological and Communicative Diseases and Stroke-Alzheimer's Disease and Related Disorders Association (NINCDS-ADRDA) (57). A clinical dementia rating (CDR) of 0

(N=242) indicated no dementia, CDR 0.5 (N=63) indicated very mild dementia, and CDR 1 (N=28) indicated mild dementia (68). Some of these CDR 0.5 participants met the criteria for mild cognitive impairment (MCI) and some were more mildly impaired and were considered "pre-MCI" (70, 441). A subset of participants (N=179) in this cohort had also undergone positron emission tomography (PET) imaging with Pittsburgh Compound-B (PIB) for assessment of in vivo amyloid burden (127, 318, 330). Apolipoprotein E (*APOE*) genotypes were determined by the WU-ADRC Genetics Core. Twenty-five to 30 mL of CSF was collected by lumbar puncture (LP) at 8 AM following overnight fasting. Samples were inverted to avoid gradient effects, centrifuged briefly (2,000g, 5 minutes, 4°C) to remove any cellular elements, and aliquoted into polypropylene tubes for freezing and storage at -80°C (107).

Analyte Measurements

CSF Aβ42, total tau, and phospho-tau181 levels (from here on referred to as 'traditional' biomarkers) were analyzed in duplicate by the WU-ADRC Biomarker Core by quantitative ELISA after a single freeze-thaw cycle according to the manufacturer's specifications (Innotest, Innogenetics, Ghent, Belgium).

CSF samples were evaluated by Rules Based Medicine, Inc. (RBM) (Austin, TX) for levels of 190 analytes using the Human Discovery Multi-Analyte Profile (MAP) 1.0 panel and a Luminex 100 platform. This 190 analyte panel (from here on referred to as 'RBM analytes') was assembled by RBM to measure a range of cytokines, chemokines, growth factors, hormones, metabolic markers, and other proteins thought to be important in disease; a complete list of analytes is available at www.rulesbasedmedicine.com.

At RBM, the samples were thawed at room temperature (RT), vortexed, spun at 13,000g for 5 minutes for clarification, and 1.0 mL was removed into a master microtiter plate for MAP analysis. Using automated pipetting, an aliquot of each sample was introduced into one of the capture microsphere multiplexes of the Human DiscoveryMAP. The mixtures of sample and capture microspheres were thoroughly mixed and incubated at RT for 1 hour. Multiplexed cocktails of biotinylated reporter antibodies for each multiplex were then added robotically, and after thorough mixing, were incubated for an additional hour at RT. Multiplexes were developed using an excess of streptavidin-phycoerythrin solution which was thoroughly mixed into each multiplex and incubated for 1 hour at RT. The volume of each multiplexed reaction was reduced by vacuum filtration and then increased by dilution into matrix buffer for analysis. Analysis was performed in a Luminex 100 instrument and the resulting data stream was interpreted using proprietary data analysis software developed at RBM. For each multiplex, both calibrators and controls were included on each microtiter plate. Eight-point calibrators were run in the first and last column of each plate and 3-level controls were included in duplicate. Testing results were determined first for the high, medium and low controls for each multiplex to ensure proper assay performance. Unknown values for each of the analytes localized in a specific multiplex were determined using 4 and 5 parameter, weighted and non-weighted curve fitting algorithms included in the data analysis package.

Statistical Analysis

Statistical analyses were performed in SAS 9.2 (SAS Institute Inc, Cary, NC) for univariate analyses, ROC/AUC calculations, and Cox proportional hazards models, and

in R version 2.10.1 for predictive modeling (442). For the RBM analytes, data below the lower detection limit (LDL) were imputed to LDL/2, and data more than five standard deviations beyond the mean were imputed using a nearest neighbor algorithm. Analytes with more than 10% of data missing or below the LDL were excluded from analysis. The distributions of analytes were tested for normalcy by Box-Cox analysis and, when appropriate, log10 transformed to approximate a normal distribution. Correlations between RBM analytes, traditional AD biomarkers, and demographic variables were evaluated using the Spearman rho correlation coefficient (α=0.05). Analysis of covariance (ANCOVA) using the General Linear Model (GLM) procedure in SAS was used to determine analytes that differed in concentration between AD and control groups while adjusting for the effects of age and gender. For each analyte showing promise by univariate analysis, the area under the receiver operating characteristic curve (AUC, ROC) was calculated for predicting CDR 0 versus CDR>0. The method of Xiong et al., 2004 was implemented to determine the optimum linear combination of analytes and to calculate the confidence interval on the AUC and the sensitivity (443).To obtain relatively unbiased estimates of expected future performance of the three marker panels in predicting CDR 0 versus CDR>0, a bootstrapping resampling technique was used to randomly divide the dataset into many subsets. Averages of performance measures were taken over 100 repetitions.

Cox proportional hazard models assessed the ability of baseline biomarkers to predict time to conversion from cognitive normalcy (CDR 0) to very mild or mild dementia (CDR 0.5 and 1). Data from subjects who did not convert were statistically censored at the date of last assessment. Biomarker measurements were treated as continuous variables and were converted to standard Z-scores to allow for comparison of hazard

ratios between different biomarkers. Baseline variables were considered for inclusion in multivariate models if they were associated with time to conversion in a univariate analysis ($p<.15$). Variables were retained in multivariate proportional hazard models if $p<.05$. AIC (Akaike Information Criterion), a measure of goodness of fit of an estimated statistical model, was used to compare different models, with a lower AIC indicating better model fit.

Several statistical machine learning techniques were utilized to predict subject outcomes as a function of baseline characteristics (e.g. age) and the candidate biomarkers. Rather than focusing on a specific model, a panel of predictive modeling techniques was applied to the data. Most of these models contain "tuning parameters" that cannot be directly estimated from the data; these values were chosen using resampling techniques. The models used were:

- Partial Least Squares (PLS) is a latent variable model that produces linear class boundaries and works well with correlated predictors (444). Candidate values of the tuning parameter, the number of PLS components, ranged from 1 to 20.
- Sparse Partial Least Squares (SPLS) is a variant of PLS that incorporates feature selection in the model fitting (445). The number of PLS components was varied in the same manner as the basic PLS model and the additional tuning parameter for regularization was varied from 0.1 to 0.9.
- Random Forests (RF) is a tree-based ensemble method (446). The number of randomly selected variables at each split was varied over five values (generally 2 to the number of predictors in the model).
- Boosted Trees are another tree-based ensemble model (447). The three tuning parameters are the depth of the tree (even values from 2 to 10 were evaluated),

the number of boosting iterations (20 iterations to 2000 in 100 iteration increments) and the learning rate (fixed at 0.1).

- Support Vector Machine (SVM) are a kernel based method (448). The radial basis function kernel was used. The kernel parameter was estimated analytically (449) and the five candidate values of the cost parameter ranged from 0.1 to 1,000 on the log10 scale.
- Nearest Shrunken Centroids (NCS) is a prototype model that incorporates feature selection (450). The tuning parameter, the shrinkage threshold, was varied over 30 values.
- Naïve Bayes (NB) is a simple classifier where each predictor variable contributes to the final class prediction independently (451). The conditional distributions were computed using a simple Gaussian distribution or using a nonparametric density estimator.
- K-Nearest Neighbors (KNN) is a simple prototype based model (451). Candidate values for the number of neighbors ranged from 5 to 15.
- Flexible Discriminant Analysis (FDA) is a partitioning based model that also incorporates feature selection (452). The multivariate adaptive spline basis function was used. Ten candidate values for the number of retained terms were evaluated.

To determine the values for the tuning parameters and to estimate performance, resampling methods were used. The entire data set was repeatedly split into training (80%) and test sets (20%). This process was repeated 200 times. Models were fit on the training sets and the associated held-out values were used to estimate performance

(sensitivity, specificity, and the area under the ROC curve). The final estimates of performance were calculated by averaging the 200 sets of performance values from the resampling procedure.

Results

Levels of 37 markers are altered in MCI/very mild and mild AD CSF

To identify new candidate biomarkers for AD, multiplexed Luminex-based immunoassays were used to evaluate the levels of 190 analytes in the CSF of 242 cognitively normal participants (CDR 0), 63 participants with very mild dementia (CDR 0.5), and 28 participants with mild dementia (CDR 1) (participant characteristics at baseline assessment in Table 6.1). Of the 190 analytes, 65 had >10% of data missing or below the LDL, and were therefore excluded from analysis, yielding 125 'measurable' analytes. The mean concentrations of 37 CSF analytes were found to differ between cognitively normal (CDR 0) and very mildly/mildly demented (CDR 0.5 and 1) participants by age and gender-adjusted analysis of covariance (ANCOVA) ($p<.05$) (Table 6.2). Additionally, participants with very mild/mild dementia exhibited the typical AD CSF biomarker profile characterized by significantly lower mean levels of CSF Aβ42 and higher mean levels of CSF tau and CSF p-tau181 (Tables 6.1 and 6.2).

Correlation of RBM analytes with demographic features and other biomarker values

Because the CDR 0, 0.5, and 1 groups showed somewhat different distributions with regard to age at LP and gender, levels of the 37 RBM analytes were evaluated for correlation with these variables. Many analytes were significantly associated with age or

gender (Table 6.3). Additionally, seeking insight into the potential roles of the analytes in AD pathology, we evaluated their association with CSF Aβ42, tau, and p-tau181, and cortical amyloid burden measured by PIB-PET imaging. Many of the analytes correlated with CSF tau and CSF p-tau181 (31 and 30, respectively), while fewer correlated with CSF Aβ42 or cortical amyloid burden (8 and 5, respectively) (Table 6.3).

Diagnostic utility of candidate biomarkers

To assess the potential of the analytes for identifying very mild/mild dementia (combined CDR 0.5 and CDR 1), ROC curves and AUCs were calculated for each of the 37 RBM analytes and for traditional AD biomarkers Aβ42, tau, p-tau181 and the ratios tau/Aβ42 and p-tau181/Aβ42 (Table 6.4). Although none of the RBM analytes alone out-performed the traditional biomarkers, combining traditional biomarkers with RBM analytes improved upon the AUC of the traditional biomarkers in many cases; e.g., Aβ42: AUC= .7552, combinations ranging from .7553-.8201; tau/Aβ42: AUC= .8443, combinations ranging from .8444-.8819; p-tau181/Aβ42: AUC= .8065, combinations ranging from .8065-.8468 (Table 6.4). For these '2-marker panels' of traditional biomarker plus RBM analyte, combinations with tau/Aβ42 consistently yielded the highest AUCs. To investigate whether combinations of three markers could yield a small panel with improved diagnostic accuracy, we utilized a targeted approach in which the four 2-marker panels with the highest AUCs (tau/Aβ42 + cystatin C, tau/Aβ42 + VEGF, tau/Aβ42 + KIM-1, tau/Aβ42 + PP) were combined with the 10 RBM analytes with the highest individual AUCs (indicated in Table 6.4). Because an independent validation cohort was not available for analysis, bootstrapping resampling with 100 iterations was performed to obtain relatively unbiased estimates of expected future performance of the

'3-marker panels' in predicting CDR 0 versus CDR>0 (Table 6.5). A number of the 3-marker panels demonstrated significantly improved AUCs compared to the corresponding 2-marker panels, with the best achieving AUCs of ~.90 and sensitivities of ~84% at 80% specificity (Table 6.5).

Because AD is a complex, multifactorial disease and likely involves alterations in multiple biological pathways, it is possible that a larger panel of biomarkers encompassing various features of AD pathophysiology may be optimal for disease diagnosis. Thus, we utilized statistical machine learning algorithms, which are more amenable to potentially large numbers of analyte combinations and can identify highly complex nonlinear relationships, to discover whether groups of markers are capable of distinguishing very mildly/mildly demented (CDR 0.5 and 1 combined) from cognitively normal participants (CDR 0). A multi-pronged analytical approach including RF, PLS, SPLS, Boosted Tree, FDA, NB, NSC, LR, KNN, and SVM was used, as each approach has its own strengths and weaknesses. Models were fit with two sets of predictors: 1) traditional biomarkers, and 2) traditional biomarkers plus RBM analytes; additionally, age, gender, and ApoE4 allele status were included in all models. Model performance measures were based on cross-validation, in which the test set results were averaged from 200 splits of the data between training (80%) and test (20%) (Table 6.6). Using either traditional biomarkers or traditional biomarkers with RBM analytes, no model clearly out-performed the others; however, the RBM analytes appeared to contribute additional specificity to the biomarker panels (traditional: sensitivity 80.6-91.4%, specificity 42.4-56.6%; traditional+ RBM: sensitivity 79.1-93.2%, specificity 59.6-77.6%). This improvement is further reflected in the Youden Index, a single statistic that captures the performance of a diagnostic test and is a function of sensitivity and specificity, which

was higher on average for the models fitted with traditional plus RBM analytes (traditional: 0.230-0.438; traditional+RBM: 0.401-0.621). Additionally, models fitted with traditional plus RBM analytes yielded mostly higher AUCs (traditional: 0.680-0.827; traditional+RBM: 0.754-0.868). For the four models with a built-in importance statistic (i.e., Boosted Tree, NSC, RF, and PLS) there was considerable overlap in the top 15 predictors for each model (Table 6.7). Importantly, nearly all of the markers found to best discriminate CDR 0 from CDR>0 participants in the more targeted ROC analyses (Table 6.5) were also identified as the top predictors in the machine learning models (Table 6.7), reconfirming the potential of these analytes as biomarkers for AD.

Prognostic utility of candidate biomarkers

Identifying individuals with AD neuropathology while they are still in the preclinical phase will be critically important, as disease-modifying therapies currently in development are likely to be most effective early in the disease process before significant synaptic and neuronal loss has occurred. Thus, we used univariate and multivariate Cox proportional hazards models to evaluate the ability of the analytes to predict risk of developing cognitive impairment (conversion from CDR 0 to CDR>0). Of the 215 CDR 0 subjects with at least one follow-up annual clinical assessment, 29 received a CDR>0 at follow-up, and thus were classified as "converters." Analyte measurements were converted to standard Z-scores to allow for comparison of hazard ratios between the different analytes. Variables with $p<.15$ in the univariate Cox analyses were considered for inclusion in the multivariate model; variables were retained in the final model if $p<.05$. The final multivariate model consisted of calbindin (HR=1.750, p=0.0063), 1/Aβ42 (HR=2.454, $p<0.0001$), and age at LP (HR=1.096, p=0.0002), with an

overall model HR of 4.704 (Table 6.8). Although calbindin and tau both had p<.05 in the univariate analysis, the significant correlation between the two (r=0.476, p<0.0001) prohibited inclusion of both variables in the multivariate model. Therefore, a second multivariate model consisted of tau (HR=1.467, p=0.0262), 1/Aβ42 (HR=2.247, p<0.0001), and age at LP (HR=1.098, p=0.0003), with an overall model HR of 3.619 (Table 6.8). However, the higher HR of calbindin than of tau, and the higher overall model HR and lower AIC of the first model support it as the better model.

Discussion

Biomarkers that can detect AD in its early stages and, importantly, predict future dementia will be invaluable for efficient clinical trial design and eventually patient care. This study identifies novel biomarkers that improve upon the ability of the best identified biomarkers to date to discriminate very mildly demented from cognitively normal participants, and identifies a novel biomarker with significant prognostic potential.

Using Luminex technology and a targeted multiplex panel, we identified 37 analytes that are increased or decreased in the CSF of participants with early AD relative to cognitively normal controls. ROC analysis revealed that small combinations of a subset of these markers (cystatin C, VEGF, TRAIL-R3, PAI-1, PP, NT-proBNP, MMP-10, MIF, GRO-α, fibrinogen, FAS, and eotaxin-3) can enhance the ability of the best-performing of the traditional biomarkers, the tau/Aβ42 ratio, to discriminate CDR 0.5 and 1 from CDR 0 participants. Using alternative statistical strategies that are more amenable to the analysis of larger combinations of markers, multiple machine learning algorithms likewise showed that the novel biomarkers improved upon the diagnostic

performance of the traditional biomarkers (Aβ42, tau, p-tau181). Importantly, nearly all of the markers found to best discriminate CDR 0 from CDR 0.5 and 1 participants in the more targeted ROC analyses were also identified as the top predictors in the machine learning models that contain a built-in importance statistic (10 of 12 markers). Thus, the potential of these analytes as biomarkers for AD is supported by alternative statistical approaches that resulted in a similar output. Further supporting these results is a recent report of the application of a smaller RBM Discovery MAP panel to a smaller cohort of AD, MCI, and control subjects (361); this study identified a number of same analytes as being differentially expressed in AD CSF as compared to control CSF and, although using different analytical approaches, included VEGF, TRAIL-R3, and eotaxin-3, in 'combined' models of novel and traditional biomarkers.

It is important to note that while the models used in our study suggest diagnostic value of the novel biomarkers, other combinations of these markers may be optimal; it will be of interest in future studies to validate the results of this discovery study in additional cohorts and to determine whether alternative combinations of these markers may demonstrate improved performance. The levels of at least 7 of the novel biomarkers have been evaluated in AD subjects in other studies: no change was observed in plasma PAI-1 levels (453); in agreement with our findings, two studies have reported increased CSF MIF in AD and MCI subjects (454, 455); also consistent with our findings, increased fibrinogen levels have been observed in AD and MCI CSF (456) and in AD plasma (457), and increased plasma levels have been associated with an increased risk of future dementia (458); results have been mixed regarding CSF FAS levels in AD (227, 459); AD plasma/serum VEGF levels have been reported to be unchanged (460, 461), decreased (462), and increased (463), while CSF levels have been reported to be

unchanged (464) or increased (465); no change in CSF or serum levels of TNF R2 in AD has been reported (218); cystatin C findings have been inconsistent, with reports of serum/plasma levels unchanged (466), increased in AD (467) or in those who later develop AD (143), and decreased (468) or decreased levels associated with increased risk of future AD (469), while CSF levels have been reported to be unchanged (466, 470), decreased (390) (Chaper 2 and 3), or increased (243). These inconsistent results may be due in part to the existence of a truncated form of cystatin C, which was found to be increased in AD CSF, while the full length protein was decreased (243, 362).

Furthermore, the potential involvement of each marker in AD pathophysiology necessitates investigation. The candidate biomarkers identified in the ROC and machine learning portions of this study belong to a wide variety of functional classes and pathways, including tissue remodeling and angiogenesis (MMP-10, VEGF), regulation of apoptosis (TRAIL-R3, FAS, MIF), neutrophil, eosinophil, and/or basophil chemotaxis (GRO-α, eotaxin-3), blood coagulation (Fibrinogen, PAI-1), intravascular volume homeostasis (NT-proBNP), and gastrointestinal and pancreatic secretions (PP). In addition, a number of molecules involved in inflammatory pathways were identified in the machine learning models (IL-7, IL-17E, TNF RII, MCP-2, FASL). The association of several of the candidate biomarkers with AD pathophysiology has already been probed, most notably for cystatin C, which appears to play a role in preventing Aβ oligomerization and amyloidogenesis (391, 393, 394, 471, 472), and to a lesser extent for PAI-1 (473-475), MIF (454, 476), fibrinogen (477, 478), FAS and FASL (479-482), VEGF (483-485), and TNF RII (486-488).

It will be important in future studies to assess each candidate biomarker's value in diagnosis in independent sample sets when combined with other existing biomarkers

or imaging tools. Additionally, to follow up on these biomarker candidates, their ability to discriminate AD from other causes of dementia needs to be examined; indeed, several of these markers have already shown promise for distinguishing AD from frontotemporal lobar degeneration (cystatin C (362), eotaxin-3 (361), and HGF (361)). Incorporation of such markers into a biomarker panel may improve diagnostic specificity. Beyond their clinical use, these markers may have great value in the design of and enrollment in trials of disease-modifying therapies. By enrolling only subjects with lower or higher values of a particular marker (or panels of markers) indicative of AD, and excluding potential subjects with intermediate or 'overlap' values, one might provide greater diagnostic certainty than is possible through clinical evaluation alone. This is especially relevant for the design and evaluation of primary prevention trials in cognitively normal cohorts. Enriching study populations for subjects displaying certain biomarker levels may result in studies of greater efficacy, translating to reduced cost.

This study also suggests a novel biomarker, CSF calbindin, that can predict risk of future dementia in individuals who are still cognitively normal. Previous studies have shown that Aβ42, tau, YKL-40 (an astrocyte marker), and the ratios tau/Aβ42 and YKL-40/Aβ42 can predict subsequent cognitive decline in non-demented cohorts (107, 132) (and Chapter 3). Using multivariate Cox proportional hazards models to determine the best combination of biomarkers for prognosis, we show here that a panel of markers consisting of calbindin, Aβ42, and age has predictive value comparable to, if not better than, a second panel consisting of tau, Aβ42, and age. Tissue culture studies have shown that increased expression of calbindin, a calcium binding protein present in central and peripheral nervous system neurons, correlates with increased resistance to cell death triggered by a variety of causes, including exposure to excitatory amino acids,

ischemic injury, and Aβ (489-492). Decreases in calbindin protein and mRNA levels (493) and number of calbindin-immunopositive neurons (400, 494, 495) have been observed in AD brains compared to controls. Further suggesting there may be a role for calbindin in AD pathophysiology is the large body of literature demonstrating that increased oxidative stress and altered calcium homeostasis appear to be interrelated mechanisms in AD pathogenesis. Interestingly, although not quite reaching statistical significance, we found that CSF calbindin levels trended higher in the very mildly/mildly demented group (p=.0660), suggesting that perhaps degenerating neurons release calbindin into the CSF. The immunohistochemical findings of a small study of 6 AD brains suggesting that calbindin-immunopositive neurons are relatively preserved in cases with moderate amyloid plaque and neurofibrillary content but are lost in more severe cases (494) prompts the question of whether CSF calbindin levels would be more significantly elevated in more severely demented individuals. Further studies are needed to confirm the prognostic potential of CSF calbindin, to determine if other complementary fluid or imaging biomarkers may improve upon its performance, and to more definitively elucidate its role in AD pathophysiology. As with the candidate diagnostic biomarkers, CSF calbindin may have value for clinical trial design by allowing for the selective enrollment of individuals who are at greater risk of developing cognitive impairment, resulting in clinical trials of shorter duration and reduced cost.

Table 6.1. Demographic, clinical, and genotypic characteristics of the 333 study participants

Characteristic	**CDR 0**	**CDR 0.5**	**CDR 1**
N	242	63	28
Gender (% Female)	65%	52%	50%
APOE genotype, % ε4+	32%	54%	57%
Mean MMSE score (SD)	28.9 (1.3)	26.3 (2.8)	22.5 (4.0)
Mean age at LP (SD), yrs	71.6 (7.4)	74.6 (7.3)	76.8 (6.2)
Mean CSF Aβ42 (SD), pg/mL	607 (234)	436 (233)	355 (119)
Mean CSF tau (SD), pg/mL	315 (169)	547 (278)	557 (266)
Mean CSF p-tau181 (SD), pg/mL	56 (25)	85 (45)	78 (38)

Abbreviations: CDR, Clinical Dementia Rating; *APOE*, apolipoprotein E; MMSE, Mini-Mental State Examination; LP, lumbar puncture; SD, standard deviation; CSF, cerebrospinal fluid; Aβ-42, amyloid-beta peptide 1-42; p-tau181, tau phosphorylated at threonine 181.

Table 6.2. Analytes that differ in levels between cognitively normal (CDR 0) and very mildly/mildly demented (CDR 0.5 and 1) participants

Marker	Adjusted mean CDR 0	Adjusted mean CDR>0	p	Raw mean CDR 0	Raw mean CDR>0
Aβ42 (pg/mL)	607.45	418.85	<.0001	606.90	411.18
Tau (pg/mL)	315.59	533.60	<.0001	314.80	549.96
p-tau181 (pg/mL)	56.30	81.01	<.0001	56.32	82.98
Growth-Regulated alpha protein (GRO-α) (pg/mL)	18.27	22.09	<.0001	18.30	22.44
Log Matrix Metalloproteinase-10 (MMP-10) (pg/mL)	24.84	31.41	<.0001	24.11	32.61
Log N-terminal pro-brain natriuretic peptide (NT-proBNP) (pg/mL)	87.00	107.75	<.0001	87.70	111.12
Log Plasminogen Activator Inhibitor 1 (PAI-1) (ng/mL)	1.05	1.28	<.0001	1.01	1.34
TNF-Related Apoptosis-Inducing Ligand Receptor 3 (TRAIL-R3) (ng/mL)	0.55	0.63	<.0001	0.55	0.65
Vascular Endothelial Growth Factor (VEGF) (pg/mL)	441.57	378.30	<.0001	437.83	386.01
Log Pancreatic Polypeptide (PP) (pg/mL)	0.94	1.30	0.0001	0.88	1.41
Log FAS (ng/mL)	0.57	0.65	0.0002	0.56	0.67
Log Macrophage Migration Inhibitory Factor (MIF) (ng/mL)	0.15	0.17	0.0004	0.15	0.18
Interleukin-7 (IL-7) (pg/mL)	12.63	9.47	0.0006	12.23	9.68
Log Cystatin C (ng/mL)	5613.84	4750.89	0.0011	5551.50	4835.30
Thrombopoietin (ng/mL)	0.43	0.37	0.0016	0.42	0.37
Sortilin (ng/mL)	6.32	6.92	0.0019	6.33	6.96
Monocyte Chemotactic Protein 2 (MCP-2) (pg/mL)	4.03	4.61	0.0020	3.97	4.67
Log Fibrinogen (ug/mL)	0.63	0.78	0.0024	0.59	0.81
Log Creatine Kinase-MB (CKMB) (pg/mL)	26.55	20.97	0.0030	26.62	20.87
Cortisol (ng/mL)	11.21	12.65	0.0034	11.17	12.89
Thymus-Expressed Chemokine (TECK) (ng/mL)	6.38	6.85	0.0039	6.30	6.96
Eotaxin-3 (pg/mL)	56.78	62.09	0.0057	55.33	63.68
Interleukin-17E (IL-17E) (pg/mL)	8.63	7.75	0.0058	8.60	7.79
Kidney Injury Molecule-1 (KIM-1) (pg/mL)	78.97	83.46	0.0074	79.05	83.08
Log Heparin-binding epidermal growth factor-like growth factor (HB-EGF)	24.98	28.77	0.0077	25.05	28.70

(pg/mL)					
Log Osteopontin (ng/mL)	173.23	197.68	0.0078	174.15	202.31
Log α-1-Antitrypsin (ug/mL)	4.87	5.37	0.0102	4.73	5.49
Fatty Acid Synthase Ligand (FASL) (pg/mL)	4.85	5.40	0.0109	4.78	5.49
Log Insulin-like Growth Factor-Binding Protein 2 (IGFBP-2) (ng/mL)	199.58	212.16	0.0111	195.93	217.47
Log Interleukin-10 (IL-10) (pg/mL)	1.14	1.29	0.0131	1.12	1.29
Log Tumor necrosis factor-a receptor 2 (TNF RII) (ng/mL)	0.53	0.59	0.0141	0.52	0.62
Log Resistin (pg/mL)	26.28	30.76	0.0146	25.20	32.14
Log Fatty Acid Binding Protein (FABP) (ng/mL)	3.03	3.62	0.0209	2.93	3.81
Log Apolipoprotein D (ApoD) (ug/mL)	4.18	4.57	0.0318	4.02	4.65
Log Hepatocyte Growth Factor (HGF) (ng/mL)	1.18	1.28	0.0349	1.18	1.30
Log Insulin (uIU/mL)	0.22	0.19	0.0359	0.21	0.19
Log Hemofiltrate cysteine-cysteine chemokine (HCC-4) (pg/mL)	30.25	33.13	0.0418	28.98	33.87
Log Interferon gamma Induced Protein 10 (IP-10) (pg/mL)	299.63	341.86	0.0432	295.14	354.74
Log Gamma-Interferon-Induced Monokine (MIG) (pg/mL)	423.80	493.91	0.0452	400.16	572.75
Thrombomodulin (ng/mL)	0.17	0.18	0.0475	0.17	0.19

Table 6.2. Analysis of covariance (ANCOVA) using the General Linear Model (GLM) procedure in SAS was used to determine analytes that differed in concentration ($p<.05$) between CDR 0 and CDR>0 groups while adjusting for the effects of age and gender ("adjusted means"). For markers that were log transformed to approximate a normal distribution, the resulting Least Squares mean (or estimated marginal mean) was back-transformed to obtain the adjusted mean shown. Also provided are the raw mean concentrations for the CDR 0 and CDR>0 groups.

Table 6.3. Correlations of RBM analytes with age, gender, and other biomarker values

Analyte	Gender	Age	Aβ42	Tau	p-tau181	tau/Aβ42	Cortical PIB
α1A	<.001	0.255 (<.0001)	0.031 (0.574)	0.117 (0.033)	0.105 (0.055)	0.048 (0.386)	-0.048 (0.525)
ApoD	<.001	0.218 (<.0001)	0.059 (0.280)	0.222 (<.0001)	0.216 (<.0001)	0.113 (0.039)	-0.103 (0.169)
Calbindin	0.001	0.196 (<.001)	0.094 (0.088)	0.476 (<.0001)	0.500 (<.0001)	0.294 (<.0001)	0.122 (0.104)
CKMB	0.524	-0.069 (0.211)	0.008 (0.877)	-0.200 (<.001)	-0.186 (0.001)	-0.148 (0.007)	0.032 (0.673)
Cortisol	0.282	0.252 (<.0001)	-0.051 (0.357)	0.187 (0.001)	0.189 (0.001)	0.159 (0.004)	0.012 (0.875)
Cystatin C	0.461	0.093 (0.089)	0.281 (<.0001)	0.536 (<.0001)	0.597 (<.0001)	0.236 (<.0001)	-0.041 (0.587)
Eotaxin-3	<.001	0.317 (<.0001)	0.058 (0.289)	0.367 (<.0001)	0.342 (<.0001)	0.217 (<.0001)	0.003 (0.971)
FABP	0.031	0.296 (<.0001)	0.012 (0.833)	0.727 (<.0001)	0.725 (<.0001)	0.505 (<.0001)	0.159 (0.034)
FAS	<.001	0.297 (<.0001)	0.083 (0.132)	0.491 (<.0001)	0.470 (<.0001)	0.288 (<.0001)	-0.074 (0.326)
FASL	0.165	0.192 (<.001)	-0.060 (0.274)	0.189 (0.001)	0.200 (<.001)	0.129 (0.018)	-0.020 (0.795)
Fibrinogen	<.001	0.284 (<.0001)	-0.044 (0.422)	0.192 (<.001)	0.178 (0.001)	0.145 (0.008)	0.034 (0.652)
GRO-α	0.178	0.279 (<.0001)	-0.105 (0.056)	0.317 (<.0001)	0.329 (<.0001)	0.259 (<.0001)	0.144 (0.054)
HB-EGF	0.975	0.017 (0.751)	0.079 (0.151)	0.348 (<.0001)	0.359 (<.0001)	0.202 (<.001)	-0.024 (0.751)
HCC-4	<.001	0.240 (<.0001)	0.007 (0.895)	0.094 (0.088)	0.037 (0.504)	0.047 (0.388)	-0.095 (0.204)
HGF	0.918	0.222 (<.0001)	0.088 (0.110)	0.619 (<.0001)	0.639 (<.0001)	0.386 (<.0001)	0.004 (0.957)
IGFBP-2	<.001	0.394 (<.0001)	0.062 (0.262)	0.462 (<.0001)	0.441 (<.0001)	0.278 (<.0001)	0.031 (0.685)
IL-17E	0.386	0.032 (0.563)	0.017 (0.760)	0.007 (0.899)	0.049 (0.371)	0.019 (0.725)	-0.101 (0.180)
IL-7	0.007	0-.002 (0.976)	0.147 (0.007)	-0.003 (0.961)	0.032 (0.557)	-0.091 (0.096)	-0.227 (0.002)
IL-10	<.001	0.055 (0.313)	-0.026 (0.637)	0.070 (0.205)	0.075 (0.170)	0.053 (0.337)	-0.071 (0.342)
IP-10	0.327	0.236 (<.0001)	0.023 (0.682)	0.249 (<.0001)	0.282 (<.0001)	0.147 (0.007)	-0.071 (0.344)
Insulin	<.001	0.094 (0.088)	0.245 (<.0001)	0.213 (<.0001)	0.214 (<.0001)	0.005 (0.921)	-0.190 (0.011)
KIM-1	0.636	0-.032 (0.561)	-0.057 (0.301)	-0.239 (<.0001)	-0.331 (<.0001)	-0.154 (0.005)	-0.060 (0.427)
MCP-2	0.013	0.146 (0.007)	-0.106 (0.053)	0.045 (0.408)	0.059 (0.282)	0.071 (0.199)	-0.011 (0.880)

MIF	0.239	0.330 (<.0001)	-0.007 (0.901)	0.579 (<.0001)	0.597 (<.0001)	0.412 (<.0001)	0.084 (0.264)
MIG	0.528	0.603 (<.0001)	-0.017 (0.762)	0.282 (<.0001)	0.289 (<.0001)	0.207 (<.001)	-0.053 (0.484)
MMP-10	0.002	0.325 (<.0001)	-0.116 (0.034)	0.458 (<.0001)	0.415 (<.0001)	0.390 (<.0001)	0.086 (0.252)
NT-proBNP	0.030	0.273 (<.0001)	0.053 (0.338)	0.331 (<.0001)	0.323 (<.0001)	0.188 (0.001)	-0.007 (0.923)
Osteopontin	0.137	0.192 (<.001)	0.030 (0.590)	0.680 (<.0001)	0.701 (<.0001)	0.466 (<.0001)	0.162 (0.030)
PP	<.001	0.374 (<.0001)	-0.072 (0.189)	0.226 (<.0001)	0.179 (0.001)	0.192 (<.001)	0.041 (0.586)
PAI-1	<.001	0.429 (<.0001)	-0.064 (0.244)	0.334 (<.0001)	0.327 (<.0001)	0.266 (<.0001)	-0.003 (0.973)
Resistin	<.001	0.355 (<.0001)	0.072 (0.189)	0.255 (<.0001)	0.198 (<.0001)	0.120 (0.029)	-0.075 (0.320)
Sortilin	0.881	0.135 (0.014)	0.139 (0.011)	0.515 (<.0001)	0.527 (<.0001)	0.273 (<.0001)	-0.003 (0.972)
TNF RII	0.205	0.426 (<.0001)	0.059 (0.282)	0.678 (<.0001)	0.702 (<.0001)	0.442 (<.0001)	0.002 (0.975)
TRAIL-R3	0.112	0.413 (<.0001)	-0.011 (0.837)	0.509 (<.0001)	0.476 (<.0001)	0.356 (<.0001)	0.008 (0.914)
Thrombomodulin	<.001	0.193 (<.001)	0.109 (0.048)	0.215 (<.0001)	0.205 (<.001)	0.076 (0.168)	-0.063 (0.406)
Thrombopoietin	0.015	0.034 (0.531)	0.194 (<.001)	-0.016 (0.768)	0.017 (0.758)	-0.130 (0.017)	-0.237 (0.001)
TECK	0.015	0.270 (<.0001)	0.047 (0.389)	0.322 (<.0001)	0.312 (<.0001)	0.193 (<.001)	0.001 (0.992)
VEGF	0.651	0.101 (0.065)	0.357 (<.0001)	0.470 (<.0001)	0.543 (<.0001)	0.154 (0.005)	-0.059 (0.429)

Table 6.3. Correlations were evaluated using the Spearman rho correlation coefficient (α=0.05); shown are the *r* and (p value). Gender differences were evaluated by Mann-Whitney test.

Table 6.4. ROC analyses

AUC of Traditional Biomarkers			
log Aβ42	0.7552		
log tau	0.7830		
log p-tau181	0.7149		
log tau/Aβ42	0.8443		
log p-tau181/Aβ42	0.8065		
AUC of RBM Biomarkers: alone and in combination with traditional biomarkers			
	Marker	**Marker+log tau/Aβ42**	**Marker+log p-tau181/Aβ42**
log α1A	0.6296	0.8578	0.8234
log ApoD	0.6136	0.8489	0.8138
log CKMB	0.6106	0.8475	0.8118
Cortisol	0.6183	0.8510	0.8155
log Cystatin C	0.5965	0.8819 §	0.8468
Eotaxin-3	0.6448 §	0.8516	0.8202
log FABP	0.6163	0.8499	0.8080
log FAS	0.6689 §	0.8518	0.8209
FASL	0.6134	0.8479	0.8116
log Fibrinogen	0.6503 §	0.8564	0.8232
GRO-α	0.7024 §	0.8609	0.8305
log HB-EGF	0.5929	0.8445	0.8081
log HCC-4	0.6172	0.8596	0.8281
log HGF	0.5972	0.8458	0.8069
log IGF-BP2	0.6378	0.8462	0.8116
IL-7	0.6029	0.8508	0.8162
log IL-10	0.6075	0.8575	0.8215
IL-17E	0.5969	0.8487	0.8145
log Insulin	0.5406	0.8453	0.8077
log IP-10	0.5970	0.8460	0.8093
KIM-1	0.5894	0.8668 §	0.8343
MCP-2	0.6264	0.8554	0.8200
log MIF	0.6651 §	0.8455	0.8117
log MIG	0.6376	0.8544	0.8207
log MMP-10	0.6929 §	0.8518	0.8232
log NT-proBNP	0.6753 §	0.8562	0.8248
log Osteopontin	0.6050	0.8508	0.8100
log PP	0.6789 §	0.8644 §	0.8356
log PAI-1	0.6814 §	0.8587	0.8273
log Resistin	0.6218	0.8522	0.8211

Sortilin	0.6177	0.8444	0.8076
log TNF RII	0.6319	0.8447	0.8065
TRAIL-R3	0.6851 §	0.8523	0.8212
Thrombomodulin	0.6004	0.8503	0.8150
Thrombopoietin	0.5898	0.8465	0.8111
TECK	0.6371	0.8525	0.8190
VEGF	0.6146	0.8766 §	0.8441

Table 6.4. To assess the ability of the markers to distinguish CDR>0 from CDR 0, ROC analyses were performed for each of the traditional biomarkers (Aβ42, tau, p-tau181 and the ratios tau/Aβ42 and p-tau181/Aβ42) and for the 37 RBM analytes with $p<.05$ in the univariate analyses. Each traditional biomarker was then combined with each RBM analyte to identify '2-marker panels' with improved AUCs. Among the traditional biomarkers, the ratios tau/Aβ42 and p-tau181/Aβ42 demonstrated the highest AUCs; additionally, combining these ratios with the RBM analytes consistently yielded 2-marker panels with AUCs higher than combinations of the individual traditional biomarkers (Aβ42, tau, p-tau181) with the RBM analytes. Thus, only the most promising 2-marker panels (those with tau/Aβ42 and p-tau181/Aβ42) are shown here. To determine whether combinations of three markers could yield a small panel with improved diagnostic accuracy, the four 2-marker panels with the highest AUCs were combined with the 10 RBM analytes with the highest individual AUCs (indicated by §, results in Table 6.5).

Table 6.5. ROC analyses of 3-marker panels

Marker Panels	AUC	Stdev	95% CI	Sensitivity (at 80% specificity)	Stdev	95% CI	P value	Stdev	95% CI
log tau/Aβ + log Cystatin C + TRAIL-R3	0.9014	0.0232	0.8969-0.9060	0.8367	0.0445	0.8280-0.8455	0.0299	0.0222	0.0255-0.0342
log tau/Aβ + log Cystatin C + log PAI-1	0.9063	0.0221	0.9020-0.9106	0.8470	0.0438	0.8384-0.8556	0.0283	0.0344	0.0215-0.0351
log tau/Aβ + log Cystatin C + log PP	0.9066	0.0203	0.9026-0.9106	0.8471	0.0400	0.8393-0.8550	0.0245	0.0319	0.0183-0.0307
log tau/Aβ + log Cystatin C + NT-proBNP	0.9041	0.0228	0.8996-0.9086	0.8422	0.0445	0.8335-0.8509	0.0287	0.0330	0.0223-0.0352
log tau/Aβ + log Cystatin C + log MMP-10	0.8987	0.0230	0.8942-0.9032	0.8317	0.0447	0.8230-0.8405	0.0647	0.0582	0.0533-0.0761
log tau/Aβ + log Cystatin C + log MIF	0.8964	0.0249	0.8915-0.9013	0.8272	0.0487	0.8177-0.8368	0.0699	0.0569	0.0588-0.0811
log tau/Aβ + log Cystatin C + GRO-α	0.9071	0.0218	0.9028-0.9113	0.8475	0.0412	0.8395-0.8556	0.0347	0.0410	0.0266-0.0427
log tau/Aβ + log Cystatin C + log Fibrinogen	0.9033	0.0219	0.8990-0.9075	0.8403	0.0429	0.8319-0.8487	0.0357	0.0502	0.0259-0.0455
log tau/Aβ + log Cystatin C + log FAS	0.9052	0.0220	0.9009-0.9095	0.8440	0.0425	0.8356-0.8523	0.0248	0.0248	0.0200-0.0297
log tau/Aβ + log Cystatin C + Eotaxin-3	0.9051	0.0219	0.9008-0.9094	0.8441	0.0427	0.8357-0.8524	0.0273	0.0350	0.0205-0.0342
log tau/Aβ + VEGF + TRAIL-R3	0.9004	0.0226	0.8960-0.9049	0.8347	0.0437	0.8262-0.8433	0.0208	0.0158	0.0177-0.0239
log tau/Aβ + VEGF + log PAI-1	0.9005	0.0225	0.8961-0.9049	0.8355	0.0445	0.8267-0.8442	0.0272	0.0320	0.0210-0.0335
log tau/Aβ + VEGF + log PP	0.9039	0.0215	0.8997-0.9081	0.8423	0.0422	0.8340-0.8506	0.0167	0.0250	0.0118-0.0216
log tau/Aβ + VEGF + NT-proBNP	0.9028	0.0224	0.8984-0.9072	0.8396	0.0439	0.8310-0.8482	0.0165	0.0207	0.0124-0.0205
log tau/Aβ + VEGF + log MMP-10	0.8947	0.0242	0.8900-0.8995	0.8241	0.0471	0.8149-0.8333	0.0534	0.0519	0.0432-0.0636
log tau/Aβ + VEGF + log MIF	0.8908	0.0261	0.8857-0.8959	0.8164	0.0506	0.8065-0.8264	0.0703	0.0570	0.0591-0.0815
log tau/Aβ + VEGF + GRO-α	0.9003	0.0238	0.8956-0.9049	0.8348	0.0452	0.8259-0.8436	0.0365	0.0371	0.0292-0.0437
log tau/Aβ + VEGF + log Fibrinogen	0.8988	0.0231	0.8943-0.9033	0.8317	0.0449	0.8229-0.8405	0.0327	0.0457	0.0237-0.0416
log tau/Aβ + VEGF + log FAS	0.9012	0.0232	0.8967-0.9058	0.8363	0.0445	0.8276-0.8451	0.0232	0.0248	0.0183-0.0281
log tau/Aβ + VEGF + Eotaxin-3	0.8991	0.0227	0.8947-0.9036	0.8325	0.0441	0.8239-0.8411	0.0293	0.0354	0.0224-0.0363
log tau/Aβ + KIM-1 + TRAIL-R3	0.8810	0.0256	0.8760-0.8860	0.7979	0.0486	0.7884-0.8075	0.1082	0.0747	0.0936-0.1229

log tau/Aβ + KIM-1 + log PAI-1	0.8866	0.0246	0.8818-0.8915	0.8087	0.0476	0.7993-0.8180	0.0614	0.0607	0.0495-0.0733
log tau/Aβ + KIM-1 + log PP	0.8905	0.0239	0.8858-0.8952	0.8162	0.0467	0.8070-0.8253	0.0357	0.0452	0.0269-0.0445
log tau/Aβ + KIM-1 + NT-proBNP	0.8821	0.0260	0.8770-0.8872	0.8001	0.0500	0.7903-0.8099	0.0926	0.0788	0.0772-0.1081
log tau/Aβ + KIM-1 + log MMP-10	0.8787	0.0270	0.8734-0.8840	0.7940	0.0511	0.7840-0.8040	0.1497	0.1015	0.1298-0.1696
log tau/Aβ + KIM-1 + log MIF	0.8775	0.0276	0.8721-0.8829	0.7918	0.0518	0.7816-0.8019	0.1478	0.0941	0.1294-0.1663
log tau/Aβ + KIM-1 + GRO-α	0.8897	0.0242	0.8850-0.8945	0.8153	0.0448	0.8065-0.8241	0.0513	0.0498	0.0416-0.0611
log tau/Aβ + KIM-1 + log Fibrinogen	0.8821	0.0267	0.8769-0.8874	0.8003	0.0507	0.7903-0.8102	0.0927	0.0809	0.0768-0.1085
log tau/Aβ + KIM-1 + log FAS	0.8806	0.0248	0.8757-0.8855	0.7973	0.0472	0.7881-0.8066	0.1157	0.0852	0.0990-0.1324
log tau/Aβ + KIM-1 + Eotaxin-3	0.8805	0.0264	0.8753-0.8857	0.7973	0.0498	0.7875-0.8071	0.1152	0.0943	0.0967-0.1337
log tau/Aβ + log PP + TRAIL-R3	0.8717	0.0249	0.8668-0.8766	0.7790	0.0488	0.7695-0.7886	0.2225	0.1023	0.2024-0.2425
log tau/Aβ + log PP + log PAI-1	0.8715	0.0250	0.8666-0.8764	0.7782	0.0498	0.7685-0.7880	0.2034	0.1052	0.1828-0.2240
log tau/Aβ + log PP + NT-proBNP	0.8723	0.0254	0.8674-0.8773	0.7806	0.0491	0.7710-0.7902	0.1705	0.1051	0.1499-0.1912
log tau/Aβ + log PP + log MMP-10	0.8702	0.0256	0.8652-0.8753	0.7761	0.0507	0.7662-0.7860	0.2394	0.1204	0.2158-0.2630
log tau/Aβ + log PP + log MIF	0.8685	0.0251	0.8635-0.8734	0.7723	0.0496	0.7625-0.7820	0.2909	0.1014	0.2711-0.3108
log tau/Aβ + log PP + GRO-α	0.8755	0.0250	0.8706-0.8804	0.7875	0.0472	0.7783-0.7968	0.1329	0.0908	0.1151-0.1507
log tau/Aβ + log PP + log Fibrinogen	0.8720	0.0255	0.8670-0.8769	0.7795	0.0498	0.7698-0.7893	0.1878	0.1160	0.1651-0.2106
log tau/Aβ + log PP + log FAS	0.8701	0.0244	0.8653-0.8749	0.7752	0.0487	0.7657-0.7847	0.2335	0.1091	0.2121-0.2548
log tau/Aβ + log PP + Eotaxin-3	0.8722	0.0245	0.8674-0.8770	0.7795	0.0487	0.7699-0.7890	0.1813	0.1087	0.1599-0.2026

Table 6.5. AUC= area under the curve; Stdev= standard deviation; CI= confidence interval. Receiver operating characteristic (ROC) analyses assessed the ability of three marker panels to discriminate CDR 0 from CDR>0 participants. Averages of performance measures were taken over 100 iterations of the bootstrap. "p-value" assesses the difference between the three marker panel and the corresponding two marker panel (e.g. log tau/Aβ + log Cystatin C + TRAIL-R3 vs. log tau/Aβ + log Cystatin C).

Table 6.6. Performance measures of machine learning algorithms in discriminating cognitively normal (CDR 0) from very mildly/mildly demented (CDR 0.5 and 1) participants

	Traditional Biomarkers				Traditional + RBM Biomarkers			
Model	**Sensitivity**	**Specificity**	**Youden Index**	**AUC**	**Sensitivity**	**Specificity**	**Youden Index**	**AUC**
Boosted Tree	0.843	0.525	0.368	0.782	0.845	0.776	0.621	0.868
Flexible Discriminant Analysis	0.882	0.546	0.428	0.827	0.827	0.672	0.499	0.808
K-Nearest Neighbors	0.866	0.552	0.418	0.813	0.886	0.627	0.513	0.814
Logistic Regression	0.902	0.490	0.392	0.819	0.791	0.667	0.458	0.757
Naïve Bayes	0.898	0.492	0.390	0.799	0.802	0.599	0.401	0.754
Partial Least Squares	0.914	0.457	0.371	0.822	0.858	0.693	0.551	0.851
Sparse Partial Least Squares	0.914	0.457	0.371	0.822	0.858	0.694	0.552	0.851
Random Forests	0.872	0.566	0.438	0.810	0.932	0.596	0.528	0.866
Nearest Shrunken Centroids	0.882	0.527	0.409	0.805	0.833	0.643	0.476	0.802
Support Vector Machine	0.806	0.424	0.230	0.680	0.929	0.645	0.574	0.868

Table 6.6. Ten statistical machine learning algorithms were used to determine groups of markers capable of distinguishing very mildly/mildly demented (CDR 0.5 and 1 combined) from cognitively normal participants (CDR 0). Models were fit with two sets of predictors: 1) traditional biomarkers, or 2) traditional biomarkers plus RBM analytes; additionally, age, gender, and ApoE4 allele status were included in all models. Model performance measures shown are based on cross-validation, in which the test set results were averaged from 200 splits of the data between training (80%) and test (20%).

Table 6.7. Top 15 predictors for machine learning algorithms with a built-in importance measure

Predictor	Boosted Tree	Nearest Shrunken Centroids	Random Forests	Partial Least Squares
1	tau	tau	Aβ42	tau
2	Aβ42	Aβ42	tau	Aβ42
3	VEGF	p-tau181	MMP-10	VEGF
4	MMP-10	GRO-α	KIM-1	p-tau181
5	PP	VEGF	VEGF	GRO-α
6	KIM-1	Eotaxin-3	IL-7	PP
7	Cystatin C	Age	IL-17E	Cystatin C
8	Calbindin	PP	PP	NT-proBNP
9	NT-proBNP	Cortisol	NT-proBNP	MMP-10
10	MIF	MCP-2	TRAIL-R3	KIM-1
11	IGFBP-2	TECK	p-tau181	Apo A1
12	TRAIL-R3	MMP-10	Cystatin C	ε3ε4
13	FSH	IL-17E	MIF	IL-7
14	FAS	IL-7	GRO-α	Insulin
15	TNF RII	FASL	CKMB	Age

Table 6.7. For the four models with a built-in importance statistic (i.e., Boosted Tree, NSC, RF, and PLS), there is considerable overlap in the top 15 predictors for each model. Additionally, nearly all of the markers found to best discriminate CDR 0 from CDR>0 participants in the more targeted ROC analyses (Table 6.5), as shown here, were also identified as the top predictors in the machine learning models.

Table 6.8. Cox proportional hazards models for predicting risk of developing cognitive impairment (conversion from CDR 0 to CDR>0)

A.	**Marker**	**HR**	**95% CI**	**p**	
	Log Calbindin	1.736	1.161-2.596	0.0072	
	Log 1/Aβ42	2.361	1.564-3.564	<0.0001	
	Age	1.094	1.043-1.147	0.0002	
	Gender	0.722	0.326-1.599	0.4216	
B.	**Marker**	**HR**	**95% CI**	**p**	**Overall model HR**
	Log Calbindin	1.750	1.172-2.613	0.0063	
	Log 1/Aβ42	2.454	1.637-3.679	<0.0001	4.704
	Age	1.096	1.045-1.149	0.0002	
C.	**Marker**	**HR**	**95% CI**	**p**	
	Log Tau	1.462	1.039-2.057	0.0294	
	Log 1/Aβ42	2.221	1.477-3.339	0.0001	
	Age	1.096	1.041-1.154	0.0005	
	Gender	0.724	0.334-1.566	0.4113	
D.	**Marker**	**HR**	**95% CI**	**p**	**Overall model HR**
	Log Tau	1.467	1.046-2.056	0.0262	
	Log 1/Aβ42	2.247	1.496-3.375	<0.0001	3.610
	Age	1.098	1.043-1.156	0.0003	

Table 6.8. Cox proportional hazards models were used to identify panels of biomarkers predictive of the risk of developing cognitive impairment (conversion from CDR 0 to CDR>0). Analyte measurements were converted to standard Z-scores to allow for comparison of hazard ratios between the different analytes. Variables with $p<.15$ in the univariate Cox analyses were considered for inclusion in multivariate models; variables were retained in the final model if $p<.05$. Because many of the analytes, including calbindin, demonstrated age and gender affects, both variables were entered into the multivariate models. However, as gender did not appear to contribute to the models (A, C), it was not included in the final panels (B, D). Although calbindin and tau both demonstrated $p<.05$ in the univariate analyses, the significant correlation between the

two (r=0.476, p<0.0001) prohibited inclusion of both variables in the multivariate model. Therefore, a separate multivariate model that included tau was evaluated (C, D). The higher HR of calbindin than of tau, and the higher overall model HR (4.704>3.610) and lower AIC (227.6<230.8) of the first model support it as the better model.

Chapter 7.

Conclusions and Future Directions

The number of individuals affected by AD is projected to increase dramatically over the coming decades, barring the development of successful treatments. Although a large number of compounds have been tested as potential therapeutics, clinical trials have been largely unsuccessful, in part, because they have targeted study subjects who already have dementia. Clinicopathological studies have made it increasingly clear there exists a 'preclinical' or 'presymptomatic' stage during which the pathological changes associated with AD begin ~10-15 years before the synaptic and neuronal loss that accompany dementia onset. Thus, to prevent neurodegeneration and the resulting cognitive impairment, disease-modifying treatments will need to be applied early in the disease process (preclinically). Currently, 'possible' or 'probable' AD is diagnosed by clinical examination. However, clinical examination cannot identify preclinical AD, and in nonspecialized settings, has limited accuracy for mild disease stages. Additionally, clinical examination cannot identify individuals at risk of developing future cognitive impairment or predict the rate of cognitive decline. Thus, there is an urgent need for biomarkers of AD. CSF Aβ42 and tau are perhaps the two most promising biomarkers identified to date. We hypothesize that there are additional CSF biomarkers that can complement Aβ42 and tau, improving upon their diagnostic and prognostic accuracy. This thesis reflects my work to identify novel biomarkers for AD that may be useful in such capacities.

We first utilized an unbiased proteomics approach (2D-DIGE LC-MS/MS) to identify CSF proteins increased or decreased in mild dementia (CDR 1, N=24) relative to cognitive normalcy (CDR 0, N=24). From this proteomic analysis, we identified 47 proteins as differing significantly in abundance between CDR 0 and CDR 1 groups. Most of these 47 candidate biomarkers could be placed into structural and/or functional categories associated with accepted neuropathophysiological changes in AD,

suggesting that many of these changes are represented by alterations in the CSF proteome. Unsupervised clustering analyses of this 2D-DIGE data, performed without the influence of CSF Aβ42, tau, p-tau and *APOE* genotype, suggested that these biomarker candidates collectively showed utility for discriminating groups with and without mild dementia. We then went on to validate these findings by measuring a subset (11) of the identified candidate biomarkers by ELISA in the original discovery sample set. Six of the candidates (NrCAM, YKL-40, chromogranin A, carnosinase I, transthyretin, cystatin C) showed differences in mean concentration between the original AD (CDR 1) and control (CDR 0) groups, and were thus subsequently evaluated in a larger independent sample set (N=292) that included CDR 0, CDR 0.5 (very mild dementia), and CDR 1 groups. In this larger independent sample set, CDR 0 and CDR>0 groups showed significant differences in mean concentrations of YKL-40, carnosinase I, tau, p-tau181 and Aβ42; CDR 1 and CDR <1 groups showed differences in carnosinase I, chromogranin A, NrCAM, tau, p-tau181 and Aβ42. ROC analyses using a stepwise logistic regression model yielded optimal biomarker panels to distinguish CDR 0 from CDR>0 (tau, YKL-40, NrCAM) and CDR 1 from CDR<1 (tau, chromogranin A, carnosinase I). These analyses suggested that these four candidate biomarkers (YKL-40, NrCAM, chromogranin A, carnosinase I) could improve the ability of tau to classify individuals into CDR 0, CDR 0.5, and CDR 1 groups. Additionally, drawing on previous work from our lab and from other groups, with these four novel biomarkers and CSF Aβ42 and tau, we were able to provide a framework for categorizing six clinicopathological stages: normal cognition without amyloid plaques, normal cognition with amyloid plaques (preclinical AD), normal cognition at increased risk to develop dementia (converters), very mild dementia (CDR 0.5), very mild dementia at increased risk for progression, and mild dementia (CDR 1). This biomarker-based

classification of six disease stages ranging from cognitively normal to mild dementia represents an important contribution to the field, as most studies have focused only on distinguishing those with AD (and often in the later stages) or those with MCI (analogous to a CDR 0.5) from cognitively normal individuals. Additionally, this small panel of CSF biomarkers may be useful to guide enrollment into and maximize the efficiency of clinical trials by classifying subjects into precise disease stages, identifying those at risk of progression, and providing study endpoints based on biomarker-defined stage transitions, rather than measures of cognitive decline.

One of the most promising candidate biomarkers to emerge from this 2D-DIGE study, in terms of novelty and fold-change, was YKL-40, a secreted glycoprotein of poorly understood function. Consistent with our 2D-DIGE findings, YKL-40 was significantly increased by ELISA in CDR 0.5 CSF of the discovery cohort, and CDR 0.5 and CDR 1 CSF of the larger validation cohort. To continue our study of this novel biomarker, we measured YKL-40 levels in plasma samples of the validation cohort, along with levels in a small cohort of FTLD and PSP CSF samples. Plasma YKL-40 levels displayed a pattern of elevation in the CDR 0.5 and 1 groups similar to that observed for CSF, and plasma and CSF levels correlated modestly. CSF YKL-40 levels trended higher in the FTLD and lower in the PSP groups relative to the AD group. Thus, this study demonstrated the promise of CSF YKL-40 as a biomarker for very early stage AD (CDR 0.5) and, although not covering the complete differential diagnosis for mild dementia, suggested that CSF YKL-40 may be useful in distinguishing AD from some other forms of neurodegenerative disease. Importantly, this study also demonstrated the potential utility of YKL-40, coupled with Aβ42, to predict cognitive decline. The CSF YKL-40/Aβ42 ratio displayed predictive value comparable to that of the best current CSF measures, tau/Aβ42 and p-tau181/Aβ42. This finding is particularly notable because,

whereas CSF tau is derived principally from neurons, based on our immunohistochemical analysis of human AD brain, YKL-40 appears to be secreted predominantly from astrocytes. To our knowledge, YKL-40 is the first astrocyte-derived marker shown to have such prognostic potential. CSF YKL-40/Aβ42 also showed promise in predicting progression of dementia from CDR 0.5 to CDR>0.5; however, tau/Aβ42 and p-tau181/Aβ42 appear to show greater utility in this regard. Unfortunately, plasma YKL-40 did not demonstrate similar prognostic utility. The finding of YKL-40 immunoreactivity predominantly within astrocytes surrounding amyloid plaques suggested a role for YKL-40 in the neuroinflammatory response to Aβ deposition. Increasing evidence suggests that, in addition to the formation of amyloid plaques and neurofibrillary tangles, brain inflammation may be considered a third key mechanism contributing to disease pathogenesis, and consequently, another potential target for therapeutics. One may speculate that perhaps neuroinflammation in response to amyloid deposits accelerates the rate of synaptic and neuronal loss or dysfunction. These different but interrelated processes may respond differently to disease-modifying therapies. Therefore, a marker of inflammation in the brain such as YKL-40 may be helpful in monitoring disease progression or response to treatment. The identification of a biomarker for AD that predicts prognosis and that marks a process different than Aβ42 or tau is a novel finding that could benefit the field.

The 2D-DIGE study presented in this work represents an expansion/validation of a previous similar proteomics experiment utilizing 2D-DIGE on a smaller scale. To follow up on several candidate biomarkers identified in that study, we evaluated the levels of ACT, ATIII, ZAG, and AGT by ELISA in a larger, independent CSF sample set (N=138). However, levels of these four proteins were not found to differ between CDR 0 and CDR>0 groups. In spite of these seemingly negative findings, these proteins may still

have potential as biomarkers for AD. It is important to note that these four proteins were first identified as differing significantly in abundance between AD and control groups by 2D-DIGE, a technique sensitive to concentration changes of minor protein isoforms and post-translational modifications which may not substantially alter global concentrations of a 'parent' protein. As these four proteins are known to have different isoforms, a thorough evaluation of their potential as biomarkers for AD would appear to require the design of ELISAs targeting specific post-translational modifications or specific 'sub-species' of interest.

A relatively unexplored source for novel biomarkers of AD is the low molecular weight components of CSF, or the CSF peptidome. To address this, we developed a protocol for the extraction and identification of peptides from CSF using Hypercarb chromatography material in a tip format and LC-MS/MS, and applied it to a CDR 0, CDR 1, and mixed/pooled clinical sample. Quantification of a subset of the peptides detected in these samples revealed differences in abundance among pooled, CDR 1, and CDR 0 CSF, albeit with a limited sample number. Additionally, recovery of internal standard BSA peptides was not statistically significantly different between sample runs, demonstrating the reproducibility of the extraction and LC-MS method. The future application of this low molecular weight protocol to larger numbers of AD and control CSF samples may identify many novel candidate biomarkers for AD; moreover, this protocol for extracting and identifying CSF peptides could be applied to studies of other neurodegenerative diseases as well.

Finally, to complement the unbiased approaches we used to identify novel biomarkers for AD, in collaboration with Pfizer we utilized a targeted proteomics approach. In this study, a large number of CSF samples (N=333) from well-characterized MCI/very early stage-AD (CDR>0) and cognitively normal (CDR 0) individuals were

chosen for protein profiling using a commercially available multiplexed immunoassay platform that measured the levels of 190 proteins belonging to a wide variety of functional classes. From this analysis, the levels of 37 proteins were found to differ between CDR 0 and CDR>0 participants by age and gender-adjusted analysis of covariance. ROC analysis revealed that small combinations of a subset of these markers (cystatin C, VEGF, TRAIL-R3, PAI-1, PP, NT-proBNP, MMP-10, MIF, GRO-α, fibrinogen, FAS, and eotaxin-3) could enhance the ability of the best-performing of the traditional biomarkers, the tau/Aβ42 ratio, to discriminate CDR 0.5 and 1 from CDR 0 participants. Using alternative statistical strategies more amenable to the analysis of larger combinations of markers, multiple machine learning algorithms likewise showed that the novel biomarkers improved upon the diagnostic performance of the traditional biomarkers (Aβ42, tau, p-tau181). Importantly, nearly all of the markers found to best discriminate CDR 0 from CDR 0.5 and 1 participants in the more targeted ROC analyses were also identified as the top predictors in the machine learning models that contain a built-in importance statistic, reconfirming the potential of these proteins as biomarkers for early-stage AD. We next used Cox proportional hazards models to evaluate the ability of the analytes to predict risk of developing cognitive impairment (conversion from CDR 0 to CDR>0) and to determine the best combination of biomarkers for use in this regard. We demonstrated that an optimal panel of markers consisted of calbindin, Aβ42, and age, and that this panel had predictive value comparable to, if not better than, a second panel consisting of tau, Aβ42, and age (the significant correlation between calbindin and tau prohibited the inclusion of both variables in the same multivariate model).

These studies have identified a number of novel candidate biomarkers that improve upon the ability of the best identified biomarkers to date to discriminate very mildly/mildly demented from cognitively normal participants (NrCAM, chromogranin A,

carnosinase I, YKL-40, cystatin C, VEGF, TRAIL-R3, PAI-1, PP, NT-proBNP, MMP-10, MIF, GRO-α, fibrinogen, FAS, and eotaxin-3). These studies have also identified two novel biomarkers (YKL-40 and calbindin) with significant prognostic potential. Although the mean concentrations of these candidate biomarkers differed between clinical groups, as with all biomarkers identified to date, considerable overlap in values was observed between the groups. This issue of overlapping values suggests that any biomarker alone will be insufficient for classifying subjects, and that a panel of complementary biomarkers will be necessary to achieve adequate sensitivity and specificity. Thus, it will be important in future studies to assess each candidate biomarker's value in diagnosis in additional independent sample sets and when combined with other existing biomarkers or imaging tools. It is worth mentioning, however, that even with overlap between groups, a biomarker that shows significant differences between groups may have great value for clinical trial design and enrollment. By enrolling only subjects with lower or higher values of a particular biomarker and excluding potential subjects with intermediate or 'overlap' values, one might provide greater diagnostic certainty than is possible through clinical diagnosis alone. Biomarkers panels such as the ones proposed here may also allow clinical trials to evaluate stage-specific responses to treatment. Furthermore, as most of these biomarkers reflect underlying pathological changes in real time, the use of biomarkers as surrogate endpoints in clinical trials may allow for the monitoring of clinically imperceptible neuropathological changes, potentially decreasing study duration. The ability of these candidate biomarkers to discriminate AD from other causes of dementia needs to be examined as well. Indeed, plans are already underway to obtain CSF from other conditions for such an analysis. Many of these proteins have not been investigated in relation to AD, and their possible roles in the disease pathophysiology will be of interest in future studies.

References

1. Association As (2010): Alzheimer's Disease Facts and Figures 2010. Alzheimer's Association.
2. Larson EB, Shadlen MF, Wang L, McCormick WC, Bowen JD, Teri L, et al. (2004): Survival after initial diagnosis of Alzheimer disease. *Ann Intern Med*. 140:501-509.
3. Molsa PK, Marttila RJ, Rinne UK (1986): Survival and cause of death in Alzheimer's disease and multi-infarct dementia. *Acta Neurol Scand*. 74:103-107.
4. Brookmeyer R, Corrada MM, Curriero FC, Kawas C (2002): Survival following a diagnosis of Alzheimer disease. *Arch Neurol*. 59:1764-1767.
5. Backman L, Small BJ, Fratiglioni L (2001): Stability of the preclinical episodic memory deficit in Alzheimer's disease. *Brain*. 124:96-102.
6. Goate A, Chartier-Harlon MC, Mullan M, Brown J, Crawford F, Fidani L, et al. (1991): Segregation of a missense mutation in the amyloid precursor protein gene with familial Alzheimer's disease. *Nature*. 349:704-706.
7. Sherrington R, Rogaev EI, Liang Y, Rogaeva EA, Levesque G, Ikeda M, et al. (1995): Cloning a a gene bearing missense mutations in early-onset familial Alzheimer's disease. *Nature*. 375:754-760.
8. Rogaev EI, Sherrington R, Rogaeva EA, Levesque G, Ikeda M, Liang Y, et al. (1995): Familial Alzheimer's disease in kindreds with missense mutations in a gene on chromosome 1 related to the Alzheimer's disease type 3 gene. *Nature*. 376:775-778.
9. Brunkan AL, Goate AM (2005): Presenilin function and gamma-secretase activity. *J Neurochem*. 93:769-792.
10. Wisniewski KE, Wisniewski HM, Wen GY (1985): Occurrence of neuropathological changes and dementia of Alzheimer's disease in Down's syndrome. *Ann Neurol*. 17:278-282.
11. Hardy J, Selkoe DJ (2002): The amyloid hypothesis of Alzheimer's disease: progress and problems on the road to therapeutics. *Science*. 297:353-356.
12. Corder EH, Saunders AM, Strittmatter WJ, Schmechel DE, Gaskell PC, Small GW, et al. (1993): Gene dose of apolipoprotein E type 4 allele and the risk of Alzheimer's disease in late onset families. *Science*. 261:921-923.
13. Mahley RW (1988): Apolipoprotein E: Cholesterol transport protein with expanding role in cell biology. *Science*. 240:622-630.
14. Saunders AM, Strittmatter WJ, Schmechel D, St. George-Hyslop PH, Pericak-Vance MA, Joo SH, et al. (1993): Association of apolipoprotein E allele ε4 with late-onset familial and sporadic Alzheimer's disease. *Neurology*. 43:1467-1472.
15. Okuizumi K, Onodera O, Tanaka H, Kobayashi H, Tsuji S, Takahashi H, et al. (1994): ApoE-ε4 and early onset Alzheimer's. *Nature Genet*. 7:10-11.
16. Chartier-Harlin MC, Parfitt M, Legrain S, Perez-Tur J, Brousseau T, Evans A, et al. (1994): Apolipoprotein E, epsilon 4 allele as a major risk factor for sporadic early and late-onset forms of Alzheimer's disease: analysis of the 19q13.2 chromosomal region. *Hum Mol Genet*. 3:569-574.
17. Sando SB, Melquist S, Cannon A, Hutton ML, Sletvold O, Saltvedt I, et al. (2008): APOE epsilon 4 lowers age at onset and is a high risk factor for Alzheimer's disease; a case control study from central Norway. *BMC Neurol*. 8:9.
18. Corder EH, Saunders AM, Risch NJ, Strittmatter WJ, Schmechel DE, Gaskell PC, et al. (1994): Protective effect of apolipoprotein E type 2 allele decreases risk of late onset Alzhimer disease. *Nature Genet*. 7:180-184.

19. West HL, Rebeck GW, Hyman BT (1994): Frequency of the apolipoprotein E ε2 allele is diminished in sporadic Alzheimer's disease. *Neurosci Lett*. 175:46-48.
20. Wilson RS, Bienias JL, Berry-Kravis E, Evans DA, Bennett DA (2002): The apolipoprotein E epsilon 2 allele and decline in episodic memory. *J Neurol Neurosurg Psychiatry*. 73:672-677.
21. Blacker D, Lee H, Muzikansky A, Martin EC, Tanzi R, McArdle JJ, et al. (2007): Neuropsychological measures in normal individuals that predict subsequent cognitive decline. *Arch Neurol*. 64:862-871.
22. Helkala EL, Koivisto K, Hanninen T, Vanhanen M, Kervinen K, Kuusisto J, et al. (1996): Memory functions in human subjects with different apolipoprotein E phenotypes during a 3-year population-based follow-up study. *Neurosci Lett*. 204:177-180.
23. Lippa CF, Smith TW, Saunders AM, Hulette C, Pulaski-Salo D, Roses AD (1997): Apolipoprotein E-epsilon 2 and Alzheimer's disease: genotype influences pathologic phenotype. *Neurology*. 48:515-519.
24. Oyama F, Shimada H, Oyama R, Ihara Y (1995): Apolipoprotein E genotype, Alzheimer's pathologies and related gene expression in the aged population. *Brain Res Mol Brain Res*. 29:92-98.
25. Tiraboschi P, Hansen LA, Masliah E, Alford M, Thal LJ, Corey-Bloom J (2004): Impact of APOE genotype on neuropathologic and neurochemical markers of Alzheimer disease. *Neurology*. 62:1977-1983.
26. Nagy Z, Esiri MM, Jobst KA, Johnston C, Litchfield S, Sim E, et al. (1995): Influence of the apolipoprotein E genotype on amyloid deposition and neurofibrillary tangle formation in Alzheimer's disease. *Neuroscience*. 69:757-761.
27. Wisniewski T, Frangione B (1992): Apolipoprotein E: a pathological chaperone protein in patients with cerebral and systemic amyloid. *Neurosci Lett*. 135:235-238.
28. Naslund J, Thyberg J, Tjernberg LO, Wernstedt C, Karlstrom AR, Bogdanovic N, et al. (1995): Characterization of stable complexes involving apolipoprotein E and the amyloid ß peptide in Alzheimer's disease brain. *Neuron*. 15:219-228.
29. Harold D, Abraham R, Hollingworth P, Sims R, Gerrish A, Hamshere ML, et al. (2009): Genome-wide association study identifies variants at CLU and PICALM associated with Alzheimer's disease. *Nat Genet*. 41:1088-1093.
30. Jun G, Naj AC, Beecham GW, Wang LS, Buros J, Gallins PJ, et al. Meta-analysis Confirms CR1, CLU, and PICALM as Alzheimer Disease Risk Loci and Reveals Interactions With APOE Genotypes. *Arch Neurol*.
31. Lambert JC, Heath S, Even G, Campion D, Sleegers K, Hiltunen M, et al. (2009): Genome-wide association study identifies variants at CLU and CR1 associated with Alzheimer's disease. *Nat Genet*. 41:1094-1099.
32. Hutton M, Lendon CL, Rizzu P, Baker M, Froelich S, Houlden H, et al. (1998): Association of missense and 5'-splice-site mutations in tau with the inherited dementia FTDP-17. *Nature*. 393:702-705.
33. Spillantini MG, Murrell JR, Goedert M, Farlow MR, Klug A, Ghetti B (1998): Mutation in the tau gene in familial multiple system tauopathy with presenile dementia. *Proc Natl Acad Sci U S A*. 95:7737-7741.
34. Mandelkow EM, Mandelkow E (1998): Tau in Alzheimer's disease. *Trends Cell Biol*. 8:425-427.
35. Lee VM, Trojanowski JQ (2006): Progress from Alzheimer's tangles to pathological tau points towards more effective therapies now. *J Alzheimers Dis*. 9:257-262.

36. Bramblett GT, Goedert M, Jakes R, Merrick SE, Trojanowski JQ, Lee VM (1993): Abnormal tau phosphorylation at Ser396 in Alzheimer's disease recapitulates development and contributes to reduced microtubule binding. *Neuron*. 10:1089-1099.
37. Small SA, Duff K (2008): Linking Abeta and tau in late-onset Alzheimer's disease: a dual pathway hypothesis. *Neuron*. 60:534-542.
38. Oddo S, Caccamo A, Kitazawa M, Tseng BP, LaFerla FM (2003): Amyloid deposition precedes tangle formation in a triple transgenic model of Alzheimer's disease. *Neurobiol Aging*. 24:1063-1070.
39. LaFerla FM, Oddo S (2005): Alzheimer's disease: Abeta, tau and synaptic dysfunction. *Trends Mol Med*. 11:170-176.
40. Oddo S, Caccamo A, Shepherd J, Murphy M, Golde T, Kayed R, et al. (2003): Triple-transgenic model of Alzheimer's disease with plaques and tangles: Intracellular Aβ and synaptic dysfunction. *Neuron*. 39:409-421.
41. Oddo S, Billings L, Kesslak JP, Cribbs DH, LaFerla FM (2004): Abeta immunotherapy leads to clearance of early, but not late, hyperphosphorylated tau aggregates via the proteasome. *Neuron*. 43:321-332.
42. Braak H, Braak E (1998): Evolution of neuronal changes in the course of Alzheimer's disease. *J Neural Transm Suppl*. 53:127-140.
43. Braak H, Braak E (1997): Frequency of stages of Alzheimer-related lesions in different age categories. *Neurobiol Aging*. 18:351-357.
44. Morris J, Price J (2001): Pathologic correlates of nondemented aging, mild cognitive impairment, and early stage Alzheimer's disease. *J Mol Neurosci*. 17:101-118.
45. Gomez-Isla T, Price JL, McKeel DW, Morris J, C. , Growdon JH, Hyman BT (1996): Profound loss of layer II entorhinal cortex neurons occurs in very mild Alzheimer's disease. *J Neurosci*. 16:4491-4500.
46. Arriagada PV, Growdon JH, Hedley-Whyte ET, Hyman BT (1992): Neurofibrillary tangles but not senile plaques parallel duration and severity of Alzheimer's disease. *Neurology*. 42:631-639.
47. Crystal H, Dickson D, Fuld P, Masur D, Scott R, Mehler M, et al. (1988): Clinico-pathologic studies in dementia: nondemented subjects with pathologically confirmed Alzheimer's disease. *Neurology*. 38:1682-1687.
48. Bierer LM, Hof PR, Purohit DP, Carlin L, Schmeidler J, Davis KL, et al. (1995): Neocortical neurofibrillary tangles correlate with dementia severity in Alzheimer's disease. *Arch Neurol*. 52:81-88.
49. Nagy Z, Jobst KA, Esiri MM, Morris JH, King EM, MacDonald B, et al. (1996): Hippocampal pathology reflects memory deficit and brain imaging measurements in Alzheimer's disease: clinicopathologic correlations using three sets of pathologic diagnostic criteria. *Dementia*. 7:76-81.
50. Giannakopoulos P, Herrmann FR, Bussiere T, Bouras C, Kovari E, Perl DP, et al. (2003): Tangle and neuron numbers, but not amyloid load, predict cognitive status in Alzheimer's disease. *Neurology*. 60:1495-1500.
51. Walsh DM, Selkoe DJ (2004): Oligomers on the brain: the emerging role of soluble protein aggregates in neurodegeneration. *Protein Pept Lett*. 11:213-228.
52. Klein WL, Krafft GA, Finch CE (2001): Targeting small Abeta oligomers: the solution to an Alzheimer's disease conundrum? *Trends Neurosci*. 24:219-224.

53. Glabe CG (2008): Structural classification of toxic amyloid oligomers. *J Biol Chem*. 283:29639-29643.
54. Jaworski T, Kugler S, Van Leuven F (2010): Modeling of tau-mediated synaptic and neuronal degeneration in Alzheimer's disease. *Int J Alzheimers Dis*. 2010.
55. Meyer-Luehmann M, Spires-Jones TL, Prada C, Garcia-Alloza M, de Calignon A, Rozkalne A, et al. (2008): Rapid appearance and local toxicity of amyloid-beta plaques in a mouse model of Alzheimer's disease. *Nature*. 451:720-724.
56. Assocation As (2010): Alzheimer's Disease Facts and Figures 2010. Alzheimer's Association.
57. McKhann G, Drachman D, Folstein M, Katzman R, Price D, Stadlan E (1984): Clinical diagnosis of Alzheimer's disease: report of the NINCDS-ADRDA Work Group under the auspices of Department of Health and Human Services Task Force on Alzheimer's Disease. *Neurology*. 34:939-944.
58. Callahan CM, Hendrie HC, Tierney WM (1995): Documentation and evaluation of cognitive impairment in elderly primary care patients. *Ann Intern Med*. 122:422-429.
59. O'Connor DW, Pollitt PA, Hyde JB, Brook CP, Reiss BB, Roth M (1988): Do general practitioners miss dementia in elderly patients? *BMJ*. 297:1107-1110.
60. Teel CS (2004): Rural practitioners' experiences in dementia diagnosis and treatment. *Aging Ment Health*. 8:422-429.
61. Hogervorst E, Bandelow S, Combrinck M, Irani SR, Smith AD (2003): The validity and reliability of 6 sets of clinical criteria to classify Alzheimer's disease and vascular dementia in cases confirmed post-mortem: added value of a decision tree approach. *Dement Geriatr Cogn Disord*. 16:170-180.
62. Ranginwala NA, Hynan LS, Weiner MF, White CL, 3rd (2008): Clinical criteria for the diagnosis of Alzheimer disease: still good after all these years. *Am J Geriatr Psychiatry*. 16:384-388.
63. Nagy Z, Esiri MM, Hindley NJ, Joachim C, Morris JH, King EM, et al. (1998): Accuracy of clinical operational diagnostic criteria for Alzheimer's disease in relation to different pathological diagnostic protocols. *Dement Geriatr Cogn Disord*. 9:219-226.
64. Group BDW (2001): Biomarkers and surrogate endpoints: preferred definitions and conceptual framework. *Clin Pharmacol Ther*. 69:89-95.
65. Price J, Ko A, Wade M, Tsou S, McKeel D, Morris J (2001): Neuron number in the entorhinal cortex and CA1 in preclinical Alzheimer's disease. *Arch Neurol*. 58:1395-1402.
66. Hulette CM, Welsh-Bohmer KA, Murray MG, Saunders AM, Mash DC, McIntyre LM (1998): Neuropathological and neuropsychological changes in "normal" aging: Evidence for preclinical Alzheimer disease in cognitively normal individuals. *J Neuropathol Exp Neurol*. 57:1168-1174.
67. Markesbery W, Schmitt F, Kryscio R, Davis D, Smith C, Wekstein D (2006): Neuropathologic substrate of Mild Cognitive Impairment. *Arch Neurol*. 63:38-46.
68. Morris JC (1993): The Clinical Dementia Rating (CDR). Current version and scoring rules. *Neurology*. 43:2412-2414.
69. Morris J, Storandt M, Miller J, McKeel D, Price J, Rubin E, et al. (2001): Mild cognitive impairment represents early-stage Alzheimer's disease. *Arch Neurol*. 58:397-405.
70. Storandt M, Grant E, Miller J, Morris J (2006): Longitudinal course and neuropathologic outcomes in original vs revised MCI and in pre-MCI. *Neurology*. 67:467-473.

71. Farias ST, Mungas D, Reed BR, Harvey D, DeCarli C (2009): Progression of mild cognitive impairment to dementia in clinic- vs community-based cohorts. *Arch Neurol*. 66:1151-1157.
72. Davies L, Wolska B, Hilbich C, Multhaup G, Martins R, Simms G, et al. (1988): A4 amyloid protein deposition and the diagnosis of Alzheimer's disease: prevalence in aged brains determined by immunocytochemistry compared with conventional neuropathologic techniques. *Neurology*. 38:1688-1693.
73. Becker RE, Greig NH, Giacobini E (2008): Why do so many drugs for Alzheimer's disease fail in development? Time for new methods and new practices? *J Alzheimers Dis*. 15:303-325.
74. Kitaguchi N, Tokushima Y, Oishi K, Takahashi Y, Shiojiri S, Nakamura S, et al. (1990): Determination of amyloid beta protein precursors harboring active form of proteinase inhibitor domains in cerebrospinal fluid of Alzheimer's disease patients by trypsin-antibody sandwich ELISA. *Biochem Biophys Res Commun*. 166:1453-1459.
75. Weidemann A, Konig G, Bunke D, Fischer P, Salbaum JM, Masters CL, et al. (1989): Identification, biogenesis, and localization of precursors of Alzheimer's disease A4 amyloid protein. *Cell*. 57:115-126.
76. Ghiso J, Tagliavini F, Timmers WF, Frangione B (1989): Alzheimer's disease amyloid precursor protein is present in senile plaques and cerebrospinal fluid: immunohistochemical and biochemical characterization. *Biochem Biophys Res Commun*. 163:430-437.
77. Prior R, Monning U, Schreiter-Gasser U, Weidemann A, Blennow K, Gottfries CG, et al. (1991): Quantitative changes in the amyloid beta A4 precursor protein in Alzheimer cerebrospinal fluid. *Neurosci Lett*. 124:69-73.
78. Henriksson T, Barbour RM, Braa S, Ward P, Fritz LC, Johnson-Wood K, et al. (1991): Analysis and quantitation of the beta-amyloid precursor protein in the cerebrospinal fluid of Alzheimer's disease patients with a monoclonal antibody-based immunoassay. *J Neurochem*. 56:1037-1042.
79. Van Nostrand WE, Wagner SL, Shankle WR, Farrow JS, Dick M, Rozemuller JM, et al. (1992): Decreased levels of soluble amyloid beta-protein precursor in cerebrospinal fluid of live Alzheimer disease patients. *Proc Natl Acad Sci U S A*. 89:2551-2555.
80. Chong JK, Miller BE, Ghanbari HA (1990): Detection of amyloid beta protein precursor immunoreactivity in normal and Alzheimer's disease cerebrospinal fluid. *Life Sci*. 47:1163-1171.
81. Palmert MR, Usiak M, Mayeux R, Raskind M, Tourtellotte WW, Younkin SG (1990): Soluble derivatives of the beta amyloid protein precursor in cerebrospinal fluid: alterations in normal aging and in Alzheimer's disease. *Neurology*. 40:1028-1034.
82. Sennvik K, Fastbom J, Blomberg M, Wahlund LO, Winblad B, Benedikz E (2000): Levels of alpha- and beta-secretase cleaved amyloid precursor protein in the cerebrospinal fluid of Alzheimer's disease patients. *Neurosci Lett*. 278:169-172.
83. Evin G, Weidemann A (2002): Biogenesis and metabolism of Alzheimer's disease Abeta amyloid peptides. *Peptides*. 23:1285-1297.
84. Roher AE, Lowenson JD, Clarke S, Woods AS, Cotter RJ, Gowing E, et al. (1993): beta-Amyloid-(1-42) is a major component of cerebrovascular amyloid deposits: implications for the pathology of Alzheimer disease. *Proc Natl Acad Sci U S A*. 90:10836-10840.
85. Southwick PC, Yamagata SK, Echols CL, Jr., Higson GJ, Neynaber SA, Parson RE, et al. (1996): Assessment of amyloid beta protein in cerebrospinal fluid as an aid in the diagnosis of Alzheimer's disease. *J Neurochem*. 66:259-265.

86. van Gool WA, Kuiper MA, Walstra GJ, Wolters EC, Bolhuis PA (1995): Concentrations of amyloid beta protein in cerebrospinal fluid of patients with Alzheimer's disease. *Ann Neurol*. 37:277-279.
87. Lannfelt L, Basun H, Vigo-Pelfrey C, Wahlund LO, Winblad B, Lieberburg I, et al. (1995): Amyloid beta-peptide in cerebrospinal fluid in individuals with the Swedish Alzheimer amyloid precursor protein mutation. *Neurosci Lett*. 199:203-206.
88. Motter R, Vigo-Pelfrey C, Kholodenko D, Barbour R, Johnson-Wood J, Galasko D, et al. (1995): Reduction of β-amyloid peptide$_{42}$ in the cerebrospinal fluid of patients with Alzheimer's disease. *Ann Neurol*. 38:643-648.
89. Ida N, Hartmann T, Pantel J, Schroder J, Zerfass R, Forstl H, et al. (1996): Analysis of heterogeneous βA4 peptides in human cerebrospinal fluid and blood by a newly developed sensitive Western blot assay. *J Biol Chem*. 271:22908-22914.
90. Tamaoka A, Sawamura N, Fukushima T, Shoji S, Matsubara E, Shoji M, et al. (1997): Amyloid β protein 42(43) in cerebrospinal fluid of patients with Alzheimer's disease. *J Neurol Sci*. 1997:41-45.
91. Galasko D, Chang L, Motter R, Clark CM, Kaye J, Knopman D, et al. (1998): High cerebrospinal fluid tau and low amyloid β42 levels in the clinical diagnosis of Alzheimer's disease and relation to apolipoprotein E genotype. *Arch Neurol*. 55:937-945.
92. Kanai M, Matsubara E, Isoe K, Urakami K, Nakashima K, Arai H, et al. (1998): Longitudinal study of cerebrospinal fluid levels of tau, Aβ1-40, and Aβ1-42(43) in Alzheimer's disease: A study in Japan. *Ann Neurol*. 44.
93. Hulstaert F, Blennow K, Ivanoiu A, Schoonderwaldt HC, Riemenschneider M, De Deyn PP, et al. (1999): Improved discrimination of AD patients using beta-amyloid(1-42) and tau levels in CSF. *Neurology*. 52:1555-1562.
94. Andreasen N, Hess C, Davidsson P, Minthon L, Wallin A, Winblad B, et al. (1999): Cerebrospinal fluid β-amyloid(1-42) in Alzheimer's disease: Differences between early- and late-onset Alzheimer's disease and stability during the course of disease. *Arch Neurol*. 56:673-680.
95. Otto M, Esselmann H, Schulz-Shaeffer W, Neumann M, Schroter A, Ratzka P, et al. (2000): Decreased beta-amyloid1-42 in cerebrospinal fluid of patients with Creutzfeldt-Jakob disease. *Neurology*. 54:1099-1102.
96. Sjogren M, Minthon L, Davidsson P, Granerus AK, Clarberg A, Vanderstichele H, et al. (2000): CSF levels of tau, beta-amyloid(1-42) and GAP-43 in frontotemporal dementia, other types of dementia and normal aging. *J Neural Transm*. 107:563-579.
97. Kanemaru K, Kameda N, Yamanouchi H (2000): Decreased CSF amyloid beta42 and normal tau levels in dementia with Lewy bodies. *Neurology*. 54:1875-1876.
98. Mehta PD, Pirttila T, Mehta SP, Sersen EA, Aisen PS, Wisniewski HM (2000): Plasma and cerebrospinal fluid levels of amyloid β proteins 1-40 and 1-42 in Alzheimer's disease. *Arch Neurol*. 57:100-105.
99. Riemenschneider M, Schmolke M, Lautenschlager N, Guder WG, Vanderstichele H, Vanmechelen E, et al. (2000): Cerebrospinal beta-amyloid ((1-42)) in early Alzheimer's disease: association with apolipoprotein E genotype and cognitive decline. *Neurosci Lett*. 284:85-88.
100. Andreasen N, Minthon L, Davidsson P, Vanmechelen V, Vanderstichele H, Winblad B, et al. (2001): Evaluation of CSF-tau and CSF-Aβ42 as diagnostic markers for Alzheimer's disease in clinical practice. *Arch Neurol*. 58:373-379.
101. Rosler N, Wichart I, Jellinger KA (2001): Clinical significance of neurobiochemical profiles in the lumbar cerebrospinal fluid of Alzheimer's disease patients. *J Neural Transm*. 108:231-246.

102. Sjogren M, Davidsson P, Wallin A, Granerus AK, Grundstrom E, Askmark H, et al. (2002): Decreased CSF-beta-amyloid 42 in Alzheimer's disease and amyotrophic lateral sclerosis may reflect mismetabolism of beta-amyloid induced by disparate mechanisms. *Dement Geriatr Cogn Disord*. 13:112-118.
103. Skoog I, Davidsson P, Aevarsson O, Vanderstichele H, Vanmechelen E, Blennow K (2003): Cerebrospinal fluid beta-amyloid 42 is reduced before the onset of sporadic dementia: A population-based study in 85-year-olds. *Dement Geriatr Cogn Disord*. 15:169-176.
104. Kapaki E, Paraskevas GP, Zalonis I, Zournas C (2003): CSF tau protein and beta-amyloid (1-42) in Alzheimer's disease diagnosis: discrimination from normal ageing and other dementias in the Greek population. *Eur J Neurol*. 10:119-128.
105. Clark C, Xie S, Chittams J, Ewbank D, Peskind E, Galasko D, et al. (2003): Cerebrospinal fluid tau and beta-amyloid: How well do these biomarkers reflect autopsy-confirmed dementia diagnoses? *Arch Neurol*. 60:1696-1702.
106. Lewczuk P, Esselmann H, Otto M, Maler JM, Henkel AW, Henkel MK, et al. (2004): Neurochemical diagnosis of Alzheimer's dementia by CSF Abeta42, Abeta42/Abeta40 ratio and total tau. *Neurobiol Aging*. 25:273-281.
107. Fagan A, Roe C, Xiong C, Mintun M, Morris J, Holtzman D (2007): Cerebrospinal fluid tau/Aβ42 ratio as a prediction of cognitive decline in nondemented older adults. *Arch Neurol*. 64:343-349.
108. Engelborghs S, De Vreese K, Van de Casteele T, Vanderstichele H, Van Everbroeck B, Cras P, et al. (2008): Diagnostic performance of a CSF-biomarker panel in autopsy-confirmed dementia. *Neurobiol Aging*. 29:1143-1159.
109. Hampel H, Teipel SJ, Fuchsberger T, Andreasen N, Wiltfang J, Otto M, et al. (2004): Value of CSF beta-amyloid1-42 and tau as predictors of Alzheimer's disease in patients with mild cognitive impairment. *Mol Psychiatry*. 9:705-710.
110. Kapaki E, Kilidireas K, Paraskevas GP, Michalopoulou M, Patsouris E (2001): Highly increased CSF tau protein and decreased beta-amyloid (1-42) in sporadic CJD: a discrimination from Alzheimer's disease? *J Neurol Neurosurg Psychiatry*. 71:401-403.
111. Mulder C, Schoonenboom SN, Wahlund LO, Scheltens P, van Kamp GJ, Veerhuis R, et al. (2002): CSF markers related to pathogenetic mechanisms in Alzheimer's disease. *J Neural Transm*. 109:1491-1498.
112. Vanderstichele H, Kerschaver EV, Hesse C, Davidsson P, Buyse M, Andreasen N, et al. (2000): Standardization of measurement of β-amyloid(1-42) in cerebrospinal fluid and plasma. *Int J Exp Clin Invest*. 7:245-258.
113. Jensen M, Schröder J, Blomberg M, Engvall B, Pantel J, Ida N, et al. (1999): Cerebrospinal fluid Aβ42 is increased early in sporadic Alzheimer's disease and declines with disease progression. *Annals of Neurology*. 45:504-511.
114. Csernansky JG, Miller JP, McKeel D, Morris JC (2002): Relationships among cerebrospinal fluid biomarkers in dementia of the Alzheimer type. *Alzheimer Dis Assoc Disord*. 16:144-149.
115. Fukuyama R, Mizuno T, Mizuno T, Mori S, Nakajima K, Fushiki S, et al. (2000): Age-dependent changes in the levels of Aβ40 and Aβ42 in cerebrospinal fluid from control subjects, and a decrease in the ratio of Aβ42 to Aβ40 level in cerebrospinal fluid from Alzheimer's disease patients. *Eur Neurol*. 43:155-160.
116. Samuels SC, Silverman JM, Marin DB, Peskind ER, Younki SG, Greenberg DA, et al. (1999): CSF beta-amyloid, cognition, and APOE genotype in Alzheimer's disease. *Neurology*. 52:547-551.

117. Riemenschneider M, Lautenschlager N, Wagenpfeil S, Diehl J, Drzezga A, Kurz A (2002): Cerebrospinal Fluid Tau and B-Amyloid 42 Proteins Identify Alzheimer Disease in Subjects With Mild Cognitive Impairment
Arch Neurol. 59:1729 - 1734.
118. Andreasen N, Vanmechelen E, Vanderstichele H, Davidsson P, Blennow K (2003): Cerebrospinal fluid levels of total-tau, phospho-tau and A beta 42 predicts development of Alzheimer's disease in patients with mild cognitive impairment. *Acta Neurol Scand Suppl*. 179:47-51.
119. Blennow K, Hampel H (2003): CSF Markers for Incipient Alzheimer's Disease. *Lancet Neurol*. 2:605 - 613.
120. Herukka S, Hallikainen M, Soininen H, Pirttila T (2005): CSF Aβ42 and tau or phosphorylated tau and prediction of progressive mild cognitive impairment. *Neurology*. 64:1294-1297
121. Hansson O, Zetterberg H, Buchhave P, Londos E, Blennow K, Minthon L (2006): Association between CSF biomarkers and incipient Alzheimer's disease in patients with mild cognitive impairment: A follow-up study. *Lancet Neurol*. 5:228-234.
122. Hansson O, Zetterberg H, Buchhave P, Andreasson U, Londos E, Minthon L, et al. (2007): Prediction of Alzheimer's disease using the CSF Abeta42/Abeta40 ratio in patients with mild cognitive impairment. *Dement Geriatr Cogn Disord*. 23:316-320.
123. Herukka SK, Helisalmi S, Hallikainen M, Tervo S, Soininen H, Pirttila T (2007): CSF Abeta42, Tau and phosphorylated Tau, APOE epsilon4 allele and MCI type in progressive MCI. *Neurobiol Aging*. 28:507-514.
124. Hansson O, Zetterberg H, Vanmechelen E, Vanderstichele H, Andreasson U, Londos E, et al. (2008): Evaluation of plasma Abeta(40) and Abeta(42) as predictors of conversion to Alzheimer's disease in patients with mild cognitive impairment. *Neurobiol Aging*.
125. DeMattos RB, Bales KR, Parsadanian M, O'Dell MA, Foss EM, Paul SM, et al. (2002): Plaque-associated disruption of CSF and plasma amyloid-β (Aβ) equilibrium in a mouse model of Alzheimer's disease. *J Neurochem*. 81:229-236.
126. Strozyk D, Blennow K, White LR, Launer LJ (2003): CSF Abeta 42 levels correlate with amyloid-neuropathology in a population-based autopsy study. *Neurology*. 60:652-656.
127. Fagan A, Mintun M, Mach R, Lee S-Y, Dence C, Shah A, et al. (2006): Inverse relation between in vivo amyloid imaging load and CSF $A\beta_{42}$ in humans. *Ann Neurol*. 59:512-519.
128. Fagan AM, Mintun MA, Shah AR, Aldea P, Roe CM, Mach RH, et al. (2009): Cerebrospinal fluid tau and ptau(181) increase with cortical amyloid deposition in cognitively normal individuals: implications for future clinical trials of Alzheimer's disease. *EMBO Mol Med*. 1:371-380.
129. Riemenschneider M, Wagenpfeil S, Diehl J, Lautenschlager N, Theml T, Heldmann B, et al. (2002): Tau and Abeta42 protein in CSF of patients with frontotemporal degeneration. *Neurology*. 58:1622-1628.
130. Holmberg B, Johnels B, Blennow K, Rosengren L (2003): Cerebrospinal fluid Abeta42 is reduced in multiple system atrophy but normal in Parkinson's disease and progressive supranuclear palsy. *Mov Disord*. 18:186-190.
131. Shoji M, Matsubara E, Kanai M, Watanabe M, Nakamura T, Tomidokoro Y, et al. (1998): Combination assay of CSF tau, A beta 1-40 and A beta 1-42(43) as a biochemical marker of Alzheimer's disease. *J Neurol Sci*. 158:134-140.

132. Li G, Sokal I, Quinn J, Leverenz J, Brodey M, Schellenberg G, et al. (2007): CSF tau/Aβ_{42} ratio for increased risk of mild cognitive impairment: A follow-up study. *Neurology*. 69:631-639.
133. Maddalena A, Papassotiropoulos A, Muller-Tillmanns B, Jung HH, Hegi T, Nitsch RM, et al. (2003): Biochemical diagnosis of Alzheimer disease by measuring the cerebrospinal fluid ratio of phosphorylated tau protein to beta-amyloid peptide42. *Arch Neurol*. 60:1202-1206.
134. Pesaresi M, Lovati C, Bertora P, Mailland E, Galimberti D, Scarpini E, et al. (2006): Plasma levels of beta-amyloid (1-42) in Alzheimer's disease and mild cognitive impairment. *Neurobiol Aging*. 27:904-905.
135. Fukumoto H, Tennis M, Locascio J, Hyman B, Growdon J, Irizarry M (2003): Age but not diagnosis is the main predictor of plasma amyloid beta-protein levels. *Arch Neurol*. 60:958-964.
136. Tamaoka A, Fukushima T, Sawamura N, Ishikawa K, Oguni E, Komatsuzaki Y, et al. (1996): Amyloid beta protein in plasma from patients with sporadic Alzheimer's disease. *J Neurol Sci*. 141:65-68.
137. Kosaka T, Imagawa M, Seki K, Arai H, Sasaki H, Tsuji S, et al. (1997): The beta APP717 Alzheimer mutation increases the percentage of plasma amyloid-beta protein ending at Abeta42(43). *Neurology*. 48:741-745.
138. Scheuner D, Eckman C, Jensen M, Song X, Citron M, Suzuki N, et al. (1996): Secreted amyloid ß-protein similar to that in the senile plaques of Alzheimer's disease is increased *in vivo* by the presenilin 1 and 2 *APP* mutations linked to familial Alzheimer's disease. *Nature Med*. 2:864-852.
139. Ertekin-Taner N, Younkin LH, Yager DM, Parfitt F, Baker MC, Asthana S, et al. (2008): Plasma amyloid beta protein is elevated in late-onset Alzheimer disease families. *Neurology*. 70:596-606.
140. Mayeux R, Tang M, Jacobs D, Manly J, Bell K, Merchant C, et al. (1999): Plasma amyloid beta-peptide 1-42 and incipient Alzheimer's disease. *Ann Neurol*. 46:412-416.
141. Mayeux R, Honig LS, Tang MX, Manly J, Stern Y, Schupf N, et al. (2003): Plasma A[beta]40 and A[beta]42 and Alzheimer's disease: relation to age, mortality, and risk. *Neurology*. 61:1185-1190.
142. van Oijen M, Hofman A, Soares H, Koudstaal P, Breteler M (2006): Plasma Aβ_{1-40} and Aβ_{1-42} and the risk of dementia: A prospective case-cohort study. *Lancet Neurol*. 5:655-660.
143. Lopez OL, Kuller LH, Mehta PD, Becker JT, Gach HM, Sweet RA, et al. (2008): Plasma amyloid levels and the risk of AD in normal subjects in the Cardiovascular Health Study. *Neurology*. 70:1664-1671.
144. Freeman SH, Raju S, Hyman BT, Frosch MP, Irizarry MC (2007): Plasma Abeta levels do not reflect brain Abeta levels. *J Neuropathol Exp Neurol*. 66:264-271.
145. Mehta P, Pirttila T, Patrick B, Barshatzky M, Mehta S (2001): Amyloid β protein 1-40 and 1-42 levels in matched cerebrospinal fluid and plasma from patients with Alzheimer disease. *Neurosci Lett*. 304:102-106.
146. Schenk D, Barbour R, Dunn W, Gordon G, Grajeda H, Guido T, et al. (1999): Immunization with amyloid-beta attenuates Alzheimer-disease-like pathology in the PDAPP mouse. *Nature*. 400:173-177.
147. Morgan D, Diamond DM, Gottschall PE, Ugen KE, Dickey C, Hardy J, et al. (2000): A beta peptide vaccination prevents memory loss in an animal model of Alzheimer's disease. *Nature*. 408:982-985.

148. Janus C, Pearson J, McLaurin J, Mathews PM, Jiang Y, Schmidt SD, et al. (2000): A beta peptide immunization reduces behavioural impairment and plaques in a model of Alzheimer's disease. *Nature*. 408:979-982.
149. Holmes C, Boche D, Wilkinson D, Yadegarfar G, Hopkins V, Bayer A, et al. (2008): Long-term effects of Abeta42 immunisation in Alzheimer's disease: follow-up of a randomised, placebo-controlled phase I trial. *Lancet*. 372:216-223.
150. Price JL, Morris JC (1999): Tangles and plaques in nondemented aging and "preclinical" Alzheimer's disease. *Ann Neurol*. 45:358-368.
151. Lewis J, Dickson DW, Lin WL, Chisholm L, Corral A, Jones G, et al. (2001): Enhanced neurofibrillary degeneration in transgenic mice expressing mutant tau and APP. *Science*. 293:1487-1491.
152. Haroutunian V, Purohit DP, Perl DP, Marin D, Khan K, Lantz M, et al. (1999): Neurofibrillary tangles in nondemented elderly subjects and mild Alzheimer disease. *Arch Neurol*. 56:713-718.
153. Price JL, Davis PB, Morris JC, White DL (1991): The distribution of tangles, plaques and related immunohistochemical markers in healthy aging and Alzheimer's disease. *Neurobiol Aging*. 12:295-312.
154. Bouras C, Hof PR, Morrison JH (1993): Neurofibrillary tangle densities in the hippocampal formation in a non-demented population define subgroups of patients with differential early pathologic changes. *Neurosci Lett*. 153:131-135.
155. Vandermeeren M, Mercken M, Vanmechelen E, Six J, van de Voorde A, Martin J, et al. (1993): Detection of tau proteins in normal and Alzheimer's disease cerebrospinal fluid with a sensitive sandwich enzyme-linked immunosorbant assay. *J Neurochem*. 61:1828-1834.
156. Arai H, Terajima M, Miura M, Higuchi S, Muramatsu T, Machida N, et al. (1995): Tau in cerebrospinal fluid: A potential diagnostic marker in Alzheimer's disease. *Ann Neurol*. 38:649-652.
157. Hock C, Golombowski S, Naser W, Muller-Spahn F (1995): Increased levels of tau protein in cerebrospinal fluid of patients with Alzheimer's disease--correlation with degree of cognitive impairment. *Ann Neurol*. 37:414-415.
158. Skoog I, Vanmechelen E, Andreasson LA, Palmertz B, Davidsson P, Hesse C, et al. (1995): A population-based study of tau protein and ubiquitin in cerebrospinal fluid in 85-year-olds: relation to severity of dementia and cerebral atrophy, but not to the apolipoprotein E4 allele. *Neurodegeneration*. 4:433-442.
159. Mori H, Hosoda K, Matsubara E, Nakamoto T, Furiya Y, Endoh R, et al. (1995): Tau in cerebrospinal fluids: establishment of the sandwich ELISA with antibody specific to the repeat sequence in tau. *Neurosci Lett*. 186:181-183.
160. Vigo-Pelfrey C, Seubert P, Barbour R, Blomquist C, Lee M, Lee D, et al. (1995): Elevation of microtubule-associated protein tau in the cerebrospinal fluid of patients with Alzheimer's disease. *Neurology*. 45:788-793.
161. Tato RE, Frank A, Hernanz A (1995): Tau protein concentrations in cerebrospinal fluid of patients with dementia of the Alzheimer type. *J Neurol Neurosurg Psychiatry*. 59:280-283.
162. Jensen M, Basun H, Lannfelt L (1995): Increased cerebrospinal fluid tau in patients with Alzheimer's disease. *Neurosci Lett*. 186:189-191.
163. Munroe WA, Southwick PC, Chang L, Scharre DW, Echols CL, Jr., Fu PC, et al. (1995): Tau protein in cerebrospinal fluid as an aid in the diagnosis of Alzheimer's disease. *Ann Clin Lab Sci*. 25:207-217.

164. Blennow K, Wallin A, Agren H, Spenger C, Siegfried J, Vanmechelen E (1995): Tau protein in cerebrospinal fluid: a biochemical marker for axonal degeneration in Alzheimer disease? *Mol Chem Neuropathol*. 26:231-245.
165. Rosler N, Wichart I, Jellinger KA (1996): Total tau protein immunoreactivity in lumbar cerebrospinal fluid of patients with Alzheimer's disease. *J Neurol Neurosurg Psychiatry*. 60:237-238.
166. Arai H, Terajima M, Miura M, Higuchi S, Muramatsu T, Matsushita S, et al. (1997): Effect of genetic risk factors and disease progression on the cerebrospinal fluid tau levels in Alzheimer's disease. *J Am Geriatr Soc*. 45:1228-1231.
167. Golombowski S, Muller-Spahn F, Romig H, Mendla K, Hock C (1997): Dependence of cerebrospinal fluid Tau protein levels on apolipoprotein E4 allele frequency in patients with Alzheimer's disease. *Neurosci Lett*. 225:213-215.
168. Andreasen N, Vanmechelen E, Van de Voorde A, Davidsson P, Hesse C, Tarvonen S, et al. (1998): Cerebrospinal fluid tau protein as a biochemical marker for Alzheimer's disease: A community based follow up study. *J Neurol Neurosurg Psych*. 64:298-305.
169. Mecocci P, Cherubini A, Bregnocchi M, Chionne F, Cecchetti R, Lowenthal DT, et al. (1998): Tau protein in cerebrospinal fluid: a new diagnostic and prognostic marker in Alzheimer disease? *Alzheimer Dis Assoc Disord*. 12:211-214.
170. Arai H, Satoh-Nakagawa T, Higuchi M, Morikawa Y, Miura M, Kawakami H, et al. (1998): No increase in cerebrospinal fluid tau protein levels in patients with vascular dementia. *Neurosci Lett*. 256:174-176.
171. Kurz A, Riemenschneider M, Buch K, Willoch F, Bartenstein P, Muller U, et al. (1998): Tau protein in cerebrospinal fluid is significantly increased at the earliest clinical stage of Alzheimer disease. *Alzheimer Dis Assoc Disord*. 12:372-377.
172. Nishimura T, Takeda M, Nakamura Y, Yosbida Y, Arai H, Sasaki H, et al. (1998): Basic and clinical studies on the measurement of tau protein in cerebrospinal fluid as a biological marker for Alzheimer's disease and related disorders: multicenter study in Japan. *Methods Find Exp Clin Pharmacol*. 20:227-235.
173. Green AJ, Harvey RJ, Thompson EJ, Rossor MN (1999): Increased tau in the cerebrospinal fluid of patients with frontotemporal dementia and Alzheimer's disease. *Neurosci Lett*. 259:133-135.
174. Hampel H, Teipel SJ, Padberg F, Haslinger A, Riemenschneider M, Schwarz MJ, et al. (1999): Discriminant power of combined cerebrospinal fluid tau protein and of the soluble interleukin-6 receptor complex in the diagnosis of Alzheimer's disease. *Brain Res*. 823:104-112.
175. Molina L, Touchon J, Herpe M, Lefranc D, Duplan L, Cristol JP, et al. (1999): Tau and apo E in CSF: potential aid for discriminating Alzheimer's disease from other dementias. *Neuroreport*. 10:3491-3495.
176. Burger nee Buch K, Padberg F, Nolde T, Teipel SJ, Stubner S, Haslinger A, et al. (1999): Cerebrospinal fluid tau protein shows a better discrimination in young old (<70 years) than in old old patients with Alzheimer's disease compared with controls. *Neurosci Lett*. 277:21-24.
177. Andreasen N, Minthon L, Clarberg A, Davidsson P, Gottfries J, Vanmechelen E, et al. (1999): Sensitivity, specificity, and stability of CSF-tau in AD in a community-based patient sample. *Neurology*. 53:1488-1494.
178. Kahle PJ, Jakowec M, Teipel SJ, Hampel H, Petzinger GM, Di Monte DA, et al. (2000): Combined assessment of tau and neuronal thread protein in Alzheimer's disease CSF. *Neurology*. 54:1498-1504.

179. Itoh N, Arai H, Urakami K, Ishiguro K, Ohno H, Hampel H, et al. (2001): Large-scale, multicenter study of cerebrospinal fluid tau protein phosphorylated at serine 199 for the antemortem diagnosis of Alzheimer's disease. *Ann Neurol*. 50:150-156.
180. Hampel H, Buerger K, Kohnken R, Teipel SJ, Zinkowski R, Moeller HJ, et al. (2001): Tracking of Alzheimer's disease progression with cerebrospinal fluid tau protein phosphorylated at threonine 231. *Ann Neurol*. 49:545-546.
181. Shoji M, Matsubara E, Murakami T, Manabe Y, Abe K, Kanai M, et al. (2002): Cerebrospinal fluid tau in dementia disorders: a large scale multicenter study by a Japanese study group. *Neurobiol Aging*. 23:363-370.
182. Ballatore C, Lee VM, Trojanowski JQ (2007): Tau-mediated neurodegeneration in Alzheimer's disease and related disorders. *Nat Rev Neurosci*. 8:663-672.
183. Hampel H, Buerger K, Zinkowski R, Teipel SJ, Goernitz A, Andreasen N, et al. (2004): Measurement of phosphorylated tau epitopes in the differential diagnosis of Alzheimer disease: a comparative cerebrospinal fluid study. *Arch Gen Psychiatry*. 61:95-102.
184. Kohnken R, Buerger K, Zinkowski R, Miller C, Kerkman D, DeBernardis J, et al. (2000): Detection of tau phosphorylated at threonine 231 in cerebrospinal fluid of Alzheimer's disease patients. *Neurosci Lett*. 287:187-190.
185. Buerger K, Teipel S, Zinkowski R, Blennow K, Arai H, Engel R, et al. (2002): CSF tau protein phosphorylated at threonine 231 correlates with cognitive decline in MCI subjects. *Neurology*. 59:627-629.
186. Lee JM, Blennow K, Andreasen N, Laterza O, Modur V, Olander J, et al. (2008): The brain injury biomarker VLP-1 is increased in the cerebrospinal fluid of Alzheimer disease patients. *Clin Chem*. 54:1617-1623.
187. Laterza OF, Modur VR, Crimmins DL, Olander JV, Landt Y, Lee JM, et al. (2006): Identification of novel brain biomarkers. *Clin Chem*. 52:1713-1721.
188. Pratico D, V MYL, Trojanowski JQ, Rokach J, Fitzgerald GA (1998): Increased F2-isoprostanes in Alzheimer's disease: evidence for enhanced lipid peroxidation in vivo. *FASEB J*. 12:1777-1783.
189. Yao Y, Zhukareva V, Sung S, Clark CM, Rokach J, Lee VM, et al. (2003): Enhanced brain levels of 8,12-iso-iPF2alpha-VI differentiate AD from frontotemporal dementia. *Neurology*. 61:475-478.
190. Montine T, Markesbery W, Roberts L, Morrow J (1998): Cerebrospinal fluid F2-isoprostane levels are increased in Alzheimer's disease. *Ann Neurol*. 44:410-413.
191. Montine TJ, Markesbery WR, Zackert W, Sanchez SC, Roberts LJ, 2nd, Morrow JD (1999): The magnitude of brain lipid peroxidation correlates with the extent of degeneration but not with density of neuritic plaques or neurofibrillary tangles or with APOE genotype in Alzheimer's disease patients. *Am J Pathol*. 155:863-868.
192. Montine T, Beal M, Cudkowicz M, O'Donnell H, Margolin R, McFarland L, et al. (1999): Increased CSF F2-isoprostane concentration in probable AD. *Neurology*. 52:562-565.
193. Pratico D, Clark C, Lee V, Trojanowski J, Rokach J, FitzGerald G (2000): Increased 8,12-iso-iPF2alpha-VI in Alzheimer's disease: Correlation of a noninvasive index of lipid peroxidation with disease severity. *Ann Neurol*. 48:809-812.
194. Montine TJ, Kaye JA, Montine KS, McFarland L, Morrow JD, Quinn JF (2001): Cerebrospinal fluid abeta42, tau, and f2-isoprostane concentrations in patients with Alzheimer disease, other dementias, and in age-matched controls. *Arch Pathol Lab Med*. 125:510-512.

195. Pratico D, Clark C, Liun F, Lee V, Trojanowski J (2002): Increased brain oxidative stress in mild cognitive impairment: A possible predictor of Alzheimer's disease. *Arch Neurol*. 59:972-976.
196. Grossman M, Farmer J, Leight S, Work M, Moore P, Van Deerlin V, et al. (2005): Cerebrospinal Fluid Profile in Frontotemporal Dementia and Alzheimer's Disease. *Ann Neurol*. 57:721 - 729.
197. Quinn JF, Montine KS, Moore M, Morrow JD, Kaye JA, Montine TJ (2004): Suppression of longitudinal increase in CSF F2-isoprostanes in Alzheimer's disease. *J Alzheimers Dis*. 6:93-97.
198. de Leon MJ, DeSanti S, Zinkowski R, Mehta PD, Pratico D, Segal S, et al. (2006): Longitudinal CSF and MRI biomarkers improve the diagnosis of mild cognitive impairment. *Neurobiol Aging*. 27:394-401.
199. de Leon M, Mosconi L, Li J, De Santi S, Yao Y, Tsui W, et al. (2007): Longitudinal CSF isoprostane and MRI atrophy in the progression to AD. *J Neurol Sci*. Nov 14.
200. Ringman JM, Younkin SG, Pratico D, Seltzer W, Cole GM, Geschwind DH, et al. (2008): Biochemical markers in persons with preclinical familial Alzheimer disease. *Neurology*. 71:85-92.
201. Irizarry MC, Yao Y, Hyman BT, Growdon JH, Pratico D (2007): Plasma F2A isoprostane levels in Alzheimer's and Parkinson's disease. *Neurodegener Dis*. 4:403-405.
202. Feillet-Coudray C, Tourtauchaux R, Niculescu M, Rock E, Tauveron I, Alexandre-Gouabau MC, et al. (1999): Plasma levels of 8-epiPGF2alpha, an in vivo marker of oxidative stress, are not affected by aging or Alzheimer's disease. *Free Radic Biol Med*. 27:463-469.
203. Montine TJ, Shinobu L, Montine KS, Roberts LJ, 2nd, Kowall NW, Beal MF, et al. (2000): No difference in plasma or urinary F2-isoprostanes among patients with Huntington's disease or Alzheimer's disease and controls. *Ann Neurol*. 48:950.
204. Tuppo EE, Forman LJ, Spur BW, Chan-Ting RE, Chopra A, Cavalieri TA (2001): Sign of lipid peroxidation as measured in the urine of patients with probable Alzheimer's disease. *Brain Res Bull*. 54:565-568.
205. Bohnstedt KC, Karlberg B, Wahlund LO, Jonhagen ME, Basun H, Schmidt S (2003): Determination of isoprostanes in urine samples from Alzheimer patients using porous graphitic carbon liquid chromatography-tandem mass spectrometry. *J Chromatogr B Analyt Technol Biomed Life Sci*. 796:11-19.
206. Flirski M, Sobow T (2005): Biochemical markers and risk factors of Alzheimer's disease. *Curr Alzheimer Res*. 2:47-64.
207. Akiyama H, Barger S, Barnum S, Bradt B, Bauer J, Cole GM, et al. (2000): Inflammation and Alzheimer's disease. *Neurobiol Aging*. 21:383-421.
208. Abraham C, Selkoe D, Potter H (1988): Immunochemical identification of the serine protease inhibitor alpha 1-antichymotrypsin in the brain amyloid deposits of Alzheimer's disease. *Cell*. 52:487-501.
209. Shoji M, Hirai S, Yamaguchi H, Harigaya Y, Ishiguro K, Matsubara E (1991): Alpha 1-antichymotrypsin is present in diffuse senile plaques. A comparative study of beta-protein and alpha 1-antichymotrypsin immunostaining in the Alzheimer brain. *Am J Pathol*. 138:247-257.
210. Roher AE, Palmer KC, Yurewicz EC, Ball MJ, Greenberg BD (1993): Morphological and biochemical analyses of amyloid plaque core proteins purified from Alzheimer disease brain tissue. *J Neurochem*. 61:1916-1926.
211. Matsubara E, Hirai S, Amari M, Shoji M, Yamaguchi H, Okamoto K, et al. (1990): Alpha 1-antichymotrypsin as a possible biochemical marker for Alzheimer-type dementia. *Ann Neurol*. 28:561-567.

212. Brugge K, Katzman R, Hill LR, Hansen LA, Saitoh T (1992): Serological alpha 1-antichymotrypsin in Down's syndrome and Alzheimer's disease. *Ann Neurol*. 32:193-197.
213. Hinds TR, Kukull WA, Van Belle G, Schellenberg GD, Villacres EC, Larson EB (1994): Relationship between serum alpha 1-antichymotrypsin and Alzheimer's disease. *Neurobiol Aging*. 15:21-27.
214. Lieberman J, Schleissner L, Tachiki KH, Kling AS (1995): Serum alpha 1-antichymotrypsin level as a marker for Alzheimer-type dementia. *Neurobiol Aging*. 16:747-753.
215. Harigaya Y, Shoji M, Nakamura T, Matsubara E, Hosoda K, Hirai S (1995): Alpha 1-antichymotrypsin level in cerebrospinal fluid is closely associated with late onset Alzheimer's disease. *Intern Med*. 34:481-484.
216. Furby A, Leys D, Delacourte A, Buee L, Soetaert G, Petit H (1991): Are alpha-1-antichymotrypsin and inter-alpha-trypsin inhibitor peripheral markers of Alzheimer's disease? *J Neurol Neurosurg Psychiatry*. 54:469.
217. Pirttila T, Mehta PD, Frey H, Wisniewski HM (1994): Alpha 1-antichymotrypsin and IL-1 beta are not increased in CSF or serum in Alzheimer's disease. *Neurobiol Aging*. 15:313-317.
218. Lanzrein AS, Johnston CM, Perry VH, Jobst KA, King EM, Smith AD (1998): Longitudinal study of inflammatory factors in serum, cerebrospinal fluid, and brain tissue in Alzheimer disease: interleukin-1beta, interleukin-6, interleukin-1 receptor antagonist, tumor necrosis factor-alpha, the soluble tumor necrosis factor receptors I and II, and alpha1-antichymotrypsin. *Alzheimer Dis Assoc Disord*. 12:215-227.
219. Licastro F, Pedrini S, Caputo L, Annoni G, Davis LJ, Ferri C, et al. (2000): Increased plasma levels of interleukin-1, interleukin-6 and alpha-1-antichymotrypsin in patients with Alzheimer's disease: peripheral inflammation or signals from the brain? *J Neuroimmunol*. 103:97-102.
220. DeKosky S, Ikonomovic MD, Wang X, Farlow M, Wisniewski S, Lopez O, et al. (2003): Plasma and Cerebrospinal Fluid 1-Antichymotrypsin Levels in Alzheimer's Disease: Correlation With Cognitive Impairnent. *Ann Neurol*. 53:81 - 90.
221. Engelhart M, Geerlings M, Meijer J, Kiliaan A, Ruitenberg A, VanSwieten J, et al. (2004): Inflammatory proteins in plasma and the risk of dementia: The Rotterdam study. *Arch Neurol*. 61:668-672.
222. Hu Y, Hosseini A, Kauwe J, Gross J, Cairns N, Goate A, et al. (2007): Identification and validation of novel CSF biomarkers for early stages of Alzheimer's disease. *Proteomics - Clin Appl*. 1:1373-1384.
223. Nielsen HM, Minthon L, Londos E, Blennow K, Miranda E, Perez J, et al. (2007): Plasma and CSF serpins in Alzheimer disease and dementia with Lewy bodies. *Neurology*. 69:1569-1579.
224. Rosler N, Wichart I, Jellinger KA (2001): Intra vitam lumbar and post mortem ventricular cerebrospinal fluid immunoreactive interleukin-6 in Alzheimer's disease patients. *Acta Neurol Scand*. 103:126-130.
225. Jia JP, Meng R, Sun YX, Sun WJ, Ji XM, Jia LF (2005): Cerebrospinal fluid tau, Abeta1-42 and inflammatory cytokines in patients with Alzheimer's disease and vascular dementia. *Neurosci Lett*. 383:12-16.
226. Blum-Degen D, Muller T, Kuhn W, Gerlach M, Przuntek H, Riederer P (1995): Interleukin-1 beta and interleukin-6 are elevated in the cerebrospinal fluid of Alzheimer's and de novo Parkinson's disease patients. *Neurosci Lett*. 202:17-20.
227. Martinez M, Fernandez-Vivancos E, Frank A, De la Fuente M, Hernanz A (2000): Increased cerebrospinal fluid fas (Apo-1) levels in Alzheimer's disease. Relationship with IL-6 concentrations. *Brain Res*. 869:216-219.

228. Yamada K, Kono K, Umegaki H, Iguchi A, Fukatsu T, Nakashima N, et al. (1995): Decreased interleukin-6 level in the cerebrospinal fluid of patients with Alzheimer-type dementia. *Neurosci Lett*. 186:219-221.
229. Engelborghs S, De Brabander M, De Cree J, D'Hooge R, Geerts H, Verhaegen H, et al. (1999): Unchanged levels of interleukins, neopterin, interferon-gamma and tumor necrosis factor-alpha in cerebrospinal fluid of patients with dementia of the Alzheimer type. *Neurochem Int*. 34:523-530.
230. Hampel H, Schoen D, Schwarz MJ, Kotter HU, Schneider C, Sunderland T, et al. (1997): Interleukin-6 is not altered in cerebrospinal fluid of first-degree relatives and patients with Alzheimer's disease. *Neurosci Lett*. 228:143-146.
231. Hasegawa Y, Sawada M, Ozaki N, Inagaki T, Suzumura A (2000): Increased soluble tumor necrosis factor receptor levels in the serum of elderly people. *Gerontology*. 46:185-188.
232. Marz P, Heese K, Hock C, Golombowski S, Muller-Spahn F, Rose-John S, et al. (1997): Interleukin-6 (IL-6) and soluble forms of IL-6 receptors are not altered in cerebrospinal fluid of Alzheimer's disease patients. *Neurosci Lett*. 239:29-32.
233. Tarkowski E, Blennow K, Wallin A, Tarkowski A (1999): Intracerebral production of tumor necrosis factor-alpha, a local neuroprotective agent, in Alzheimer disease and vascular dementia. *J Clin Immunol*. 19:223-230.
234. Kalman J, Juhasz A, Laird G, Dickens P, Jardanhazy T, Rimanoczy A, et al. (1997): Serum interleukin-6 levels correlate with the severity of dementia in Down syndrome and in Alzheimer's disease. *Acta Neurol Scand*. 96:236-240.
235. Angelis P, Scharf S, Mander A, Vajda F, Christophidis N (1998): Serum interleukin-6 and interleukin-6 soluble receptor in Alzheimer's disease. *Neurosci Lett*. 244:106-108.
236. Maes M, DeVos N, Wauters A, Demedts P, Maurits VW, Neels H, et al. (1999): Inflammatory markers in younger vs elderly normal volunteers and in patients with Alzheimer's disease. *J Psychiatr Res*. 33:397-405.
237. Wada-Isoe K, Wakutani Y, Urakami K, Nakashima K (2004): Elevated interleukin-6 levels in cerebrospinal fluid of vascular dementia patients. *Acta Neurol Scand*. 110:124-127.
238. Teunissen CE, de Vente J, Steinbusch HW, De Bruijn C (2002): Biochemical markers related to Alzheimer's dementia in serum and cerebrospinal fluid. *Neurobiol Aging*. 23:485-508.
239. Pan S, Zhu D, Quinn JF, Peskind ER, Montine TJ, Lin B, et al. (2007): A combined dataset of human cerebrospinal fluid proteins identified by multi-dimensional chromatography and tandem mass spectrometry. *Proteomics*. 7:469-473.
240. Zougman A, Pilch B, Podtelejnikov A, Kiehntopf M, Schnabel C, Kumar C, et al. (2008): Integrated analysis of the cerebrospinal fluid peptidome and proteome. *J Proteome Res*. 7:386-399.
241. Davidsson P, Westman-Brinkmalm A, Nilsson C, Lindbjer M, Paulson L, Andreasen N, et al. (2002): Proteome analysis of cerebrospinal fluid proteins in Alzheimer patients. *NeuroReport*. 13:611-615.
242. Puchades M, Folkesson Hansson S, Nilsson C, Andreasen N, Blennow K, Davidsson P (2003): Proteomic studies of potential cerebrospinal fluid protein markers for Alzheimer's disease. *Mol Brain Res*. 118:140-146.
243. Carrette O, Demalte I, Scherl A, Yalkinoglu O, Corthals G, Burkhard P, et al. (2003): A panel of cerebrospinal fluid potential biomarkers for the diagnosis of Alzheimer's disease. *Proteomics*. 3:1486-1494.

244. Selle H, Lamerz J, Buerger K, Dessauer A, Hager K, Hampel H, et al. (2005): Identification of novel biomarker candidates by differential peptidomics analysis of cerebrospinal fluid in Alzheimer's disease. *Comb Chem High Throughput Screen*. 8:801-806.
245. Zhang J, Goodlett DR, Quinn JF, Peskind E, Kaye JA, Zhou Y, et al. (2005): Quantitative proteomics of cerebrospinal fluid from patients with Alzheimer disease. *J Alzheimers Dis*. 7:125-133; discussion 173-180.
246. Abdi F, Quinn J, Jankovic J, McIntosh M, Leverenz J, Peskind E, et al. (2006): Detection of biomarkers with a multiplex quantitative proteomic platform in cerebrospinal fluid of patients with neurodegenerative disorders. *J Alzheimers Dis*. 9:293-348.
247. Choe L, Dutt M, Relkin N, Lee K (2002): Studies of potential cerebrospinal fluid molecular markers for Alzheimer's disease. *Electrophoresis*. 23:2247-2251.
248. Castano E, Roher A, Esh C, Kokjohn T, Beach T (2006): Comparative proteomics of cerebrospinal fluid in neuropathologically-confirmed Alzheimer's disease and non-demented elderly subjects. *Neurol Res*. 28:155-163.
249. Finehout EJ, Franck Z, Relkin N, Lee KH (2006): Proteomic analysis of cerebrospinal fluid changes related to postmortem interval. *Clin Chem*. 52:1906-1913.
250. Simonsen A, McGuire J, Hansson O, Zetterberg H, Podust V, Davies H, et al. (2007): Novel panel of cerebrospinal fluid biomarkers for the prediction of progression to Alzheimer dementia in patients with mild cognitive impairment. *Arch Neurol*. 64:366-370.
251. Hu Y, Malone J, Fagan A, Townsend R, Holtzman D (2005): Comparative proteomic analysis of intra- and interindividual variation in human cerebrospinal fluid. *Mol & Cell Proteom*. 4:2000-2009.
252. Gorevic PD, Casey TT, Stone WJ, DiRaimondo CR, Prelli FC, Frangione B (1985): Beta-2 microglobulin is an amyloidogenic protein in man. *J Clin Invest*. 76:2425-2429.
253. Gejyo F, Yamada T, Odani S, Nakagawa Y, Arakawa M, Kunitomo T, et al. (1985): A new form of amyloid protein associated with chronic hemodialysis was identified as beta 2-microglobulin. *Biochem Biophys Res Commun*. 129:701-706.
254. Schwarzman AL, Gregori L, Vitek MP, Lyubski S, Strittmatter WJ, Enghilde JJ, et al. (1994): Transthyretin sequesters amyloid beta protein and prevents amyloid formation. *Proc Natl Acad Sci U S A*. 91:8368-8372.
255. Schwarzman AL, Goldgaber D (1996): Interaction of transthyretin with amyloid beta-protein: binding and inhibition of amyloid formation. *Ciba Found Symp*. 199:146-160; discussion 160-144.
256. Tsuzuki K, Fukatsu R, Yamaguchi H, Tateno M, Imai K, Fujii N, et al. (2000): Transthyretin binds amyloid beta peptides, Abeta1-42 and Abeta1-40 to form complex in the autopsied human kidney - possible role of transthyretin for abeta sequestration. *Neurosci Lett*. 281:171-174.
257. Merched A, Serot J, Visvikis S, Aguillon D, Faure G, Siest G (1998): Apolipoprotein E, transthyretin and actin in the CSF of Alzheimer's patients: Relation with the senile plaques and cytoskeleton biochemistry. *FEBS Lett*. 425:225-228.
258. Finehout E, Franck Z, Choe L, Relkin N, Lee K (2006): Cerebrospinal fluid proteomic biomarkers for Alzheimer's disease. *Ann Neurol*. 61:120-129.
259. Portelius E, Zetterberg H, Andreasson W, Brinkmalm G, Andreasen N, Wallin A, et al. (2006): An Alzheimer's Disease -Specific B-Amyloid Fragment Signature in Cerebrospinal Fluid. *Neurosci Lett*. 409:215 - 219.

260. Lopez MF, Mikulskis A, Kuzdzal S, Bennett DA, Kelly J, Golenko E, et al. (2005): High-resolution serum proteomic profiling of Alzheimer disease samples reveals disease-specific, carrier-protein-bound mass signatures. *Clin Chem*. 51:1946-1954.
261. German DC, Gurnani P, Nandi A, Garner HR, Fisher W, Diaz-Arrastia R, et al. (2007): Serum biomarkers for Alzheimer's disease: proteomic discovery. *Biomed Pharmacother*. 61:383-389.
262. Hye A, Lynham S, Thambisetty M, Causevic M, Campbell J, Byers HL, et al. (2006): Proteome-based plasma biomarkers for Alzheimer's disease. *Brain*. 129:3042-3050.
263. Ray S, Britschgi M, Herbert C, Takeda-Uchimura Y, Boxer A, Blennow K, et al. (2007): Classification and prediction of clinical Alzheimer's diagnosis based on plasma signaling proteins. *Nat Med*. 13:1359-1362.
264. Jobst KA, Smith AD, Barker CS, Wear A, King EM, Smith A, et al. (1992): Association of atrophy of the medial temporal lobe with reduced blood flow in the posterior parietotemporal cortex in patients with a clinical and pathological diagnosis of Alzheimer's disease. *J Neurol Neurosurg Psychiatry*. 55:190-194.
265. De Leon MJ, George AE, Golomb J, Tarshish C, Convit A, Kluger A, et al. (1997): Frequency of hippocampal formation atrophy in normal aging and Alzheimer's disease. *Neurobiol Aging*. 18:1-11.
266. Killiany RJ, Gomez-Isla T, Moss M, Kikinis R, Sandor T, Jolesz F, et al. (2000): Use of structural magnetic resonance imaging to predict who will get Alzheimer's disease. *Ann Neurol*. 47:430-439.
267. deToledo-Morrell L, Stoub TR, Bulgakova M, Wilson RS, Bennett DA, Leurgans S, et al. (2004): MRI-derived entorhinal volume is a good predictor of conversion from MCI to AD. *Neurobiol Aging*. 25:1197-1203.
268. Tapiola T, Pennanen C, Tapiola M, Tervo S, Kivipelto M, Hanninen T, et al. (2008): MRI of hippocampus and entorhinal cortex in mild cognitive impairment: a follow-up study. *Neurobiol Aging*. 29:31-38.
269. Fotenos AF, Snyder AZ, Girton LE, Morris JC, Buckner RL (2005): Normative estimates of cross-sectional and longitudinal brain volume decline in aging and AD. *Neurology*. 64:1032-1039.
270. Thompson PM, Hayashi KM, de Zubicaray G, Janke AL, Rose SE, Semple J, et al. (2003): Dynamics of gray matter loss in Alzheimer's disease. *J Neurosci*. 23:994-1005.
271. Barnes J, Godbolt AK, Frost C, Boyes RG, Jones BF, Scahill RI, et al. (2007): Atrophy rates of the cingulate gyrus and hippocampus in AD and FTLD. *Neurobiol Aging*. 28:20-28.
272. Barnes J, Whitwell JL, Frost C, Josephs KA, Rossor M, Fox NC (2006): Measurements of the amygdala and hippocampus in pathologically confirmed Alzheimer disease and frontotemporal lobar degeneration. *Arch Neurol*. 63:1434-1439.
273. Whitwell JL, Jack CR, Jr. (2005): Comparisons between Alzheimer disease, frontotemporal lobar degeneration, and normal aging with brain mapping. *Top Magn Reson Imaging*. 16:409-425.
274. Whitwell JL, Weigand SD, Shiung MM, Boeve BF, Ferman TJ, Smith GE, et al. (2007): Focal atrophy in dementia with Lewy bodies on MRI: a distinct pattern from Alzheimer's disease. *Brain*. 130:708-719.
275. Kato T, Knopman D, Liu H (2001): Dissociation of regional activation in mild AD during visual encoding: a functional MRI study. *Neurology*. 57:812-816.

276. Dickerson BC, Salat DH, Greve DN, Chua EF, Rand-Giovannetti E, Rentz DM, et al. (2005): Increased hippocampal activation in mild cognitive impairment compared to normal aging and AD. *Neurology*. 65:404-411.
277. Machulda MM, Ward HA, Borowski B, Gunter JL, Cha RH, O'Brien PC, et al. (2003): Comparison of memory fMRI response among normal, MCI, and Alzheimer's patients. *Neurology*. 61:500-506.
278. Rombouts SA, Barkhof F, Veltman DJ, Machielsen WC, Witter MP, Bierlaagh MA, et al. (2000): Functional MR imaging in Alzheimer's disease during memory encoding. *AJNR Am J Neuroradiol*. 21:1869-1875.
279. Dickerson B, Salat D, Bates J, Atiya M, Killiany R, Greve D, et al. (2004): Medial temporal lobe function and structure in mild cognitive impairment. *Ann Neurol*. 56:27-35.
280. Kircher TT, Weis S, Freymann K, Erb M, Jessen F, Grodd W, et al. (2007): Hippocampal activation in patients with mild cognitive impairment is necessary for successful memory encoding. *J Neurol Neurosurg Psychiatry*. 78:812-818.
281. Johnson SC, Schmitz TW, Moritz CH, Meyerand ME, Rowley HA, Alexander AL, et al. (2006): Activation of brain regions vulnerable to Alzheimer's disease: the effect of mild cognitive impairment. *Neurobiol Aging*. 27:1604-1612.
282. Petrella JR, Krishnan S, Slavin MJ, Tran TT, Murty L, Doraiswamy PM (2006): Mild cognitive impairment: evaluation with 4-T functional MR imaging. *Radiology*. 240:177-186.
283. Celone KA, Calhoun VD, Dickerson BC, Atri A, Chua EF, Miller SL, et al. (2006): Alterations in memory networks in mild cognitive impairment and Alzheimer's disease: an independent component analysis. *J Neurosci*. 26:10222-10231.
284. Hamalainen A, Pihlajamaki M, Tanila H, Hanninen T, Niskanen E, Tervo S, et al. (2007): Increased fMRI responses during encoding in mild cognitive impairment. *Neurobiol Aging*. 28:1889-1903.
285. Dickerson BC, Sperling RA (2008): Functional abnormalities of the medial temporal lobe memory system in mild cognitive impairment and Alzheimer's disease: Insights from functional MRI studies. *Neuropsychologia*. 46:1624-1635.
286. Burns A, Philpot MP, Costa DC, Ell PJ, Levy R (1989): The investigation of Alzheimer's disease with single photon emission tomography. *J Neurol Neurosurg Psychiatry*. 52:248-253.
287. Montaldi D, Brooks DN, McColl JH, Wyper D, Patterson J, Barron E, et al. (1990): Measurements of regional cerebral blood flow and cognitive performance in Alzheimer's disease. *J Neurol Neurosurg Psychiatry*. 53:33-38.
288. Harris GJ, Lewis RF, Satlin A, English CD, Scott TM, Yurgelun-Todd DA, et al. (1998): Dynamic susceptibility contrast MR imaging of regional cerebral blood volume in Alzheimer disease: a promising alternative to nuclear medicine. *AJNR Am J Neuroradiol*. 19:1727-1732.
289. Hunter R, McLuskie R, Wyper D, Patterson J, Christie JE, Brooks DN, et al. (1989): The pattern of function-related regional cerebral blood flow investigated by single photon emission tomography with 99mTc-HMPAO in patients with presenile Alzheimer's disease and Korsakoff's psychosis. *Psychol Med*. 19:847-855.
290. Leys D, Steinling M, Petit H, Salomez JL, Gaudet Y, Ovelacq E, et al. (1989): [Alzheimer's disease: study by single photon emission tomography (Hm PAO Tc99m)]. *Rev Neurol (Paris)*. 145:443-450.
291. Perani D, Di Piero V, Vallar G, Cappa S, Messa C, Bottini G, et al. (1988): Technetium-99m HM-PAO-SPECT study of regional cerebral perfusion in early Alzheimer's disease. *J Nucl Med*. 29:1507-1514.

292. Huang C, Wahlund LO, Almkvist O, Elehu D, Svensson L, Jonsson T, et al. (2003): Voxel- and VOI-based analysis of SPECT CBF in relation to clinical and psychological heterogeneity of mild cognitive impairment. *Neuroimage*. 19:1137-1144.
293. Huang C, Eidelberg D, Habeck C, Moeller J, Svensson L, Tarabula T, et al. (2007): Imaging markers of mild cognitive impairment: multivariate analysis of CBF SPECT. *Neurobiol Aging*. 28:1062-1069.
294. Huang C, Wahlund LO, Svensson L, Winblad B, Julin P (2002): Cingulate cortex hypoperfusion predicts Alzheimer's disease in mild cognitive impairment. *BMC Neurol*. 2:9.
295. Kogure D, Matsuda H, Ohnishi T, Asada T, Uno M, Kunihiro T, et al. (2000): Longitudinal evaluation of early Alzheimer's disease using brain perfusion SPECT. *J Nucl Med*. 41:1155-1162.
296. Hirao K, Ohnishi T, Hirata Y, Yamashita F, Mori T, Moriguchi Y, et al. (2005): The prediction of rapid conversion to Alzheimer's disease in mild cognitive impairment using regional cerebral blood flow SPECT. *Neuroimage*. 28:1014-1021.
297. Borroni B, Anchisi D, Paghera B, Vicini B, Kerrouche N, Garibotto V, et al. (2006): Combined 99mTc-ECD SPECT and neuropsychological studies in MCI for the assessment of conversion to AD. *Neurobiol Aging*. 27:24-31.
298. Bradley KM, O'Sullivan VT, Soper ND, Nagy Z, King EM, Smith AD, et al. (2002): Cerebral perfusion SPET correlated with Braak pathological stage in Alzheimer's disease. *Brain*. 125:1772-1781.
299. Alsop DC, Detre JA, Grossman M (2000): Assessment of cerebral blood flow in Alzheimer's disease by spin-labeled magnetic resonance imaging. *Ann Neurol*. 47:93-100.
300. Johnson NA, Jahng GH, Weiner MW, Miller BL, Chui HC, Jagust WJ, et al. (2005): Pattern of cerebral hypoperfusion in Alzheimer disease and mild cognitive impairment measured with arterial spin-labeling MR imaging: initial experience. *Radiology*. 234:851-859.
301. Du AT, Jahng GH, Hayasaka S, Kramer JH, Rosen HJ, Gorno-Tempini ML, et al. (2006): Hypoperfusion in frontotemporal dementia and Alzheimer disease by arterial spin labeling MRI. *Neurology*. 67:1215-1220.
302. Hoffman JM, Welsh-Bohmer KA, Hanson M, Crain B, Hulette C, Earl N, et al. (2000): FDG PET imaging in patients with pathologically verified dementia. *J Nucl Med*. 41:1920-1928.
303. Sakamoto S, Ishii K, Sasaki M, Hosaka K, Mori T, Matsui M, et al. (2002): Differences in cerebral metabolic impairment between early and late onset types of Alzheimer's disease. *J Neurol Sci*. 200:27-32.
304. Minoshima S, Giordani B, Berent S, Frey KA, Foster NL, Kuhl DE (1997): Metabolic reduction in the posterior cingulate cortex in very early Alzheimer's disease. *Ann Neurol*. 42:85-94.
305. Nestor P, Fryer T, Smielewski P, Hodges J (2003): Limbic hypometabolism in Alzheimer's disease and mild cognitive impairment. *Ann Neurol*. 54:343-351.
306. de Leon MJ, Convit A, Wolf OT, Tarshish CY, DeSanti S, Rusinek H, et al. (2001): Prediction of cognitive decline in normal elderly subjects with 2-[(18)F]fluoro-2-deoxy-D-glucose/poitron-emission tomography (FDG/PET). *Proc Natl Acad Sci U S A*. 98:10966-10971.
307. Arnaiz E, Jelic V, Almkvist O, Wahlund LO, Winblad B, Valind S, et al. (2001): Impaired cerebral glucose metabolism and cognitive functioning predict deterioration in mild cognitive impairment. *Neuroreport*. 12:851-855.
308. Chetelat G, Landeau B, Eustache F, Mezenge F, Viader F, Sayette V, et al. (2005): Using Voxel-Based Morphometry to Map the Structural Changes Associated with Rapid Conversion in MCI: A Longitudinal MRI Study. *NeuroImage*.1 - 13.

309. Drzezga A, Grimmer T, Riemenschneider M, Lautenschlager N, Siebner H, Alexopoulus P, et al. (2005): Prediction of individual clinical outcome in MCI by means of genetic assessment and (18)F-FDG PET. *J Nucl Med*. 46:1625-1632.
310. Mosconi L, Perani D, Sorbi S, Herholz K, Nacmias B, Holthoff V, et al. (2004): MCI conversion to dementia and the APOE genotype: A prediction study with FDG-PET. *Neurology*. 63:2332-2340.
311. Cagnin A, Brooks DJ, Kennedy AM, Gunn RN, Myers R, Turkheimer FE, et al. (2001): In-vivo measurement of activated microglia in dementia. *Lancet*. 358:461-467.
312. Versijpt JJ, Dumont F, Van Laere KJ, Decoo D, Santens P, Audenaert K, et al. (2003): Assessment of neuroinflammation and microglial activation in Alzheimer's disease with radiolabelled PK11195 and single photon emission computed tomography. A pilot study. *Eur Neurol*. 50:39-47.
313. Zhang MR, Maeda J, Ogawa M, Noguchi J, Ito T, Yoshida Y, et al. (2004): Development of a new radioligand, N-(5-fluoro-2-phenoxyphenyl)-N-(2-[18F]fluoroethyl-5-methoxybenzyl)acetami de, for pet imaging of peripheral benzodiazepine receptor in primate brain. *J Med Chem*. 47:2228-2235.
314. Maeda J, Ji B, Irie T, Tomiyama T, Maruyama M, Okauchi T, et al. (2007): Longitudinal, quantitative assessment of amyloid, neuroinflammation, and anti-amyloid treatment in a living mouse model of Alzheimer's disease enabled by positron emission tomography. *J Neurosci*. 27:10957-10968.
315. Verhoeff NP, Wilson AA, Takeshita S, Trop L, Hussey D, Singh K, et al. (2004): In-vivo imaging of Alzheimer disease beta-amyloid with [11C]SB-13 PET. *Am J Geriatr Psychiatry*. 12:584-595.
316. Kudo Y, Okamura N, Furumoto S, Tashiro M, Furukawa K, Maruyama M, et al. (2007): 2-(2-[2-Dimethylaminothiazol-5-yl]ethenyl)-6- (2-[fluoro]ethoxy)benzoxazole: a novel PET agent for in vivo detection of dense amyloid plaques in Alzheimer's disease patients. *J Nucl Med*. 48:553-561.
317. Mathis C, Wang Y, Holt D, Huang G, Debnath M, Klunk W (2003): Synthesis and evaluation of ^{11}C-labeled 6-substituted 2-arylbenzothiazoles as amyloid imaging agents. *J Med Chem*. 46:2740-2754.
318. Klunk W, Engler H, Nordberg A, Wang Y, Blomqvist G, Holt D, et al. (2004): Imaging brain amyloid in Alzheimer's disease with Pittsburgh Compound-B. *Ann Neurol*. 55:306-319.
319. Rabinovici GD, Furst AJ, O'Neil JP, Racine CA, Mormino EC, Baker SL, et al. (2007): 11C-PIB PET imaging in Alzheimer disease and frontotemporal lobar degeneration. *Neurology*. 68:1205-1212.
320. Rowe CC, Ng S, Ackermann U, Gong SJ, Pike K, Savage G, et al. (2007): Imaging beta-amyloid burden in aging and dementia. *Neurology*. 68:1718-1725.
321. Pike KE, Savage G, Villemagne VL, Ng S, Moss SA, Maruff P, et al. (2007): Beta-amyloid imaging and memory in non-demented individuals: evidence for preclinical Alzheimer's disease. *Brain*. 130:2837-2844.
322. Kemppainen NM, Aalto S, Wilson IA, Nagren K, Helin S, Bruck A, et al. (2006): Voxel-based analysis of PET amyloid ligand [11C]PIB uptake in Alzheimer disease. *Neurology*. 67:1575-1580.
323. Price J, Klunk W, Lopresti B, Lu X, Hoge J, Ziolko S, et al. (2005): Kinetic modeling of amyloid binding in humans using PET imaging and Pittsburgh Compound-B. *J Cereb Blood Flow & Metab*. in press.

324. Small GW, Kepe V, Ercoli LM, Siddarth P, Bookheimer SY, Miller KJ, et al. (2006): PET of brain amyloid and tau in mild cognitive impairment. *N Engl J Med*. 355:2652-2663.
325. Archer H, Edison P, Brooks D, Barnes J, Frost C, Yeatman T, et al. (2006): Amyloid load and cerebral atrophy in Alzheimer's disease: An ^{11}C-PIB positron emission tomography study. *Ann Neurol*. 60:145-147.
326. Forsberg A, Engler H, Almkvist O, Blomquist G, Hagman G, Wall A, et al. (2007): PET imaging of amyloid deposition in patients with mild cognitive impairment. *Neurobiol Aging*.
327. Engler H, Forsberg A, Almkvist O, Blomquist G, Larsson E, Savitcheva I, et al. (2006): Two-year follow-up of amyloid deposition in patients with Alzheimer's disease. *Brain*. 129:2856-2866.
328. Kemppainen NM, Aalto S, Wilson IA, Nagren K, Helin S, Bruck A, et al. (2007): PET amyloid ligand [11C]PIB uptake is increased in mild cognitive impairment. *Neurology*. 68:1603-1606.
329. Jack CR, Jr., Lowe VJ, Senjem ML, Weigand SD, Kemp BJ, Shiung MM, et al. (2008): 11C PiB and structural MRI provide complementary information in imaging of Alzheimer's disease and amnestic mild cognitive impairment. *Brain*. 131:665-680.
330. Mintun M, LaRossa G, Sheline Y, Dence C, Lee S-Y, Mach R, et al. (2006): [^{11}C]PIB in a nondemented population: Potential antecedent marker of Alzheimer disease. *Neurology*. 67:446-452.
331. Lopresti BJ, Klunk WE, Mathis CA, Hoge JA, Ziolko SK, Lu X, et al. (2005): Simplified quantification of Pittsburgh Compound B amyloid imaging PET studies: a comparative analysis. *J Nucl Med*. 46:1959-1972.
332. Klunk WE, Price JC, Mathis CA, Tsopelas ND, Lopresti BJ, Ziolko SK, et al. (2007): Amyloid deposition begins in the striatum of presenilin-1 mutation carriers from two unrelated pedigrees. *J Neurosci*. 27:6174-6184.
333. Drzezga A, Grimmer T, Henriksen G, Stangier I, Perneczky R, Diehl-Schmid J, et al. (2008): Imaging of amyloid plaques and cerebral glucose metabolism in semantic dementia and Alzheimer's disease. *Neuroimage*. 39:619-633.
334. Johnson KA, Gregas M, Becker JA, Kinnecom C, Salat DH, Moran EK, et al. (2007): Imaging of amyloid burden and distribution in cerebral amyloid angiopathy. *Ann Neurol*. 62:229-234.
335. Bacskai BJ, Frosch MP, Freeman SH, Raymond SB, Augustinack JC, Johnson KA, et al. (2007): Molecular imaging with Pittsburgh Compound B confirmed at autopsy: a case report. *Arch Neurol*. 64:431-434.
336. Klunk WE, Mathis CA (2008): The future of amyloid-beta imaging: a tale of radionuclides and tracer proliferation. *Curr Opin Neurol*. 21:683-687.
337. Shoghi-Jadid K, Small GW, Agdeppa ED, Kepe V, Ercoli LM, Siddarth P, et al. (2002): Localization of neurofibrillary tangles and beta-amyloid plaques in the brains of living patients with Alzheimer disease. *Am J Geriatr Psychiatry*. 10:24-35.
338. Bresjanac M, Smid LM, Vovko TD, Petric A, Barrio JR, Popovic M (2003): Molecular-imaging probe 2-(1-[6-[(2-fluoroethyl)(methyl) amino]-2-naphthyl]ethylidene) malononitrile labels prion plaques in vitro. *J Neurosci*. 23:8029-8033.
339. Agdeppa ED, Kepe V, Liu J, Flores-Torres S, Satyamurthy N, Petric A, et al. (2001): Binding characteristics of radiofluorinated 6-dialkylamino-2-naphthylethylidene derivatives as positron emission tomography imaging probes for beta-amyloid plaques in Alzheimer's disease. *J Neurosci*. 21:RC189.

340. Rowe CC, Ackerman U, Browne W, Mulligan R, Pike KL, O'Keefe G, et al. (2008): Imaging of amyloid beta in Alzheimer's disease with 18F-BAY94-9172, a novel PET tracer: proof of mechanism. *Lancet Neurol*. 7:129-135.
341. Koole M, Lewis DM, Buckley C, Nelissen N, Vandenbulcke M, Brooks DJ, et al. (2009): Whole-body biodistribution and radiation dosimetry of 18F-GE067: a radioligand for in vivo brain amyloid imaging. *J Nucl Med*. 50:818-822.
342. Mathis C, Lopresti B, Mason N, Price J, Flatt N, Bi W, et al. (2007): Comparison of the amyloid imaging agents [F-18]3'-F-PIB and [C-11]PIB in Alzheimer's disease and control subjects. *J NUCL MED MEETING ABSTRACTS*. 48:56P-b-.
343. Wong DF, Rosenberg PB, Zhou Y, Kumar A, Raymont V, Ravert HT, et al. (2010): In vivo imaging of amyloid deposition in Alzheimer disease using the radioligand 18F-AV-45 (florbetapir [corrected] F 18). *J Nucl Med*. 51:913-920.
344. Choi SR, Golding G, Zhuang Z, Zhang W, Lim N, Hefti F, et al. (2009): Preclinical properties of 18F-AV-45: a PET agent for Abeta plaques in the brain. *J Nucl Med*. 50:1887-1894.
345. Lin KJ, Hsu WC, Hsiao IT, Wey SP, Jin LW, Skovronsky D, et al. (2010): Whole-body biodistribution and brain PET imaging with [18F]AV-45, a novel amyloid imaging agent--a pilot study. *Nucl Med Biol*. 37:497-508.
346. Sunderland T, Linker G, Mirza N, Putnam K, Friedman D, Kimmel L, et al. (2003): Decreased β-amyloid$_{1-42}$ and increased tau levels in cerebrospinal fluid of patients with Alzheimer's disease. *JAMA*. 289:2094-2103.
347. Buerger K, Zinowski R, Teipel S, Tapiola T, Arai H, Blennow K, et al. (2002): Differential diagnosis of Alzheimer's disease with cerebrospinal fluid levels of tau protein phosphorylated at threonine 231. *Arch Neurol*. 59:1267-1272.
348. Hansson O, Zetterberg H, Buchhave P, Londos E, Blennow K, Minthon L (2006): Association Between CSF Biomarkers and Incipient Alzheimer's Disease in Patients with Mild Cognitive Impairment: A Follow-Up Study. *Lancent Neurology*. 5:228 - 234.
349. DeKosky S, Ikonomovic M, Wang X, Farlow M, Wisniewski S, Lopez O, et al. (2003): Plasma and cerebrospinal fluid α1-antichymotrypsin levels in Alzheimer's disease: Correlation with cognitive impairment
Ann Neurol. 53:81-90.
350. Bosscher L SP (2001): *MRI of the temporal lobe*. Oxford: Blackwell.
351. Carlson NE, Moore MM, Dame A, Howieson D, Silbert LC, Quinn JF, et al. (2008): Trajectories of brain loss in aging and the development of cognitive impairment. *Neurology*. 70:828-833.
352. Sperling RA, Bates JF, Chua EF, Cocchiarella AJ, Rentz DM, Rosen BR, et al. (2003): fMRI studies of associative encoding in young and elderly controls and mild Alzheimer's disease. *J Neurol Neurosurg Psychiatry*. 74:44-50.
353. Becker JT, Mintun MA, Aleva K, Wiseman MB, Nichols T, DeKosky ST (1996): Compensatory reallocation of brain resources supporting verbal episodic memory in Alzheimer's disease. *Neurology*. 46:692-700.
354. Woodard JL, Grafton ST, Votaw JR, Green RC, Dobraski ME, Hoffman JM (1998): Compensatory recruitment of neural resources during overt rehearsal of word lists in Alzheimer's disease. *Neuropsychology*. 12:491-504.
355. Grady CL, Furey ML, Pietrini P, Horwitz B, Rapoport SI (2001): Altered brain functional connectivity and impaired short-term memory in Alzheimer's disease. *Brain*. 124:739-756.

356. Moulin CJ, Laine M, Rinne JO, Kaasinen V, Sipila H, Hiltunen J, et al. (2007): Brain function during multi-trial learning in mild cognitive impairment: a PET activation study. *Brain Res*. 1136:132-141.
357. Bozzao A, Floris R, Baviera ME, Apruzzese A, Simonetti G (2001): Diffusion and perfusion MR imaging in cases of Alzheimer's disease: correlations with cortical atrophy and lesion load. *AJNR Am J Neuroradiol*. 22:1030-1036.
358. Gonzalez RG, Fischman AJ, Guimaraes AR, Carr CA, Stern CE, Halpern EF, et al. (1995): Functional MR in the evaluation of dementia: correlation of abnormal dynamic cerebral blood volume measurements with changes in cerebral metabolism on positron emission tomography with fludeoxyglucose F 18. *AJNR Am J Neuroradiol*. 16:1763-1770.
359. Barnes L, Schneider J, Boyle P, Bienias J, Bennett D (2006): Memory complaints are related to Alzheimer disease pathology in older persons. *Neurology*. 67:1581-1585.
360. Jagust WJ, Landau SM, Shaw LM, Trojanowski JQ, Koeppe RA, Reiman EM, et al. (2009): Relationships between biomarkers in aging and dementia. *Neurology*. 73:1193-1199.
361. Hu WT, Chen-Plotkin A, Arnold SE, Grossman M, Clark CM, Shaw LM, et al. (2010): Novel CSF biomarkers for Alzheimer's disease and mild cognitive impairment. *Acta Neuropathol*. 119:669-678.
362. Simonsen AH, McGuire J, Podust VN, Hagnelius NO, Nilsson TK, Kapaki E, et al. (2007): A novel panel of cerebrospinal fluid biomarkers for the differential diagnosis of Alzheimer's disease versus normal aging and frontotemporal dementia. *Dement Geriatr Cogn Disord*. 24:434-440.
363. Simonsen AH, McGuire J, Podust VN, Davies H, Minthon L, Skoog I, et al. (2008): Identification of a novel panel of cerebrospinal fluid biomarkers for Alzheimer's disease. *Neurobiol Aging* 29:961-968.
364. Finehout EJ, Franck Z, Choe LH, Relkin N, Lee KH (2007): Cerebrospinal fluid proteomic biomarkers for Alzheimer's disease. *Ann Neurol*. 61:120-129.
365. Choe L DAM, Relkin NR, Pappin D, Ross P, Williamson B, Guertin S, Pribil P, Lee KH (2007): 8-plex quantitation of changes in cerebrospinal fluid protein expression in subjects undergoing intravenous immunoglobulin treatment for Alzheimer's disease. *Proteomics*. 7:3651-3660.
366. Suzuki N, Cheung TT, Cai XD, Odaka A, Otvos L, Jr., Eckman C, et al. (1994): An increased percentage of long amyloid beta protein secreted by familial amyloid beta protein precursor (beta APP717) mutants. *Science*. 264:1336-1340.
367. Alban A, David S, Bjorkesten L, Andersson C, Sloge E, Lewis S, et al. (2003): A novel experimental design for comparative two-dimensional gel analysis: Two-dimensional difference gel electrophoresis incorporating a pooled internal standard. *Proteomics*. 3:36-44.
368. Havlis J TH, Sebela M, Shevchenko A (2003): Fast-response proteomics by accelerated in-gel digestion of proteins. *Anal Chem* 75:1300-1306.
369. King J, Gross J, Lovly C, Rohrs H, Piwnica-Worms H, Townsend R (2006): Accurate mass-driven analysis for the characterization of protein phosphorylation. Study of the human chk2 protein kinase *Anal Chem*. 78:2171-2181.
370. Bredemeyer A, Lewis R, Malone J, Davis A, Gross J, Townsend R, et al. (2004): A proteomic approach for the discovery of protease substrates. *Proc Natl Acad Sci USA*. 101:11785-11790.
371. Liu H, Sadygov RG, Yates JR, 3rd (2004): A model for random sampling and estimation of relative protein abundance in shotgun proteomics. *Anal Chem*. 76:4193-4201.

372. Craig-Schapiro R, Perrin RJ, Roe CM, Xiong C, Carter D, Cairns NJ, et al. (2010): YKL-40: A Novel Prognostic Fluid Biomarker for Preclinical Alzheimer's Disease. *Biological Psychiatry*. in press.
373. Colton CA, Mott RT, Sharpe H, Xu Q, Van Nostrand WE, Vitek MP (2006): Expression profiles for macrophage alternative activation genes in AD and in mouse models of AD. *J Neuroinflammation*. 3:27.
374. Kolson DL (2008): YKL-40: a candidate biomarker for simian immunodeficiency virus and human immunodeficiency virus encephalitis? *Am J Pathol*. 173:25-29.
375. Bonneh-Barkay D, Bissel SJ, Wang G, Fish KN, Nicholl GC, Darko SW, et al. (2008): YKL-40, a marker of simian immunodeficiency virus encephalitis, modulates the biological activity of basic fibroblast growth factor. *Am J Pathol*. 173:130-143.
376. Ostergaard C, Johansen JS, Benfield T, Price PA, Lundgren JD (2002): YKL-40 is elevated in cerebrospinal fluid from patients with purulent meningitis. *Clin Diagn Lab Immunol*. 9:598-604.
377. Kaynar MY, Tanriverdi T, Kafadar AM, Kacira T, Yurdakul F, Uzun H, et al. (2005): YKL-40 levels in the cerebrospinal fluid and serum of patients with aneurysmal subarachnoid hemorrhage: preliminary results. *J Clin Neurosci* 12:754-757.
378. Junker N, Johansen JS, Hansen LT, Lund EL, Kristjansen PE (2005): Regulation of YKL-40 expression during genotoxic or microenvironmental stress in human glioblastoma cells. *Cancer Sci*. 96:183-190.
379. Hakala BE, White C, Recklies AD (1993): Human cartilage gp-39, a major secretory product of articular chondrocytes and synovial cells, is a mammalian member of a chitinase protein family. *J Biol Chem*. 268:25803-25810.
380. Chupp GL, Lee CG, Jarjour N, Shim YM, Holm CT, He S, et al. (2007): A chitinase-like protein in the lung and circulation of patients with severe asthma. *N Engl J Med*. 357:2016-2027.
381. Ling H, Recklies AD (2004): The chitinase 3-like protein human cartilage glycoprotein 39 inhibits cellular responses to the inflammatory cytokines interleukin-1 and tumour necrosis factor-alpha. *Biochem J*. 380:651-659.
382. Letuve S, Kozhich A, Arouche N, Grandsaigne M, Reed J, Dombret MC, et al. (2008): YKL-40 is elevated in patients with chronic obstructive pulmonary disease and activates alveolar macrophages. *J Immunol*. 181:5167-5173.
383. Roberts ES, Zandonatti MA, Watry DD, Madden LJ, Henriksen SJ, Taffe MA, et al. (2003): Induction of pathogenic sets of genes in macrophages and neurons in NeuroAIDS. *Am J Pathol*. 162:2041-2057.
384. Wati H, Kawarabayashi T, Matsubara E, Kasai A, Hirasawa T, Kubota T, et al. (2009): Transthyretin accelerates vascular Abeta deposition in a mouse model of Alzheimer's disease. *Brain Pathol* 19:48-57.
385. Buxbaum JN, Ye Z, Reixach N, Friske L, Levy C, Das P, et al. (2008): Transthyretin protects Alzheimer's mice from the behavioral and biochemical effects of Abeta toxicity. *Proc Natl Acad Sci U S A*. 105:2681-2686.
386. Buxbaum JN, Reixach N (2009): Transthyretin: the servant of many masters. *Cell Mol Life Sci*. 66:3095-3101.
387. Costa R, Goncalves A, Saraiva MJ, Cardoso I (2008): Transthyretin binding to A-Beta peptide--impact on A-Beta fibrillogenesis and toxicity. *FEBS Lett*. 582:936-942.

388. Choi SH, Leight SN, Lee VM, Li T, Wong PC, Johnson JA, et al. (2007): Accelerated Abeta deposition in APPswe/PS1deltaE9 mice with hemizygous deletions of TTR (transthyretin). *J Neurosci*. 27:7006-7010.
389. Lovell MA, Lynn BC, Xiong S, Quinn JF, Kaye J, WR M (2008): An aberrant protein complex in CSF as a biomarker of Alzheimer disease. *Neurology*. 70:2212-2218.
390. Hansson SF, Andreasson U, Wall M, Skoog I, Andreasen N, Wallin A, et al. (2009): Reduced levels of amyloid-beta-binding proteins in cerebrospinal fluid from Alzheimer's disease patients. *J Alzheimers Dis*. 16:389-397.
391. Kaeser SA, Herzig MC, Coomaraswamy J, Kilger E, Selenica ML, Winkler DT, et al. (2007): Cystatin C modulates cerebral beta-amyloidosis. *Nat Genet*. 39:1437-1439.
392. Sun B, Zhou Y, Halabisky B, Lo I, Cho SH, Mueller-Steiner S, et al. (2008): Cystatin C-cathepsin B axis regulates amyloid beta levels and associated neuronal deficits in an animal model of Alzheimer's disease. *Neuron*. 60:247-257.
393. Mi W, Pawlik M, Sastre M, Jung SS, Radvinsky DS, Klein AM, et al. (2007): Cystatin C inhibits amyloid-beta deposition in Alzheimer's disease mouse models. *Nat Genet*. 39:1440-1442.
394. Selenica ML, Wang X, Ostergaard-Pedersen L, Westlind-Danielsson A, Grubb A (2007): Cystatin C reduces the in vitro formation of soluble Abeta1-42 oligomers and protofibrils. *Scand J Clin Lab Invest*. 67:179-190.
395. Kalus I, Bormann U, Mzoughi M, Schachner M, Kleene.R (2006): Proteolytic cleavage of the neural cell adhesion molecule by ADAM17/TACE is involved in neurite outgrowth. *J Neurochem* 98:78-88.
396. Yin GN, Lee HW, Cho JY, Suk K (2009): Neuronal pentraxin receptor in cerebrospinal fluid as a potential biomarker for neurodegenerative diseases. *Brain Res*. 1265:158-170.
397. Aisa B, Gil-Bea FJ, Solas M, García-Alloza M, Chen CP, Lai MK, et al. (2010): Altered NCAM Expression Associated with the Cholinergic System in Alzheimer's Disease *Journal of Alzheimers Disease*. 20:659-668.
398. Storan MJ, Magnaldo T, Biol-N'Garagba MC, Zick Y, Key-B (2004): Expression and putative role of lactoseries carbohydrates present on NCAM in the rat primary olfactory pathway. *J Comp Neurol* 475:289-302.
399. Hosaka M, Suda M, Sakai Y, Izumi T, Watanabe T, T. T (2004): Secretogranin III binds to cholesterol in the secretory granule membrane as an adapter for chromogranin A. *J Biol Chem*. 279:3627-3634.
400. Lechner T, Adlassnig C, Humpel C, Kaufmann WA, Maier H, Reinstadler-Kramer K, et al. (2004): Chromogranin peptides in Alzheimer's disease. *Exp Gerontol*. 39:101-113.
401. Lassmann H, Weiler R, Fischer P, Bancher C, Jellinger K, Floor E, et al. (1992): Synaptic pathology in Alzheimer's disease: immunological data for markers of synaptic and large dense-core vesicles. *Neuroscience*. 46:1-8.
402. Eder U, Leitner B, Kirchmair R, Pohl P, Jobst KA, Smith AD, et al. (1998): Levels and proteolytic processing of chromogranin A and B and secretogranin II in cerebrospinal fluid in neurological diseases. *J Neural Transm*. 105:39-51.
403. Balion CM, Benson C, Raina PS, Papaioannou A, Patterson C, AS I (2007): Brain type carnosinase in dementia: a pilot study. *BMC Neurol* 7:38.
404. Guiotto A, Calderan A, Ruzza P, Borin-G (2005): Carnosine and carnosine-related antioxidants: a review. *Curr Med Chem* 12:2293-2315.

405. Hipkiss-AR (2007): Could carnosine or related structures suppress Alzheimer's disease? *J Alzheimers Dis*. 11:229-240.
406. Kapaki E, Paraskevas GP, Papageorgiou SG, Bonakis A, Kalfakis N, Zalonis I, et al. (2008): Diagnostic value of CSF biomarker profile in frontotemporal lobar degeneration. *Alzheimer Dis Assoc Disord* 22:47-53.
407. Bian H, Van Swieten JC, Leight S, Massimo L, Wood E, Forman M, et al. (2008): CSF biomarkers in frontotemporal lobar degeneration with known pathology. *Neurology*. 70:1827-1835.
408. Mollenhauer B, Cullen V, Kahn I, Krastins B, Outeiro TF, Pepivani I, et al. (2008): Direct quantification of CSF alpha-synuclein by ELISA and first cross-sectional study in patients with neurodegeneration. *Exp Neurol* 213:315-325.
409. Bateman RJ, Siemers ER, Mawuenyega KG, Wen G, Browning KR, Sigurdson WC, et al. (2009): A gamma-secretase inhibitor decreases amyloid-beta production in the central nervous system. *Ann Neurol*. 66:48-54.
410. Craig-Schapiro R, Fagan AM, Holtzman DM (2009): Biomarkers of Alzheimer's disease. *Neurobiol Dis*. 35:128-140.
411. Perrin RJ, Fagan AM, Holtzman DM (2009): Multimodal techniques for diagnosis and prognosis of Alzheimer's disease. *Nature*. 461:916-922.
412. Hampel H, Burger K, Teipel SJ, Bokde AL, Zetterberg H, Blennow K (2008): Core candidate neurochemical and imaging biomarkers of Alzheimer's disease. *Alzheimers Dement*. 4:38-48.
413. Jack CR, Jr., Knopman DS, Jagust WJ, Shaw LM, Aisen PS, Weiner MW, et al. (2010): Hypothetical model of dynamic biomarkers of the Alzheimer's pathological cascade. *Lancet Neurol*. 9:119-128.
414. Johansen JS (2006): Studies on serum YKL-40 as a biomarker in diseases with inflammation, tissue remodelling, fibroses and cancer. *Dan Med Bull*. 53:172-209.
415. Johansen JS, Schultz NA, Jensen BV (2009): Plasma YKL-40: a potential new cancer biomarker? *Future Oncol*. 5:1065-1082.
416. Comabella M, Fernandez M, Martin R, Rivera-Vallve S, Borras E, Chiva C, et al. Cerebrospinal fluid chitinase 3-like 1 levels are associated with conversion to multiple sclerosis. *Brain*. 133:1082-1093.
417. Neary D, Snowden JS, Gustafson L, Passant U, Stuss D, Black S, et al. (1998): Frontotemporal lobar degeneration: a consensus on clinical diagnostic criteria. *Neurology*. 51:1546-1554.
418. Litvan I, Agid Y, Calne D, Campbell G, Dubois B, Duvoisin RC, et al. (1996): Clinical research criteria for the diagnosis of progressive supranuclear palsy (Steele-Richardson-Olszewski syndrome): report of the NINDS-SPSP international workshop. *Neurology*. 47:1-9.
419. Snider BJ, Fagan AM, Roe C, Shah AR, Grant EA, Xiong C, et al. (2009): Cerebrospinal fluid biomarkers and rate of cognitive decline in very mild dementia of the Alzheimer type. *Arch Neurol*. 66:638-645.
420. Suarez-Sola ML, Gonzalez-Delgado FJ, Pueyo-Morlans M, Medina-Bolivar OC, Hernandez-Acosta NC, Gonzalez-Gomez M, et al. (2009): Neurons in the white matter of the adult human neocortex. *Front Neuroanat*. 3:7.
421. Kacira T, Hanimoglu H, Kucur M, Sanus GZ, Kafadar AM, Tanriverdi T, et al. (2008): Elevated cerebrospinal fluid and serum YKL-40 levels are not associated with symptomatic

vasospasm in patients with aneurysmal subarachnoid haemorrhage. *J Clin Neurosci*. 15:1011-1016.
422. Bonneh-Barkay D, Wang G, Starkey A, Hamilton RL, Wiley CA In vivo CHI3L1 (YKL-40) expression in astrocytes in acute and chronic neurological diseases. *J Neuroinflammation*. 7:34.
423. Zetterberg H, Pedersen M, Lind K, Svensson M, Rolstad S, Eckerstrom C, et al. (2007): Intra-individual stability of CSF biomarkers for Alzheimer's disease over two years. *J Alzheimers Dis*. 12:255-260.
424. Wyss-Coray T, Mucke L (2002): Inflammation in neurodegenerative disease--a double-edged sword. *Neuron*. 35:419-432.
425. Heneka MT, O'Banion MK (2007): Inflammatory processes in Alzheimer's disease. *J Neuroimmunol*. 184:69-91.
426. Recklies AD, Ling H, White C, Bernier SM (2005): Inflammatory cytokines induce production of CHI3L1 by articular chondrocytes. *J Biol Chem*. 280:41213-41221.
427. De Ceuninck F, Gaufillier S, Bonnaud A, Sabatini M, Lesur C, Pastoureau P (2001): YKL-40 (cartilage gp-39) induces proliferative events in cultured chondrocytes and synoviocytes and increases glycosaminoglycan synthesis in chondrocytes. *Biochem Biophys Res Commun*. 285:926-931.
428. Recklies AD, White C, Ling H (2002): The chitinase 3-like protein human cartilage glycoprotein 39 (HC-gp39) stimulates proliferation of human connective-tissue cells and activates both extracellular signal-regulated kinase- and protein kinase B-mediated signalling pathways. *Biochem J*. 365:119-126.
429. Bigg HF, Wait R, Rowan AD, Cawston TE (2006): The mammalian chitinase-like lectin, YKL-40, binds specifically to type I collagen and modulates the rate of type I collagen fibril formation. *J Biol Chem*. 281:21082-21095.
430. Malinda KM, Ponce L, Kleinman HK, Shackelton LM, Millis AJ (1999): Gp38k, a protein synthesized by vascular smooth muscle cells, stimulates directional migration of human umbilical vein endothelial cells. *Exp Cell Res*. 250:168-173.
431. Nishikawa KC, Millis AJ (2003): gp38k (CHI3L1) is a novel adhesion and migration factor for vascular cells. *Exp Cell Res*. 287:79-87.
432. Lee CG, Hartl D, Lee GR, Koller B, Matsuura H, Da Silva CA, et al. (2009): Role of breast regression protein 39 (BRP-39)/chitinase 3-like-1 in Th2 and IL-13-induced tissue responses and apoptosis. *J Exp Med*. 206:1149-1166.
433. Morris JC, Roe CM, Xiong C, Fagan AM, Goate AM, Holtzman DM, et al. (2010): *APOE* Predicts Abeta but not Tau Alzheimer's Pathology in Cognitively Normal Aging. *Ann Neurol*. In Press.
434. Gimenez-Roqueplo AP, Celerier J, Lucarelli G, Corvol P, Jeunemaitre X (1998): Role of N-glycosylation in human angiotensinogen. *J Biol Chem*. 273:21232-21238.
435. Jirka M, Blanicky P (1980): Polymorphism of human serum Zn-alpha 2-glycoprotein and its behaviour during ontogenesis using quantitative crossed starch gel immunoelectrophoresis. *Clin Chim Acta*. 103:61-66.
436. Uria JA, Fueyo A, Balbin M, Velasco G, Pendas AM, Lopez-Otin C (1996): Alternative splicing gives rise to two novel long isoforms of Zn-alpha 2-glycoprotein, a member of the immunoglobulin superfamily. *Gene*. 169:233-236.
437. Carlson TH, Babcock T, Atencio AC, Levinson C, Mora HR (1988): Behavior of antithrombin III isoforms on immobilized heparins. Evidence that the isoforms bind to different numbers of low-affinity heparin sites. *J Biol Chem*. 263:2187-2194.

438. Maurer MH (2008): Proteomics of brain extracellular fluid (ECF) and cerebrospinal fluid (CSF). *Mass Spectrom Rev*.
439. Andersson C, Blennow K, Almkvist O, Andreasen N, Engfeldt P, Johansson SE, et al. (2008): Increasing CSF phospho-tau levels during cognitive decline and progression to dementia. *Neurobiol Aging*. 29:1466-1473.
440. Buchhave P, Blennow K, Zetterberg H, Stomrud E, Londos E, Andreasen N, et al. (2009): Longitudinal study of CSF biomarkers in patients with Alzheimer's disease. *PLoS One*. 4:e6294.
441. Petersen R, Smith G, Waring S, Ivnik R, Tabgalos E, Kokmen E (1999): Mild cognitive impairment: Clinical characterization and outcome. *Arch Neurol*. 56:303-308.
442. Team RDC (2010): R: A language and environment for statistical computing. *R Foundation for Statistical Computing*.
443. Xiong C, McKeel D, Miller J, Morris J (2004): Combining correlated diagnostic tests---application to neuropathologic diagnosis of Alzheimer's disease. *Medical Decision Making*. 24:659-669.
444. Gerlach RW, Kowalski BR, Wold HOA (1979): Partial least-squares path modelling with latent variables. *Analytica Chimica Acta*. 112:417-421.
445. Chun H, Keleş S Sparse partial least squares regression for simultaneous dimension reduction and variable selection. *Journal of the Royal Statistical Society: Series B (Statistical Methodology)*. 72:3-25.
446. Breiman L (2001): Random Forests. *Mach Learn*. 45:5-32.
447. Friedman JH (2001): Greedy Function Approximation: A Gradient Boosting Machine. *The Annals of Statistics*. 29:1189-1232.
448. Boser BE, Guyon IM, Vapnik VN (1992): A training algorithm for optimal margin classifiers. *Proceedings of the fifth annual workshop on Computational learning theory*. Pittsburgh, Pennsylvania, United States: ACM.
449. Caputo B, Sim K, Furesjo F, Smola A (2001): Appearance-based object recognition using SVMs: which kernel should I use? *Proceedings of Neural Information Processing Systems Workshop on Statistical methods for Computational Experiments In Visual Processing and Computer Vision*. Whistler.
450. Tibshirani R, Hastie T, Narasimhan B, Chu G (2003): Class Prediction by Nearest Shrunken Centroids, with Applications to DNA Microarrays. *Statistical Science*. 18:104-117.
451. Hastie T, Tibshirani R, Friedman JH (2001): *The Elements of Statistical Learning*. Springer-Verlag, New York.
452. Hastie T, Tibshirani R, Buja A (1993): Flexible Discriminant Analysis by Optimal Scoring. *Journal of the American Statistical Association*. 89:1255-1270.
453. Ban Y, Watanabe T, Suguro T, Matsuyama TA, Iso Y, Sakai T, et al. (2009): Increased plasma urotensin-II and carotid atherosclerosis are associated with vascular dementia. *J Atheroscler Thromb*. 16:179-187.
454. Bacher M, Deuster O, Aljabari B, Egensperger R, Neff F, Jessen F, et al. (2010): The role of macrophage migration inhibitory factor in Alzheimer's disease. *Mol Med*. 16:116-121.
455. Popp J, Bacher M, Kolsch H, Noelker C, Deuster O, Dodel R, et al. (2009): Macrophage migration inhibitory factor in mild cognitive impairment and Alzheimer's disease. *J Psychiatr Res*. 43:749-753.
456. Lee JW, Namkoong H, Kim HK, Kim S, Hwang DW, Na HR, et al. (2007): Fibrinogen gamma-A chain precursor in CSF: a candidate biomarker for Alzheimer's disease. *BMC Neurol*. 7:14.

457. Chang CY, Liang HJ, Chow SY, Chen SM, Liu DZ (2007): Hemorheological mechanisms in Alzheimer's disease. *Microcirculation*. 14:627-634.
458. van Oijen M, Witteman JC, Hofman A, Koudstaal PJ, Breteler MM (2005): Fibrinogen is associated with an increased risk of Alzheimer disease and vascular dementia. *Stroke*. 36:2637-2641.
459. Tarkowski E, Wallin A, Regland B, Blennow K, Tarkowski A (2001): Local and systemic GM-CSF increase in Alzheimer's disease and vascular dementia. *Acta Neurol Scand*. 103:166-174.
460. Leyhe T, Hoffmann N, Stransky E, Laske C (2009): Increase of SCF plasma concentration during donepezil treatment of patients with early Alzheimer's disease. *Int J Neuropsychopharmacol*. 12:1319-1326.
461. Del Bo R, Scarlato M, Ghezzi S, Martinelli Boneschi F, Fenoglio C, Galbiati S, et al. (2005): Vascular endothelial growth factor gene variability is associated with increased risk for AD. *Ann Neurol*. 57:373-380.
462. Mateo I, Llorca J, Infante J, Rodriguez-Rodriguez E, Fernandez-Viadero C, Pena N, et al. (2007): Low serum VEGF levels are associated with Alzheimer's disease. *Acta Neurol Scand*. 116:56-58.
463. Chiappelli M, Borroni B, Archetti S, Calabrese E, Corsi MM, Franceschi M, et al. (2006): VEGF gene and phenotype relation with Alzheimer's disease and mild cognitive impairment. *Rejuvenation Res*. 9:485-493.
464. Blasko I, Lederer W, Oberbauer H, Walch T, Kemmler G, Hinterhuber H, et al. (2006): Measurement of thirteen biological markers in CSF of patients with Alzheimer's disease and other dementias. *Dement Geriatr Cogn Disord*. 21:9-15.
465. Tarkowski E, Issa R, Sjogren M, Wallin A, Blennow K, Tarkowski A, et al. (2002): Increased intrathecal levels of the angiogenic factors VEGF and TGF-beta in Alzheimer's disease and vascular dementia. *Neurobiol Aging*. 23:237-243.
466. Kalman J, Marki-Zay J, Juhasz A, Santha A, Dux L, Janka Z (2000): Serum and cerebrospinal fluid cystatin C levels in vascular and Alzheimer's dementia. *Acta Neurol Scand*. 101:279-282.
467. Straface E, Matarrese P, Gambardella L, Vona R, Sgadari A, Silveri MC, et al. (2005): Oxidative imbalance and cathepsin D changes as peripheral blood biomarkers of Alzheimer disease: a pilot study. *FEBS Lett*. 579:2759-2766.
468. Chuo LJ, Sheu WH, Pai MC, Kuo YM (2007): Genotype and plasma concentration of cystatin C in patients with late-onset Alzheimer disease. *Dement Geriatr Cogn Disord*. 23:251-257.
469. Sundelof J, Arnlov J, Ingelsson E, Sundstrom J, Basu S, Zethelius B, et al. (2008): Serum cystatin C and the risk of Alzheimer disease in elderly men. *Neurology*. 71:1072-1079.
470. Brettschneider J, Riepe MW, Petereit HF, Ludolph AC, Tumani H (2004): Meningeal derived cerebrospinal fluid proteins in different forms of dementia: is a meningopathy involved in normal pressure hydrocephalus? *J Neurol Neurosurg Psychiatry*. 75:1614-1616.
471. Sastre M, Calero M, Pawlik M, Mathews PM, Kumar A, Danilov V, et al. (2004): Binding of cystatin C to Alzheimer's amyloid beta inhibits in vitro amyloid fibril formation. *Neurobiol Aging*. 25:1033-1043.
472. Tizon B, Ribe EM, Mi W, Troy CM, Levy E (2010): Cystatin C protects neuronal cells from amyloid-beta-induced toxicity. *J Alzheimers Dis*. 19:885-894.
473. Fabbro S, Seeds NW (2009): Plasminogen activator activity is inhibited while neuroserpin is up-regulated in the Alzheimer disease brain. *Journal of Neurochemistry*. 109:303-315.

474. Melchor JP, Pawlak R, Strickland S (2003): The tissue plasminogen activator-plasminogen proteolytic cascade accelerates amyloid-beta (Abeta) degradation and inhibits Abeta-induced neurodegeneration. *J Neurosci*. 23:8867-8871.
475. Cacquevel M, Launay S, Castel H, Benchenane K, Cheenne S, Buee L, et al. (2007): Ageing and amyloid-beta peptide deposition contribute to an impaired brain tissue plasminogen activator activity by different mechanisms. *Neurobiol Dis*. 27:164-173.
476. Oyama R, Yamamoto H, Titani K (2000): Glutamine synthetase, hemoglobin alpha-chain, and macrophage migration inhibitory factor binding to amyloid beta-protein: their identification in rat brain by a novel affinity chromatography and in Alzheimer's disease brain by immunoprecipitation. *Biochim Biophys Acta*. 1479:91-102.
477. Cortes-Canteli M, Paul J, Norris EH, Bronstein R, Ahn HJ, Zamolodchikov D, et al. (2010): Fibrinogen and beta-amyloid association alters thrombosis and fibrinolysis: a possible contributing factor to Alzheimer's disease. *Neuron*. 66:695-709.
478. Paul J, Strickland S, Melchor JP (2007): Fibrin deposition accelerates neurovascular damage and neuroinflammation in mouse models of Alzheimer's disease. *J Exp Med*. 204:1999-2008.
479. Su JH, Anderson AJ, Cribbs DH, Tu C, Tong L, Kesslack P, et al. (2003): Fas and Fas ligand are associated with neuritic degeneration in the AD brain and participate in beta-amyloid-induced neuronal death. *Neurobiol Dis*. 12:182-193.
480. Erten-Lyons D, Jacobson A, Kramer P, Grupe A, Kaye J (2010): The FAS gene, brain volume, and disease progression in Alzheimer's disease. *Alzheimers Dement*. 6:118-124.
481. Ethell DW, Kinloch R, Green DR (2002): Metalloproteinase shedding of Fas ligand regulates beta-amyloid neurotoxicity. *Curr Biol*. 12:1595-1600.
482. Morishima Y, Gotoh Y, Zieg J, Barrett T, Takano H, Flavell R, et al. (2001): Beta-amyloid induces neuronal apoptosis via a mechanism that involves the c-Jun N-terminal kinase pathway and the induction of Fas ligand. *J Neurosci*. 21:7551-7560.
483. Burger S, Noack M, Kirazov LP, Kirazov EP, Naydenov CL, Kouznetsova E, et al. (2009): Vascular endothelial growth factor (VEGF) affects processing of amyloid precursor protein and beta-amyloidogenesis in brain slice cultures derived from transgenic Tg2576 mouse brain. *Int J Dev Neurosci*. 27:517-523.
484. Del Bo R, Ghezzi S, Scarpini E, Bresolin N, Comi GP (2009): VEGF genetic variability is associated with increased risk of developing Alzheimer's disease. *J Neurol Sci*. 283:66-68.
485. Patel NS, Mathura VS, Bachmeier C, Beaulieu-Abdelahad D, Laporte V, Weeks O, et al. (2010): Alzheimer's beta-amyloid peptide blocks vascular endothelial growth factor mediated signaling via direct interaction with VEGFR-2. *J Neurochem*. 112:66-76.
486. Cheng X, Yang L, He P, Li R, Shen Y (2010): Differential activation of tumor necrosis factor receptors distinguishes between brains from Alzheimer's disease and non-demented patients. *J Alzheimers Dis*. 19:621-630.
487. Patel JR, Brewer GJ (2008): Age-related differences in NFkappaB translocation and Bcl-2/Bax ratio caused by TNFalpha and Abeta42 promote survival in middle-age neurons and death in old neurons. *Exp Neurol*. 213:93-100.
488. Zhao M, Cribbs DH, Anderson AJ, Cummings BJ, Su JH, Wasserman AJ, et al. (2003): The induction of the TNFalpha death domain signaling pathway in Alzheimer's disease brain. *Neurochem Res*. 28:307-318.

489. Guo Q, Christakos S, Robinson N, Mattson MP (1998): Calbindin D28k blocks the proapoptotic actions of mutant presenilin 1: reduced oxidative stress and preserved mitochondrial function. *Proc Natl Acad Sci U S A*. 95:3227-3232.
490. Goodman JH, Wasterlain CG, Massarweh WF, Dean E, Sollas AL, Sloviter RS (1993): Calbindin-D28k immunoreactivity and selective vulnerability to ischemia in the dentate gyrus of the developing rat. *Brain Res*. 606:309-314.
491. Mattson MP, Rychlik B, Chu C, Christakos S (1991): Evidence for calcium-reducing and excito-protective roles for the calcium-binding protein calbindin-D28k in cultured hippocampal neurons. *Neuron*. 6:41-51.
492. Prehn JH, Bindokas VP, Jordan J, Galindo MF, Ghadge GD, Roos RP, et al. (1996): Protective effect of transforming growth factor-beta 1 on beta-amyloid neurotoxicity in rat hippocampal neurons. *Mol Pharmacol*. 49:319-328.
493. Iacopino AM, Christakos S (1990): Specific reduction of calcium-binding protein (28-kilodalton calbindin-D) gene expression in aging and neurodegenerative diseases. *Proc Natl Acad Sci U S A*. 87:4078-4082.
494. Iritani S, Niizato K, Emson PC (2001): Relationship of calbindin D28K-immunoreactive cells and neuropathological changes in the hippocampal formation of Alzheimer's disease. *Neuropathology*. 21:162-167.
495. Greene JR, Radenahmad N, Wilcock GK, Neal JW, Pearson RC (2001): Accumulation of calbindin in cortical pyramidal cells with ageing; a putative protective mechanism which fails in Alzheimer's disease. *Neuropathol Appl Neurobiol*. 27:339-342.